N° d'ordre :

الجمهورية الجزائرية الديمقراطية الشعبية

République Algérienne Démocratique et Populaire

وزارة التعليم العالي والبحث العلمي

Ministère de L'enseignement Supérieur et de La Recherche Scientifique

جامعة عين تموشنت بلحاج بوشعيب

Université Ain Témouchent-Belhadj Bouchaib

Faculté :Faculté des Sciences et Technologie
Departement : Biologie
Laboratoire : Hydrologie Appliquée et Environnement

THÈSE

Présentée pour l'obtention du **diplôme de DOCTORAT**
Domaine : Sciences de la Nature et de la Vie
Filière : Sciences Biologiques
Spécialité : Biochimie

Par : BENCHIKH Imen

Intitulé

Study the effect of common contaminants on rat pancreatic cell physiology

Soutenue publiquement, le 12 /07 /2025, devant le jury composé de :

Nom & Prénom(s)	Grade	Qualité	Établissement de rattachement
BRIXI GORMAT Nassima	Maître de conférences A	Présidente	Université de Ain Témouchent
ZIANI Kaddour	Professeur	Rapporteur	Université de Saida Dr Moulay Tahar
KHALED Méghit Boumediène	Professeur	Co-rapporteur	Université Djillali Liabés de Sidi Bel Abbés
BERROUKECHE Farid	Maître de conférences A	Examinateur	Université de Béchar
YAZIT sidi Mohammed	Maître de conférences A	Examinateur	Université de Ain Témouchent
KHALFA Ali	Maître de conférences A	Examinateur	Université de Ain Témouchent

Année Universitaire : 2024/2025

ACKNOWLEDGMENTS

First and foremost, I would like to express my sincere gratitude to **Allah**, the Almighty, for bestowing upon me the blessings of courage, strength, and patience, enabling me to complete this work. As He says in the Holy Quran, ﴿ وَقُلْ رَبِّ زِدْنِي عِلْمًا﴾, Surah Ta-Ha, Verse 114.

I would like to extend my sincere special thanks to my supervisor **Prof. Kaddour ZIANI**, for his continuous support for this study and for his patience, motivation, and the wealth of knowledge he shared. His invaluable guidance was instrumental throughout my PhD journey. Also, I would like to express my deepest gratitude to my co-supervisor **Prof. Méghit Boumédiène KHALED**, for his constant support, invaluable advice, motivation, and regular feedback. Their guidance significantly enhanced my scientific skills and fostered a strong team spirit.

I would also like to express my sincere gratitude to my thesis committee members for their valuable time and insightful feedback during the evaluation of this work. My deepest thanks go to the committee president, **Dr. BRIXI GORMAT Nassima**, as well as to **Dr. BERROUKECHE Farid**, **Dr. YAZIT Sidi Mohammed**, and **Dr. KHALFA Ali**.

I am deeply grateful to **Prof. Antonio Gonzalez Matheos** for his supervision, collaboration, and guidance during my internship in Spain. I would like to extend my sincere thanks to his team of cell biology and communication research group, particularly **Candido Ortiz-Placin** and **Alba Castillejo-Rufo**, for their support, encouragement, and the excellent teamwork I experienced during my stay in their lab.

I would like to thank **Dr. Abdelkarim BENALIA** for his invaluable help, assistance, and guidance during the animal experiments.

I wish to express my sincere gratitude to **Dr. Hayat ARGOUB** and **Dr. Youcef ATTAR** for their valuable collaboration and guidance during the histological study.

I am deeply indebted to my **friends** and **colleagues** whose unwavering support and encouragement were instrumental in the successful completion of this thesis.

Last, but not least, I deeply thank **my parents** for their endless support and encouragement. Your support has played a crucial role in my personal and academic growth. I am incredibly thankful for your unwavering belief in me and for the encouragement that has helped me in each step of the way. I am grateful also to **my sisters** and **brothers-in-law** for their continuous support and love.

Finally, I also place on record, sense of gratitude to one and all, who directly or indirectly have participated in this venture.

ABSTRACT

The neonicotinoid insecticide acetamiprid has been linked to toxicity in various organs and organisms. However, its effects on the exocrine pancreas remain largely unexplored. This study aimed to investigate the toxic effects of acetamiprid on the exocrine pancreas through *in-vivo* and *in-vitro* investigations. We also explored the potential preventive effects of carnosine. In the *in-vivo* study, male *Wistar* rats were administered acetamiprid orally at two doses (21.7 and 43.4 mg/kg/day, respectively) with or without carnosine supplementation (200mg/kg/day) for 30 days. The body and pancreatic weight were measured, malonaldehyde, glucose, lipase, amylase levels, and histopathological examination were evaluated. In the *in-vitro* study, AR42J pancreatic cells were exposed to acetamiprid with or without carnosine, and the cell viability, MAPK signaling pathway, intracellular calcium levels, and trypsin secretion were investigated. Sub-acute acetamiprid exposure led to significant adverse effects, including decreased body weight and pancreatic somatic index, increased blood glucose, altered pancreatic enzyme levels (decreased amylase and increased lipase levels), and elevated malondialdehyde levels. Histological examination revealed damage to pancreatic tissue. While carnosine supplementation partially mitigated these adverse effects. Acetamiprid exposure altered AR42J pancreatic cell viability in a dose-dependent manner, while co-treatment with carnosine significantly improved cell survival, and activated the MAPK signaling pathway, which was attenuated by carnosine. While acetamiprid increased intracellular calcium levels, it did not significantly affect trypsin secretion. This study shows that acetamiprid harms the exocrine pancreas. However, carnosine supplementation may offer protection against these harmful effects.

Key words: Neonicotinoid insecticide, exocrine pancreas, carnosine, subacute toxicity, AR42J cells, acetamiprid, *Wistar* rats.

RÉSUMÉ

L'insecticide néonicotinoïde acétamipride a été associé à une toxicité dans divers organes et organismes. Cependant, ses effets sur le pancréas exocrine restent largement inexplorés. Cette étude visait à étudier les effets toxiques de l'acétamipride sur le pancréas exocrine à travers des investigations *in-vivo* et *in-vitro*. Nous avons également exploré les effets préventifs potentiels de la carnosine. Dans l'étude *in-vivo*, des rats *Wistar* mâles ont reçu de l'acétamipride par voie orale à deux doses (21,7 et 43,4 mg/kg/jour, respectivement) avec ou sans supplémentation en carnosine (200 mg/kg/jour) pendant 30 jours. Le poids corporel et le poids pancréatique ont été mesurés, les niveaux de malondialdéhyde, de glucose, de lipase, d'amylase et un examen histopathologique ont été évalués. Dans l'étude *in-vitro*, des cellules pancréatiques AR42J ont été exposées à l'acétamipride avec ou sans carnosine, et la viabilité cellulaire, la voie de signalisation MAPK, les niveaux de calcium intracellulaire et la sécrétion de trypsine ont été étudiées. L'exposition sous-aiguë à l'acétamipride a entraîné des effets indésirables significatifs, notamment une diminution du poids corporel et de l'indice somatique pancréatique, une augmentation de la glycémie, des modifications des niveaux d'enzymes pancréatiques (diminution de l'amylase et augmentation des niveaux de lipase) et une élévation des niveaux de malondialdéhyde. L'examen histologique a révélé des lésions tissulaires pancréatiques. La supplémentation en carnosine a atténué partiellement ces effets indésirables. L'exposition à l'acétamipride a modifié la viabilité cellulaire des cellules pancréatiques AR42J de manière dose-dépendante, tandis que le traitement concomitant avec la carnosine a amélioré significativement la survie cellulaire et activé la voie de signalisation MAPK, qui a été atténuée par la carnosine. Bien que l'acétamipride ait augmenté les niveaux de calcium intracellulaire, elle n'a pas affecté de manière significative la sécrétion de trypsine. Cette étude montre que l'acétamipride nuit au pancréas exocrine. Cependant, la supplémentation en carnosine peut offrir une protection contre ces effets néfastes.

Mots-clés : Insecticide néonicotinoïde, pancréas exocrine, carnosine, toxicité subaiguë, cellules AR42J, acétamipride, rats *Wistar*.

ملخص

أظهرت الدراسة الحالية أن مبيد الحشرات النيونيكوتينويدي أسيتاميبريد يرتبط بالسمية في أعضاء وكائنات حية مختلفة. ومع ذلك، فإن آثاره على البنكرياس خارجي الافراز لم يتم استكشافها بشكل كامل. هدفت هذه الدراسة إلى إلى دراسة الآثار السامة للأستاميبريد على البنكرياس خارجي الافراز باستخدام جرذان المختبر والخلايا. كما استكشفنا الآثار الوقائية المحتملة للكارنوزين. في الدراسة على الجسم الحي، تم إعطاء جرعات مختلفة من الأسيتامبريد (21.7 و43.4 ملغ/كغ/يوم) لذكور الجرذان البيضاء عن طريق الفم، مع أو بدون مكملات الكارنوزين (200 ملغ/كغ/يوم) لمدة 30 يومًا. تم قياس وزن الجسم والوزن البنكرياسي، ومستويات المالونديالدهيد، والجلوكوز، والليباز، والأميلوز، وتم إجراء التقييم النّسيجي. في الدراسة على الخلايا، تم تعريض خلايا البنكرياس AR42J للأسيتامبريد مع أو بدون الكارنوزين، وتم تقييم حيوية الخلية والإشارات الخلوية MAPK، مستويات الكالسيوم داخل الخلية، وإفراز التربسين. أدى التعرض للأسيتامبريد إلى آثار ضارة كبيرة، بما في ذلك انخفاض في وزن الجسم والوزن البنكرياسي، وزيادة في نسبة السكر في الدم، وتغيرات في مستويات إنزيمات البنكرياس (انخفاض الأميلوز وزيادة مستويات الليباز)، وارتفاع في مستويات المالونديالدهيد. كشف التقييم النّسيجي عن تلف في أنسجة البنكرياس. أدت مكملات الكارنوزين إلى تخفيف جزئي لهذه الآثار الضارة. أدى التعرض للأسيتامبريد إلى تغيير قابلية بقاء الخلايا البنكرياسية AR42J بشكل يعتمد على الجرعة، بينما أدى العلاج المصاحب بالكارنوزين إلى تحسين بقاء الخلايا بشكل كبير وفعّل الأسيتامبريد مسار والإشارات الخلويةMAPK ، والذي تم تخفيفه بواسطة الكارنوزين. على الرغم من أن الأسيتامبريد زاد من مستويات الكالسيوم داخل الخلية، إلا أنه لم يؤثر بشكل كبير على إفراز التربسين. توضح هذه الدراسة أن الأسيتامبريد يضر بالبنكرياس خارجي الافراز. ومع ذلك، فإن مكملات الكارنوزين قد توفر حماية ضد هذه الآثار الضارة.

الكلمات المفتاحية: مبيدات الحشرات النيونيكوتينويد، البنكرياس خارجي الافراز، الكارنوزين، السمية تحت الحادة، خلايا AR42J ، الأسيتاميبريد، جرذان ويستار

TABLE OF CONTENTS

LIST OF FIGURES

LIST OF TABLES

LIST OF ABBREVIATIONS

ACE 2: angiotensin-converting enzyme 2

ACE: acetamiprid

Ach: acetylcholine

ADP: adenosine di-phosphate

AMP: adenosine mono-phosphate

ARE: antioxidant response element

ATP: adenosine tri-phosphate

ATPGD1: ATP-Grasp domain containing protein 1

cAMP: cyclic denosine mono-phosphate

CARN: carnosine

CARNMT: carnosine N-methyltransferase

CARNS1: carnosine synthetase 1

CCK: cholecystokinin

CNDP 1: carnosine dipeptidase 1

CNDP 2: carnosine dipeptidase 2

DNA: Deoxyribonucleic acid

ER: endoplasmic reticulum

G6Pase: glucose-6-phosphatase

GSH: glutathione

GSK: glycogen synthase kinase

HCDs: histidine containing dipeptides

HIF-1α: hypoxia-inducible factor-1 alpha

IGF-1: Insulin-like Growth Factor 1

IGFBP1: Insulin-like Growth Factor Binding Protein 1

IL-10: interleukin-10

IL-6: interleukin-6

IL-8: interleukin-8

MAPK: mitogen-activated protein kinases

MDA: malondialdehyde

mTOR: mammalian target of rapamycin

n.s: non stimulated

nAChRs:Nicotinic Acetylcholine Receptors

NF-κB: Nuclear fFctor-κB

Nrf2: Nuclear factor erythroid 2-related factor 2

PABNA: N-a-benzoyl-DL-arginine-p-nitroanilide

POT: roton-coupled oliOgopeptide Transporter

PSI: Pancreatic Somatic Index

ROS: Reactive Oxygen Species

SLC 15: Solute Carrier Family 15

SOD: Superoxide Dismutase

Stauro: Staurosporine

TNF-α: Tumor Necrosis Factor α

Tps: Thapsigargin

UPR: Unfolded Protein Response

INTRODUCTION

INTRODUCTION

The pervasive presence of chemicals in the environment, driven by industrialization and urbanization, poses significant exposure risks to living beings, leading to increased health hazards for both humans and wildlife **(Bisesi & Lee, 2024)**. Within this context, pesticide exposure constitutes a significant global health concern, contributing in an estimated 150,000 to 300,000 fatalities annually **(Eddleston, 2020; Traore et al., 2016)**. This issue is particularly prevalent in rural regions of developing nations due to widespread access to pesticides **(Lee & Cha, 2009)**.

Pesticides, particularly insecticides, warrant extensive scientific investigation alongside conventional contaminants such as heavy metals, due to their unique toxicity profiles, environmental persistence, and profound implications for human health and ecosystems. These substances have been associated with a range of disorders, including neurodevelopmental abnormalities, endocrine disruption, and carcinogenesis. Furthermore, their propensity to bioaccumulate within food chains poses long-term ecological and public health risks **(Adil et al., 2023)**. Among insecticides, neonicotinoids have emerged as the most widely used and rapidly expanding class globally, recognized for their efficacy against a broad range of pests (**Jeschke et al., 2011; Jeschke & Nauen, 2008**). Their selective action on insect nicotinic acetylcholine receptors contributes to their high target specificity and adaptability across various application methods (**Kundoo et al., 2018**).

Acetamiprid (ACE), a widely utilized neonicotinoid insecticide, is extensively employed in agricultural practices to manage a broad spectrum of pests (**Zuščíková et al., 2023**). However, apprehensions have arisen concerning its potential environmental and health repercussions. Indeed, ACE has been shown to persist in soil environments and accumulate in nectar and pollen, potentially impacting non-target species, such as pollinators and aquatic invertebrates (**Goulson, 2013**). Furthermore, its widespread occurrence in the environment, drinking water sources, and food supply has prompted concerns regarding potential human health hazards (**Devan et al., 2015**).

A growing body of evidence highlights the necessity for a thorough understanding of the risks associated with ACE exposure. Animal studies have demonstrated potential for genotoxicity and cytotoxicity **(Thompson et al., 2020**). Additionally, ACE has been confirmed to induce oxidative stress, disrupt spermatogenesis, and cause endocrine disruption within the reproductive systems of animals **(El-Hak et al., 2022; Phogat et al., 2023; Zuščíková et al., 2023**). Despite these findings, the majority of research on insecticides toxicity, including ACE, have primarily focused on direct mechanisms of action, often overlooking secondary effects on specific organs such as the pancreas which could be a target organ for such toxicity.

Chemicals such as heavy metals have been shown to alter pancreatic function, particularly by disrupting mitochondrial activity and inducing oxidative stress (**Linţa et al., 2024**). These toxins can also interfere with glucose and glucagon metabolism and enzyme activity, primarily by disrupting the function of ß-cells, α-cells, and acinar cells **(Im et al., 2024; Javaid et al., 2021**). Besides, neonicotinoid insecticides may exhibit analogous effects. For instance, imidacloprid has been demonstrated to disrupt glucose metabolism and induce insulin resistance (**Khalil et al., 2017**). Additionally, ACE has been proven to induce genotoxicity and cytotoxicity in the AR42J pancreatic cell line (**Kara et al., 2019**).

Carnosine (CARN), a naturally occurring dipeptide, is found in high concentrations in skeletal muscle, brain tissue, and other organs. It is renowned for its antioxidants, anti-glycation, and pH-buffering properties, which play a critical role in maintaining cellular homeostasis and protecting against oxidative stress **(Turner et al. 2021)**. Extensive research has highlighted CARN's ability to scavenge free radicals, chelate metal ions, and inhibit the formation of advanced glycation end-products, which are implicated in aging and various chronic diseases **(Boldyrev et al. 2013)**. Additionally, CARN has demonstrated protective effects in numerous physiological and pathological contexts, including neurodegenerative diseases, diabetes, and cardiovascular disorders **(Boldyrev 2012; Peters et al. 2020)**. Given its multifaceted therapeutic potential, CARN is increasingly being explored as a potential intervention to counteract the adverse effects of toxic substances on cellular and organ function.

To date, the toxicity of insecticides, particularly ACE, on the exocrine pancreas remains poorly understood and warrants further investigation. Similarly, the potential

efficacy of natural compounds such as CARN in mitigating these toxic effects requires in-depth exploration.

This study aims to elucidate the effects of ACE on the physiology of exocrine pancreatic cells, identify the underlying mechanisms involved, and explore its potential role in the pathogenesis of pancreatic disorders. Furthermore, it investigates the preventive effects of CARN against these alterations.

The experimental design was conducted in multiple phases. Male *Wistar* rats were selected as the animal model, and subacute toxicity was induced using ACE at doses of 43.4 mg/kg/day and 21.7 mg/kg/day. Concurrently, CARN was administered at a dose of 200 mg/kg/day as a preventive treatment. Biochemical analyses were performed to assess blood glucose levels, amylase and lipase activity, as well as oxidative stress markers in pancreatic tissues. Histological examinations were conducted to assess tissue damage, and in-vitro analyses using AR42J cells were carried out to evaluate cell viability, the MAPK signaling pathway, intracellular calcium mobilization, and trypsin secretion. These investigations provide critical insights into the molecular mechanisms underlying ACE-induced toxicity and the potential protective role of CARN.

CHAPTER 1

ACETAMIPRID: PROPERTIES, ENVIRONMENTAL IMPACT, AND TOXICITY

CHAPTER 1

ACETAMIPRID: PROPERTIES, ENVIRONMENTAL IMPACT, AND TOXICITY

1.1 Pesticides use

Pesticides encompass any substance or combination of substances designed to control or eliminate organisms deemed harmful. These substances, often chemical in nature, target pests such as insects, weeds, and disease-causing organisms that threaten agricultural productivity **(US EPA, 2014; World Health Organization, 2020)**.

Over the past few decades, pesticide usage has dramatically increased, with a particularly notable fortyfold rise in the application of modern synthetic pesticides over the last three decades **(Alavanja, 2009)**. Although these chemicals have contributed to increased crop yields and enhanced food security, their widespread use raises significant concerns **(Sharma et al., 2019)**. This is because of their persistent nature and potential for bioaccumulation, which poses risks to both the environment and human health **(Sharma et al., 2020)**.

1.1.1 In the world

Global pesticide use has surged in recent decades, reaching approximately 2.7 million tons in 2020, with an average application rate of 1.8 kilograms per hectare. This marks a substantial 50% increase since 1990, driven largely by a significant rise in herbicide use **(Wisnujati, 2023)**. Notably, low-income countries have experienced a dramatic 153% increase in pesticide usage over the past decade, underscoring the likely underreporting of pesticide use trends in these regions **(Shattuck et al., 2023)**.

Pesticide use has surged across Asia, with Southeast Asia accounting for approximately 20% of global consumption **(Schreinemachers & Tipraqsa, 2012)**.

Countries like India, a major producer, saw production skyrocket from 5,000 to 90,000 metric tons annually **(Pozo et al., 2011)**. While China, now the world's largest producer, experienced a dramatic increase in consumption more than doubled between 1991 and 2006, increasing from 76 million tons to 146 million tons **(Qiao et al., 2022)**. Whereas 45% of worldwide consumption is used by Europe and 25% by the USA **(De et al., 2014)**.

1.1.2 In Algeria

The expansion of agricultural land in Algeria has led to a significant increase in the use of pesticides, reaching an estimated 6,000-10,000 tons per year **(Youcefi & Mokhtari, 2024)**. The market currently boasts a wide array of pesticide options, with approximately 400 active substances and nearly 7000 commercial formulations available. In the El-Oued region, 41.7% of all pesticides used are insecticides, and within this category, acetamiprid constitutes 25.58% of the active ingredients **(Zamoum et al., 2023)**. Whereas in the Biskra region, extensive pesticide use was recorded, with acetamiprid applied at rates of 500-600 g per hectare, significantly exceeding the registered dose limit of 125 g/hectare **(Soudani et al., 2022)**.

1.2 Pesticide classification

The classification of pesticides is essential for understanding their applications, mechanisms, and potential impacts on health and the environment. It can be classified by their target organism (e.g., insecticides, herbicides, fungicides), chemical class (e.g., organophosphates, pyrethroids, neonicotinoids), mode of action (contact, systemic, fumigant), and origin (synthetic or biopesticides) **(Figure 1.1) (Hassaan & El Nemr, 2020)**.

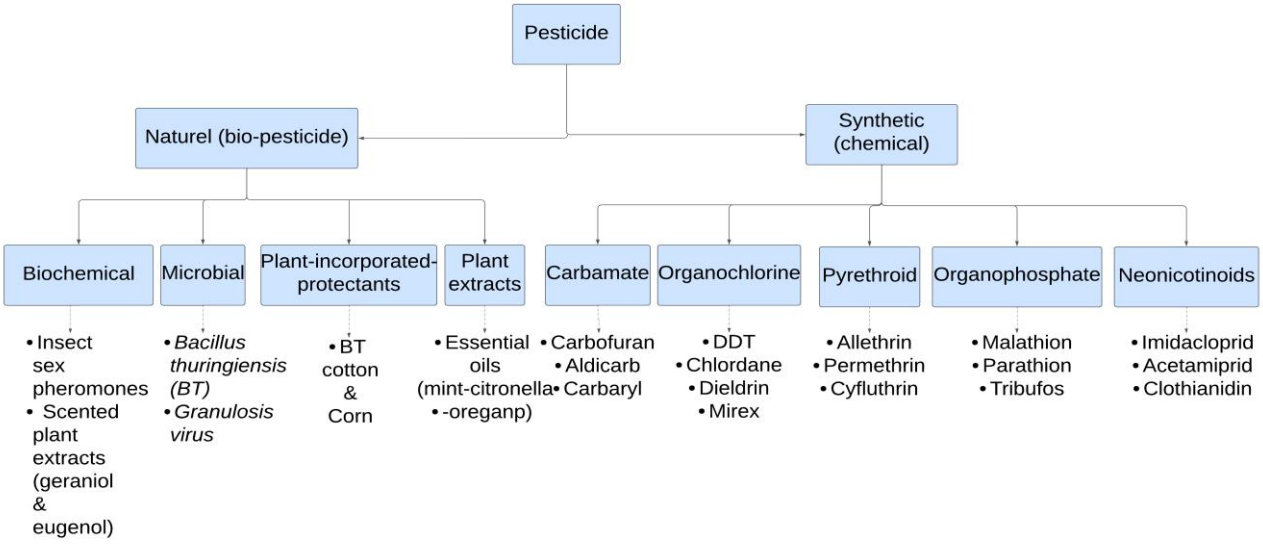

Figure 1.1 Pesticides classification **(I. Ansari et al., 2021)**

1.3 Neonicotinoids insecticides

Neonicotinoids constitute a major class of systemic insecticides widely employed in agriculture for pest control. These insecticides function by mimicking the action of acetylcholine at insect nicotinic acetylcholine receptors, disrupting their nervous systems which lead to death **(Garud et al., 2024)**.

This class of pesticides covers seven insecticides based on their active compounds, as depicted in **Figure 1.2.**

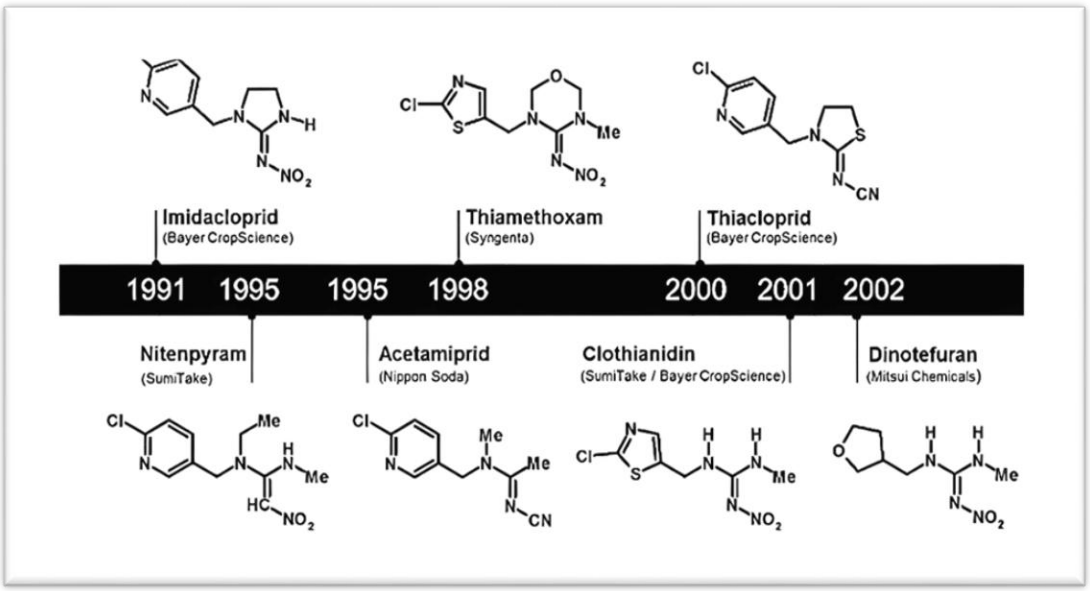

Figure 1.2 Neonicotinoid insecticides **(Bass et al., 2015)**

1.4 Acetamiprid

Acetamiprid ($C_{10}H_{11}ClN_4$) is a neonicotinoid insecticide that was primarily developed by the Japanese chemical company (Nippon Soda Co., Ltd.) in the early 1990s. The company was working to produce a new powerful insecticide that could be used against a wide range of insects without affecting harmful effect on non-target organisms **(Bass et al., 2015)**.

Acetamiprid (or N-((6-chloro-3-pyridinyl) methyl)-N'-cyano-N-methylethanimidamide) can be described as a carboxamidine compound where the amino hydrogens are replaced by a (6-chloropyridin-3-yl) methyl group and a methyl group. Additionally, the hydrogen attached to the imino nitrogen is substituted by a cyano group **(Figure 1.3) (X. Zhang et al., 2023)**.

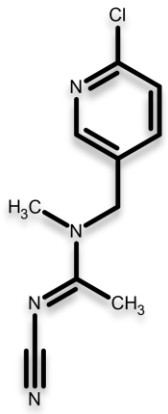

Figure 1.3 Chemical structure of acetamiprid **(PubChem)**

1.5 Physicochemical properties

Acetamiprid exists as a white crystalline solid with a very slight identifiable odor. It comes in various formulations, such as dusts, granules, and liquid concentrates **(Sheets et al., 2016)**. The specific physical characteristics and odor of acetamiprid can vary, contingent upon the formulation and purity of the compound **(Bondareva & Fedorova, 2021)**. **Table 1.1** summarized the physicochemical properties of acetamiprid.

Table1.1 Physicochemical properties of acetamiprid (extracted from **PubChem**)

Property	Value
Chemical formula	$C_{10}H_{11}ClN_4$
International Union of Pure and Applied Chemistry (IUPAC) nomenclature	N-[(6-chloropyridin-3-yl) methyl]-N'-cyano-N-methylethanimidamide
Molecular weight	222.67 g/mol
Hydrogen bond donor count	0
Hydrogen bond acceptor count	1
Melting point	98.9 °C
Solubility (in water)	4.25X10+3 mg/L at 25 °C
Vapor pressure	0.000044 millimeter of mercury (mmHg) at 25 °C
Density	1.33 g/cm^3 at 20° C
Henry's Law Constant	6.92X10-8 mol/(L·Pa) at 25 °C
Ionization mode	Positive
pH	2.7
Dissociation Constants (pKa)	0.7
Log kow	0.80 at 25 °C

Henry's Law Constant is the concentration of a gas in a liquid to the partial pressure of that gas above the liquid, know (Octanol-Water Partition Coefficient) is a measure of a substance's tendency to partition between organic and aqueous phases. Acetamiprid has a relatively high Kow value, indicating that it has a greater affinity for organic solvents than for water.

1.6 Mode of action

Acetamiprid is one of the neonicotinoid insecticides that acts similarly to nicotine **(Figure 1.4)**. Its involves an irreversible interaction with the nicotinic acetylcholine receptors (nAchRs) in the nervous system of insects **(Shamsi et al., 2021)**.

When acetamiprid attaches to nAChRs, it triggers their activation, causing irregular nerve signal transmission that results in paralysis and death of the targeted insect. This binding process is highly selective for insects, making it less harmful to non-target organisms **(Zuščíková et al., 2023)**. This selectivity is due to the differences in nAChR structure and composition between insects and other organisms. Acetamiprid has a much stronger affinity for insect nAChRs compared to mammalian nAChRs **(EFSA PPR et al., 2022)**.

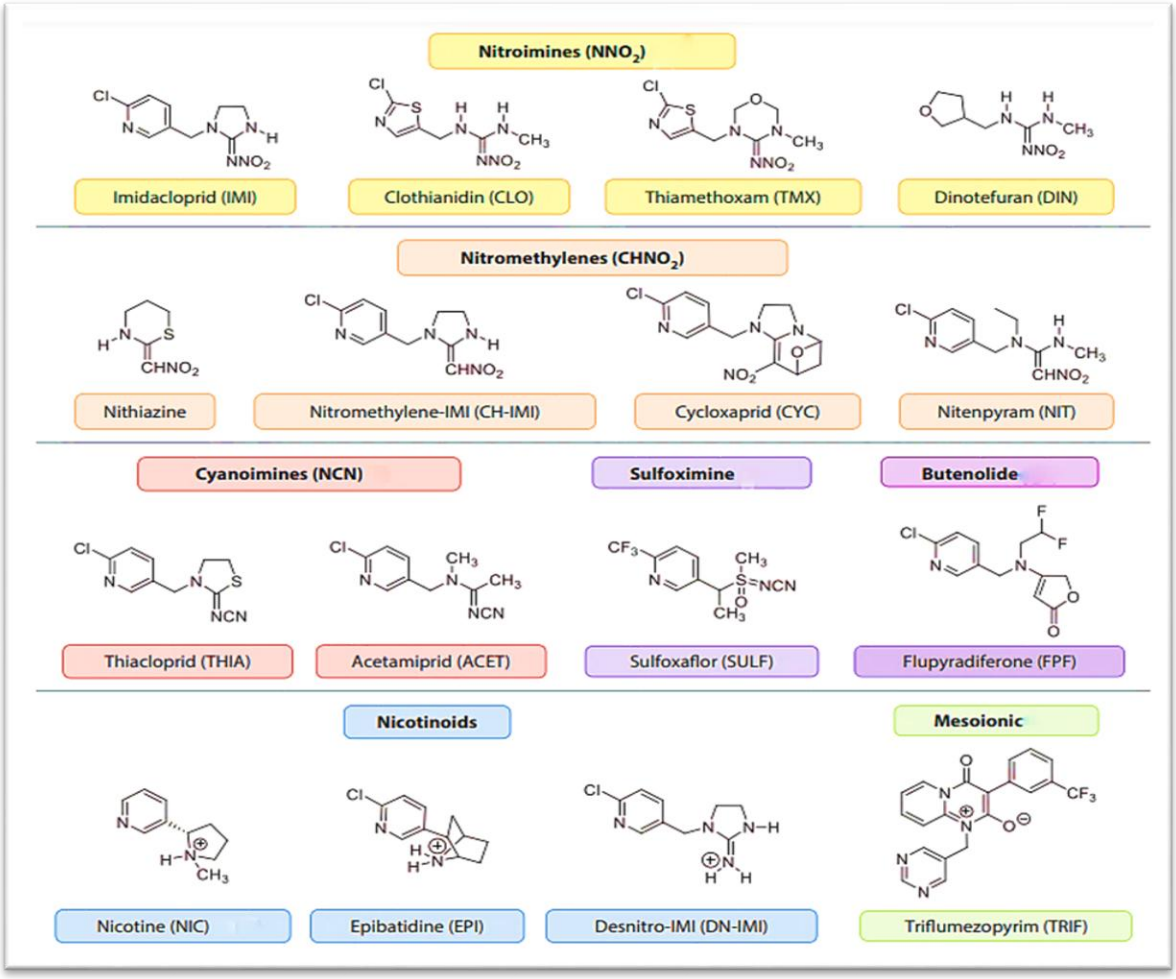

Figure 1.4 Agonists of nAchRs including neonicotinoid insecticides **(Casida, 2018)**

Certainly, acetamiprid's binding to nAChRs initiates a surge in neurotransmitter release, including acetylcholine, which overstimulates nerve cells. This overstimulation leads to hyperexcitability in the insect's nervous system. Furthermore, acetamiprid downregulates the enzyme acetylcholinesterase (AChE), the enzyme that breaks down acetylcholine in the synapses. By blocking AChE, acetamiprid prolongs the action of acetylcholine, intensifying the overstimulation of the insect's nervous system **(Figure 1.5) (Wallace, 2024)**.

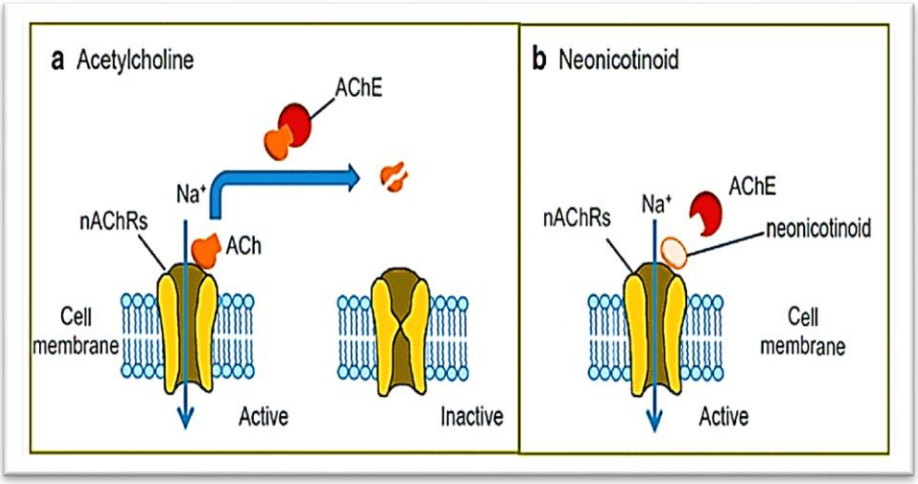

Figure 1.5 Nicotinic acetylcholine receptor's action in front of acetylcholine or neonicotinoid insecticide **(Zuščíková et al., 2023)**

1.7 Toxicokinetic

1.7.1 Absorption

According to several studies, intestinal absorption is considered the primary route of administration. In the study of **Brunet et al. (2008)**, the apparent permeability coefficient of acetamiprid flux was determined to be 26.10^{6} cm/s in a bidirectional manner using the Caco-2 cell line at a temperature of 37°C. This finding indicates that acetamiprid crosses the cell transepithelial barrier in substantial quantities. Furthermore, in Wistar rats, it has been demonstrated that acetamiprid is rapidly absorbed from the intestine. This absorption results in increased permeability of the intestinal epithelium and initiates the initial damage in the body **(Matsuo et al., 1998)**.

1.7.2 Distribution

The distribution of acetamiprid in various tissues has been extensively studied. In the study of **Devan et al. (2015)**, acetamiprid was detected in multiple tissues of Wistar rat including the liver, muscles, fat, kidneys, spleen, and brain, following oral administration. In another interesting investigation conducted by **Yeter and Aydın (2014)**, using HPLC analysis, acetamiprid and its metabolites were identified in the stomach (47.35 µg/g), liver (0.79 µg/g), and blood (2.7 µg/mL) of a postmortem human following a fatal intoxication case.

Hence, according to **Nimako et al. (2021)**, both acetamiprid and imidacloprid, along with their respective metabolites, were identified in eight different tissues of mice after prolonged exposure to 0.6 mg/kg in powdered diet. The highest levels were detected in the blood, followed by the testes, lungs, brain, inguinal white adipose tissue, kidneys, gonadal white adipose tissue, and lastly, the pancreas. Whereas a single study detected N-desmethyl-acetamiprid, the primary metabolite of acetamiprid, at higher levels in cord serum compared to other metabolites **(Zhang et al., 2022)**.

1.7.3 Metabolism

Acetamiprid is metabolized within both human and animal bodies, although the exact processes involved are not fully understood. It appears that this insecticide is broken down primarily through aldehyde oxidase and cytochrome P450 enzymes, undergoing a nitro-reduction reaction to produce nitro/amino metabolites in the liver **(Swenson & Casida, 2013)**. Additionally, the metabolite N-desmethyl-acetamiprid has been observed in both rainbow trout and rats, indicating a conserved metabolic pathway across these species **(Kolanczyk et al., 2020)**.

1.7.4 Excretion

Excretion through urine and feces facilitates the elimination of this compound in both humans and animals, regardless of the exposure route. A study using Liquid Chromatography/Time-of-Flight Mass Spectrometry (LC/TOFMS) identified seven insecticides metabolites in human urine samples, with N-desmethyl-acetamiprid, 5-hydroxy-imidacloprid, and N-desmethyl-clothianidin being the most prevalent **(Taira et al., 2013)**. Additionally, urine samples from 24 adults who were given a single 5 µg dose of acetamiprid revealed the presence of the parent compound, with concentrations of 1.14 µg/day. The half-life of this chemical was reported to be between 0.17 to 1.45 days **(Harada et al., 2016)**.

1.8 Persistence and environmental contamination

1.8.1 Soil

Acetamiprid demonstrates different sorption and dissipation patterns depending on the soil type. Biochar addition to agricultural soils enhances acetamiprid

sorption, decreasing its dissipation **(Yu et al., 2011)**. However, in sandy soils, acetamiprid exhibits high persistence and mobility, with low sorption values and slow mineralization rates, increasing the risk to soil organisms and potential transfer to water sources **(Potts et al., 2022)**. In Brazilian tropical soils, acetamiprid sorption is relatively low, indicating a high risk of surface and groundwater contamination **(Carbo et al., 2007)**. Encouragingly, a strain of Pigmentiphaga sp. AAP-1 has been identified that can degrade acetamiprid, suggesting the potential for bioremediation of acetamiprid-contaminated environments **(Wang et al., 2013)**.

1.8.2 Water

The insecticide acetamiprid has the potential to contaminate water sources, thereby threatening aquatic ecosystems and humans **(Qamruzzaman & Nasar, 2014)**. Nevertheless, implementing proper forestry practices can help mitigate this risk, as evidenced by Thomas et al. **(2023)** research on chemical runoff from trees treated with acetamiprid. Several approaches have been suggested for eliminating acetamiprid from water, such as ozonation **(Fasnabi et al., 2012)** and Fenton and Fenton-like oxidation **(Mitsika et al., 2013)**. These studies underscore the importance of developing efficient water treatment strategies to address the potential consequences of acetamiprid contamination.

1.8.3 Crops

Recent research has given great interest in developing methods for detecting and analyzing acetamiprid in food products. Surface-enhanced Raman spectroscopy has been utilized as a quick and precise approach for identifying acetamiprid in apple juice and on apple surfaces **(Wijaya et al., 2014)**. A combined strategy using HPLC-MS and QueChERS extraction revealed the presence of acetamiprid in hazel leaves, honey, and pollen, as well as various transformation products **(Calza et al., 2022)**. A label-free fluorescent assay based on a triplex-to-G-quadruplex molecular switch exhibited strong sensitivity and selectivity for acetamiprid detection in food extracts **(Tang et al., 2018)**.

Indeed, acetamiprid residues were strongly present in cucumber, cauliflower, tomato, chilies, apple, and mango after extraction with ethyl acetate **(Nawaz et al., 2015)**. Additionally, when acetamiprid was used at 200-400 ppm to treat tomato fruits,

the amount was over five times higher than the safe limit (i.e., 0.2 mg/kg) after 7 days of application **(Ali, 2018)**. All these studies contribute to understanding the persistence of acetamiprid in food products, as well as its potential effects on human health **(Figure 1.6)**.

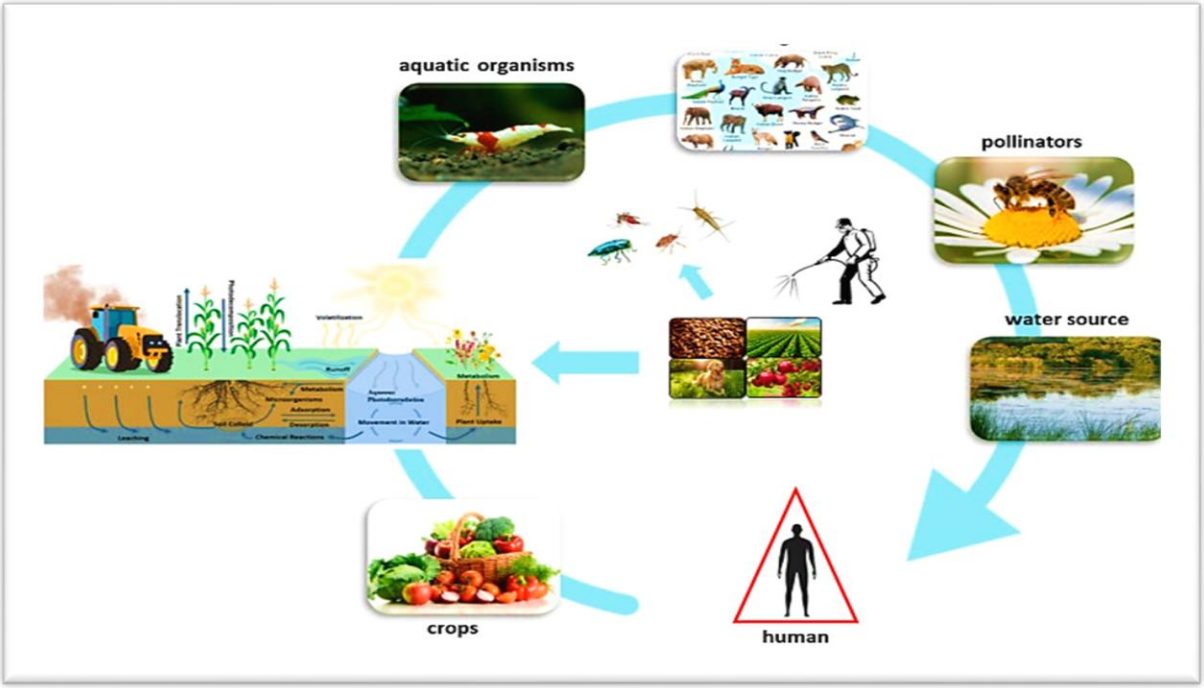

Figure 1.6 Assessing the environmental degradation and exposure pathways of acetamiprid Post-Application **(Zuščíková et al., 2023)**

1.9 Effect of acetamiprid

1.9.1 Target organisms

Acetamiprid is a potent insecticide effective against a broad range of insects and pests. This efficacy is attributed to its wide spectrum of action, long-lasting residual effect, and relatively low potential for pests to develop resistance **(Kundoo et al., 2018)**.

The effectiveness of acetamiprid extends even further. In the study by **Waqas et al. (2019)**, acetamiprid was shown to reduce the reproductive capacity of *Solenopsis mealybug* by impacting oviposition, fecundity, and feeding behavior at sublethal doses. Furthermore, similar effect was observed on *Eriopis connexa,* where acetamiprid disturbed embryogenesis by up to 45% and reduced egg producing by up to 100% **(Fogel et al., 2013)**.

Indeed, in apple orchards, acetamiprid showed reduced effectiveness (78.3-86.7%) against rosy apple aphid in four out of six locations but maintained high efficacy (89.7-95.3%) in two orchards **(Holdaj et al., 2020)**. For cotton pests, acetamiprid at 20 grams of active ingredient per hectare was highly effective against *Aphis gossypii* and *Amrasca biguttula biguttula*, with increased efficacy at higher concentrations **(Kanna et al., 2007)**. It also significantly reduced jassid, whitefly, and thrips populations in cotton for up to nine days **(Raghuraman et al., 2008)**. However, while acetamiprid effectively controlled *Bemisia tabaci* in cotton, it negatively impacted six predator species, potentially disrupting integrated pest management programs **(Naranjo & Akey, 2004)**. Overall, acetamiprid demonstrates high efficacy against various pests but may have unintended effects on beneficial insects, requiring careful consideration in pest management strategies.

1.9.2 Non-target organisms

Recent research indicates that acetamiprid can have considerable negative impacts on non-target organisms. In aquatic habitats, both the active ingredient and commercial formulations of acetamiprid impair detoxification and oxidative metabolism in snails **(Cossi et al., 2020)**, and expose high toxicity to crustaceans such as *Daphnia magna* and *Plea minutissima* **(Gacem et al., 2023)**. Terrestrial insects are also disturbed, with field studies showing up to 78% decline in plant bug populations following exposure to acetamiprid-based insecticides **(Sedlmeier et al., 2024)**. Interestingly, some non-target insects demonstrated nearly 10,000 times greater sensitivity to acetamiprid than honeybees, with males being more sensitive than females in certain species **(Renaud et al., 2018)**.

Moreover, acetamiprid has been associated with reproductive system disruptions in mammals, including oxidative stress in testes and pathological changes in ovarian follicles **(Zuščíková et al., 2023)**. These findings underscore the potential risks of acetamiprid to various non-target organisms across diverse ecosystems.

1.10 Toxicity of acetamiprid

There is a significant concern regarding the potential organotoxic effects of acetamiprid on non-target organisms, including human beings. Various findings have

shown that exposure to this neonicotinoid insecticide can lead to disruptions in the function of different organs and tissues, including the liver, kidneys, nervous system, and reproductive system.

1.10.1 Neurotoxicity

Numerous studies have demonstrated that acetamiprid can cause neurotoxicity in mammals. Exposure to this insecticide during prenatal development can result in neurodevelopmental toxicity, impacting neurogenesis and neuronal distribution in the developing brain **(Kagawa & Nagao, 2018)**. In adult rats, administration of acetamiprid leads to oxidative stress, altering brain physiology and behavior **(Gasmi et al., 2016)**. It can also induce neuronal apoptosis and structural changes in the hippocampus **(Abdallah et al., 2021)**. Besides, **Dhouib et al. (2017)**, Gasmi et al. **(2019)**, and Shamsi et al. **(2021)**, stated that acetamiprid exposure has been shown to increase adrenaline levels, decrease the activity of acetylcholine esterase, butyrylcholine esterase, dopamine, and serotonin in the cerebellum of male rats. It has also been found to induce oxidative stress in the brain **(Gasmi et al., 2017)**.

However, certain natural compounds have exhibited protective effects against acetamiprid-induced neurotoxicity. Supplementation with quercetin has been shown to improve biochemical parameters and reduce oxidative stress in rats treated with this compound **(Gasmi et al., 2016)**. Likewise, Moringa oleifera extract has displayed neuroprotective and anti-apoptotic properties, reducing oxidative stress markers and downregulating apoptosis-related genes **(Albrakati, 2024)**. Administration of curcumin has also demonstrated neuroprotective effects, significantly reducing nitric oxide levels and mitigating acetamiprid-induced structural changes in the hippocampus **(Abd El-Kader et al., 2022)**.

1.10.2 Hepatotoxicity and nephrotoxicity

Extensive studies have been conducted on the potential liver and kidney toxicity of acetamiprid. In rats, repeated exposure to acetamiprid resulted in liver and kidney damage, with more severe effects observed at higher doses **(Didenko et al., 2022)**. Sub-chronic exposure also caused oxidative damage and affected liver function markers (such as ASAT and ALAT levels) **(Figure 1.7)**, with histopathological examinations

revealing greater toxicity to the liver than the kidney **(Karaca et al., 2019a)**. In mice, sublethal doses of acetamiprid induced oxidative stress along with histological alterations in liver and kidney tissues **(El-Gendy et al., 2022)**.

Furthermore, comparative studies suggest that acetamiprid may be less hepatotoxic and nephrotoxic than other neonicotinoids like thiamethoxam, though both compounds induced alterations in liver and kidney function tests and caused histological changes in these organs **(Hataba et al., 2014)**. Overall, these studies indicate that acetamiprid can cause liver and kidney damage, particularly at higher doses or with prolonged exposure.

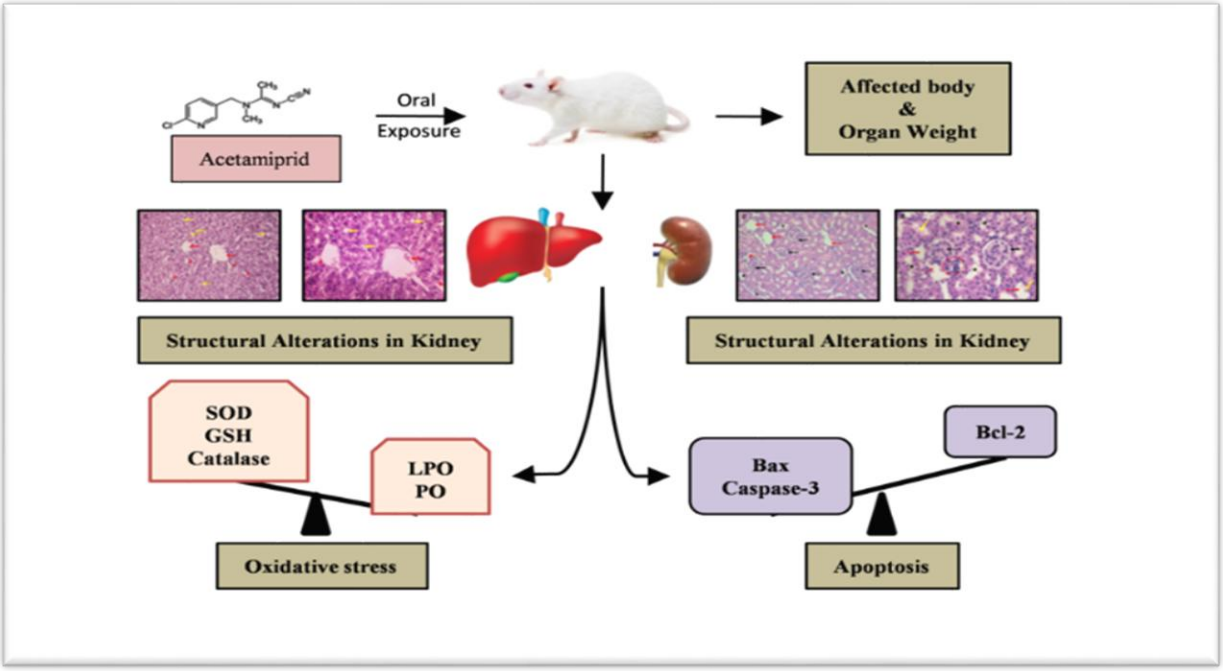

Figure 1.7 Effect of acetamiprid on liver and kidneys **(Phogat et al., 2023)**

1.10.3 Reproductive toxicity and immunotoxicity

Besides other pesticides, acetamiprid tend to impair the reproductive system of rodents. Exposure to this insecticide led to a decrease in sperm count, motility, and viability of male Wistar rats **(Arıcan et al., 2020; Hataba et al., 2014; Terayama et al., 2018; Zhang et al., 2011)**. Moreover, it leads to a reduction in testosterone levels and the weight of reproductive organs, while simultaneously increasing the number of abnormal sperm cells. These toxic effects seem to be linked to oxidative stress,

hormonal imbalances, and apoptosis in the testicular tissue **(Karaca et al., 2019; Toghan et al., 2022)**.

In humans, the study of **Mahai et al. (2022)** and **Pan et al. (2022)** have shown that acetamiprid beside other insecticides and its metabolites can negatively affect birth outcomes, including gestational age, ponderal index, and head circumference. Additionally, two cross-sectional studies have provided evidence that acetamiprid and thiamethoxam, are positively associated with reduced levels of dehydroepiandrosterone, testosterone, and dehydrocorticosterone in 143 male farmworkers, as reported by **Suwannarin et al. (2021)**.

The sub-chronic toxicity of acetamiprid in Swiss albino mice has been linked to immunotoxic effects. According to **Marzouki et al. (2017)**, these effects include a decrease in spleen weight and an increase in IgG antibody levels. Additionally, **Shakthi Devan et al. (2015)** observed a reduction in ß-cell proliferation, further indicating immunotoxicity caused by this compound exposure in these mice.

1.10.4 Oxidative stress induction

Acetamiprid has been found to induce oxidative stress in a range of organisms. Research on earthworms **(Li et al., 2018)**, silkworms **(Lu et al., 2021)**, Wistar rats **(Chakroun et al., 2016)**, and human umbilical cord blood erythrocytes **(Quintana et al., 2018)** has shown that exposure to acetamiprid results in increased production of reactive oxygen species (ROS) and alterations in antioxidant enzyme activities.

In both earthworms and silkworms, acetamiprid exposure led to changes in the activities of superoxide dismutase (SOD), catalase (CAT), and glutathione S-transferase (GST) **(Li et al., 2018**; **Lu et al., 2021)**. Male Wistar rats exposed to acetamiprid exhibited increased levels of malondialdehyde and catalase activity, while glutathione levels decreased **(Chakroun et al., 2016)**.

In human umbilical cord blood erythrocytes, this exposure resulted in elevated ROS levels and decreased activities of CAT and SOD **(Quintana et al., 2018)**. These findings collectively indicate that oxidative stress induced by acetamiprid can lead to various harmful effects, including DNA damage, reproductive toxicity, and developmental issues in non-target organisms.

1.10.5 Pancreatic toxicity

Regarding pancreas toxicity, few of the findings have investigated this toxic effect of acetamiprid insecticide.

Research has shown its cytotoxic and genotoxic potential on pancreatic cells, with a dose-dependent decrease in cell viability and an increase in DNA damage **(Kara et al., 2015)**. In rats, exposure to acetamiprid resulted in significant increases in plasma glucose, glycosylated hemoglobin, serum amylase, and lipase, while decreasing plasma insulin levels **(El-Nagdy et al., 2024)**. These changes were accompanied by histological alterations in pancreatic tissue and reduced ß-cell insulin reactivity.

Furthermore, acetamiprid exposure induced oxidative stress, affecting antioxidant enzymes and increasing inflammatory markers **(Toghan et al., 2022)**. These findings suggest that acetamiprid can have detrimental effects on pancreatic function and may contribute to the development of pancreatic disorders.

CHAPTER 2

PANCREAS: ANATOMY, PHYSIOLOGY, AND PATHOPHYSIOLOGY

CHAPTER 2

PANCREAS: ANATOMY, PHYSIOLOGY, AND PATHOPHYSIOLOGY

2.1 Pancreatic anatomy

The pancreas represents an amphicrine gland consisting of two distinct types of tissue: endocrine and exocrine. These tissues are organized into lobes that are macroscopically visible and are separated by connective tissue septa containing blood vessels, lymphatics, and nerves. In humans, most of the pancreatic volume, approximately 80-85%, is made up of exocrine tissue, while 10-15% comprises the extracellular matrix and vessels. However, the endocrine portion constitutes around 2% of the pancreatic volume **(Sastre et al., 2005)**.

In an adult human, the pancreas typically has an average volume of 72 cm^3, with the parenchyma comprising 44 cm^3 and fat making up 28 cm^3. Macroscopically, the pancreas can be divided into four parts: the head, neck, body, and tail. Positioned as a secondarily retroperitoneal organ, it rests against the posterior wall of the abdominal cavity. The head of the pancreas is adjacent to the duodenum, the neck is in proximity to the superior mesenteric vessels, the body lies posterior to the stomach's rear wall, and the tail extends towards the hilum of the spleen (**Figure 2.1**). Unlike most glands in the human body, the pancreas lacks a distinct fibrous capsule **(Henry et al., 2019)**.

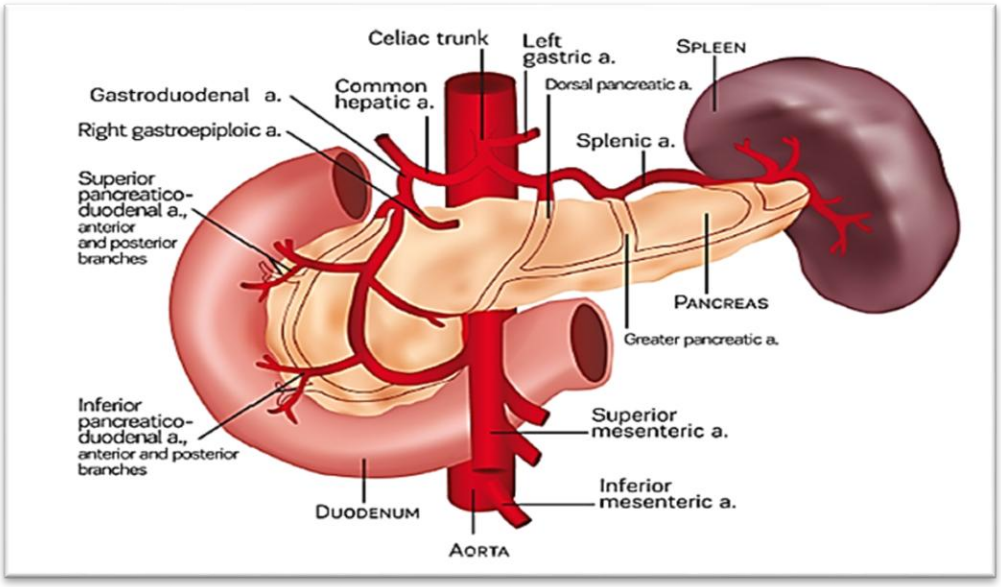

Figure 2.1 Pancreatic anatomy **(Henry et al., 2019)**

2.2 Innervation

The pancreas is conveyed to the central nervous system through both vagal and spinal pathways. The cell bodies of spinal afferent pancreatic neurons reside in the dorsal root ganglia of the T6-L2 spinal segments. These neurons' axons travel through the splanchnic nerves and celiac plexus before reaching the pancreas **(Travagli, 2016)**. Innervation is regulated by the autonomic nervous system, which consists of its parasympathetic and sympathetic divisions **(Bachem et al., 1998)**.

2.2.1 Sympathetic innervation

It arises from sympathetic preganglionic neurons located in the lower thoracic and upper lumbar segments of the spinal cord. Axons stemming from these neurons exit the spinal cord through the ventral roots. They then distribute either to the paravertebral ganglia of the sympathetic chain via communicating rami of the thoracic and lumbar nerves, or to the celiac and mesenteric ganglia via the splanchnic nerves (**Figure 2.2.a**) **(Travagli, 2016)**. This innervation primarily operates indirectly, exerting its effects by reducing blood flow and suppressing transmission in pancreatic ganglia, ultimately leading to inhibition of secretion **(Love et al., 2007)**.

2.2.2 Parasympathetic innervation

It serves as the primary excitatory input to the pancreas. Preganglionic parasympathetic neurons responsible for pancreas innervation originate in the dorsal motor nucleus of the vagus. These neurons stimulate parasympathetic post-ganglionic neurons in the pancreatic ganglia, predominantly through activation of nicotinic acetylcholine receptors (**Figure 2.2.b**). The vagus nerve acts as the principal cholinergic component influencing exocrine pancreas secretion, with its prominent neurotransmitters being acetylcholine and vasoactive intestinal peptide **(Love et al., 2007)**.

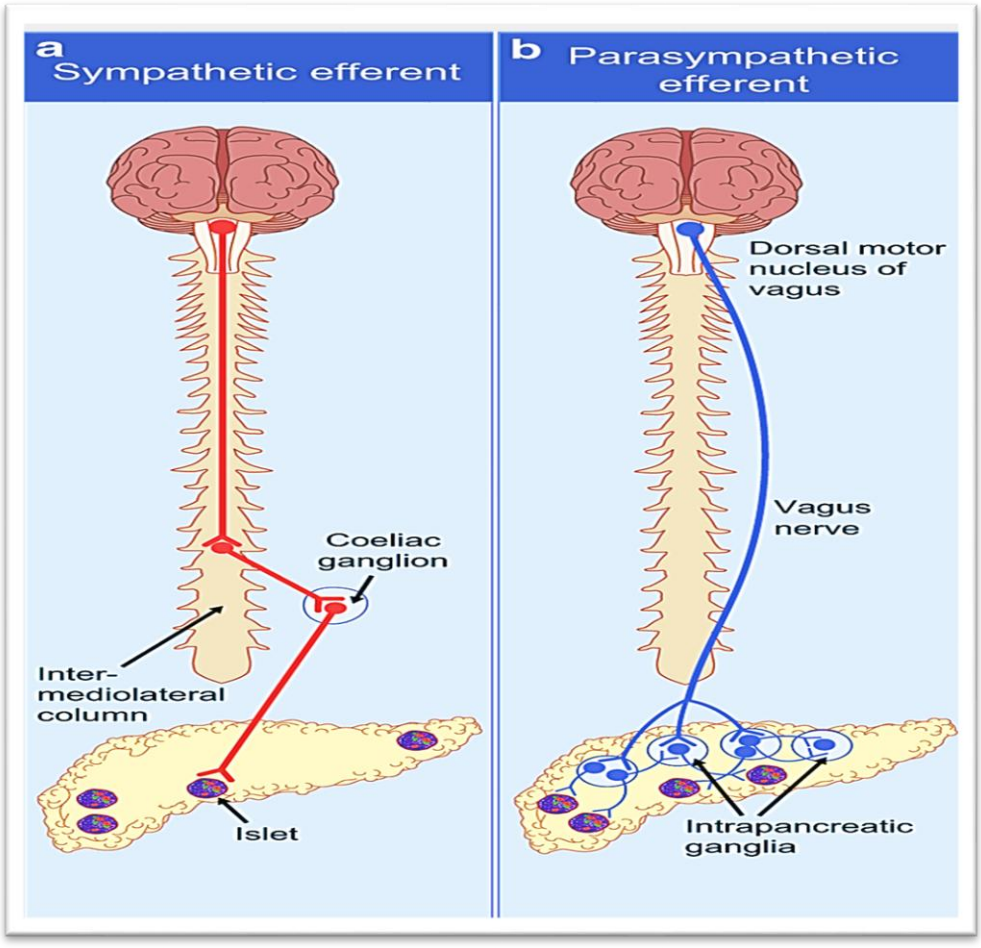

Figure 2.2 Pancreatic innervation **(Hampton et al., 2022)**

2.3 Histology

The pancreas can be functionally segregated into two intermixed tissues: an exocrine tissue primarily comprising acini, which are clusters of acinar cells that lead

into ductules, and an endocrine tissue consisting of the islets. It is enveloped by a capsule of non-pattern connective tissue, which extends partitions into the interior, dividing it into lobes and lobules. This connective tissue serves supportive functions and facilitates the innervation and irrigation of the gland **(Omary et al., 2007)**.

2.3.1 Acinar cells

Pancreatic acinar cells are responsible for synthesizing and secreting nearly all the digestive enzymes required for nutrient digestion in the lumen of the small intestine **(Williams, 2010)**. Each fundamental functional unit comprises acinar secretory cells, centroacinar cells, and ductal cells, organized in rounded or tubular clusters (**Figure 2.3**). It typically exhibits polygonal or pyramidal morphology, with their apex facing the central lumen of the acinus. The nucleus is situated basally, while the cytoplasm is characterized by abundant rough endoplasmic reticulum, imparting an intense basophilia. Additionally, acinar cells feature a prominent Golgi apparatus, surrounded by numerous acidophilic granules or zymogen granules. These granules are membrane-bound and house the enzymes constituting pancreatic secretion **(Sastre et al., 2005)**.

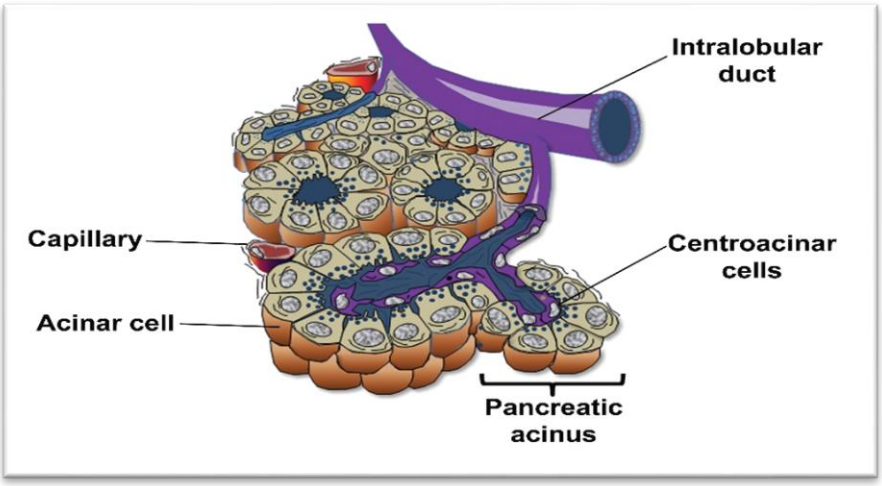

Figure 2.3 Schematic illustration of pancreatic acinar cell, centroacinar cells, and the pancreatic duct **(Foster, 2014)**

2.3.2 Islets of Langerhans

The islets of Langerhans are scattered throughout the acinar lobules of the pancreas, with larger islets often found along the main and interlobular ducts. In adults of most mammalian species, the islets constitute approximately 1-2% of the pancreas.

The majority of cells within the islets are ß-cells, which make up about 75-80% of the islet cell population, followed by α-cells at approximately 15%, δ-cells at about 5%, and a small number of pancreatic polypeptide (PP)-cells (**Figure 2.4**) **(Longnecker, 2014)**.

When examining the ultrastructure of these cells, the α-cells, ß-cells, and δ-cells can be differentiated primarily based on the characteristics of their granules. Typically, α-cell granules are slightly larger than those found in ß-cells, while δ-cell granules tend to be less densely stained in comparison to the granules in α- and ß-cells **(Shahid & Singh, 2024)**.

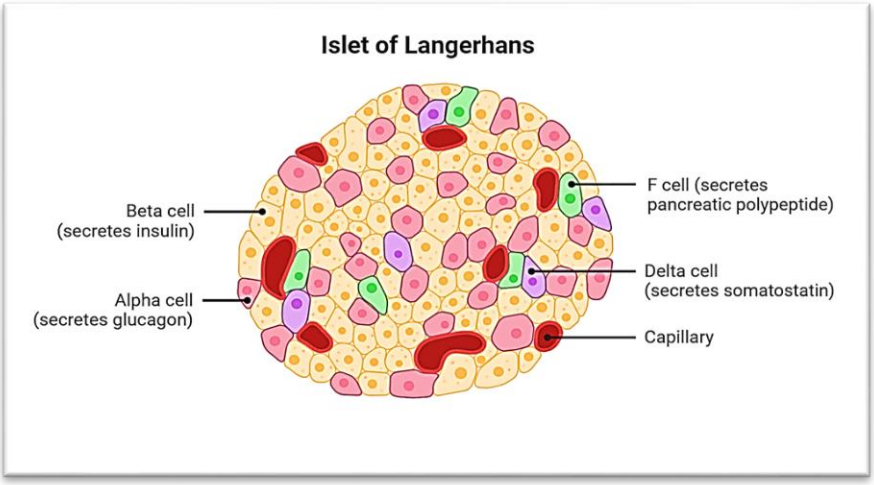

Figure 2.4 Schematic illustration of islets of Langerhans **(Tamang, 2024)**

2.4 Physiology

The pancreas can be functionally divided into an exocrine gland, which produces enzymes that aid digestion in the gastrointestinal tract, and an endocrine gland composed of the islets, which, among other functions, secretes hormones that regulate carbohydrate metabolism **(El Sayed & Mukherjee, 2024)**.

2.4.1 Endocrine pancreas

Pancreatic hormones are secreted directly into the bloodstream in an endocrine manner. These hormones are produced by the islets of Langerhans. These small, island-like structures are located within the exocrine pancreatic tissue and make up only 1-2% of the pancreas' total volume **(Röder et al., 2016)**. The five main cell types within the islets, each releasing different hormones:

- α-cells, which produce glucagon and make up 15-20% of the islet cells,
- ß-cells, which produce amylin, C-peptide, and insulin and account for 65-80% of the cells,
- γ-cells, which produce pancreatic polypeptide and constitute 3-5% of the cells,
- δ-cells, which produce somatostatin and make up 3-10% of the cells,
- ε-cells, which produce ghrelin and represent less than 1% of the cells **(Golson & Kaestner, 2017)**.

Each hormone has a specific role. Glucagon raises blood glucose levels, while insulin lowers it. Somatostatin inhibits the release of both glucagon and insulin, and pancreatic polypeptide regulates the secretion activities of both the exocrine and endocrine pancreas. These hormones work together to maintain glucose homeostasis in vertebrates. Once secreted, they travel through the bloodstream to reach their target organs and tissues **(Henry et al., 2019)**.

2.4.2 Exocrine pancreas

The exocrine pancreas consists of two primary cell types: acinar cells and duct cells. Acinar cells release a small amount of isotonic, plasma-like fluid containing NaCl and digestive enzymes. Duct cells, on the other hand, alter the ionic composition of the fluid and secrete the majority of the fluid and HCO_3 in the pancreatic juice. The main triggers for acinar cell secretion are acetylcholine, which is released by vagal postganglionic neurons, and CCK, which is released by intestinal endocrine cells **(Williams, 2010)**.

2.4.2.1 Hydro-electrolytic secretion

Centroacinar and duct cells are responsible for electrolyte secretion in the exocrine pancreas. This secretion primarily consists of water (98%) and is highly enriched in sodium and bicarbonate. The cation concentrations, including sodium (154 ± 7 mEq/l), potassium (4.8 ± 0.9 mEq/l), calcium (1.7 ± 0.3 mEq/l), and magnesium (0.27 ± 0.08 mEq/l), remain relatively constant and similar to those found in plasma. The main anions are chlorine and bicarbonate. Bicarbonate equilibrium concentration in plasma is approximately 25 mM, and its secretion increases in response to food intake **(Jun et al., 2017)**.

The secretion of water and electrolytes in the exocrine pancreas is primarily stimulated by secretin, which consequently regulates the volume of pancreatic juice. Secretin triggers an increase in bicarbonate secretion by ductal cells and activates adenylate cyclase in centroacinar cells, leading to an increase in cyclic adenosine monophosphate levels **(Sastre et al., 2005)**.

2.4.2.2 Enzymatic secretion

Acinar cells are responsible for the synthesis and secretion of digestive enzymes, which can be classified into four groups based on their function: proteolytic, lipolytic, glycolytic, and nucleolytic (**Table 2.1**). The synthesis of these enzymes occurs in the rough endoplasmic reticulum, where they are then transported to the Golgi apparatus. During their passage through the Golgi apparatus, the enzymes undergo various post-translational modifications, particularly glycosylation. After these modifications, the enzymes are concentrated and stored in zymogen granules. The secretion of these enzymes occurs through exocytosis **(Karpińska & Czauderna, 2022)**.

Table 2.1 Pancreatic enzymes (**Sastre et al., 2005**)

Enzyme	Activator	Function-action
Trypsin	Enteroquinase	breaks peptide bonds
Chymotrypsin	Trypsin	breaks peptide bonds
Elastase	Trypsin	breaks peptide bonds
Carboxypeptidase A	Trypsin	Slices residues of Phe, Tyr and Trp from the carboxy terminal end of a polypeptide
Carboxypeptidase B	Trypsin	Slices Arg and Lys residues from the carboxy terminal end of a polypeptide
Phospholipase A2	Trypsin	Split fatty acid of phospholipids
Amylase	-	Digest the starch into small polymers of Glu, maltose and Glu
Lipase	-	Split fatty acid of glycerol
Carboxylesterase	-	Hydrolyzes cholesterol esters
Ribonuclease	-	Slices RNA to form short chains
Deoxyribonuclease	-	Slices DNA to form short chains

Arg: Arginine; Phe: Phenylalanine; Glu: Glucose; Lys: Lysine; Trp: Tryptophan; Tyr: Tyrosine.

2.5 Exocrine pancreatic diseases

The exocrine pancreas is susceptible to two major diseases: pancreatitis and pancreatic cancer. In both conditions, acinar cells are believed to play a crucial role in their pathogenesis.

In pancreatitis, the activation of digestive enzymes within acinar cells leads to cell damage and inflammation. This intracellular activation of enzymes can cause autodigestion of the pancreas, resulting in acute or chronic pancreatitis **(Mayerle et al., 2019)**.

In pancreatic cancer, acinar cell plasticity is thought to contribute to the formation of ductal tumors. This process involves the transformation of acinar cells into duct-like cells, which can then give rise to pancreatic ductal adenocarcinoma, the most common type of pancreatic cancer. Overall, understanding the role of acinar cells in these diseases is crucial for developing effective treatments and improving patient outcomes **(Karpińska & Czauderna, 2022)**.

2.5.1 Acute pancreatitis

Acute pancreatitis is a prevalent condition characterized by sudden inflammation of the pancreas. The severity of acute pancreatitis can range from mild cases that can be managed conservatively to severe and complex cases with high morbidity and mortality. Mortality rates for acute pancreatitis range from 3% in patients with mild edematous pancreatitis to as high as 20% in those with pancreatic necrosis **(Gapp et al., 2024)**.

Microscopically, it is marked by the death of acinar cells and the presence of inflammatory cells infiltrating the pancreatic tissue **(Bhatia et al., 2005)**. While macroscopically, it is characterized by pancreatic enzyme activation (i.e., trypsinogen and protease) and disruption of both intracellular and extracellular separation, which includes impaired exocytosis, retention of zymogens, and the formation of endocytic vacuoles that facilitate the conversion of trypsinogen to active trypsin. Active trypsin predominantly triggers apoptosis, dampening inflammatory responses, whereas unregulated calcium release can induce necrosis and elicit inflammatory reactions.

Additionally, endocytic vacuoles harboring trypsin and cathepsin B merge with lysosomes, releasing these enzymes into the cytosol and resulting in either apoptosis or necrosis of pancreatic acinar cells. Necrosis leads to the release of cellular components into the extracellular space, activating leukocytes via the inflammasome signaling pathway. Furthermore, TNFα can promote necroptosis in acinar cells (**Figure 2.5**) **(Mayerle et al., 2019)**.

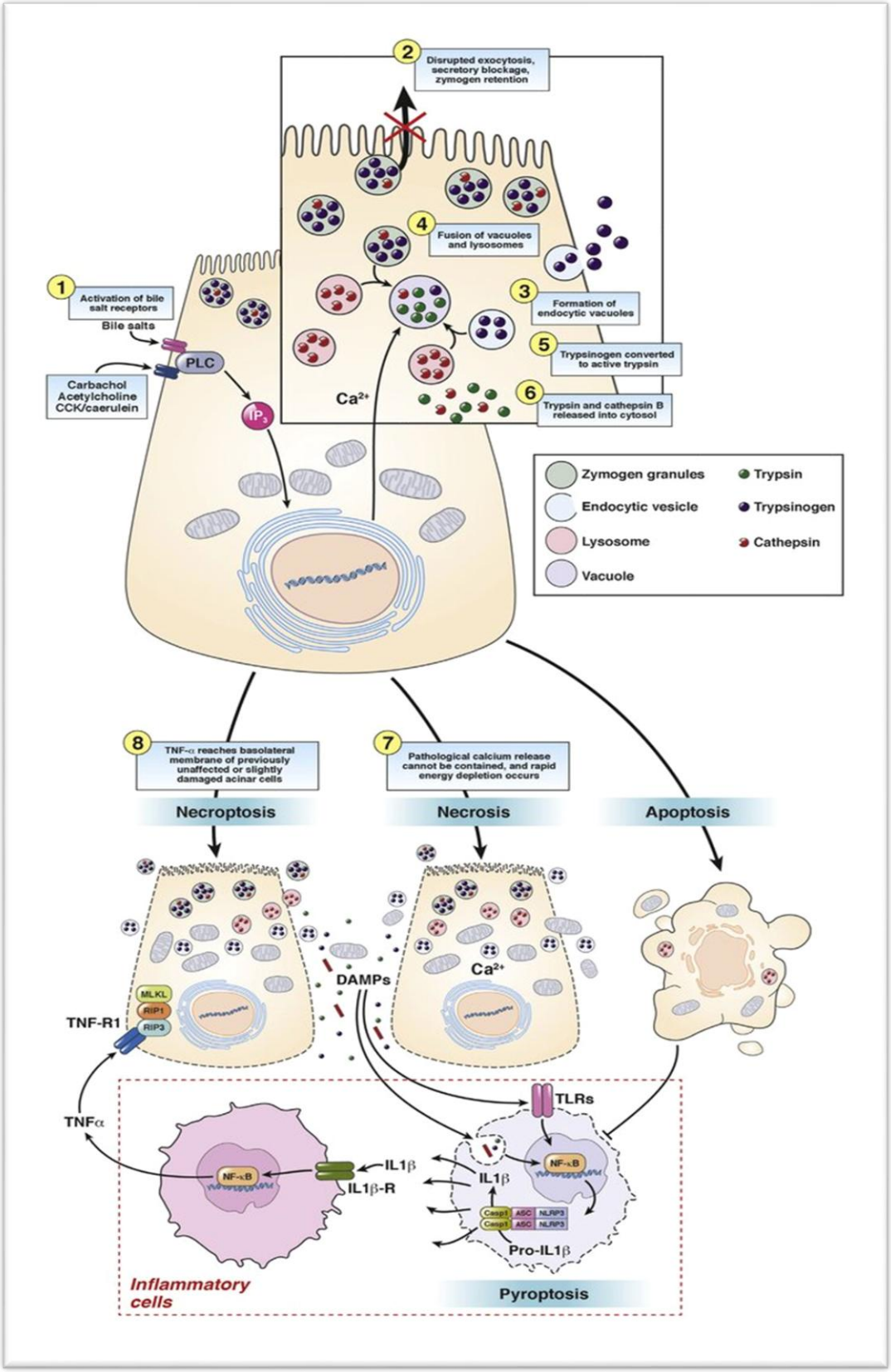

Figure 2.5 Molecular mechanisms of acute pancreatitis **(Mayerle et al., 2019)**

2.5.2 Chronic pancreatitis

Chronic pancreatitis represents a fibroinflammatory syndrome of the exocrine pancreas that is characterized by recurrent episodes of pancreatic inflammation with varying intensity and duration, ultimately leading to irreversible damage to pancreatic tissue. Definitive signs of chronic pancreatitis include parenchymal or intraductal calcifications, pancreatic fibrosis, impairment of both exocrine and endocrine pancreatic functions resulting in malabsorption and diabetes, persistent pain, and an elevated risk of pancreatic cancer **(Beyer et al., 2020)**.

Indeed, five mechanisms are hypothesized to contribute to the development of chronic pancreatitis (**Figure 2.6**):

1) Necrosis-fibrosis sequence: Chronic pancreatitis may arise from repeated episodes of acute pancreatitis, leading to fibrosis.
2) Sentinel acute pancreatitis event: A single acute pancreatitis event triggers inflammation and fibrosis, with ongoing damage driving further fibrosis.
3) Direct metabolic-toxic effect: Environmental factors like alcohol and tobacco may directly harm acinar cells, but this effect is not fully understood.
4) Oxidative stress: Free radicals in acinar cells cause inflammation and fibrosis through various pathways.
5) Ductal dysfunction: Abnormalities in pancreatic duct function, such as CFTR mutations, may lead to protein plug formation and ductal obstruction, contributing to chronic pancreatitis.

These mechanisms are not mutually exclusive and may interact in complex ways to cause chronic pancreatitis **(Kleeff et al., 2017)**.

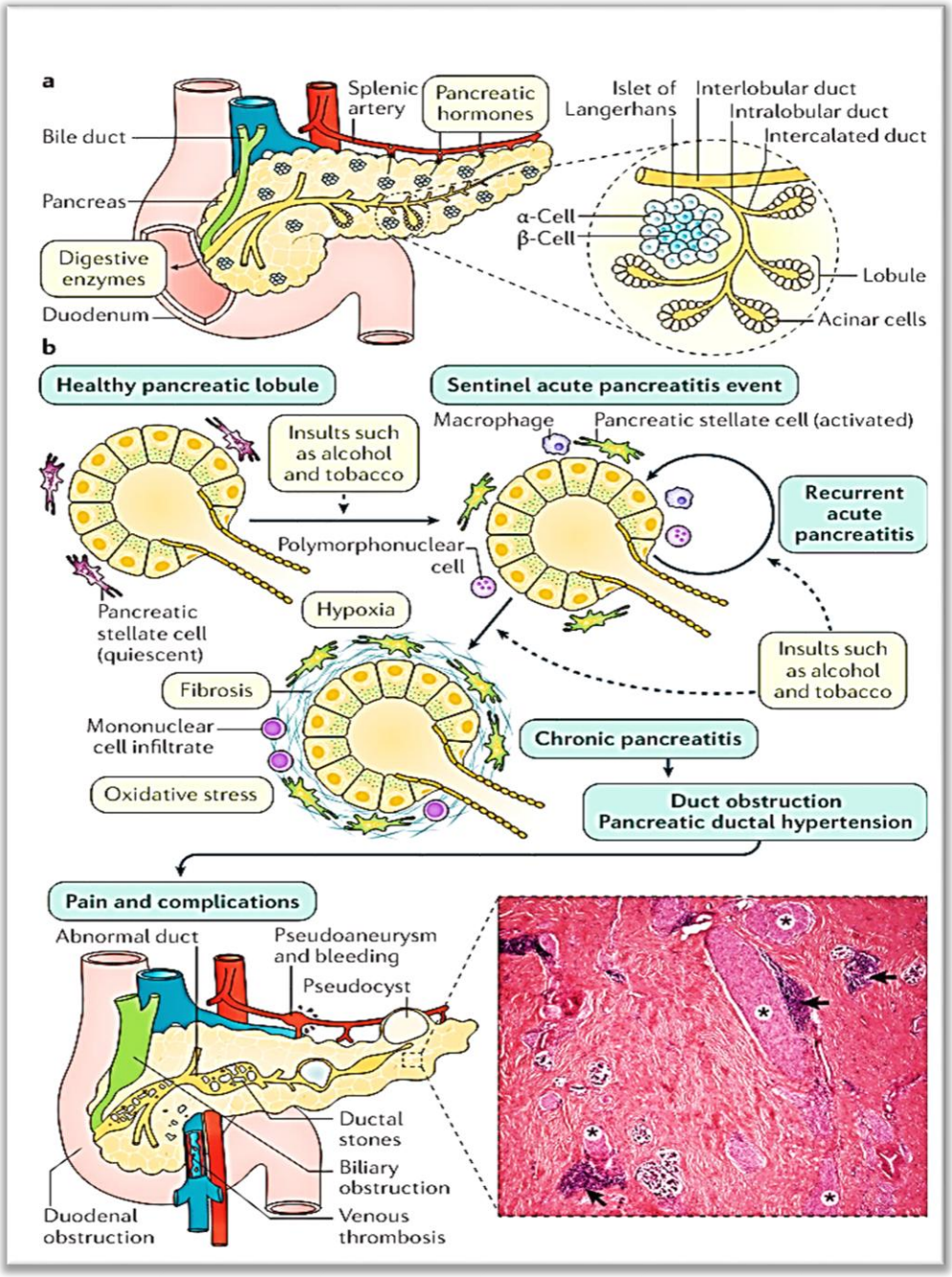

Figure 2.6 Main mechanisms of chronic pancreatitis a) Pancreas anatomy. b) Chronic pancreatitis pathophysiology, tobacco or alcohol trigger the initial episode of acute pancreatitis, characterized by inflammation and immune cell recruitment, continued exposure to these factors leads to recurrent acute pancreatitis attacks, activating pancreatic stellate cells and initiating fibrosis. A specimen from a patient with chronic pancreatitis appears hypertrophic and dystrophic nerves (asterisks) enclosed by massive fibrotic tissue and infiltration of lymphocytes (arrows) **(Kleeff et al., 2017)**.

2.5.3 Pancreatic cancer

Pancreatic cancer is a significant global health issue, responsible for approximately 227,000 deaths annually **(Vincent et al., 2011)**. In recent years, the incidence of this disease has risen. Despite comprising only 2% of all cancers, pancreatic cancer is responsible for 5% of cancer-related deaths. The most prevalent form of pancreatic cancer is pancreatic ductal adenocarcinoma (PDAC), which affects the majority of patients diagnosed with this disease **(Zhao & Liu, 2020)**.

PDACs progress through noninvasive precursor lesions, primarily pancreatic intraepithelial neoplasia, accumulating genetic and epigenetic changes along the way. They can also develop from intraductal papillary mucinous neoplasms or mucinous cystic neoplasms. Interactions between cancer-related fibroblasts (the main stromal cell type) and neoplastic cells may contribute to tumor initiation, progression, and metastasis **(Vincent et al., 2011)**.

The immune system's role in pancreatic cancer progression has been studied, with a focus on inhibiting T regulatory lymphocytes (cells that suppress anti-tumor immune responses) or using vaccines, such as irradiated genetically modified pancreatic cancer cells or immunostimulatory pancreatic cancer antigens (e.g., overexpressed or mutated proteins) **(Figure 2.7)**. Researchers have also investigated how cancer cells and cancer-associated fibroblasts evade immune responses **(Ansari et al., 2016)**. The existence and role of tumor-initiating cells (cancer stem cells) in pancreatic cancer development is debated. While potential cells have been identified, reconciling the concept of tumor-initiating cells with the clonal selection provided by tumorigenic mutations is challenging. One hypothesis is that cancer stem-cell markers identify cells most likely to survive specific cellular stresses, such as growth in nude mice or resistance to chemotherapeutic agents **(Vincent et al., 2011)**.

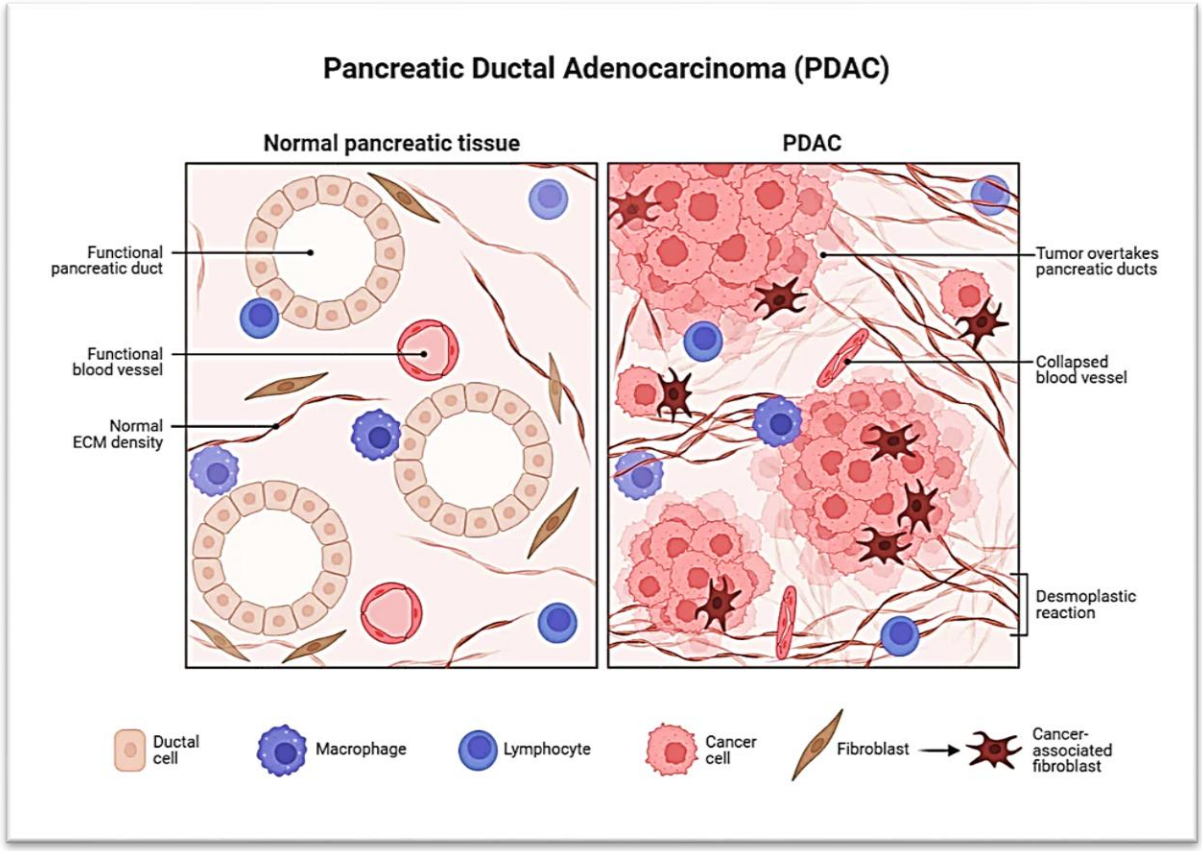

Figure 2.7 Schematic illustration of pancreatic tissue in normal and PDAC conditions **(Tamang, 2024)**

CHAPTER 3

CARNOSINE: A PHYSIOLOGICAL AND THERAPEUTIC OVERVIEW

CHAPTER 3

CARNOSINE: A PHYSIOLOGICAL AND THERAPEUTIC OVERVIEW

3.1 Carnosine discovery

Carnosine ($C_9H_{14}N_4O_3$) represents a biological active dipeptide discovered for the first time by the Russian biochemist Gulevich V.S. in the early XX century. It was isolated from the muscular tissue of beef and was given its name "carnosine" refer to caro, carni in *Latin* that means meat **(Gulewitsch & Amiradžibi, 1900)**. It is composed of ß-alanine and L-histidine and has naturally occurring derivatives. The most common variant of this substance are the methylated analogues (i.e., anserine and ophidine), whereas the acetylated analogues represent an important variant also such as acetylcarnosine and carcinine (**Figure 3.1**) **(Boldyrev et al., 2013).**

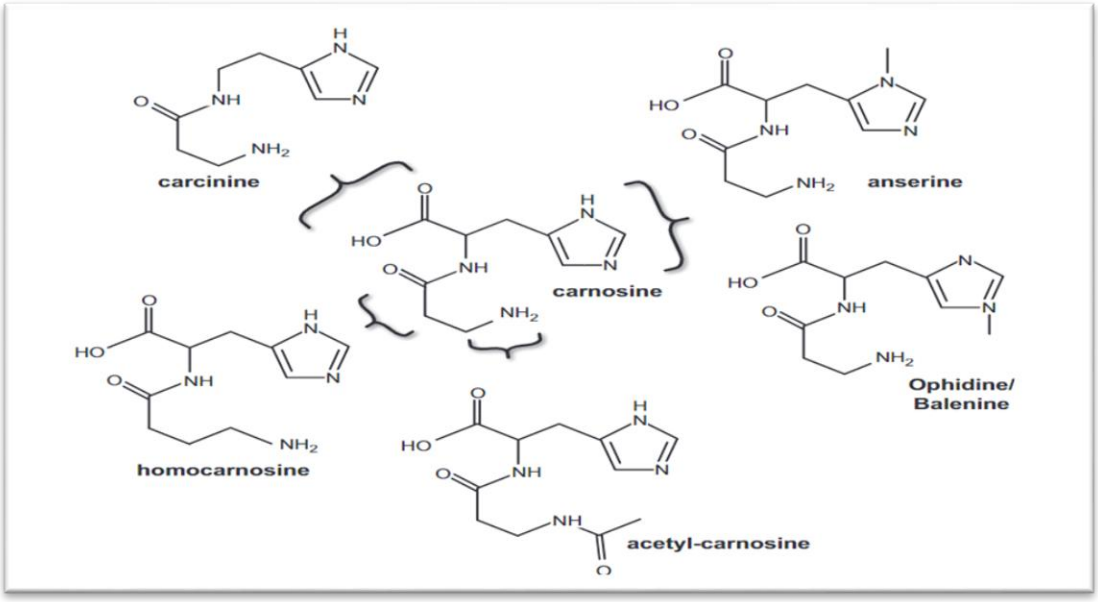

Figure 3.1 The chemical structure of carnosine and its derivatives **(Boldyrev et al., 2013)**

Carnosine is highly present in muscular tissues. However, it can be found as well in brain, kidneys, skin, and liver of vertebrates **(Boldyrev & Severin, 1990)**.

Instead, another methylated variant of carnosine was found in snake and whale muscle named, respectively, ophidine and balenine, all these dipeptides are called the histidine containing dipeptides (HCDs) **(Menon et al., 2020)** that characterizes by the imidazole ring which is the responsible of the physiological activities (**Table 3.1**) **(Boldyrev et al., 2013)**.

Table 3.1 HCDs in different tissues and organisms

Compound	Localization
ß-alanyl-L-histidine (carnosine)	Skeletal muscles of vertebrates
ß-alanyl-1-*N*-methylhistidine (anserine)	Skeletal muscles of vertebrates
ß-alanyl-3-*N*-methylhistidine (ophidine)	Snake and whale musculature
ϒ-aminobutyrylhistidine (homocarnosine)	Human and animal brain
ϒ-aminobutyryl- 1 -*N*-methylhistidine (homoanserine)	Bovine brain
N-acetylhistidine	Central nervous system and ocular tissues of frogs and fishes
ß-alanylhistamine (carcinine)	Central nervous system and musculature of crab
N-acetylanserine	Myocardium

3.2 Tissue distribution of carnosine

In mammals, one of the methylated carnosine analogs (eighter anserine or ophidine) are present with carnosine, except in human beings, where only the nonmethylated carnosine itself is present **(Hall, 2001)**.

In tissues, only skeletal muscle and the olfactory bulbs have higher carnosine concentrations that are in the millimolar range. Since only the former makes up a significant percentage of the body's overall mass, it may be estimated that skeletal muscle tissue contains more than 99% of an organism's carnosine. Additionally, it's measurable in other tissues such as the brain and body fluids with lower concentration compared to muscles **(Boldyrev et al., 2013)**.

3.3 Physiological and biochemical properties of carnosine

3.3.1 Buffering activity

Carnosine is soluble in water (1g in 3.1 ml of water at 25°C), characterized by 3 ionizable groups: the carboxylic group (Pk_a 2.76), the amino group of the ß-alanine residue (pK_a 9.32), and the nitrogen of the imidazole ring (pK_a 6.72). According to the pK_a values, carnosine is mostly found in the zwitterionic form at the physiological pH, with both the carboxyl and amino group of ß-alanine in their ionized forms **(Wu, 2020)**. The control of buffering activity of carnosine is regulated by the imidazole ring. This function is suggested by the pK_a values of carnosine that is very close to 7 which their proton sequestering capacity is high **(Turner et al., 2021)**.

3.3.2 Carnosine and metal ion

Carnosine has a capacity to bind with metals from the first transition metals series, including Cu^{2+}, Zn^{2+}, and Co^{2+}, to form a complex with different biological roles.

On one hand, the complex copper-carnosine can be formed in both monomeric and dimeric forms, with the dimeric form being favored at neutral pH **(Baran, 2000)**. The ligand of this complex can bind through carboxylate, amid, and amino donor atoms. While imidazole rings bind the copper (II) ions through the N3 nitrogen atoms **(Torreggiani et al., 2000)**.

On the other hand, the zinc-carnosine complex represents an interesting biological complex. It was proved that Zn (II)-carnosine complex protects gastric mucosa from ulcers **(Mustafa et al., 2009)** and gastritis affected by Helicobacter pylori infection **(You & Jiao, 2006)**.

3.3.3 Quencher of reactive carbonyl species

reactive carbonyl species represent a group of oxylipins that have both α and ß unsaturated carbonyl structure, including acrolein and 4-hydroxy-E-2-nonenal (HNE) **(Biswas & Mano, 2021)**. Carnosine has the ability to quenching this species through an autocatalytic process which engages both imidazole ring and ß-alanine group (**Figure 3.2**) **(Aldini et al., 2005)**.

Additionally, this capacity was detected as endogenous agent in skeletal muscle and the nervous system of rat **(Aldini et al., 2011)**, by reducing acrolein-protein adduct formation which lead to suppress the activity of inflammation **(Spaas et al., 2021)**.

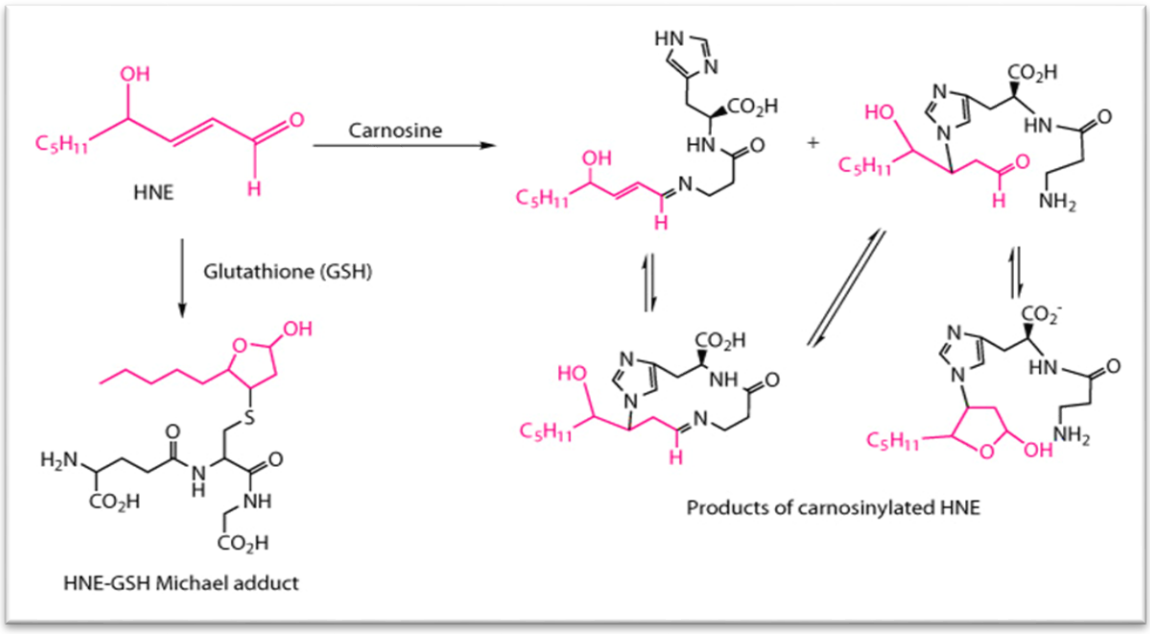

Figure 3.2 Quenching of HNE by carnosine and GSH **(Reddy et al., 2005)**

Moreover, the ability of carnosine to counteract carbonyl compounds can be primarily attributed to the peptide's metal-chelating properties, with a minor direct capacity for carbonyl sequestration **(Price et al., 2001)**, as a similar effect to the inhibitors of lipid peroxidation end products such as aminoguanidine and pyridoxamine **(Zhao et al., 2019, Orioli et al., 2007)**.

3.3.4 Antioxidant properties

The major studied property of carnosine is its antioxidant activity, in both physiological and pathophysiological conditions.

In physiological conditions, carnosine tend to be oxidated to 2-oxocarnosine **(Ihara et al., 2019)** (**Figure 3.3**). This metabolite was a result of histidyl imidazole radical formation with addition to a molecule of oxygen, becoming a greater antioxidant molecule in excess of glutathione and ascorbate **(Aldini et al., 2021)**. Indeed, the study of Klebanov et al. **(1997)** demonstrated that carnosine interacts with superoxide union

such as superoxide dismutase (SOD) as a quencher molecule of this free radicals. In addition, carnosine could react on reactive oxygen species (ROS) such as hydroxyl radicals, by formation of a transient intermediate through water elimination reaction catalyzed commonly by a base **(Boldyrev et al., 2013)**.

Another carnosine ability is to become a protective agent against nitration by peroxynitrite. The study of **Fontana et al. (2002)** showed that carnosine and its derivative (i.e., anserine) protects the amino acid tyrosine against nitration, inactivation of α1-antiproteinase, and significantly decreases the oxidation of low-density lipoprotein by $ONOO^-$.

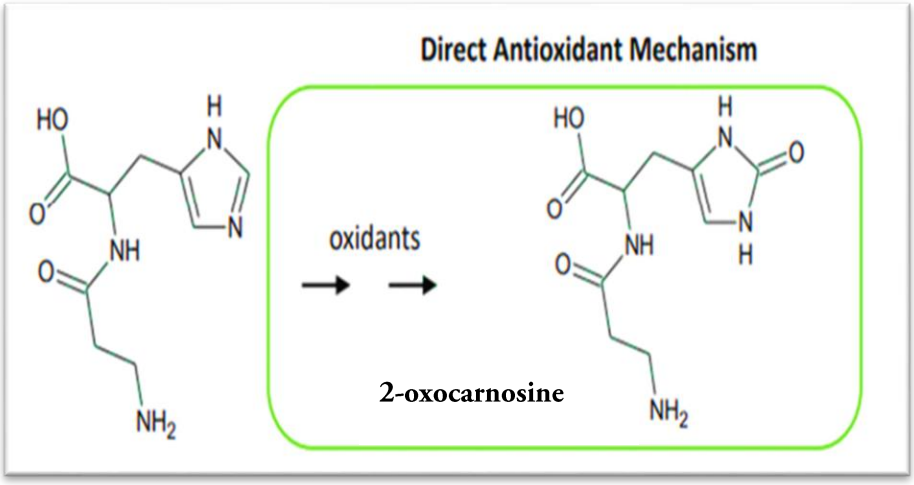

Figure 3.3 Oxidation of carnosine **(Aldini et al., 2021)**

Furthermore, detoxification of hypochlorite is also an ability of carnosine, as was investigated by several studies**. Formaziuk et al. (1992)** firstly discovered that carnosine reacts promptly with hypochlorite to make poorly and less reactive species with a long live for these molecules. Importantly, the direct antioxidant influence, particularly concerning H_2O_2, has been substantiated in ex vivo samples by detecting the resulting oxidation product **(Kulikova et al., 2020)**.

Moreover, recent studies have reported that carnosine can indirectly mitigate oxidative stress by amplifying the expression and activation of the nuclear factor erythroid 2-related factor 2 (Nrf2) pathway. This pathway controls the transcription of over two hundred genes containing an antioxidant response element (ARE) in their promoter region **(Aldini et al., 2021)**. Among these genes are those encoding antioxidant proteins and enzymes related to phases I, II, and III, as well as enzymes involved in lipid, carbohydrate, and amino acid metabolism, proteasome components,

and regulators of inflammation. Collectively, these genes form a comprehensive stress-response network aimed at preserving microenvironmental homeostasis (**Figure 3.4**) **(Mou et al., 2020)**.

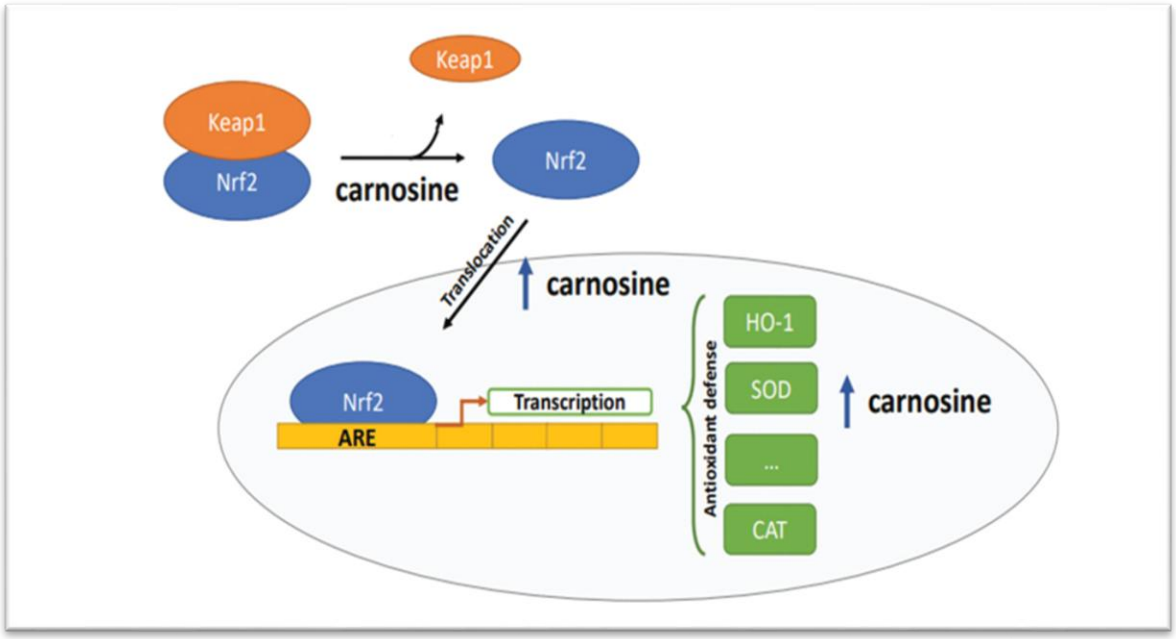

Figure 3.4 Activation of Nrf2-Keap1 pathways by carnosine **(Matsumaru & Motohashi, 2021)**

Hence, when carnosine was administered after a liver injury caused by CCl_4, it restored Nrf2 expression compared to the group treated only with CCl_4. This carnosine-induced Nrf2 nuclear translocation was found to account for its notable antioxidant effects and its ability to alleviate inflammation, as indicated by a reduction in hepatic tumor necrosis factor (TNF) levels and the restoration of interleukin-10 (IL-10) levels **(Nagai et al., 1990)**. Similar effect was observed in rats, were carnosine improved learning and memory functions by modulation of signaling pathway of nuclear factor-κB and Nrf2 **(Ahshin-Majd et al., 2016)**.

3.3.5 Anti-aging activity

The anti-aging property of carnosine was first reported in 1994 by the study of McFarland & Holliday **(1994)**. It was approved that carnosine can improve cell division of human fibroblasts and rejuvenate senescent cells.

In the brain, it was demonstrated that carnosine at concentration of 10 mM protected SH-SY5Y cells from aging caused by D-galactose, through the up-regulation

of neuronal markers and antioxidant enzymes (i.e., GSH and SOD) and decrease in IL-10 and TNF α **(Kim & Kim, 2020)**. Similar effect was observed in brain tissue of rats treated with d-galactose for 8 weeks, in addition with an increase in malondialdehyde (MDA) and caspase-3 expression **(Aydın et al., 2016)**. Furthermore, carnosine protected spermatogonia and Sertoli cells in mice accelerated aging stain **(Gopko et al., 2005)**, and decreased MDA level which lead to improve oxidative status in seminal plasma **(Rocha et al., 2018)**. While some studies attribute the anti-aging effect to its antioxidant properties, and other studies suggest that its gero-protective benefits are linked to its capacity to inhibit protein carbonylation and regulate the degradation of aged proteins **(Boldyrev et al., 2013).**

3.4 Metabolism of carnosine

The synthesis of carnosine is facilitated by carnosine synthetase 1 (CARNS1), an enzyme responsible for catalyzing the formation of the dipeptide (ß-alanyl-L-histidine) using ß-alanine and L-histidine amino acids through an ATP-dependent process **(Wang-Eckhardt et al., 2020; Drozak et al., 2010)**.

CARNS1, a member of the ATP-grasp superfamily of adenosine 5′-diphosphate (ADP)-producing ligases, also known as ATPGD1 (ATP-Grasp domain containing protein 1), is primarily found in the cytosol of skeletal and cardiac muscles as well as in the olfactory bulb of the brain **(She et al., 2022; Jukić et al., 2021).**

Various proteins from the proton-coupled oligopeptide transporter (POT) family, alternatively recognized as solute carrier family 15 (SLC15), facilitate the transport of carnosine across cellular membranes **(Sasawatari et al., 2011)**. In humans, multiple transmembrane proteins within the SLC15 family, namely SLC15A1 (PEPT1), SLC15A2 (PEPT2), SLC15A4 (PHT1), and SLC15A3 (PHT2), are capable of transporting di- and tripeptides, including carnosine. These proteins are responsible for either the uptake or release of carnosine **(Andou et al., 2009)**.

The expression levels of genes responsible for carnosine transporters in humans are generally minimal. On one hand, detectable expression of SLC15A2 and SLC15A4 is observed in microglia, while mature astrocytes exhibit expression only of SLC15A2 **(Caruso et al., 201)**. Neurons, on the other hand, demonstrate very low expression

levels of these transporters, although possibly adequate for carnosine imports **(Schön et al., 2019)**.

Carnosine absorption occurs in the small intestine, with a portion entering the bloodstream unchanged upon oral intake **(Asatoor et al., 1970)**. The transportation of carnosine across the brush-border membrane is facilitated by PEPT1 (**Figure 3.5**). Within enterocytes, carnosine is likely hydrolyzed, possibly by CNDP2 (or CN2), or transported across the basolateral membrane (**Gardner et al., 1991)**. In renal tubules, PEPT2 aids in the reabsorption of filtered peptides, primarily situated in the apical membrane of epithelial cells. Removal of PEPT2 significantly hinders carnosine reabsorption in the kidneys, affecting renal carnosine clearance close to the glomerular filtration rate **(Peters et al., 2015)**. Although PEPT2 is crucial in renal carnosine reabsorption, the overall movement of carnosine across epithelial cells is restricted, likely resulting in the breakdown of the dipeptide during renal passage **(Elbarbary et al., 2018)**.

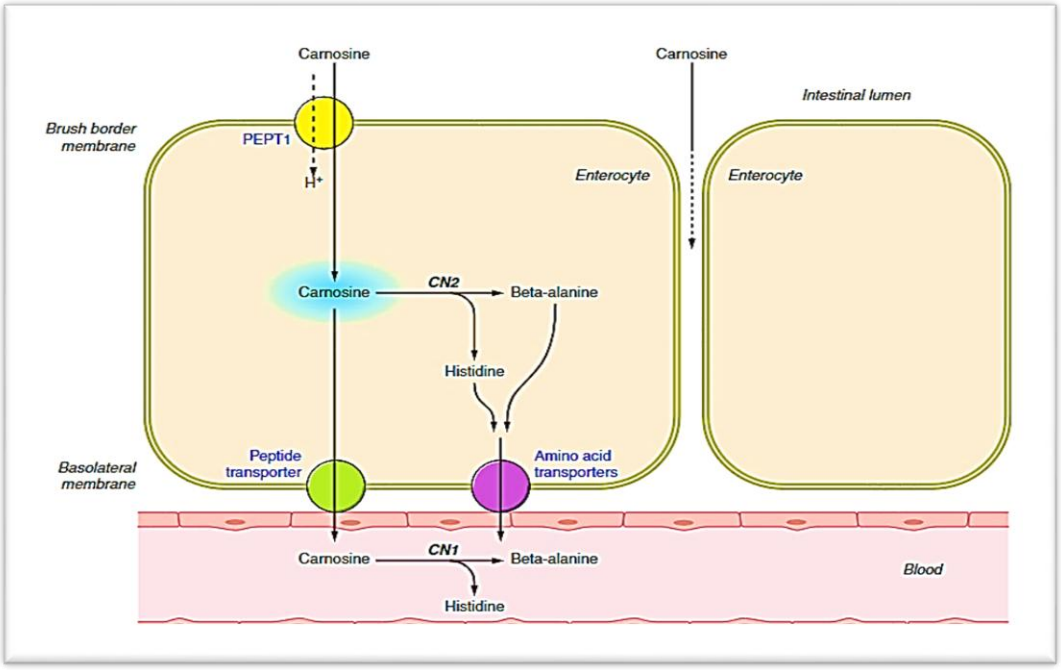

Figure 3.5 Intestinal absorption of carnosine in mammals **(Boldyrev et al., 2013)**

Regarding degradation, carnosine levels in tissues and biological fluids are regulated mainly through degradation mechanisms involving two distinct dipeptidases from the M20 metalloprotease family: carnosine dipeptidase 1 (CNDP1) in serum, and carnosine dipeptidase 2 (CNDP2) in the cytosol **(Bellia et al., 2014)**. CNDP1, prevalent in human serum, exhibits specific degradation activity toward carnosine and its analogs anserine

and homocarnosine **(Solana-Manrique et al., 2022)**. It is predominantly expressed in the liver and the brain, particularly in oligodendrocytes **(Toviwek et al., 2023)**. CNDP2, a Mn^{2+}-dependent cytosolic enzyme, possesses a broader substrate spectrum compared to CNDP1 and is ubiquitously expressed in human tissues, albeit at lower levels in the brain **(Solana-Manrique et al., 2022)**.

Additionally, carnosine can be converted into its analogue, anserine, by carnosine N-methyltransferase enzyme (CARNMT). Similarly, it methylates other HCDs (i.e., homocarnosine) and demonstrates weak expression in brain cells (**Figure 3.6**) **(Drozak et al., 2015)**.

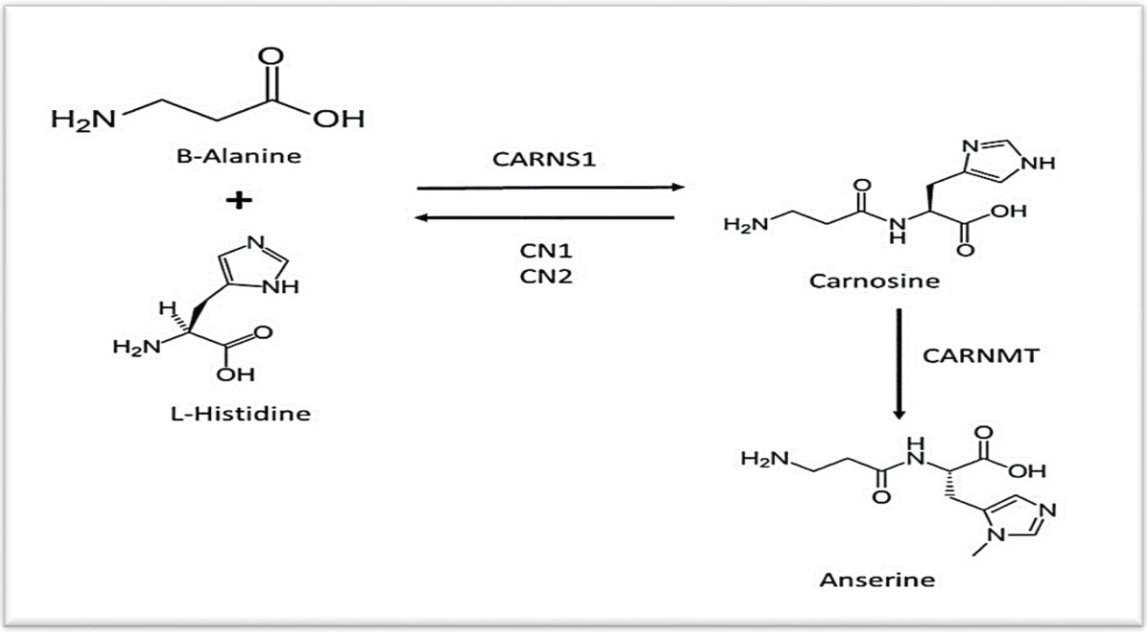

Figure 3.6 Reaction mechanisms of carnosine's metabolism **(Solana-Manrique et al., 2022)**

3.5 Carnosine's role in various health conditions

3.5.1 Brain and neurodegenerative diseases

It was demonstrated that the concentration of carnosine is significantly higher in the olfactory system than other brain regions. Based on this significant presence, there's a hypothesis suggesting carnosine's involvement in sensory neurotransmission, either as a neurotransmitter or a neuromodulator **(Colín-Barenque et al., 2018)**.

In most sensory pathways, glutamate serves as the primary excitatory neurotransmitter within the synapse between olfactory neurons and target cells (i.e., periglomerular and mitral cells) in the olfactory bulb. Intriguingly, studies utilizing immunohistochemistry have revealed the coexistence of carnosine and glutamate within the terminal of synapses olfactory neurons in mice and the bipolar cells within the retina of frogs **(Nicoll et al., 1980; Sakai et al., 1988)**. This observation supports the proposal for a potential role of this dipeptide in modulating glutamatergic sensory neurons.

Carnosine, specific brain areas, is thought to offer protective effects via its antioxidant, anti-glycation activities, and metal chelating, potentially compensating for low levels of other endogenous antioxidants in the nervous system (**Figure 3.7**). While its therapeutic potential is recognized, its precise physiological role in normal function remains to be fully understood. Additionally, carnosine's ability to chelate transition metals like copper and zinc might indirectly impact neurotransmission, contributing to its role in neural function **(Boldyrev et al., 2013, Solana-Manrique et al., 2022)**.

A growing body of evidence is concentrated on carnosine homeostasis and its relationship with neurodegenerative diseases such as Alzheimer's disease. This neurological disorder recognized by a memory loss and cognitive decline due to brain cell degeneration **(Niu et al., 2017)**. Carnosine has demonstrated the inhibition of Aß aggregation within the central nervous system of transgenic mouse models of Alzheimer's patients **(Kitazawa et al., 2012)**. Additionally, it diminishes the in vitro formation of Aß1-42 fibrils **(Wu et al., 2013; Shen et al., 2022) (Greco et al., 2020)**. The suggestion is that carnosine may disrupt both the elongation process of fibrils and the formation of globular oligomeric species during the assembly phase **(Aloisi et al., 2013)**. Furthermore, in the study of **Fonteh *et* al. (2007)** comparing patients of Alzheimer's disease to non-diseased subjects, lower carnosine and higher anserine levels were observed in the plasma of these patients. However, the total amount of carnosine and anserine together was reduced in these patients.

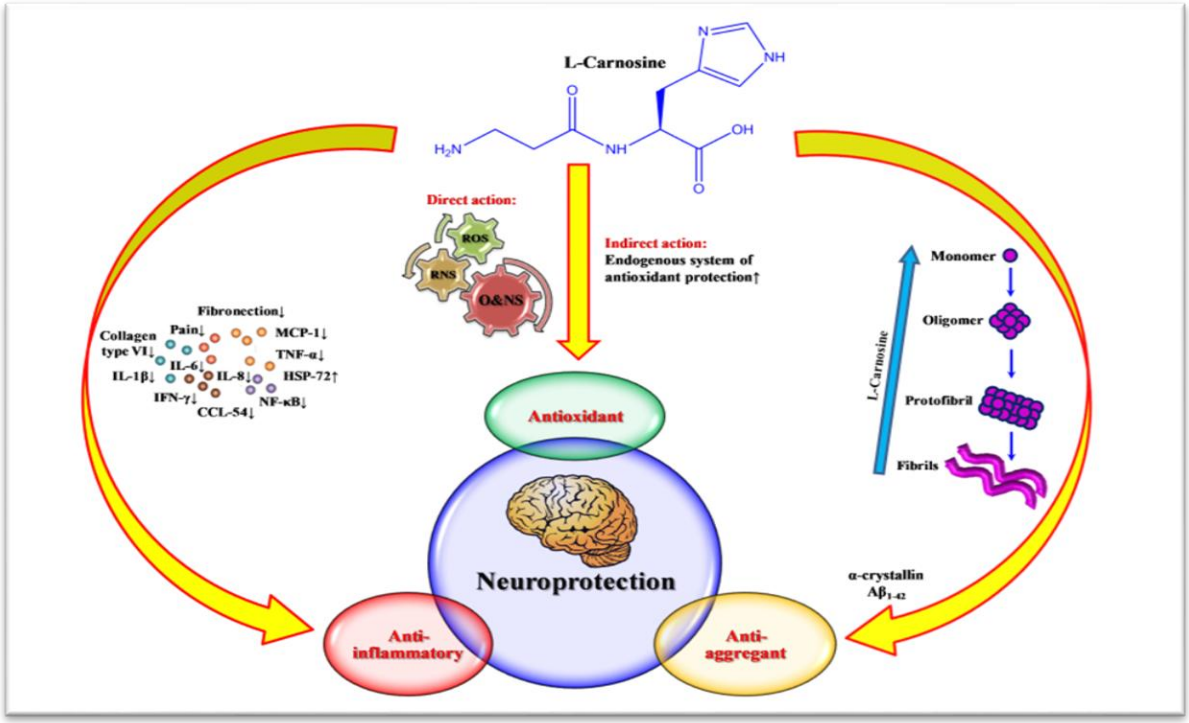

Figure 3.7 Probable mechanisms of action of carnosine as a neuroprotector **(Caruso et al., 2019)**

Another neurodegenerative disorder that is Parkinson's disease were related to carnosine metabolism. It was shown that carnosine was accumulated in serum of Parkinson's disease patients, as a result of a reduction of CNDP1 activity **(Wassif et al., 1994)**. Hence, carnosine was demonstrated as an inhibitor of α-synuclein in oligomerization process in model systems, and to mitigate certain modifications observed in animal models mimicking Parkinson's disease **(Boldyrev et al., 2013)**.

3.5.2 Muscular disorders

The reduction in carnosine levels within skeletal muscles, observed with age or in muscular diseases, may lead to functional decline and structural alterations due to diminished antioxidant protection. This decline could potentially interact with specific atrophic and pathological mechanisms. Analysis of free carnosine concentrations in skeletal muscles, both from patients with muscular diseases and rats of varying ages, revealed a significant negative correlation with age. The study indicated that age is a noteworthy negative predictor of carnosine concentrations in skeletal muscles, with a 63% decrease observed between the ages of 10 and 70 in human subjects **(Stuerenburg, 2000)**.

Hence, during exercise and the contraction of skeletal muscles, carnosine is released into both the interstitium and the blood circulation. This release helps in decreasing acidosis that caused muscular fatigue (**Figure 3.8**) **(Holeček, 2020)**. Indeed, an increase in muscle carnosine levels via ß-alanine supplementation enhances exercise capacity and performance lasting from 30 seconds to 10 minutes. This is likely achieved by serving as a pH buffer to mitigate fatigue induced by the accumulation of H+ ions **(Matthews et al., 2019)**. In contrast, the quantity of carnosine was observed to decrease by 53.2% in type II fibers of patients with osteoarthritis, emphasizing the importance of its homeostasis in muscle to prevent such disorders **(Tallon et al., 2007)**.

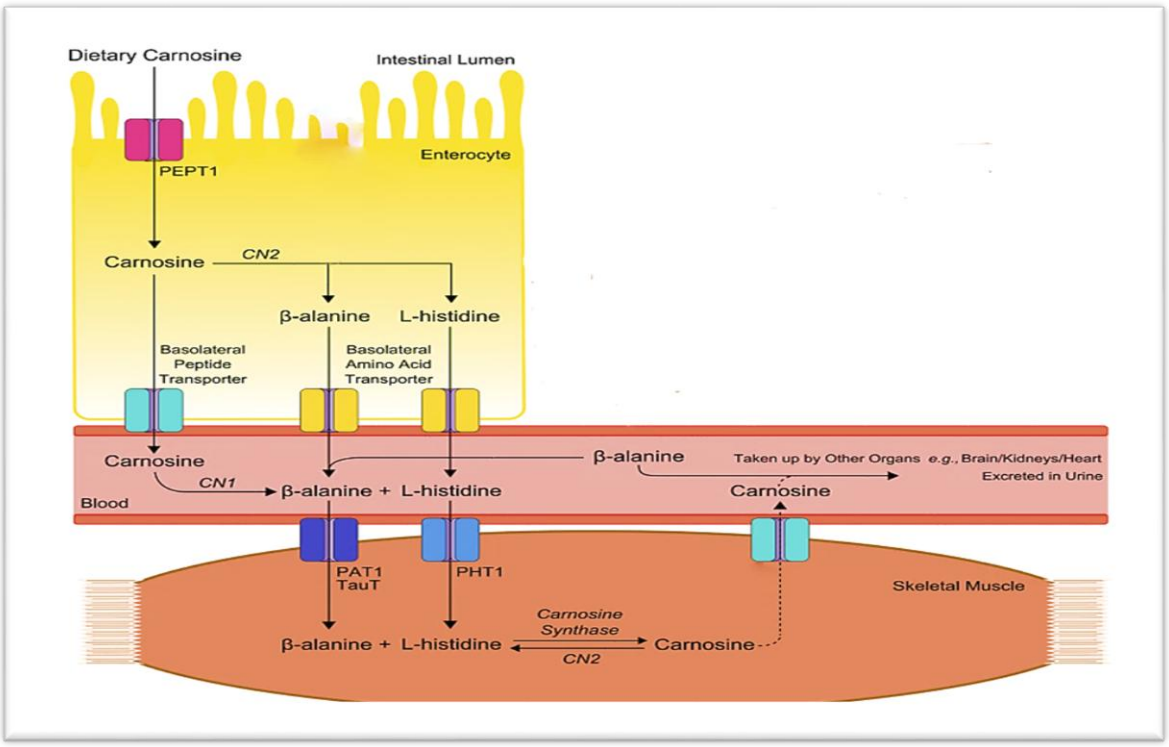

Figure 3.8 Carnosine absorption and release in muscles (Adapted from **(Stuerenburg, 2000)**

3.5.3 Endocrine disorders

A growing body of evidence studied the relationship between carnosine and endocrine disorders such as diabetes and thyroid diseases due to its diverse function in the organism.

In diabetic disorder, carnosine plays a protective role. This action is related to its capacity to maintain glycemic control and mitigate or ameliorate diabetic complications (e.g., nephropathy) **(Boldyrev et al., 2013)**. Numerous studies have

assessed this protective effect, **Lee et al. (2005)** and **Albrecht et al. (2017)** indicated that treatment with carnosine (at 200 mg/kg) in diabetic mice was the result of decreasing hyperglycemia and maintaining blood glucose levels all with reducing dyslipidemia.

Indeed, De Courten et al. **(2016)** assessed the effect of carnosine supplementation during 12 weeks to decrease the resistance of insulin in overweight persons. Furthermore, the administration of carnosine was observed to prevent diabetes-induced nephropathy, specifically by inhibiting glomerular apoptosis, preventing the loss of podocytes, and reducing the expression of Bcl-2-associated X protein and cytochrome c, which are widely recognized as pro-apoptotic proteins **(Riedl et al., 2011)**. Additionally, carnosine was found to improve diabetic neuropathies, particularly in terms of abnormal sensory perception **(Kamei et al., 2008)**.

Hence, carnosinase deficiency was found to be significantly correlated with serum thyroxine level in hypothyroidism patients, suggesting that carnosine homeostasis could play a crucial role in thyroid dysfunction **(Bando et al., 1986)**. Moreover, carnosine daily supplementation was observed to elevated serum triiodothyronine and thyroxine levels **(Maurin & Garnuszek, 2010)**.

In sum, the endocrine system could be enhanced and protected by carnosine, particularly by increasing pancreatic secretion, maintaining glycemic blood level, and improving endocrine hormonal secretion.

3.5.4 Cardiovascular diseases

Carnosine improves cardiac contractility via calcium handling and raising pH buffering capacity **(Boldyrev et al., 1999)**. This evidence suggested that carnosine could play an effect in cardiovascular disease such as atherosclerosis.

Barski et al. (2013) conducted a study using an atherosclerosis model with ApoE−/− mice on a high-fat diet. They found that dietary carnosine supplementation prevented the formation of early atherosclerotic lesions. This effect was attributed to the positive modulation of oxidative stress-related processes. Similarly, **Menini et al. (2012)** found that carnosine supplementation affected a reduce in inflammation and carbonyl stress that caused atherosclerosis. Additionally, when administered intraperitoneally, carnosine exhibited cardioprotective effects in rats by mitigating cardiac ischemia and enhancing heart function. These protective actions were

associated with carnosine's capacity to reduce lipid peroxidation in cell membranes **(Caruso et al., 2019)**. Accordingly, carnosine is thought to enhance angiogenesis, boost exercise performance, improve vasodilatory response, and concurrently offering protection against ischemic tissue damage (**Figure 3.9**) **(Feehan et al., 2022)**.

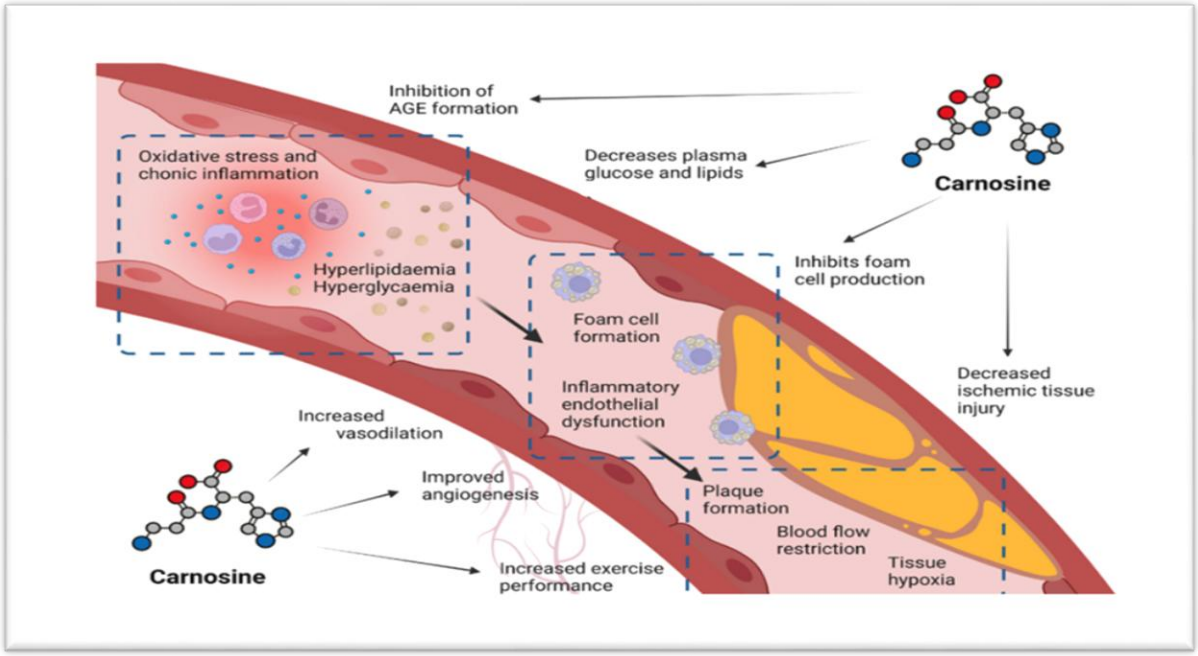

Figure 3.9 Role of carnosine in perivascular diseases **(Feehan et al., 2022)**

3.5.5 Cancer

In the latter part of the 20th century, the anti-neoplastic property of carnosine was discovered by Nagai and Suda **(1986)**. The study demonstrated that 50 mg/kg/day of carnosine induced a reduction in the growth of sarcoma-180 tumor cells. Lately, it was shown that 20 mM of carnosine inhibited neoplastic cells growth without altering the growth of human fibroblasts **(Holliday & McFarland, 1996)**. Indeed, it decreases the generation of ATP in cancer cells that primarily use glycolysis for energy without exerting inhibition on differentiated fibroblasts, which rely more on oxidative phosphorylation for ATP synthesis **(Boldyrev et al., 2013)**.

Furthermore, growing research indicating carnosine's anti-proliferative effects on glioblastoma models, a particularly aggressive form of brain cancer, has been first conducted and then expanded to other cancer cell lines. These include colorectal cancer cells, intestinal cancer cells, and ovarian cancer cells **(Artioli et al., 2019)**.

3.5.6 Bone damage

In physiological conditions, numerous studies suggested that carnosine can promote bone formation by stimulating the proliferation and activity of osteoblasts, suppressing bone resorption by osteoclasts, and influencing the differentiation of bone marrow mesenchymal stem cells (**Figure 3.10**) **(Yang et al., 2022)**. Yet, in pathological conditions, carnosine is observed to have a significant impact on various conditions related to bone damage.

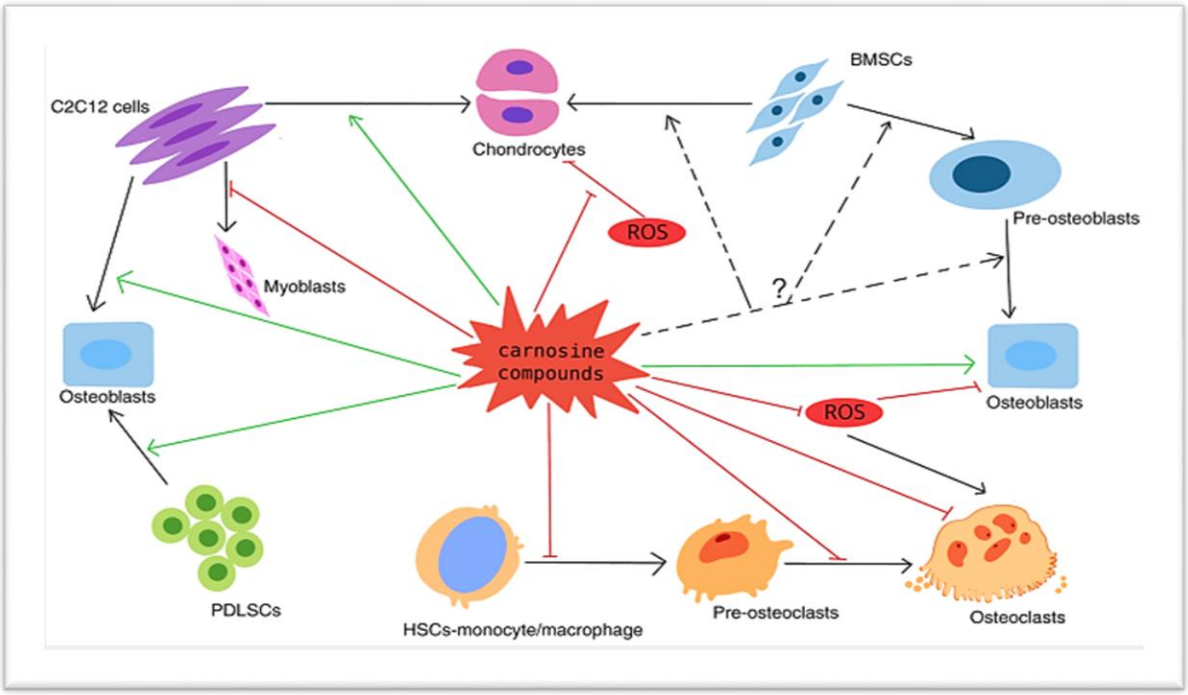

Figure 3.10 Effect of carnosine on bone metabolism **(Yang et al., 2022)**

Carnosine participates in the control of bone marrow mesenchymal stem cells (BMSCs), C2C12 myogenic stem cells, periodontal ligament stem cells (PDLSCs), and bone marrow macrophages (BMMs) differentiation, along with the regulation of chondrocyte, osteoblast, and osteoclast activity through the reduction of ROS **(Ko et al., 2022)**.

Hence, carnosine is suggested to potentially inhibit sympathetic nerve activity while enhancing parasympathetic nerve activity through the activity of natural killer cells in spleen or the regulation of the autonomic nervous system via the histidine H3 receptor, these mechanisms are involved in postmenopausal osteoporosis **(Ciaffaglione & Rizzarelli, 2023)**. Additionally, in hydrocortisone-induced osteopathy, carnosine regulated parathyroid hormone levels, alkaline phosphatase

activity, and enhanced both zinc and DNA contents **(Segawa et al., 1992)**. Alternatively, numerous research indicates that carnosine has the ability to boost the expression of protein components and the release of cytokines in the process of bone remodeling following a fracture, thereby supporting bone formation **(Ko et al. 2022 , Igarashi & Yamaguchi 2003)**. Thus, carnosine's potential bioactive impact in bone tissue may occur via the mitogen-activated protein kinases (MAPK) signaling pathway or protein kinase C mediated stimulation of albumin synthesis, thereby playing a role in maintaining bone mass and contributing to homeostasis during bone reconstruction **(Yang et al., 2022)**.

Furthermore, carnosine exhibits antitumor properties and inhibits glycolysis, which could impact the growth and spread of bone tumor cells (via MAPK, mTOR, and STAT3 signaling pathway), all with enhancing genomic stability and shields cells from DNA damage **(Hipkiss & Gaunitz, 2014)**.

3.5.7 Castro-intestinal disorders

Castro-intestinal disorders cover a variety of issues, from typical minor conditions like acute infections or irritations leading to sickness and diarrhea, ambiguous and undetermined symptoms, to significant diseases such as cancer and acute abdominal emergencies, and specific organic disorders like peptic ulcers, hernias, and piles **(Fry, 1985)**.

A number of studies have investigated the effects of carnosine in these disorders. In the study of Arakawa et al. **(1990)**, carnosine at 10 and 30 mg/kg protected gastric mucosa of rat from irritation caused by ethanol. A similar study has assessed the same effect in rat where inflammatory cytokines (e.g., IL-8, IL-6, and TNF-α) were decreased and expression of antioxidant enzymes and growth factors were upregulated **(Choi et al., 2013)**. In inflammatory bowel disease, which is ulcerative colitis, investigations are underway to anticipate disease relapse. Diminished histidine levels in the plasma, a component of carnosine, serve as an indicator for the likelihood of relapse in this disease **(Hisamatsu et al., 2015)**. In addition, carnosine induce inhibition of mRNA expression of IL-8 in human intestinal epithelial cells stimulated by hydrogen peroxide and TNF-α **(Jukić et al., 2021)**.

A growing body of evidence evaluated the effectiveness of zinc-L carnosine in improving intestinal damage. The study by **Mahmood et al. (2007)** involved an *In-*

vitro investigation utilizing both colonic human cells and intestinal epithelial rat cells treated with zinc-L carnosine. The findings indicated that this compound enhanced both migration and proliferation. Moreover, zinc-L carnosine suppressed the proliferation of human gastric carcinoma by arresting the cell cycle, triggering apoptosis, and downregulating the mTOR signaling pathway **(Zhang et al., 2014)**. Hence, it reduced the expression of inflammatory cytokines (such as TNF-α, IFN-γ, and interleukins) in murine colitis, growth factors (i.e., IGF-1), and upregulated the expression of heat shock proteins (HSP 72) (**Figure 3.11**) **(Efthymakis & Neri, 2022)**.

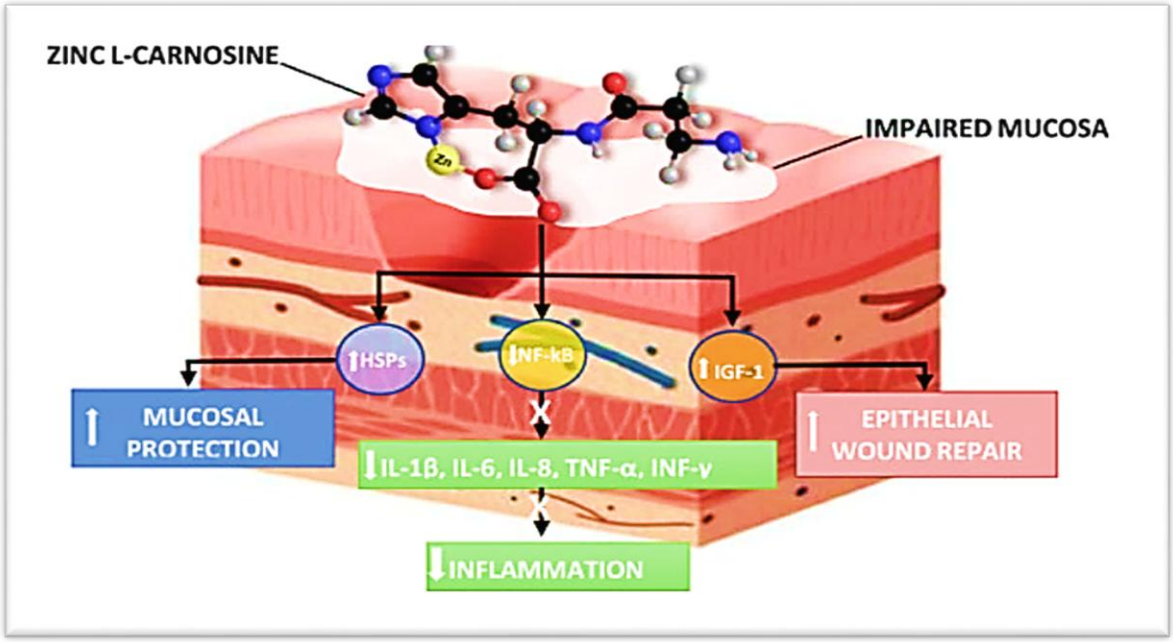

Figure 3.11 Mechanisms of zinc-L carnosine in gastric mucosa **(Efthymakis & Neri, 2022)**

3.5.8 Kidney diseases

Recent studies have been interested in the relationship between carnosine and kidney diseases such as acute kidney failure.

Acute kidney failure represents a sudden decline in kidney function, resulting in reduced filtration rate, imbalance of electrolyte, and reduce in pH regulation **(Kilis-Pstrusinska, 2020)**. Carnosine tends to have a reno-protective effect against acute kidney failure by suppressing adrenergic activity and activating histamine H3 receptors in the central nervous system **(Kurata et al., 2006)**.

Moreover, it decreased the oxidative stress and inhibited matrix metalloproteinase-2 which decreased urate nephrolithiasis development **(Zharikov et**

al., 2023). Additionally, carnosine was observed to decrease urea, creatinine, and serum lipid levels via its anti-glycation and antioxidant activities in diabetic nephropathy in male rats **(Fatih Aydın et al., 2017)**.

3.5.9 Carnosine and COVID

Since December 2019, the world has witnessed the rapid spread of the novel severe acute respiratory syndrome coronavirus 2. This virus has led to severe complications affecting multiple organs, including the lung, pancreas, and kidneys **(Gusev et al., 2022)**. A few studies have investigated the role of carnosine in COVID-19 patients.

In a study conducted by Lopachev et al. **(2020)**, Wistar rats afflicted with ulcers were utilized as a model of severe inflammation to investigate the effects of a combined molecule of salicylic acid and carnosine (salicyl-carnosine). The study also assessed the antioxidant properties on leukocyte cells and the antithrombotic effect using human thrombocyte cells. The findings led the researchers to conclude that salicyl-carnosine could play a crucial role in mitigating factors such as thrombosis, inflammation, and oxidative stress, which are prominent pathogenetic factors in severe cases of COVID-19.

Additionally, in an in-silico study, **Saadah et al. (2020)** explored the inhibitory effects of carnosine on both the angiotensin-converting enzyme 2 (ACE 2) and the spike protein of the coronavirus. Their findings suggest a promising potential for carnosine in mitigating the effects of the COVID-19 pandemic. Hence, the multi-properties of carnosine (e.g., antioxidant, anti-inflammation, and anti-hyperglycemia) has been suggested to enhance the severe complications in COVID-19 patients (**Figure 3.12**) **(Diniz et al., 2022)**.

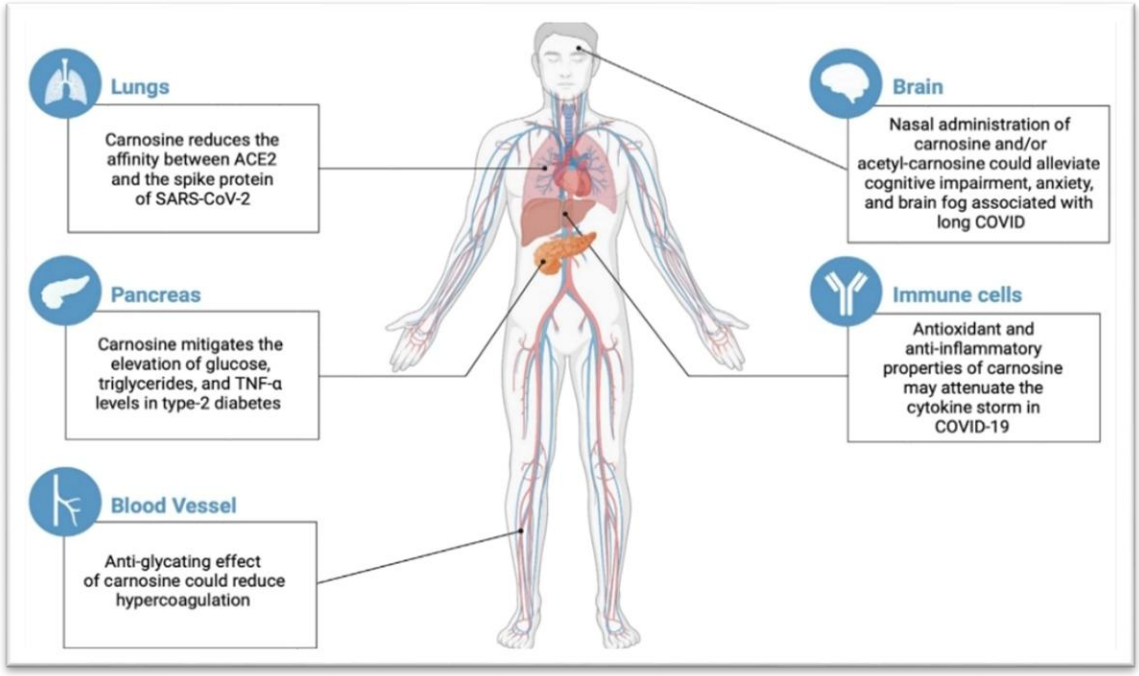

Figure 3.12 The possible impact of carnosine on various organs prone to COVID-19 infection **(Diniz et al., 2022)**

3.6 Supplementing with carnosine

3.6.1 Carnosine as nutritional supplements

When it comes to carnosine supplementation, there are two possibilities to increase carnosine concentration in the organism. The major source is derived from dietary intake. Various nutrients contain a considerable amount of carnosine, such as meat (chicken and beef), seafood like fish and shrimps, along with vegetables such as asparagus, white mushrooms, and green peas. While consuming 30 g of dehydrated beef daily has the potential to fully meet the daily carnosine needs of a 70 kg adult, contributing to the improvement of human nutrition and overall health **(Cesak et al., 2023)**.

The commercial form of carnosine could be an alternative source. This form could be as a naturally occurring form (that is L-carnosine), conjugated, or in a complex formulation. The most common formulation is L-carnosine, plays various roles in enhancing the health, from the antioxidant scavenger in different tissues and anti-aging effects to improving several organ's function (such as the cardiovascular, cognitive, and ocular functions) **(Hoffman et al., 2018)**.

The conjugated forms of carnosine could be a good choice as a supplement. N-acetyl-carnosine supplementation has been potentially investigated in improving ocular diseases such as cataracts and retinal disorders **(Babizhayev, 2009)**. Furthermore, salicyl-carnosine which is a combined form of carnosine and salicylic acid represent a new formulation that was studied for its anti-ulcer and anti-inflammation properties **(Kulikova et al., 2020)**. The combination form between zinc and carnosine is widely used as a gastrointestinal tract protector, which play a role in improving gastric and intestinal damage, preventing mucositis, and enhancing loss of taste **(Cesak et al., 2023)**.

In the meanwhile, carnosine could be combined to form complexes with vitamin E, α-lipoic acid, and resveratrol where it is used as a neuroprotective agent and cardiovascular protective agent **(Aryal et al., 2021; Kulikova et al., 2018)**.

3.6.2 Potential side effects of carnosine supplement

The adverse side effects of carnosine supplementation remain infrequent due to its rapid metabolization by CNDP1 and CNDP2. However, it could be referred to the effects of alanine and histidine overdose (mainly the components) where no adverse effect were highlighted except some transient paresthesia **(HOLEČEK, 2022)**.

CHAPTER 4

MATERIALS & METHODS

CHAPTER 4

MATERIALS & METHODS

4.1 Study aims

The primary aims of the present investigation were to enhance comprehension of the impact of an insecticide acetamiprid (ACE), $C_{10}H_{11}ClN_4$, chosen to carry out this study, on exocrine pancreatic cell physiology and to elucidate the underlying mechanisms involved in its effects on pancreatic function and its potential role in disease induction. Secondary aims included the preventive effect of carnosine (CARN) against these alterations. The study was conducted in several steps:

1) *Selection of the insecticide ACE and male Wistar rats* as an animal model for *in-vivo* study;
2) *Induction of sub-acute toxicity* using ACE doses of 43.4 and 21.7 mg/kg/day in male Wistar rats, with CARN administered at 200 mg/kg/day as a preventive treatment. This phase was carried out in the animal house of the laboratory of Nutrition, Pathology, Biotechnology, and Health (Lab-NuPABS), Sidi Bel-Abbes, during the period of June-July 2021 and December 2022-January 2023;
3) *Biochemical assessment* of blood glucose, amylase, and lipase levels, as well as measurement of MDA level in pancreatic tissue homogenates. This step took place at Lab-NuPABS, from January to February 2023;
4) *Histological analysis and scoring* of pancreatic tissue, conducted at the service of anatomy & pathology, University Hospital Center HASSANI ABDELKADER, Sidi-Bel-Abbès, during the period of September-December 2021 and to January 2023-April 2023;
5) *In-vitro investigation* using AR42J pancreatic cells to delve deeper into the molecular pathways of ACE toxicity and the preventive effects of CARN on exocrine pancreatic function. This step was carried out in the laboratory of cell biology and communication research group, department of biology,

university of Extremadura, Caceres, Spain, from March-July 2023 and November-December 2024.

4.2 Experimental design

The study was divided into two main parts as described in **Figure 4.1**.

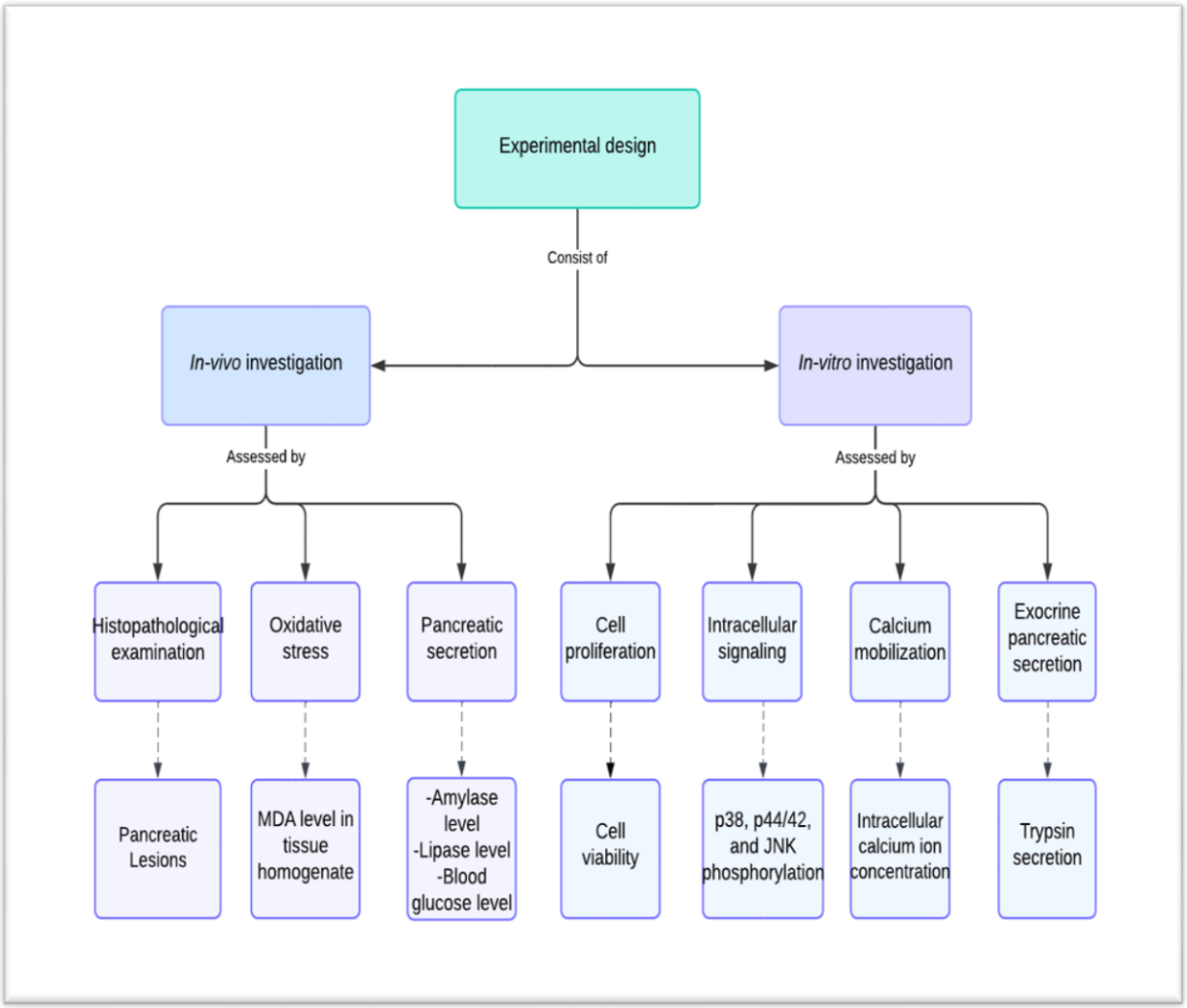

Figure 4.1 *In-vivo* and *In-vitro* assessment diagram

4.3 In-vivo procedures

4.3.1 Animals

Thirty-six male albino Wistar rats (**Figure 4.2**), aged 5 weeks and an average weight of 110±16 (g), were purchased from the Pasteur Institute in Algiers. The rodents were placed in plastic cages within a controlled environment, maintaining

a constant temperature of 22 ± 2 °C, a relative humidity of 55 ± 10%, and a regular 12-hour light/dark cycle. Additionally, they were granted unrestricted access to standard laboratory chow and water in the animal house of the Laboratory Lab-NuPABS, Sidi Bel-Abbes. The rats were treated ethically, following the international guidelines for treating laboratory animals (ethical approval No. IRB-A001/03.2022 from LA B-NUPABS-IRB).

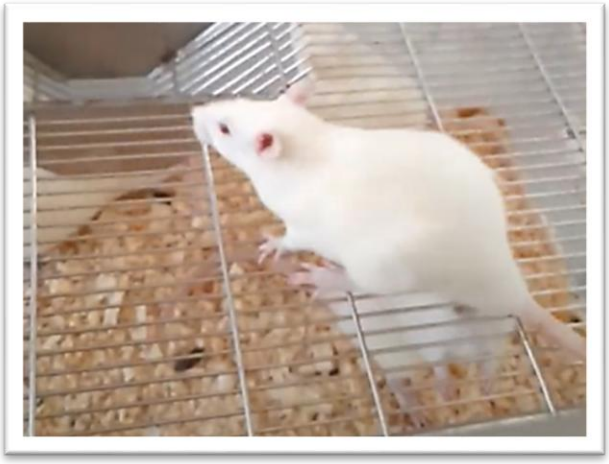

F*igure 4.*2 Male albino Wistar rat

4.3.2 ACE solution preparation

The commercial product of ACE, Mospilan®20 SL (Mospilan Max - Certis Belchim), contains 20% as an active ingredient (95% purity). The quantity of the two doses used in this study (i.e., 43.4 mg/kg and 21.7 mg/kg of ACE), following the methodology outlined by **Chakroun et al. (2016)**, was calculated as follows:

$$Mass\ of\ ACE\ (mg) = \frac{dose\ of\ ACE\ (mg) \times weight\ of\ animal\ (g)}{1000g} \times D \quad \text{.....(I)}$$

Were the dose of ACE either 43.4 mg or 21.7 mg, the concentration factor (D) is 5 (as mentioned, the product contains only 20% of ACE).

The calculated mass of ACE for each dose was dissolved in 1 mL of distilled water for administration to each respective rat.

4.3.3 Carnosine solution preparation

The concentration of the CARN solution (Pure Carnosine in capsules - 500mg , 99,9% pure - dynveo.fr) used in this study (200 mg/kg), as outlined by **Fadda et al. (2020)**, was calculated as follows:

$$Mass\ of\ CARN\ (mg) = \frac{dose\ of\ CARN\ (mg) \times weight\ of\ animal\ (g)}{1000g} \quad \text{.....(II)}$$

The calculated mass of CARN was dissolved in 1 mL of distilled water for administration to each respective rat.

4.3.4 Rodents' treatment

The animals underwent an eight-day acclimatization period. Subsequently, the rats were randomly assigned to six groups (six rats per group) using Research Randomizer©, as outlined below:

- Group I (Control): Received 1 mL of distilled water (vehicle solvent).
- Group II (CARN): Administered 1 mL of the CARN solution.
- Group III (High Dose; HD): Administered 1 mL of ACE (43.4 mg/kg) solution.
- Group IV (Low Dose; LD): Administered 1 mL of ACE (21.7 mg/kg) solution.
- Group V (HD+CARN): Administered 1 mL of ACE (43.4 mg/kg) solution, 4 hours after receiving 1 mL of CARN solution.
- Group VI (LD+CARN): Administered 1 mL of ACE (21.7 mg/kg) solution, 4 hours after receiving 1 mL of CARN solution.

All solutions were administered using a syringe attached to an oral gavage probe (**Figure 4.3**), and the treatment continued for 30 consecutive days and the body weight was recorded each week.

Figure 4.3 Oral gavage administration procedure

On the day following the cessation of treatment, the rats were euthanized under chloroform anesthesia. Blood samples were immediately collected via cardiac puncture and stored in tubes. Subsequently, the rats were sacrificed, and the pancreas were extracted, weighed using an analytical balance, and promptly rinsed with a sodium chloride buffer (0.9%) (**Figure 4.4**).

The Pancreatic Somatic Index (PSI) was calculated by multiplying the weight of each pancreas by 100 and dividing the result by the body weight measured directly before sacrifice. Subsequently, half of the organs were preserved in a 10% formaldehyde solution for histological examination, while the remaining half was frozen at -18 °C for lipid peroxidation analysis.

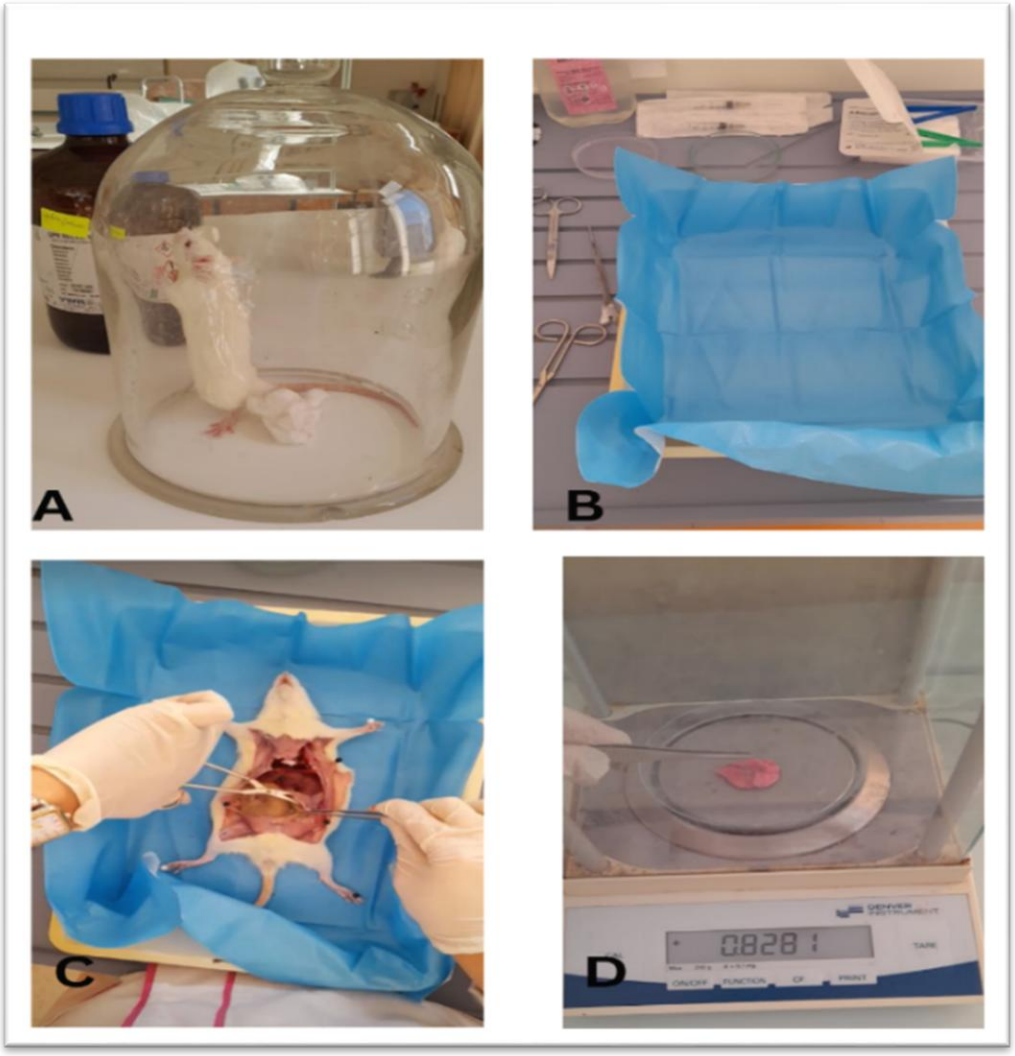

Figure 4.4 Experimental procedure. A) Rat under anesthesia, B) sacrifice instrument, C) sacrifice procedure, D) organ weight measurement

4.3.5 Biochemical Assay

4.3.5.1 Blood glucose level

The glucose level was measured using a colorimetric technique that employed an enzymatic method incorporating glucose oxidase and peroxidase following the method of **Trinder (1969)** (**Figure 4.5**).

Firstly, the blood was centrifugated for 10 min at 1500 rpm. The serum was collected in tubes, and the glucose level was determined using standard kits by a colorimetric technique.

Using a micropipette, 10 µL of serum is dispensed into a test tube, followed by the addition of 1000 µL of reagent buffer 1, which contains p-hydroxybenzoic acid, glucose oxidase, peroxidase, and 4-aminoantipyrine. Additionally, 10 µL of reagent buffer 2 (glucose standard solution) is introduced into another tube (standard) along with 1000 µL of reagent buffer 1. In a separate tube (blank), 1 mL of distilled water is added. The three tubes are then placed in a water bath at 37 °C for 10 min, resulting in the observation of a pink color. Subsequently, the absorbance measured at 505-510 nm against the blank (Ref. 05269397001, 2010).

The concentration of glucose level (g/L) is calculated as follows:

$$C\left(\frac{g}{L}\right) = \frac{A_{sample}}{A_{standard}} \times C_{standard} \quad \text{.....(III)}$$

Where: A $_{sample}$ is the absorbance of the sample, C $_{standard}$ is 100 g/L of D-glucose containing in standard, A $_{standard}$ is the absorbance of 100 g/L of D-glucose of the standard detected against the blank.

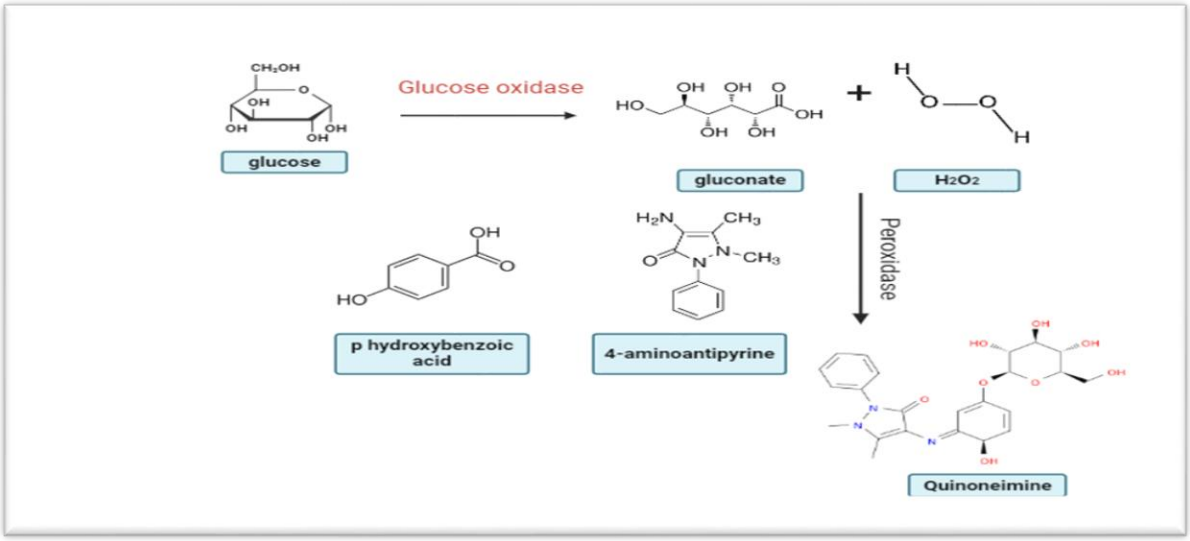

Figure 4.5 Glucose assay reactions (created using BioRender)

4.3.5.2 Amylase level

Alpha-amylase was measured using a colorimetric technique involving an enzymatic reaction that hydrolyzes 4,6-ethylidene- (G7)-p-nitrophenyl-(G1)-α-D-maltoheptaoside (EPS-G7) into ethylidene-glucoside and glucose(7-X)-p-nitrophenol

(G(7-X)-pNP). This product (G(7-X)-pNP) is further hydrolyzed into glucose and pNP, forming a yellow product that is quantified at 405 nm**(Zafer et al., 2021)** (**Figure 4.6**).

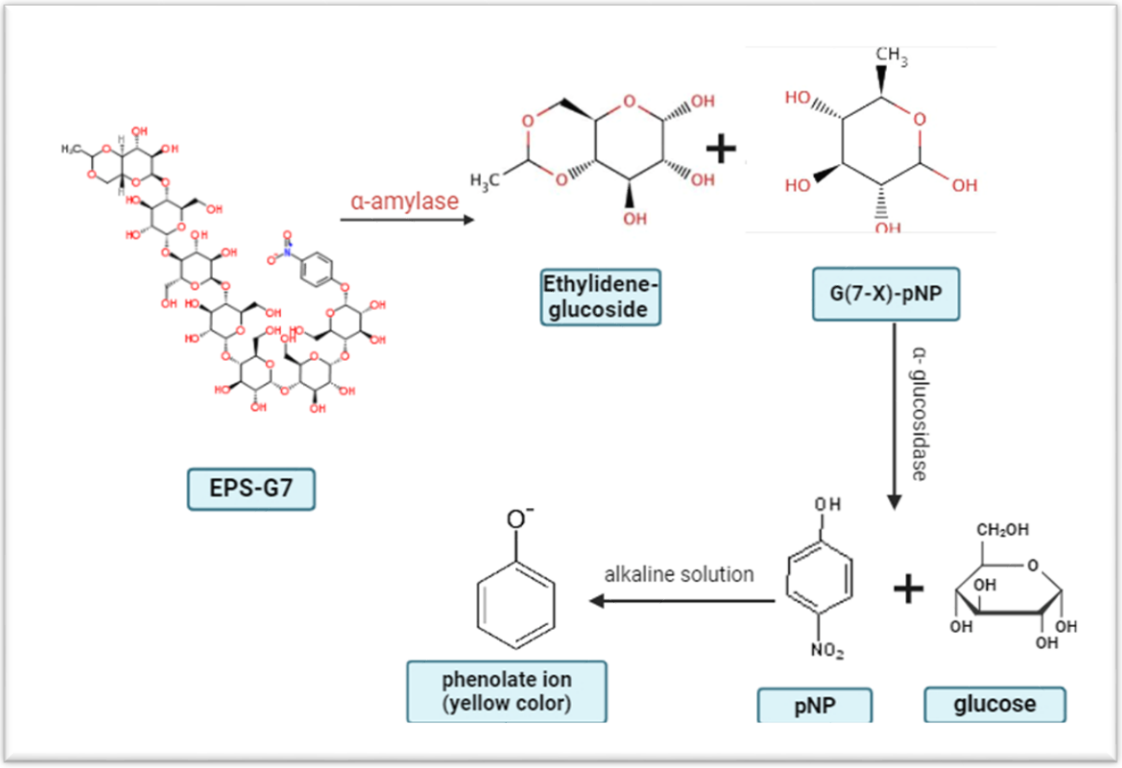

Figure 4.6 α-amylase assay reactions (created using BioRender)

Using a micropipette, 50 µL of serum is dispensed into a test tube, followed by the addition of 100 µL of amylase assay buffer, which contains 50% of EPS-G7, and 50% of α-glucosidase. Additionally, 50 µL of standard solution is introduced into another tube (standard) along with 100 µL of amylase assay buffer. In a separate tube (positive control), 50 µL of amylase positive control is added with 100 µL of amylase assay buffer. Subsequently, the absorbance is directly measured at 405 nm (Ref. 05269397001, 2010), and an incubation of 10 minutes is conducted, followed by a remeasurement of the absorbance at various time intervals. Each 1 unit represents the quantity of amylase required to hydrolyze EPS-G7 to produce 1 µmol of pNP per minute.

α-amylase activity (U/mL) is calculated as follows:

$$\alpha - \text{amylase activity } ({}^{U}/_{mL}) = \frac{C}{\Delta T \times V} \ldots\ldots\ldots\ldots\ldots\ldots\ldots\ldots\text{(IV)}$$

Where: C is the concentration of nitrophenol(nmol) produced by α-amylase during incubation time (10 min), ΔT is incubation time (10 min), and V is the volume of samples (ml).

4.3.5.3 Lipase level

Lipase level was measured using a colorimetric technique that involves an enzymatic reaction that cleaves 1,2-O-dilaurylrac-glycero-3-glutaric acid-(6'methyl-resorufin)-ester (glycerol-derived compound) into 1,2-O-dilauryl-rac-glycerol and glutaric acid-6'-methylresorufinester in the presence of emulsifies. These products further decompose to form glutaric acid and methylresorufin, forming a bluish-purple product that is quantified at 570-580 nm **(Panteghini et al., 2001)** (**Figure 4.7**).

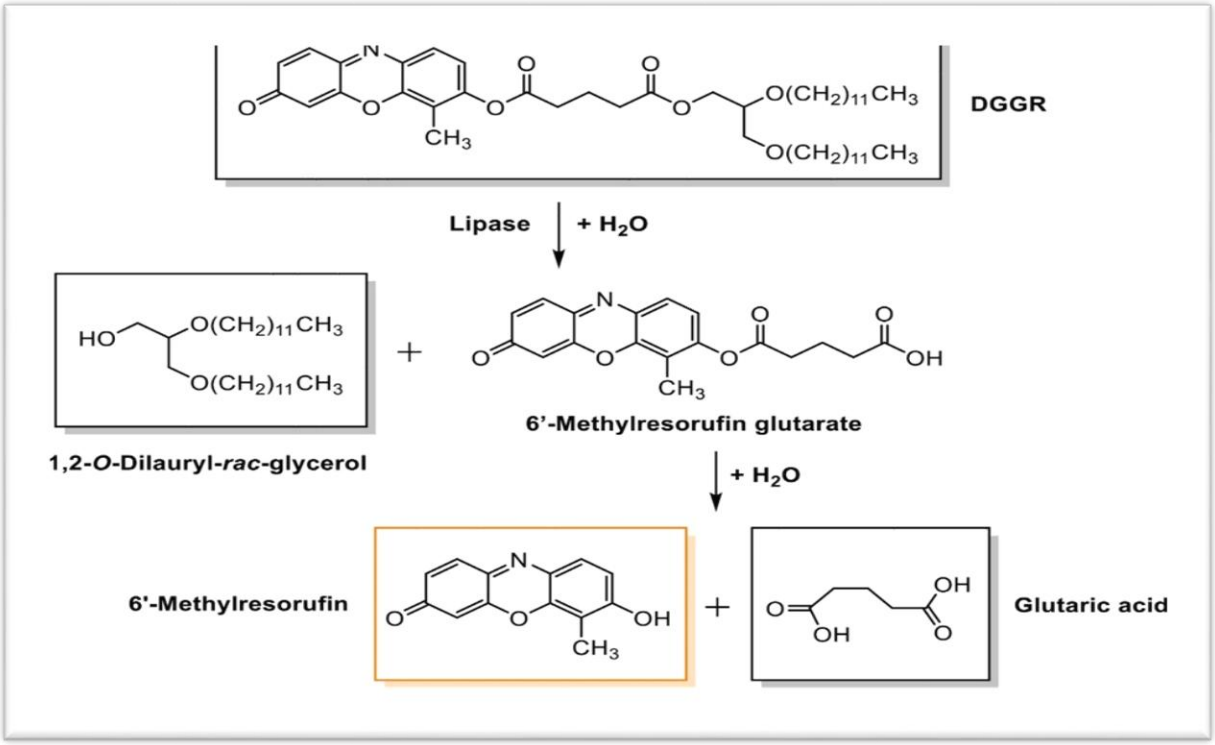

Figure 4.7 Lipase assay reactions **(Rocha et al., 2023)**

Using a micropipette, 10 µL of serum is dispensed into a test tube. Then, 1000 µL of reagent buffer 1, which contains the substrate and the emulsifies. Additionally, 10 µL of standard solution is introduced into another tube (standard) along with 1000 µL of reagent buffer 1. In a separate tube (blank), 10 µL of distilled water is added with 1000 µL of reagent buffer 1. The three tubes are then placed in a water bath at 37 °C for 5-10 min. After the time spent out, 600 µl of stop solution is added and the

absorbance is measured directly at 570-580 nm (Ref. 05269397001, 2010) against the blank. One unit represents the quantity of lipase enzyme that formed 1 µmol/min of methylresorufin.

The concentration of lipase level (mU/mL) is calculated as follows:

$$lipase\ activity\ = \frac{\Delta_{sample}}{\Delta_{standard}} \times Standard\ acticity \ldots\ldots\ldots\ldots\ldots\ldots (V)$$

Where: Δ_{sample} represents the absorbance of samples per unit of time, $\Delta_{standard}$ represents the absorbance of a standard used per unit of time, and standard activity represents the activity of the standard used calculated from the standard curve.

4.3.5.4 Malondialdehyde (MDA) measurement

MDA level in the pancreatic tissue was determined following the methods of **Nagasawa** et al. **(2001)** and **Kebièche et al. (2011)**. The approach involves measuring the product (MDA-TBA_2 adduct) formed by the reaction between malondialdehyde (MDA), the final product of lipid peroxidation in cells, and 2 molecules of thiobarbituric acid (TBA) (**Figure 4.8**). MDA-TBA_2 adduct is a pink chromophore that is quantified at 532 nm.

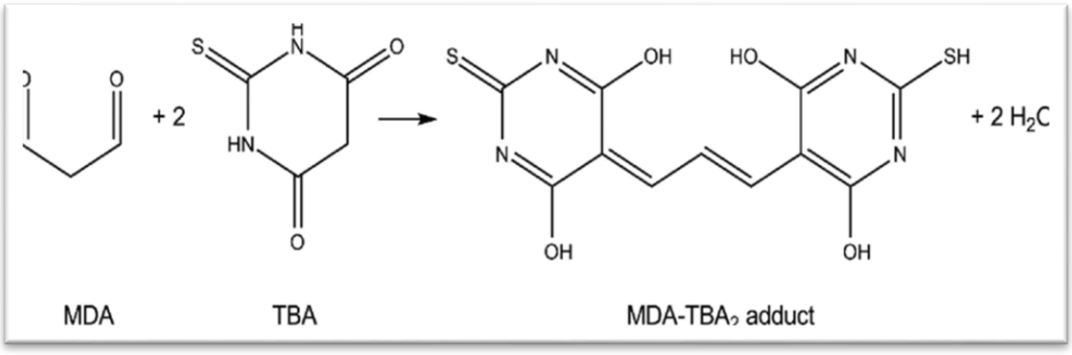

Figure 4.8 MDA and TBA reaction **(Jablan, 2016)**

The homogenate of pancreatic tissue was prepared by blending 1 g of tissue with 3 ml of potassium chloride solution (1.15 M). Subsequently, 0.5 mL the homogenate was combined with 0.5 mL of trichloroacetic acid (20%) and 1mL of thiobarbituric acid (0.67%). The resulting mixture was then heated for 15 minutes at 100°C, and 4 mL of

n-butanol was added. Following centrifugation for 15 minutes at 3000 rpm, the absorbance of the 1 mL of the supernatant at 532 nm was determined (**Figure 4.9**).

MDA concentration (nmol/mL) is calculated as follows:

$$C_{MDA} = \frac{OD}{\varepsilon} \ldots\ldots\ldots\ldots\ldots\ldots (VI)$$

Where: OD: optical density of samples subtracted from the blank at 532 nm, ε: extinction coefficient (156,000 M^{-1} cm^{-1}).

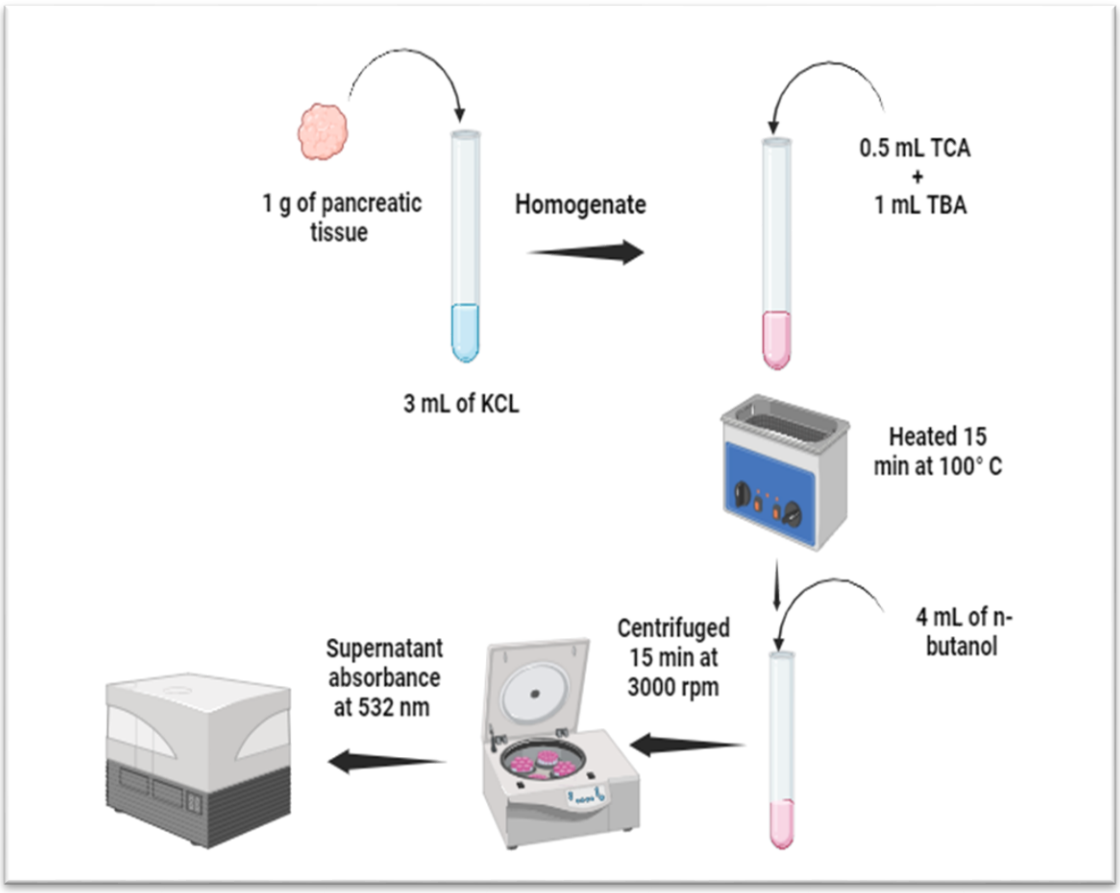

Figure 4.9 MDA quantification procedure (created by BioRender)

4.3.6 Histological Evaluation & Scoring

4.3.6.1 Histological evaluation

In the current study, pancreatic tissue was fixed in a 10% formaldehyde solution for 48h. Then, it was embedded in paraffin using a Leica TP1020 automatic Benchtop

(**Figure 4.10**) tissue processor as described in (**Table 4.1**). Subsequently, re-embedded manually in paraffin was using Histo-Line TEC2900 embedding center (**Figure 4.10**). After the hardening of blocks, it was sectioned into 3-4 µm slices using Histo-Line manual rotatory microtome (**Figure 4.10**). Sections were placed onto warm water at 45°C affixed onto AmScope microscope slides and left to dry. Furthermore, the slides underwent staining using Hematoxylin and Eosin (H&E) stains by Leica ST4040 linear staining system (**Figure 4.10**) as described in (**Table 4.2**). Finally, microscope slides were mounted using DPX mountant under cover glass (**Figure 4.11**).

Table 4.1 Embedding process

Step	Solution	Time
1	Ethanol (70%)	1h
2	Ethanol (90%)	1h
3	Ethanol (100%)	1h
4	Ethanol (100%)	1h 30min
5	Ethanol (100%)	1h 30min
6	Xylene	1h
7	Xylene	1h
8	Paraffin wax	1h
9	Paraffin wax	2h
10	Paraffin wax	2h

Table 4.2 Staining process

Step	Solution	Time
1	Ethanol (80%)	2 min
2	Running water	3 min
3	Harris's hematoxylin	5 min
4	Running water	3 min
5	Ethanol (70%)	2 min
6	Ethanol (95%)	2 min
7	Orange G-solution	5 min
8	Ethanol (95%)	1 min
9	EA-50	5 min
10	Ethanol (95%)	1 min
11	Ethanol (100%)	1 min
12	Xylene	3 min

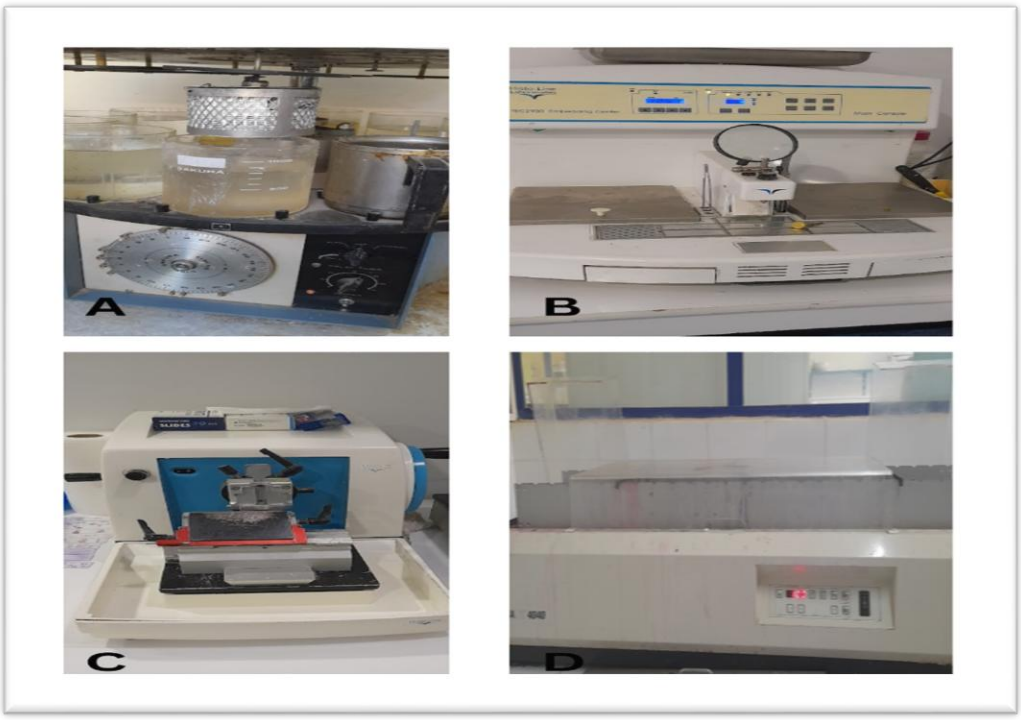

Figure 4.10 Instrumentation for Histological Processing. A) Leica TP1020 automatic Benchtop, B) Histo-Line TEC2900 embedding center, C) Histo-Line manually rotatory microtome, D) Leica ST4040 linear staining system

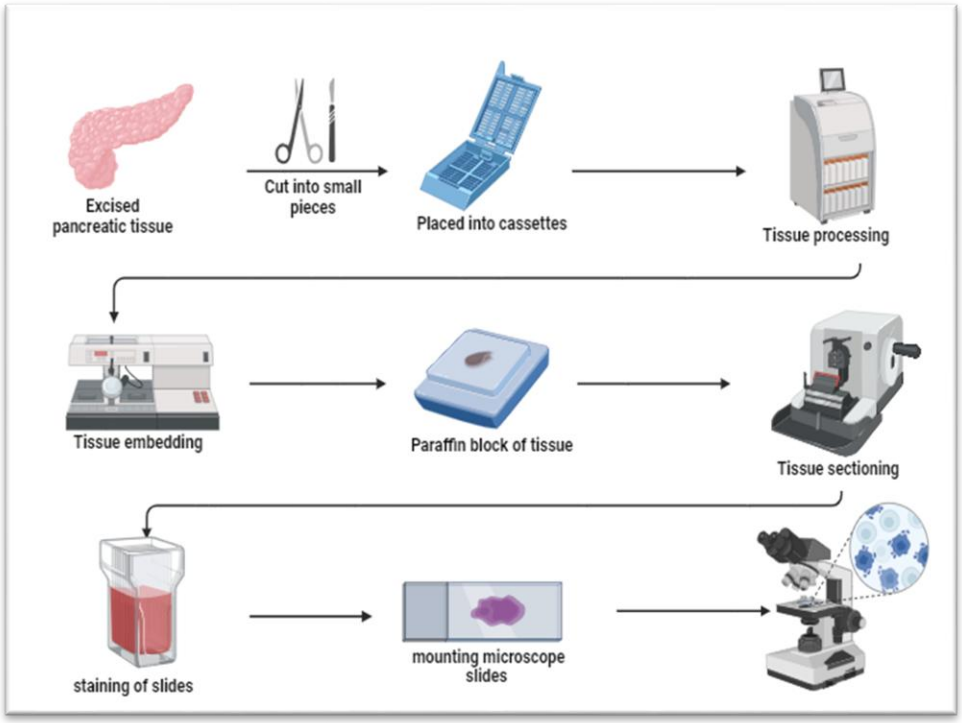

Figure 4.11 Histology process (created by BioRender)

4.3.6.2 Histological scoring

In the present study, pancreatic histological scoring was conducted as previously described by **Dembiński et al. (2006)**. After (H&E) staining, eight microscope slides per rat underwent an examination to assess histopathological features (i.e., edema, inflammatory infiltration, and vacuolization), utilizing an ordinal scale ranging from 0 to 3 to grade severity levels (**Table 4.3**). Blinding procedures were strictly adhered to by assigning codes to all slides. The evaluation was initially performed by one pathologist and subsequently validated by another, ensuring thorough verification.

Table 4.3 Histological score based on Dembiński et al. **(2006)**

Histological feature	Score	Description
Edema	0	Absent
	1	Presence of interlobular edema
	2	Presence of interlobular with moderate intralobular edema
	3	Interlobular with severe intralobular edema
Inflammatory infiltration	0	Absent
	1	Presence of scarce perivascular infiltration
	2	Presence of moderate perivascular and scarce diffuse infiltration
	3	Presence of abundant diffuse infiltration
Vacuolization	0	Absent
	1	Presence of 25% of vacuolated acinar cells
	2	Presence of 25-50% of vacuolated acinar cells
	3	Presence of <50% of vacuolated acinar cells

4.4 *In-vitro* procedures

4.4.1 Cell line used

To investigate the effect of ACE and/or CARN on the exocrine pancreas using *in-vitro* techniques, the AR42J cell line was used in this study. It was acquired from the university of Extremadura, service of applied techniques, Badajoz, Spain, and stored at -90°C until needed.

4.4.2 Preparation of cell culture

Firstly, the cells were rapidly defrizzed under running water. Under a biological safety cabinet Telstar EN12469, 3 mL of the supplemented RPMI-1640 medium was added **(cf. Appendix**). The tube was centrifuged (Eppendorf Centrifuge 5430 R) for 5 min at 2000 rpm (23°C). subsequently, the supernatant was removed, and the cell pellet was recovered in a new conical tube with 12 mL of the supplemented RPMI-1640 medium. Finally, using an electronic pipette, the cell suspension was suspended in a cell culture flask and incubated in an incubator (New Brunswick Galaxy 170 S, USA) with 5% CO_2 at 37°C (**Figure 4.12**).

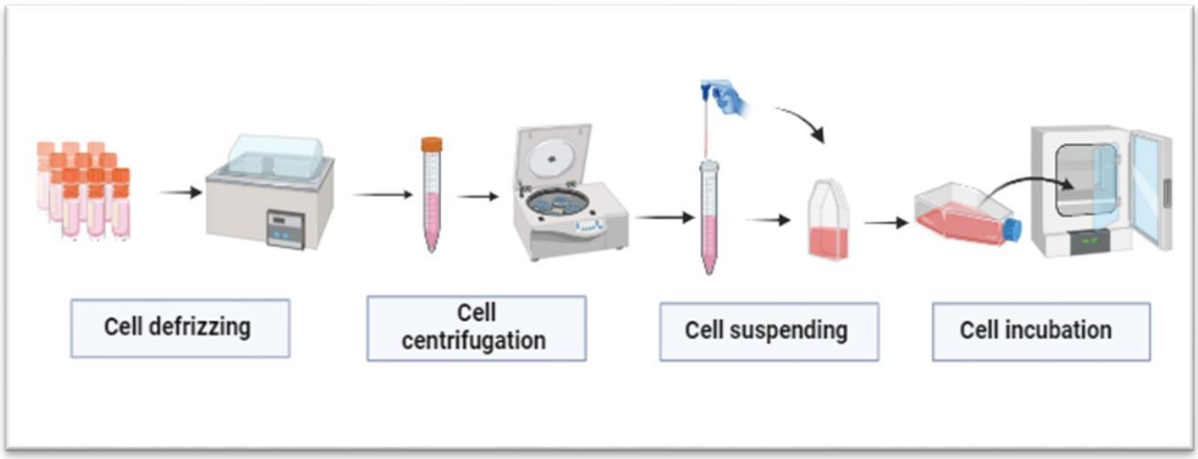

Figure 4.12 Cell culturing process (created by BioRender)

4.4.3 Cell viability assay

In the current study, the commercial cell viability assay Alamar Blue® was used to determine the effect of ACE and/or CARN on pancreatic AR42J cell proliferation following the method of **O'Brien et al. (2000)**.

4.4.3.1 Cell counting and seeding

Cell counting is a preliminary step in determining cell concentrations before seeding the cells for a cell viability assay. Trypan blue was used for this procedure **(Strober, 2001)**. In aseptic conditions, 2 mL of cell media was removed (transferred to a new tube), and 2 mL of trypsin solution (0.25% in PBS) was added to initiate trypsinization. After 5 min of incubation, the 2 mL of original media was reintroduced to the cell suspension, and the entire mixture was transferred to a new conical tube for centrifugation at 3000 rpm for 5 min. The resulting cell pellet was resuspended in 12 mL of fresh RPMI-1460 medium (**Figure 4.13**). In an Eppendorf tube, 10 µL of cell suspension was mixed with 40 µL of trypan blue solution (0.4%). Subsequently, the mixture was gently drawn into a glass hemocytometer (BLAUBRAND®, Germany) (**Figure 4.14**), and under a microscope NIKON ECLISPE (NIKON instruments, USA) equipped with a 10X objective, viable cells were counted within the grid lines (**Figure 4.14**).

Cell concentration was calculated as follows:

$$cell\ concentration\ \left(\frac{cell}{ml}\right) = \frac{average\ cell\ count\ per\ square}{4} \times dilution\ factor \times 10^4 \text{.....(VII)}$$

Where: 4 is the number of squares, the dilution factor is 5, and 10^4 is to convert 0.1 mm^3 to 1 mL.

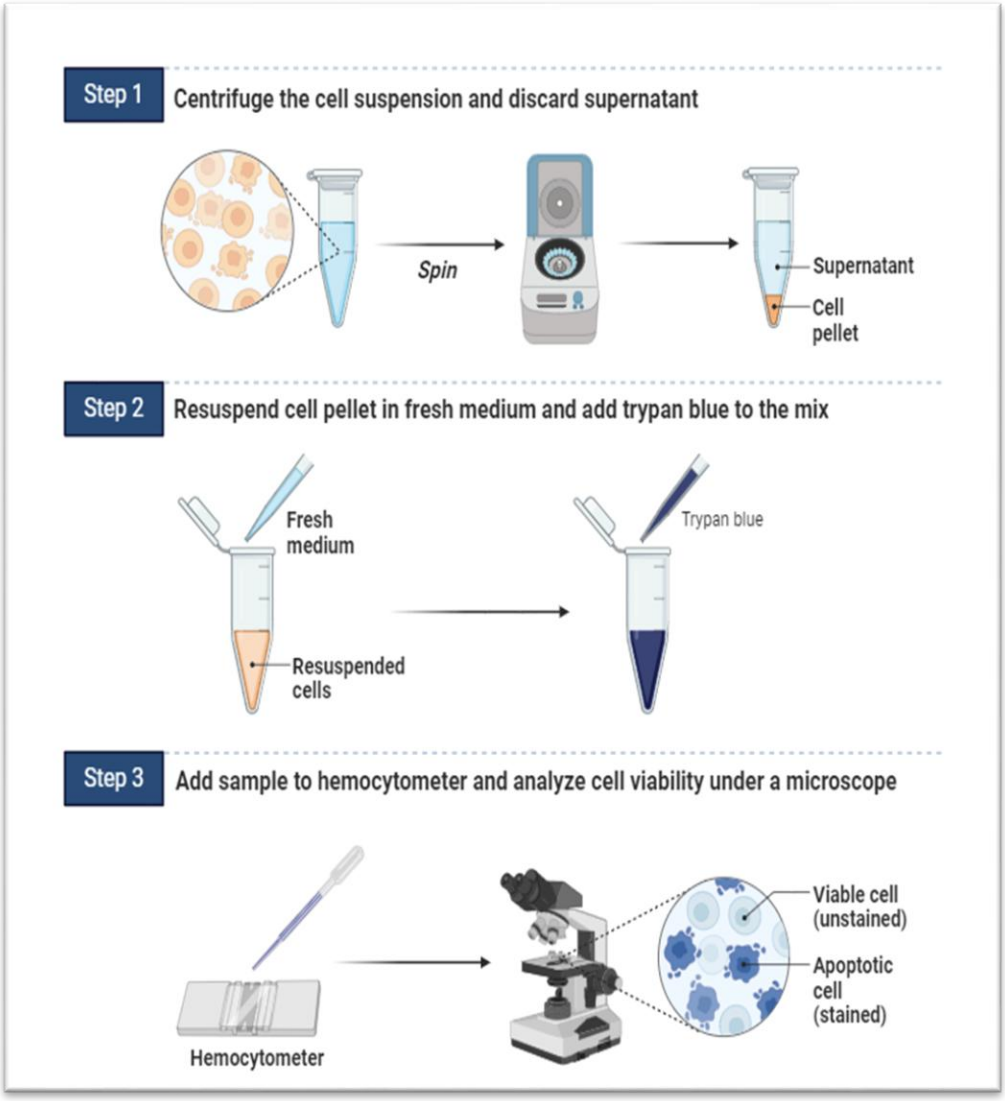

Figure 4.13 Cell counting process using Trypan blue (created by BioRender)

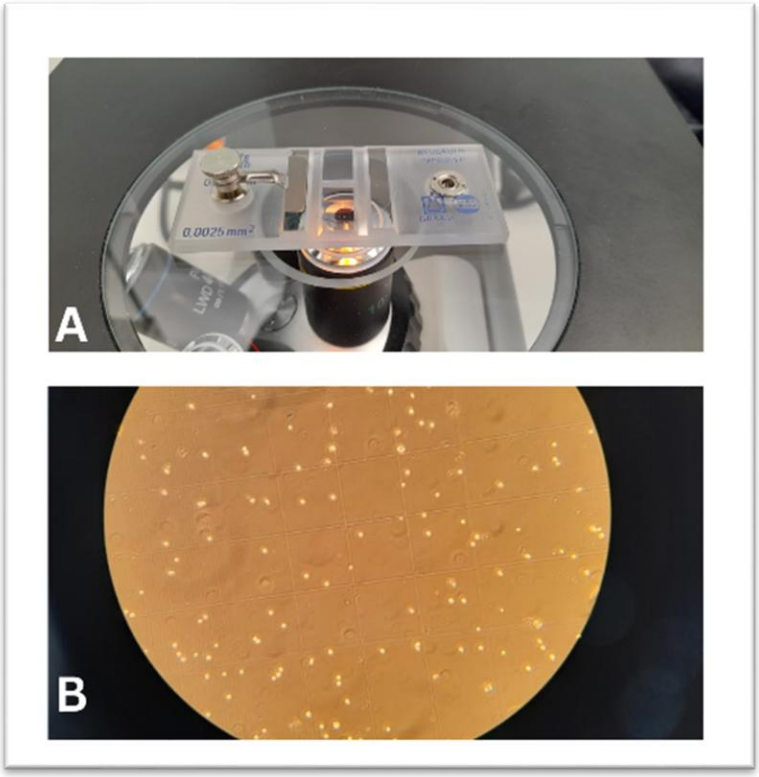

Figure 4.14 Cell counting. A) hemocytometer, B) Viable cells under a microscope (10X)

4.4.3.2 Alamar Blue® assay

The commercial cell viability assay Alamar Blue® operates on the principle of resazurin reduction **(O'Brien et al., 2000)**.

In a 96-well plate, cells were seeded at a density of 5000 cells per well in 100 µL of medium and incubated at 37°C, 95% humidity, and 5% of CO_2 for 24 hours. Subsequently, the ACE stock solution was dissolved in the RPMI-1640 medium, and various dilutions were prepared with fresh medium to achieve the desired concentrations (from 0.1 µM to 10 mM of ACE). For the ACE/CARN combination, cells were pretreated with 50 µL of 10 mM CARN for 5 min before adding the ACE solution. 2 µl of Staurosporine (2 µM) was used as positive control. The plates were then further incubated for 24, 48, and 72 hours.

After 24 hours, 20 µL of Alamar Blue was added to each well. The plate was then incubated for 4 hours in the incubator (**Figure 4.15**), following which the fluorescence

was measured with excitation at a wavelength of 560 nm and emission at 590 nm (RF-6000 Spectro-fluorophotometer, Shimadzu, USA).

Cell viability (%) was calculated as follows:

$$viable\ cells\ (\%) = \frac{absorbance\ of\ the\ sapmle - absorbance\ of\ the\ blank}{absorbance\ of\ the\ control\ well - absorbance\ of\ the\ blank} \times 100 \ldots\ldots\ldots (VIII)$$

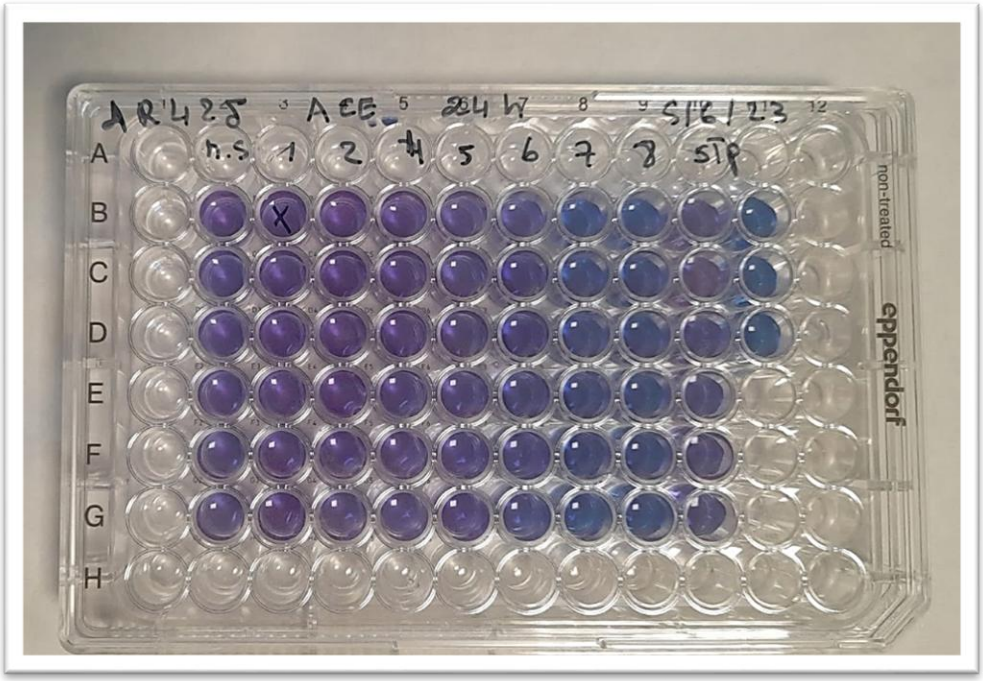

Figure 4.15 AR42J cells stimulated with ACE and/or CARN in 96 wells plate

4.4.4 Proteins quantification by Western blotting

In the present study, the focus was on three MAPKs pathways (**Figure 4.16**). The phosphorylation form of P44/42, p38, and JNK proteins was quantified to assess the effect of ACE and CARN on the intracellular signaling pathways of AR42J cells. ß-actin was used as a loading control. Therefore, Western blotting techniques were used to quantify proteins **(Towbin et al., 1979)**.

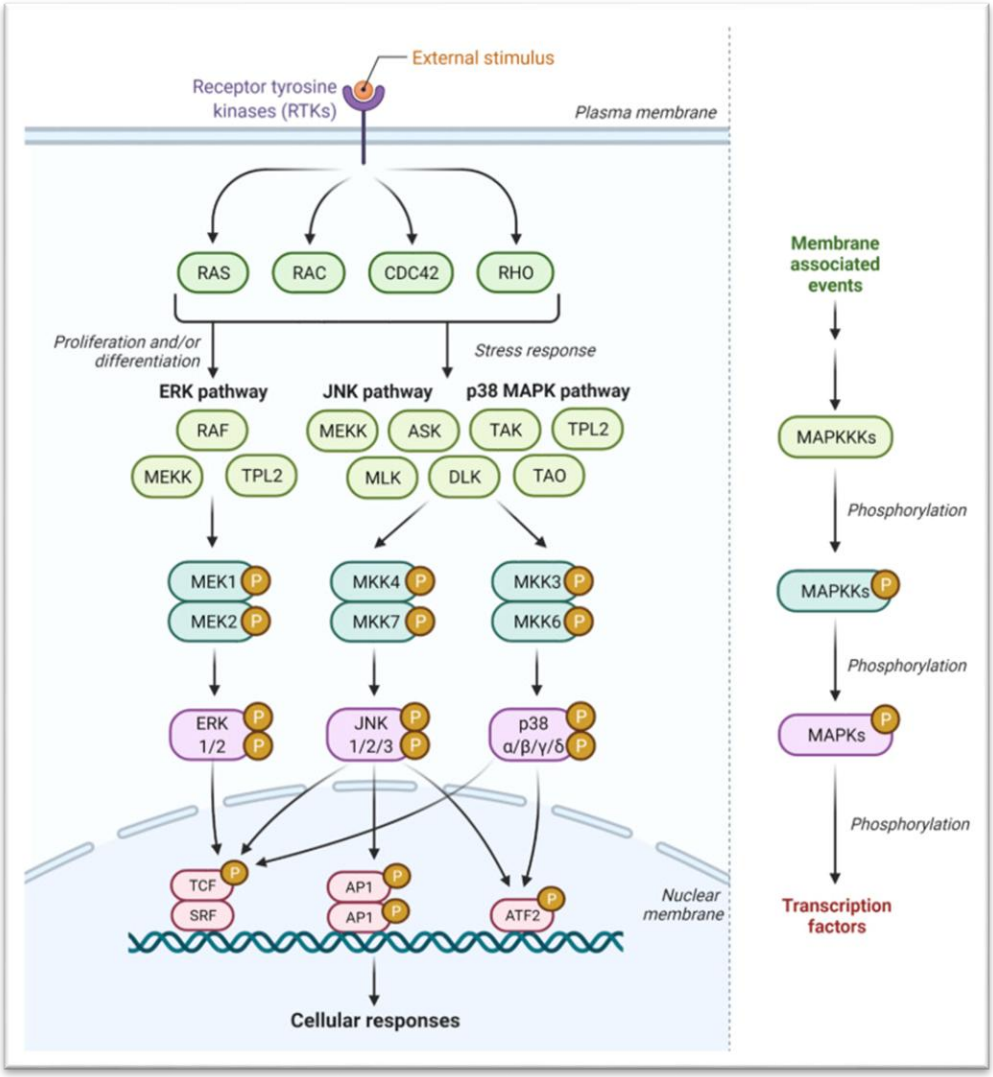

Figure 4.16 MAPKs signaling by ERK, JNK, and p38 pathways **(Pua et al., 2022)**

4.4.4.1 Cell stimulation

AR42J cells were detached, counted, and seeded at a density of 10^5 cells per well in 100 µL of medium in a 6-well plate, as previously described. Subsequently, the plate was incubated at 37°C, 95% humidity, and 5% CO2 for 24 hours. Following this incubation period, the cells were stimulated with ACE solution (from 0.5, 1, 2, and 3 mM) alone or combined with 10 mM of CARN, and subsequently incubated for 1h (**Figure 4.17**).

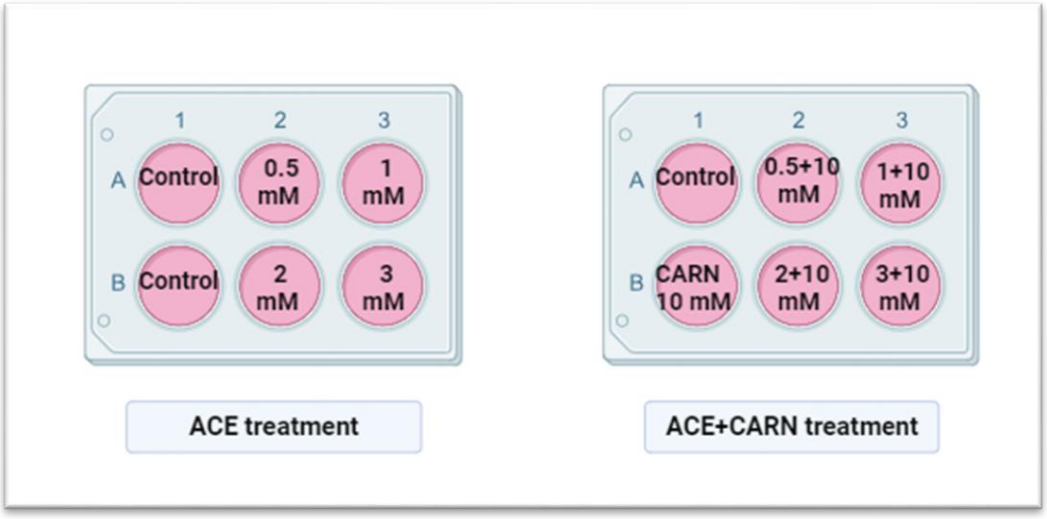

Figure 4.17 ACE and CARN stimulation cells in 6 wells plate (created by BioRender)

4.4.4.2 Cell lysis

In this study, cell lysis was performed using both chemical and physical methods. The chemical method entailed the utilization of cell lysis buffer. Whereas the physical approach entailed the use of sonication.

The medium was aspirated on ice using an aspirator (AFT 1 aspirator, Biosan, Lativia), and the wells were quickly washed three times with 1 mL of cold PBS. Then, 50 µL of lysis buffer (cf. Appendix) was added to each well and the cells were gently scraped using a scraper. The lysates were subsequently collected in Eppendorf tubes and placed on ice. Next, the tubes were sonicated for 1 minute using a sonicator (SONOplus sonicator, BANDELIN, Germany). After sonication, the tubes were incubated for 15 minutes and then centrifuged at 14,000 rpm for 15 minutes at 4°C. Following centrifugation, the supernatants were carefully collected in new Eppendorf tubes. A dilution of 1:10 (5 µL of sample + 45 µL of MilliQ water) was prepared in new Eppendorf tubes and stored at -20°C until use.

4.4.4.3 Total protein quantification

The determination of protein concentration is carried out using the colorimetric Bradford method **(Bradford, 1976)**. This technique allows the calculation of proteins concentration in a sample based on the formation of a complex between the brilliant

blue dye Coomassie G250 and the proteins in solution. This complex is then compared to a standard curve established by the reaction of known quantities of a standard protein, typically bovine serum albumin (BSA).

To perform the assay, BSA standard tubes are thawed, and 5 µL of lysis buffer and 5 µL of MilliQ H_2O are added. The blank was prepared by mixing 45 µL of MilliQ H_2O with 5 µL of lysis buffer. Subsequently, the tubes were subjected to centrifugation, to bring all the contents to the bottom. Afterwards, the tubes of 1:10 dilution were thawed, and Bradford solution was prepared (80 mL of MilliQ H2O with 20 mL of Bradford stock solution). 10 µL of each solution (standards, blank, and the samples) was added to a 96-well plate as depicted in **Figure 4.18**. Using an electronic pipette, 190 µL of Bradford solution was added to each well, and the absorbance was measured at 595 nm using a micro-plate reader (CLARIO star Plus, BMG LABTECH, Germany).

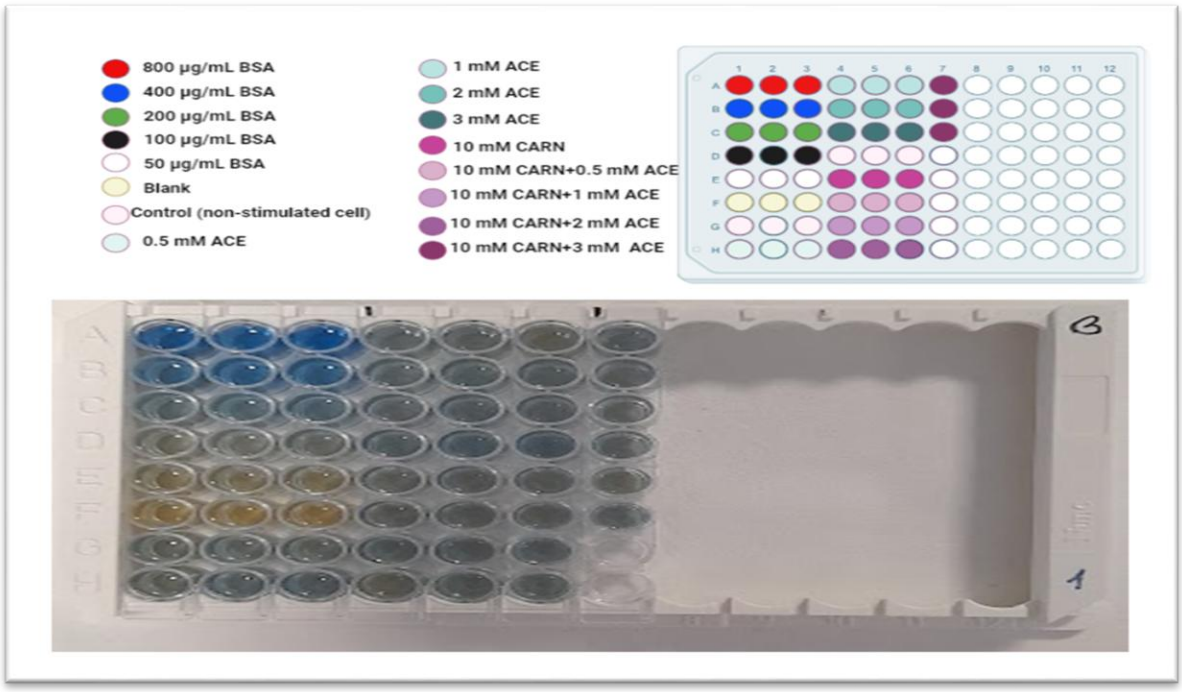

Figure 4.18 96 wells plate filled with standards, blank, and samples (created by BioRender)

The concentration of proteins was calculated using the following equation:

$$Y = aX + b \text{.....(IX)}$$

Where: Y is the absorbance at 595 nm, X is the protein concentration, a= 0.0008, and b= 0.0289 calculated using the standard curve (**Figure 4.19**).

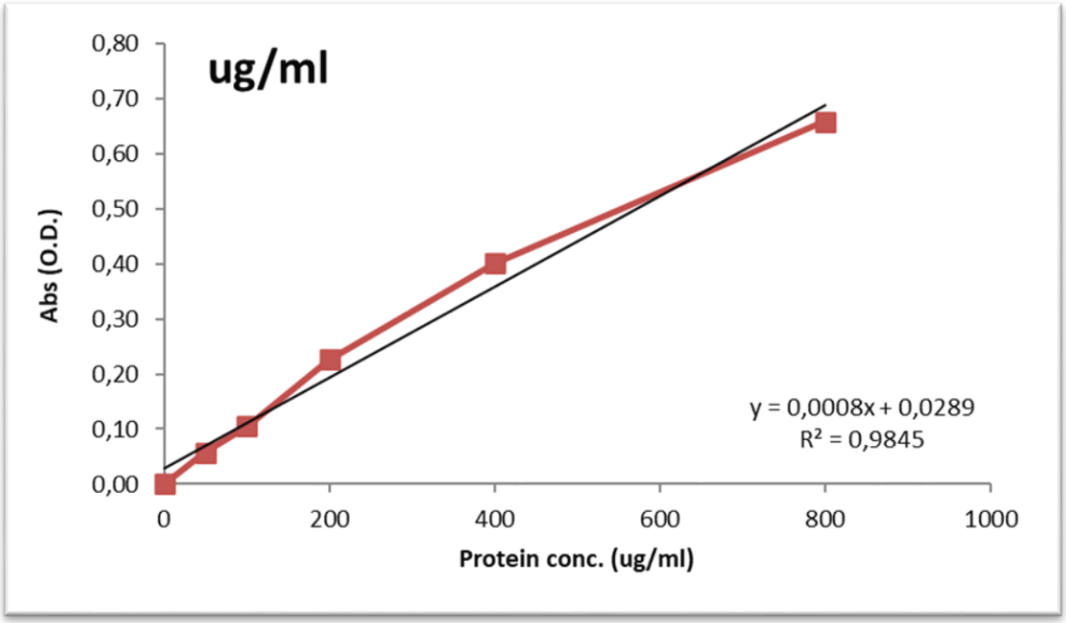

Figure 4.19 Standard curve of concentration (µg/mL) versus absorbance

4.4.4.4 Electrophoresis

The separation of total proteins was conducted using sodium dodecyl sulfate polyacrylamide gel electrophoresis (SDS-PAGE) **(Laemmli, 1970)**. This approach includes denaturing the proteins prior to electrophoresis.

Initially, the samples were diluted with lysis buffer to attain a total protein concentration of 12 µg/ml. The volume of lysis buffer to add was calculated by the difference between the volume of the most diluted sample and the volume of each sample.

The loading buffer was prepared by combining 100 µL of ß-mercaptoethanol with 900 µL of Laemmli buffer. Subsequently, this buffer was added to the samples and stored at -20°C until needed. The following calculation is used to determine the required volume of loading buffer:

Loading buffer volume (µL) = Target protein amount (µg) x Final volume in well/Sample protein amount ……..(X)

On the day of electrophoresis, the glass plate containing the polyacrylamide gels was placed into the electrophoresis chamber and filled with the running buffer (cf. Appendix). The sample tubes were subjected to heating at 70°C for duration of 10 minutes, vortexed, and carefully loaded into the wells of the gel. The first and the last wells were loaded with 2 µL of the molecular weight marker. The electrophoresis was initially run at 90 V, and when the samples reached 2 cm from the wells, the voltage was increased to 110 V. Finally, the electrophoresis was stopped when the samples (blue front) reached the end (**Figure 4.20**).

Figure 4.20 SDS-PAGE process

4.4.4.5 Blotting

At the end of the electrophoresis, the glass plates were carefully removed, and the gels were transferred to a container containing transfer buffer 1X (cf. Appendix) and allowed to equilibrate for a few minutes. The sandwich was then assembled in the following order: sponge, followed by 3 Whatman papers, then the nitrocellulose membrane, the gel, another 3 Whatman papers, and finally another sponge. The assembled transfer sandwiches were placed in the cassettes, and the cassettes were placed in the transfer tank. The transfer tank was filled with cooled transfer buffer 1X,

and placed in a container filled with ice, and the transfer was performed at 100 V for 1 h and 30 min at 4°C (**Figure 4.21**).

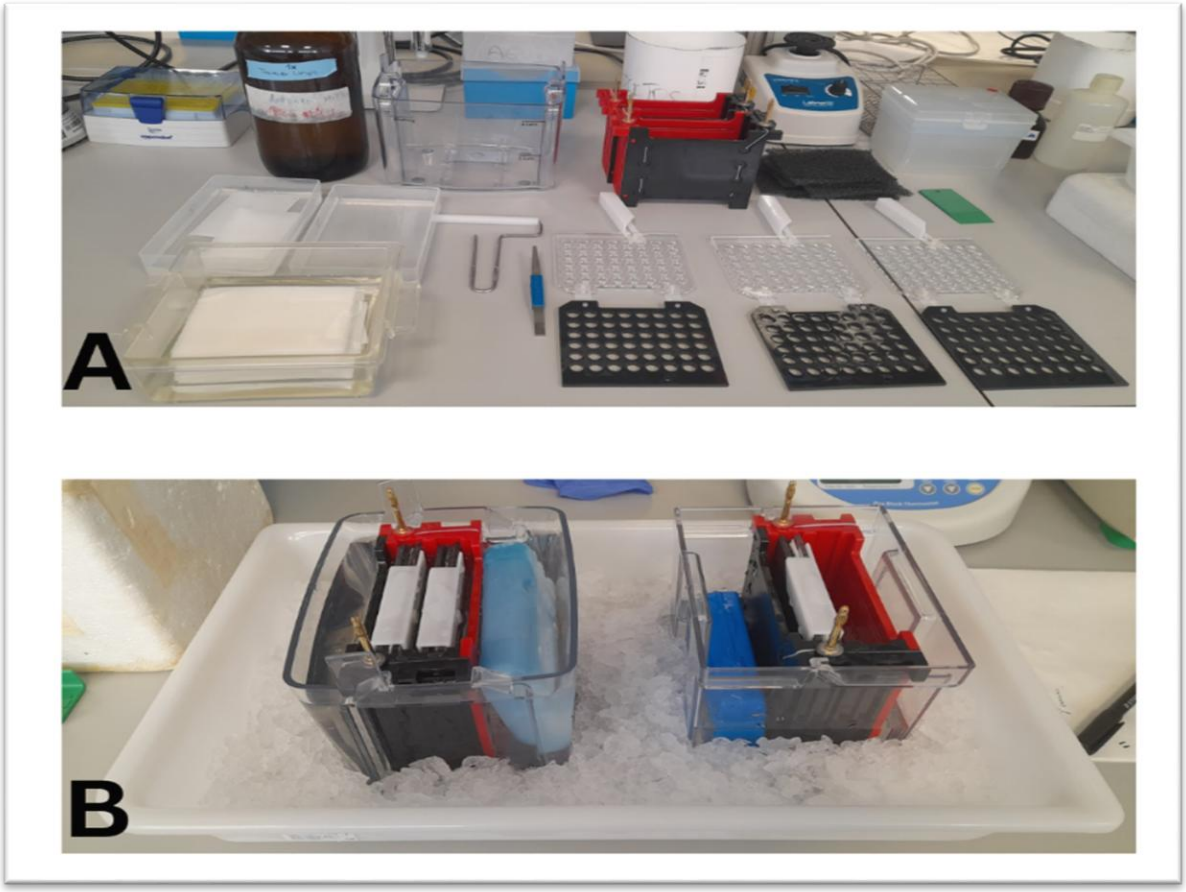

Figure 4.21 Blotting process. A) instrument used, B) transfer tank on ice

4.4.4.6 Blocking and antibody incubation

After the end of the blotting process, the membranes were placed in small boxes for Ponceau staining. The objective of this method is to confirm that the lanes have been accurately transferred from the gel to the nitrocellulose membrane. 3 mL of Ponceau solution was added to each membrane, and they were gently agitated until the lanes became visible (**Figure 4.22**). Following this, photographs were taken (by G: Box Chemi XX6/XX9, Syngene) using the Ponceau reader through the GeneSys software after the membranes were washed three times with distilled water.

Figure 4.22 Nitrocellulose membrane with visible lanes by ponceau solution

The membranes were then washed 3 times with the 10 mL blocking solution (cf. Appendix) for 10 min each time and then incubated with 10 mL of block solution for 1 h at room temperature with gentle agitation. Once blocking was complete, the membranes were washed with 10 mL of TBST 1X (3 times) to remove any traces of milk and prevent antibody contamination (**Figure 4.23**). To improve the performance of Western Blot, the membranes were cut using a scalpel and ruler to separate them into different fragments and isolate proteins of interest based on their molecular weight.

Figure 4.23 Membrane wash with TBST solution

After the blocking, the membranes were incubated with the first antibody solution (for p-p38 (1:1000 dilution), p-JNK (1:1000 dilution), and p-P-44/42 (1:2000 dilution) proteins detection in gentle agitation for 24 h at 4°C (**Figure 4.24**). After the first incubation, the membranes were recuperated in small boxes and washed twice with 10 mL of blocking solution with rapid agitation. Finally, the membranes were incubated with the appropriate IgG-HRP conjugated secondary antibody at a 1:5000 dilution in blocking solution (2 µL of antibody with 10 mL of blocking solution) for 1 h at room temperature with gentle agitation. The membranes were then washed with 10 ml blocking solution for the first time and twice with 10 ml TBST 1X solution, also under rapid agitation and for 10 minutes each.

For the loading control, and after the blocking, the membranes were incubated with ß-actin solution (1:50000 dilution) in gentle agitation for 24 h at 4°C. Subsequently, the membranes were washed with 10 mL of blocking solution for 10 min at rapid agitation and then twice with 10 mL of TBST 1X solution with rapid agitation for 10 min each.

Figure 4.24 Membrane incubation with 1st antibody

The proteins were detected using the chemiluminescent detector SuperSignal™ West Femto by adding 200 µL of it to the specific area of the protein interest and then the signal was detected by the G: Box Chemi XX6/XX9, Syngene equipment using GeneSys software. The detected intensity bands were quantified using the ImageJ program.

The protein amount (%) was calculated as follows:

$$Intensity\ bands\ (\%) = \frac{Intensity\ of\ \ protein\ of\ interest}{Intensity\ of\ total\ proteins} / Intensity\ of\ protiens\ of\ control \times 100 \ldots\ldots\ldots (XI)$$

4.4.5 Measurement of intracellular free-calcium concentration

Intracellular free calcium concentration was measured using the calcium-sensitive fluorescent probe Fura-2/AM (**Figure 4.25**), following the method of Grynkiewicz et al. **(1985)**. When exposed to ultraviolet light, the compound becomes activated, and its highest absorption point changes from 380 nm when there's no calcium present to 340 nm when calcium is bound to it. In both scenarios, the maximum emission intensity is observed at a wavelength of 510 nm (**Figure 4.26**). Fura-2 exhibits

a notable binding affinity for calcium, which is commensurate with the calcium levels observed in resting conditions **(Barreto-Chang & Dolmetsch, 2009)**.

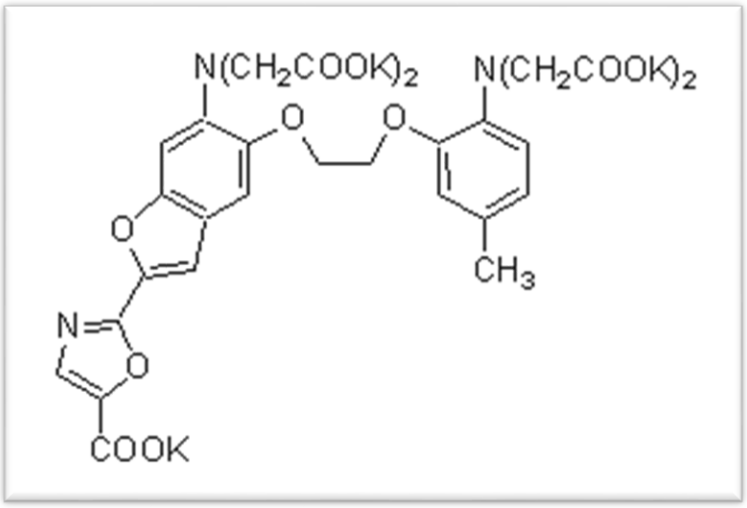

Figure 4. 25 Fura 2/AM chemical composition **(de Melo Reis et al., 2020)**

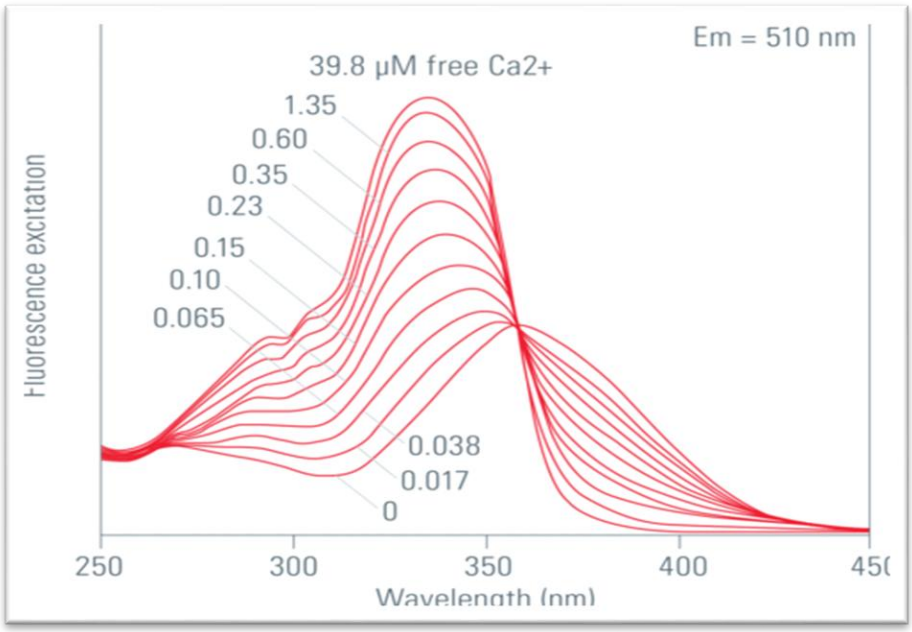

Figure 4.26 The fluorescence excitation spectra of Fura-2 were recorded at various calcium concentrations **(Burger & Diehl, 2013)**

Firstly, the cells were detached and counted as previously described. The cells were seeded at a density of 100,000 cells per dish in a 35 x 15 mm petri dish containing a sterilized coverslip with a diameter of 16 mm. The dishes were then incubated for 72 hours in the incubator. After incubation, 1.5 µL of dexamethasone (10^{-4}) was added to

the cells and they were incubated for 24 hours. Subsequently, Fura-2/AM was added to the cells at a concentration of 4 µM (4 µL/mL) and incubated for 40 minutes in obscurity (**Figure 4.27**).

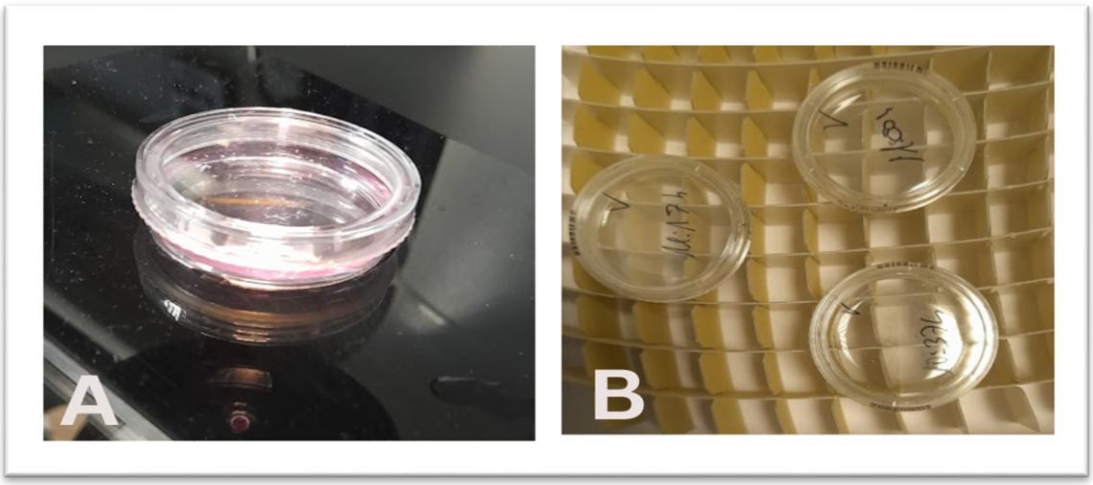

Figure 4.27 AR42J cells for calcium detection. A) Incubation of cells in a petri dish, B) Incubation of cells with Fura-2

The medium was then removed, and the cells were suspended in Na-Hepes solution 1X (cf. Appendix). The coverslip was then mounted into an experimental perfusion chamber positioned on an epifluorescence inverted microscope (RF-5001-PC; Shimadzu, Kyoto, Japan) (**Figure 4.28**). The experiment began with a 40-second wash of cells using Na-Hepes solution 1X, followed by another 40-second wash with Na-Hepes solution without Ca2+. Subsequently, the cells were treated with 1 mM of ACE or 1 µM of Thapsigargin (Tps) in Ha-Hepes solution 1X without Ca^{2+} for 5 minutes. Fluorescence excitation at wavelengths of 340 nm and 380 nm was employed to stimulate the cells using a monochromator (Polychrome IV, Photonics, Hamamatsu, Japan), while fluorescence emission at 505 nm was detected using an ORCA Flash 4.0 V2 digital CMOS camera (Hamamatsu Photonics-France, Barcelona, Spain) and recorded using dedicated software (HCImage from Hamamatsu Corp., Sewickley, PA, USA).

The results are presented as the ratio of fluorescence emitted when excited at 340 nm and 380 nm, adjusted to the baseline fluorescence level. To facilitate a comparative analysis of the responses, the average peak of the intracellular calcium concentration was determined. This calculated response, determined as the maximum value attained following cell stimulation with ACE. Furthermore, the overall calcium mobilization was

determined by calculating the integral of the increase in $[Ca^{2+}]_i$ relative to baseline values over a 5-min period after cell stimulation with ACE. All fluorescence readings were taken from regions identified as individual cells.

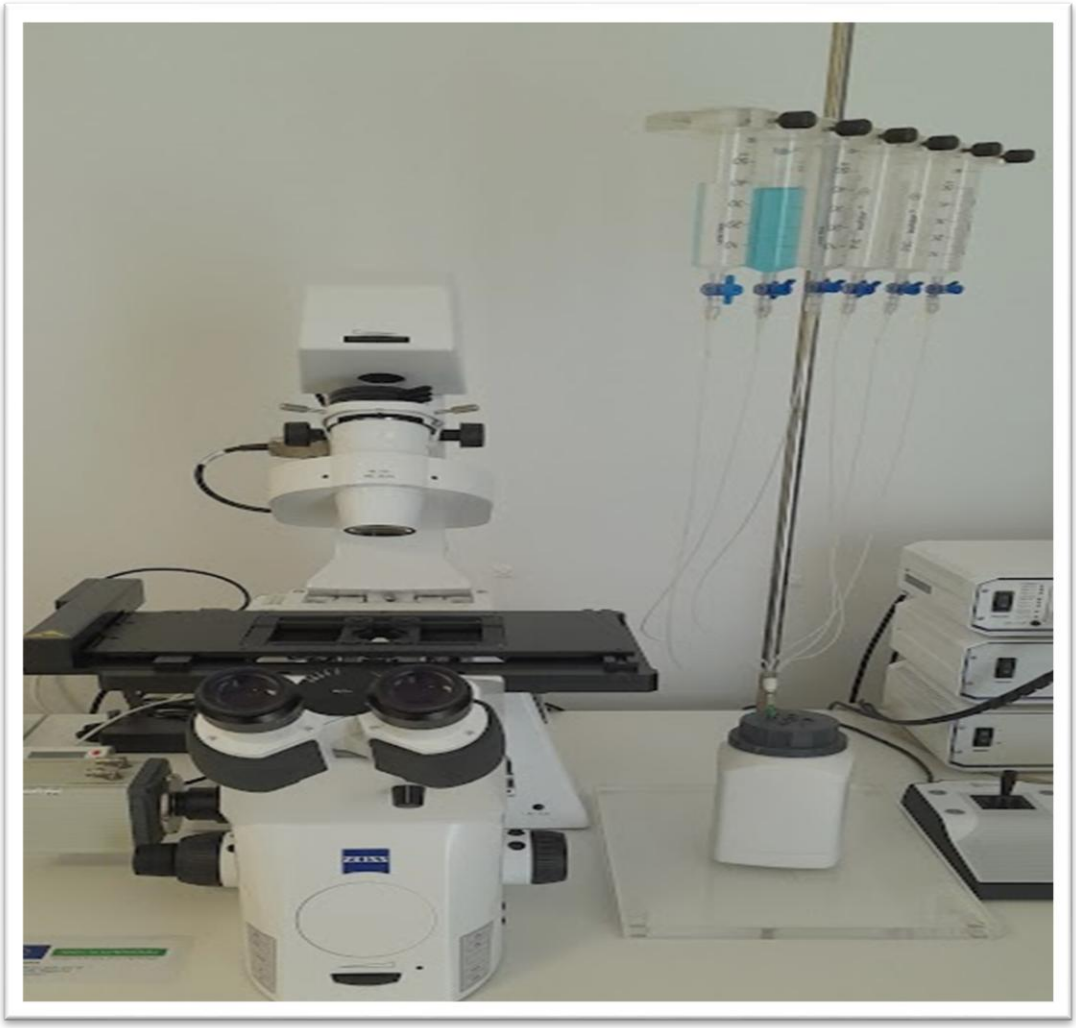

Figure 4.28 Perfusion chamber and the epifluorescence inverted microscope used in this study

4.4.6 Measurement of trypsin secretion

The current study aimed to assess trypsin secretion in the exocrine pancreas following treatment with ACE and/or CARN by measuring its levels in AR42J cells following the method of **Tapia et al. (1997)**.

The assay involves the conversion of trypsinogen secreted by AR42J cells to trypsin by enterokinase. Subsequently, the former trypsin hydrolyzes BAPNA to generate 4-nitroaniline, which is then detected at a wavelength of 405 nm. The color intensity is directly proportional to the concentration of p-NA, allowing for accurate quantification of trypsin activity. Trypsin secretion was quantified using a calibration curve established with known concentrations of trypsin, and the results are expressed in units of trypsin (UT).

The cells were detached and counted as previously described. Then, they were seeded in a 24-well plate at a density of 40000 cells/well and allowed to incubate for 72h. After the first incubation, the cells were differentiated by adding 1.8 µL of dexamethasone (10^{-4} M) and incubated for 24h. Then, the cells were stimulated with 1 µL of cholecystokinin (CCK) at 0.15 M, ACE at 1 mM in RPMI medium (5 min before), and CARN at 10 mM in RPMI medium (5 min before) (**Figure 4.29**). The cells were then incubated for 1 h.

The enterokinase and BAPNA solutions were prepared by first combining 1.8 mL of $CaCl_2$ (1M) with 1.8 mL of Trizma Base solution (0.1 M). This mixture was then augmented with 120 µL of enterokinase and 9 µL of BAPNA. For the preparation of the standard curve, a known trypsin solution (10 U/µL) was utilized to prepare different concentrations ranging from 0 to 50 through dilution with Na-Hepes solution 1X.

In a 96-well plate, 25 µL each of the BAPNA and enterokinase solutions were combined and incubated for 10 min. Subsequently, 150 µL of each sample was added. The absorbances at 405 nm were then measured every 5 min over a period of 60 min using a microplate reader (CLARIO Star Plus, BMG LABTECH, Germany). The results were expressed as a unit of trypsin secreted by cells.

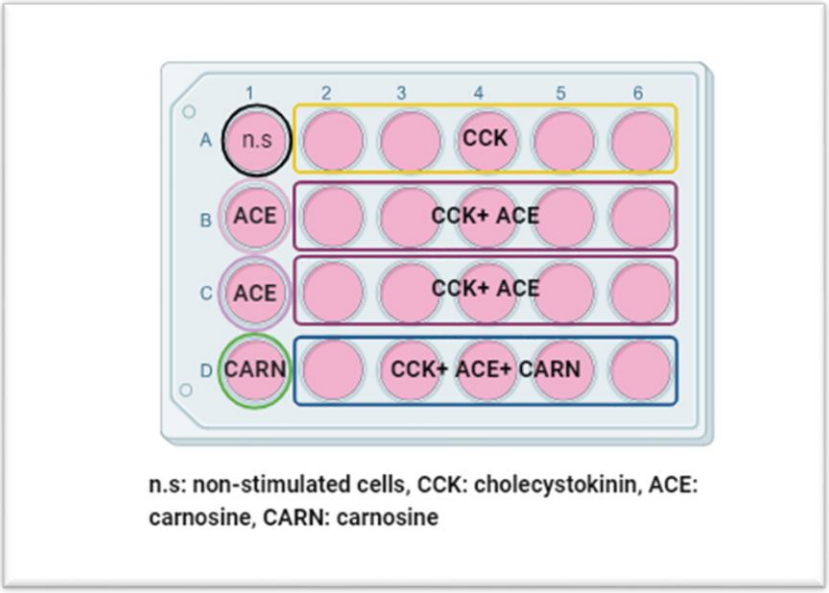

Figure 4.29 AR42J cells with different stimuli in 24 wells plate (created with BioRender)

4.5 Statistical analysis

All statistical analyses for this study were performed using Prism version 8.0.2 for Windows (GraphPad Software, La Jolla, California, USA). The normal distribution of the data was verified using the Shapiro-Wilk test and the assumption of equal variance was verified using Levene's test. The Statistical differences between groups were estimated by one-way analysis of variance (ANOVA) and Tukey's multiple comparisons, while the tests and statistical differences between individual treatments were estimated by Student's t-test. The statistical significance level for significant findings was determined as $P \leq 0.05$ and data were presented as mean values ± SD.

The results were considered to be significant (*) if the P value fell within the range of 0.01 to 0.05, highly significant (**) if it ranged from 0.01 to 0.001, and extremely significant (***) (***) if the P value was between 0.001 to 0.0001, respectively.

CHAPTER 5

RESULTS

CHAPTER 5

RESULTS

5.1 *In-vivo* study

5.1.1 Clinical signs of toxicity

During this experimentation, noticeable clinical signs of ACE toxicity were observed following ACE administration. The evident symptoms included piloerection, which was displayed by the erection of fur; plowing manifested as nose plowing through the cage bedding; and increased salivation after dosing. Challenges during handling and dosing, trembling, and hair loss were also reported. These clinical signs were consistently observed in both groups treated with ACE (III and IV). In contrast, no similar toxicity signs were detected in the groups treated with CARN (II, V, and VI).

5.1.2 Body weight and PSI

The body weight of each animal was measured before sacrifice to calculate PSI. The variations in body weight (g) between the different groups studied are illustrated in **Figure 5.1.** The body weight of all treated groups (groups III, V, IV, and VI) was extremely decreased compared to the control group (I) ($p < 0.0001$). In the groups treated with both ACE and CARN (V and VI), it was noted that CARN did not significantly prevent body loss compared to those receiving ACE treatment alone (III and V).

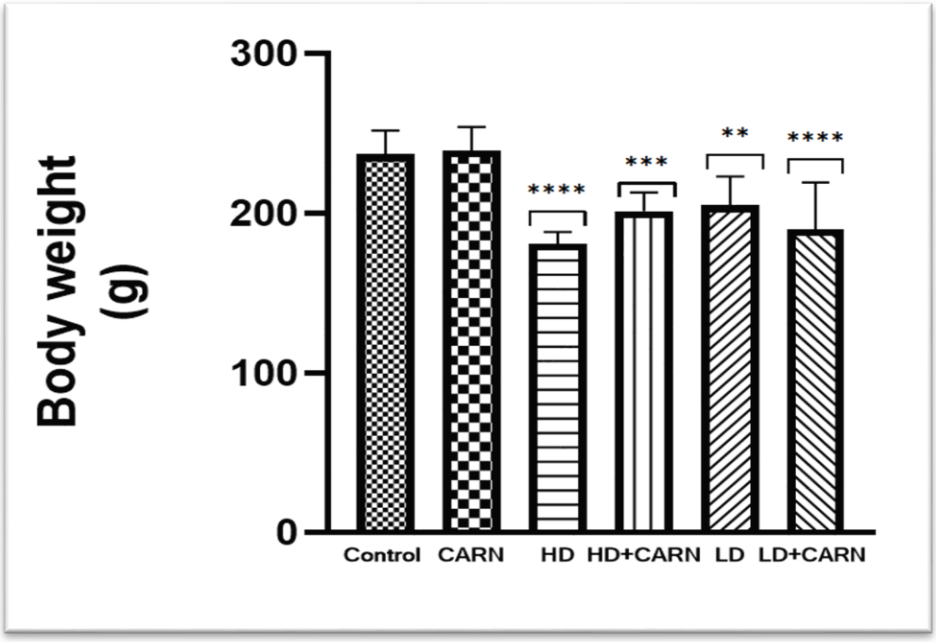

Figure 5.1 The effect of ACE and CARN doses on body weight in experimental groups compared to a control group (**p < 0.01, ***p < 0.001, and ****p < 0.0001)

Figure 5.2 represents the PSI (%) of the different groups used. Both doses of ACE (groups III and IV) exerted an extremely significant decrease in PSI compared to the control (group I) with $p < 0.001$. In contrast, the groups treated with both ACE and CARN (groups V and VI) showed an insignificant decrease in PSI compared to the control ($p > 0.06$). This indicates that CARN may have a preventative effect against the decrease in PSI caused by the two doses of ACE, especially when the prevention of CARN was highly significant between the lowest dose of ACE alone (IV) alone compared to the same dose of ACE with CARN administration (VI) ($p < 0.001$).

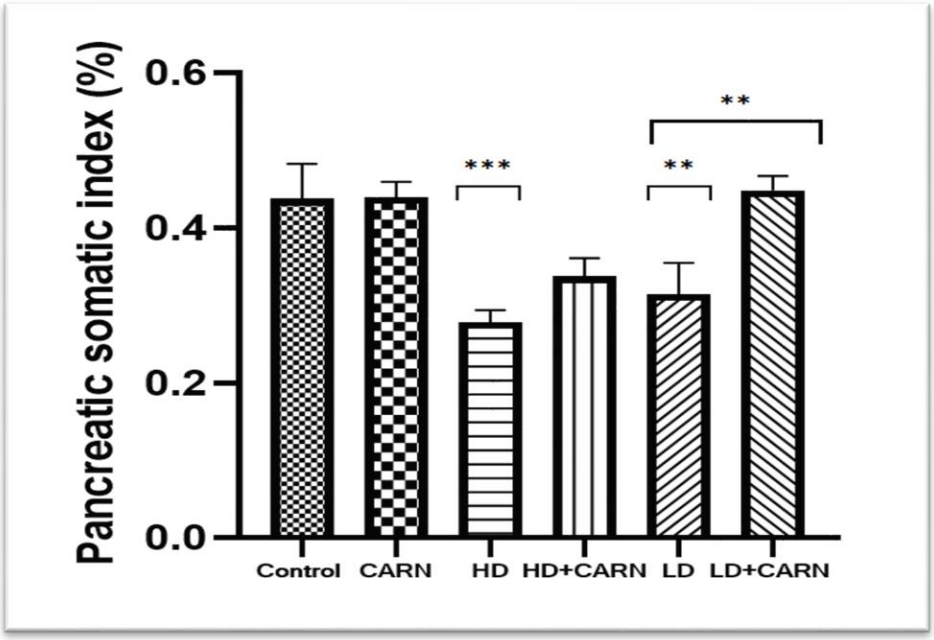

Figure 5.2 Pancreatic somatic index (PSI) of male Wistar rats after ACE and CARN administration **p value < 0.01, and ***p value < 0.001

5.1.3 Biochemical dosage

The effect of subacute ACE toxicity on exocrine pancreatic secretion was assessed. Amylase, lipase, and blood glucose levels were measured. In addition, the preventive effect of CARN administration against ACE toxicity was examined. Indeed, no significant changes were observed between the CARN and the control group (I *vs.* II) across all the biochemical analyses.

5.1.3.1 Blood glucose level

The blood glucose level (g/L) of all groups is represented in **Figure 5.3**. The highest dose of ACE, whether administered alone or with CARN (groups III and V), significantly increased blood glucose levels compared to groups (I and II) ($p \leq 0.001$). Conversely, the lowest dose of ACE, either alone or with CARN, caused an insignificant increase in blood glucose level ($p = 0.06$). Furthermore, CARN administration slightly reduced blood glucose levels in the groups treated with both ACE and CARN compared to those treated with ACE alone. This observation suggests that CARN may have a preventative role against ACE-induced hyperglycemia.

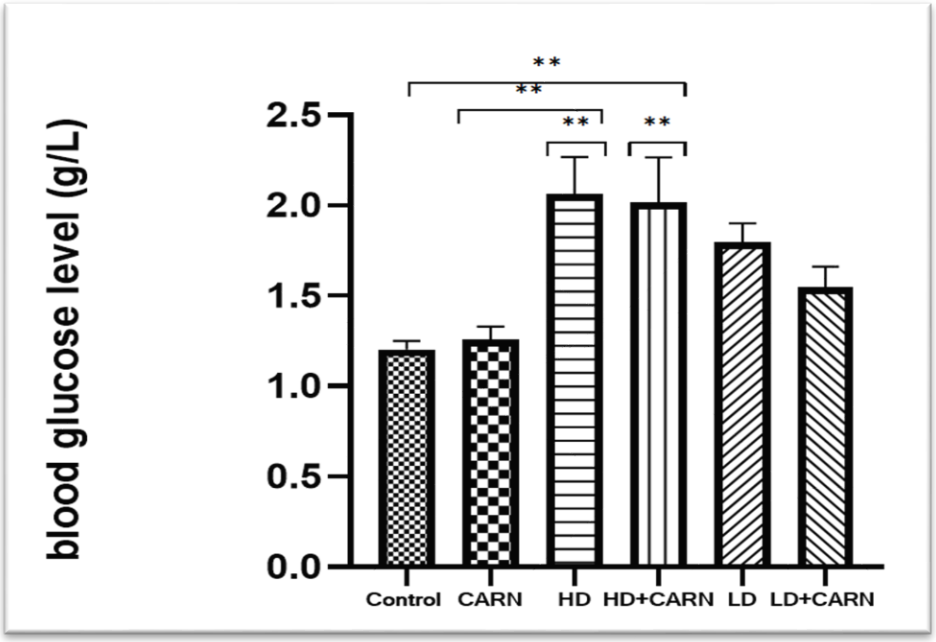

Figure 5.3 Blood glycose level (g/L) in treated male Wistar rat with ACE and/or CARN

**p < 0.001 as a significant difference in comparison to the control group and between groups.

5.1.3.2 Amylase level

The amylase level (U/mL) of all groups is shown in **Figure 5.4**. Both the highest and the lowest dose of ACE, administered either alone or with CARN (groups III, V, IV, and VI), affected an extremely significant decrease in amylase levels ($p \leq 0.001$), with the greatest reduction observed in HD+ACE group ($p \leq 0.0001$) compared to control. Simultaneously, the HD+CARN group (V) showed a significant increase in amylase levels compared to the HD group (III) ($p < 0.001$). This suggests that CARN may have a preventative effect against the ACE-induced reduction in amylase levels.

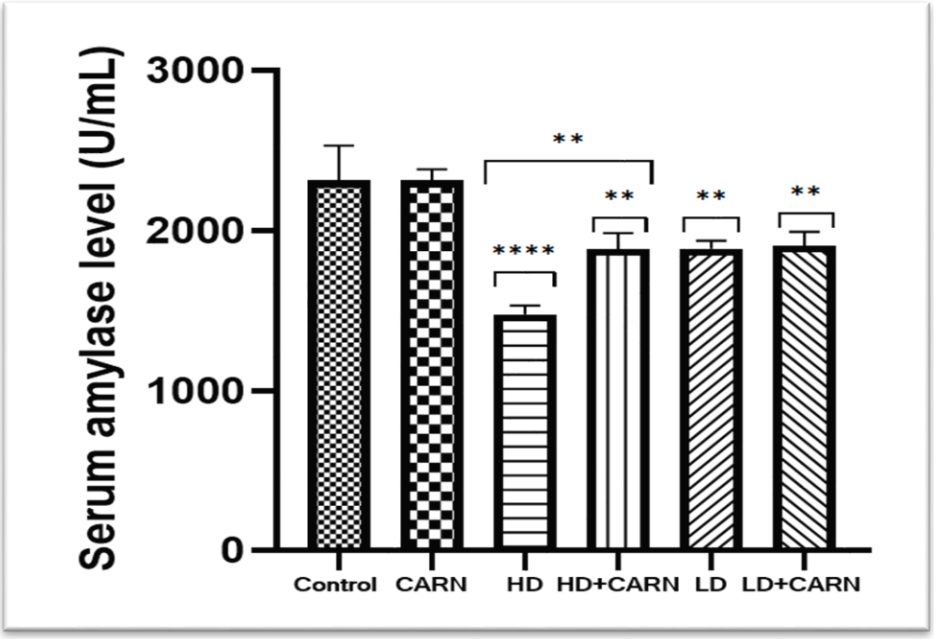

Figure 5.4 Serum amylase levels (U/mL) in response to ACE and CARN treatments

**p < 0.001, ****p < 0.0001 as a significant difference in comparison to the control group and between groups.

5.1.3.3 Lipase level

Figure 5.5 illustrates the lipase levels (mU/mL) across all groups. Both the highest and the lowest dose of ACE, administered either alone or with CARN (groups III, V, IV, and VI), caused an extremely significant increase in lipase levels ($p \leq 0.0001$) compared to Group I (control). Simultaneously, a significant decrease in lipase levels of ACE + CARN groups (V and VI) was observed compared to ACE groups (III and IV) ($p < 0.05$). This indicates that CARN may exert a preventative role in mitigating the ACE-induced increase in lipase levels.

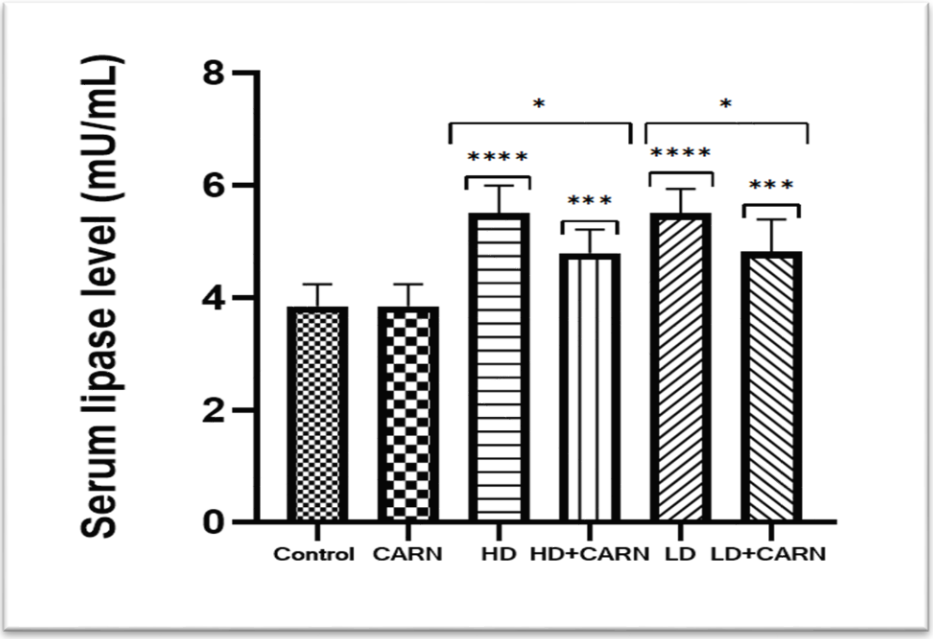

Figure 5.5 Serum lipase level (mU/mL) in response to ACE and CARN treatments

*p < 0.05, ***p < 0.001, ****p < 0.0001 as significant difference in comparison to control group and between groups.

5.1.3.4 MDA level in pancreatic tissue

As shown in **Figure 5.6**, MDA levels significantly increased in the groups treated with HD, LD, and HD+CARN (Groups III, IV, and V) compared to the control group (Group I) ($0.01 < p < 0.0001$). Although the administration of CARN did not result in a statistically significant effect. However, it showed a noticeable trend toward preventing the increase in MDA levels in the ACE+CARN-treated groups compared to those treated with ACE alone. This observation implies that CARN may exert a preventive effect against the ACE-induced elevation of MDA levels in pancreatic tissue homogenates.

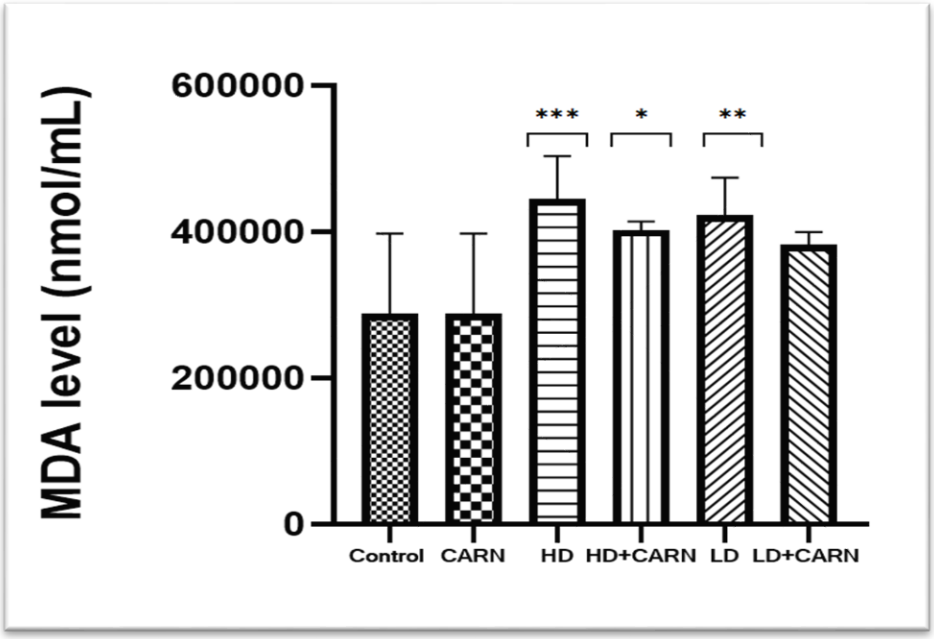

Figure 5.6 MDA level of pancreatic tissue homogenate (nmol/mL)

*p < 0.01, **p < 0.001, ***p < 0.0001 as significant difference in comparison to control group.

5.1.4 Histological evaluation and scoring

Histopathological analysis of pancreatic sections was performed using hematoxylin and eosin (H&E) staining to ensure a detailed examination of the tissue. Both the control and CARN groups exhibited typical acinar cells and intact Langerhans islets (**Figure 5.7**).

The histological scoring of pancreatic alterations induced by ACE administration is summarized in **Table 5.1.**

The appearance of moderate interlobular and intralobular edema (score 2) was extremely significant in the highest dose of ACE (III) ($p < 0.0001$). Additionally, interlobular edema (score 1) was extremely significant in the HD+CARN, LD, and LD+CARN groups (Groups IV, V, and VI, respectively) when compared to the control ($p < 0.0001$).

Furthermore, moderate perivascular and slightly diffuse infiltration (score 2) was observed to be extremely significant in the highest dose of the ACE group (Group III)

($p < 0.0001$). In contrast, scarce perivascular infiltration (score 1) was significant in the HD+CARN group ($p < 0.01$) but insignificant in the LD and LD+CARN groups compared to the control.

The presence of less than 25% of vacuolated acinar cells was highly significant in the groups treated with the highest dose of ACE alone or with CARN (Groups III and V) ($p < 0.001$ and $p < 0.01$, respectively), While this observation was insignificant in the groups treated with the lowest dose of ACE alone or with CARN (Groups IV and VI) ($p > 0.06$).

Table 5.1 Histological scoring of pancreatic damage of male Wistar rats treated with ACE alone or with CARN for consecutive 30 days

Group	Edema	Inflammatory infiltration	Vacuolization
Control	0 ± 0	0.1 ± 0	0 ± 0
CARN	0.1 ± 0	0 ± 0	0 ± 0
HD	1.79 ± 0.23 [c]	1.89 ± 0.35 [c]	1.35 ± 0.38 [b]
HD+CARN	1.36 ± 0.22 [c]	1.11 ± 0.26 [a]	0.90 ± 0.24 [a]
LD	1.21 ± 0.24 [c]	0.85 ± 0.25	0.65 ± 0.19
LD+CARN	0.89 ± 0.18 [c]	0.78 ± 0.22	0.55 ± 0.15

[a]p value < 0.01, [b]p value < 0.001, [c]p value < 0.0001 as a significant difference in comparison to the control group.

Subsequently, several histological lesions were observed in the group that received the highest dose of ACE (Group III). These included the following: hyperplasia, hypertrophy, and atrophy of acinar cells and a reduction in the number of Langerhans islets, and zymogen granules (**Figure 5.8**).

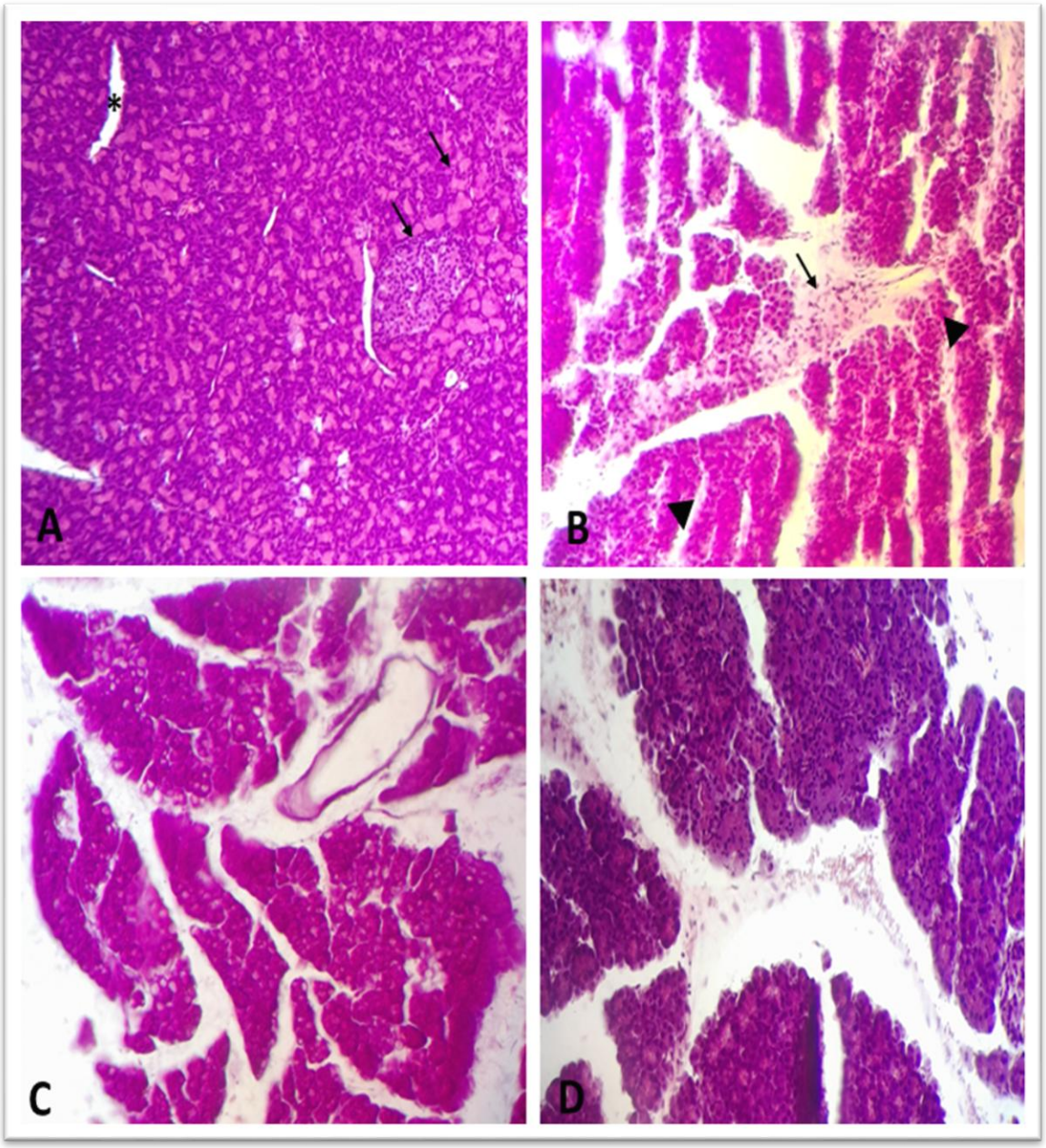

Figure 5.7 Histological findings of pancreatic tissue stained with hematoxylin-eosin (X 100). A) Normal pancreatic tissue displaying an intralobular pancreatic duct (star), along with acini and endocrine islets (arrows). B) pancreatic tissue showing interlobular (arrow) and intralobular (arrowhead) edema. C) Vacuolization of acinar cells. D) lobular atrophy with a decrease in the number of zymogene granules in treated groups with ACE.

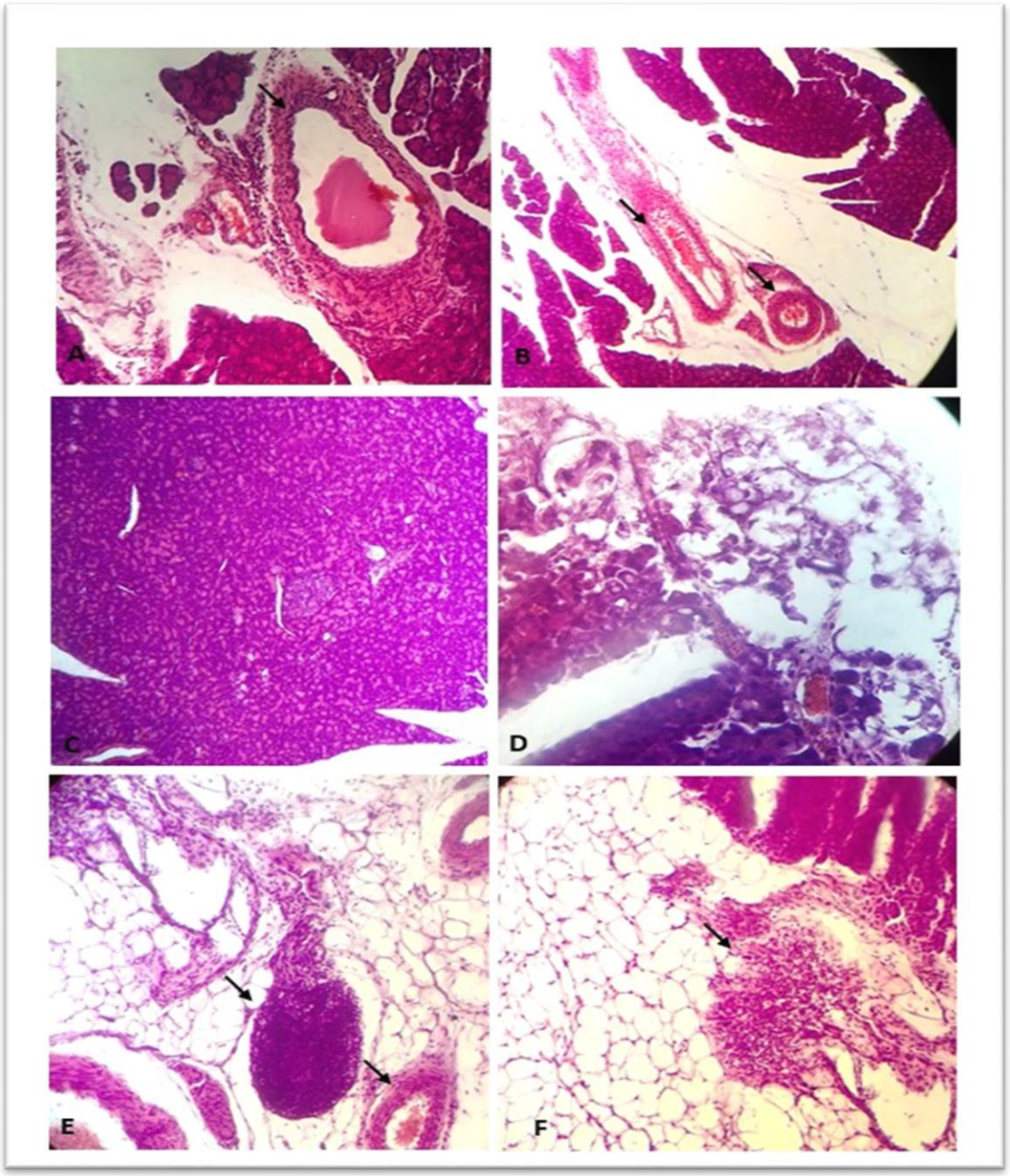

Figure 5.8 Histological alterations observed in the group treated with the highest dose of ACE (H&E staining, X100, X400). (A) Canal dilatation (arrow). (B) Vascular congestion (arrows). C) Acinar cells hyperplasia. (D) Focus of atrophied acinar cells with increased basophilia. (E) Peripancreatic lymphadenopathy with vascular congestion(arrows). (F) Inflammatory infiltration in pancreatic parenchyma (arrow).

5.2 *In-Vitro* study

5.2.1 Cell culture

After incubation, AR42J cells were used for experiments upon reaching 60-70 % confluency every 5-6 days (**Figure 5.9**). Differentiation into the exocrine phenotype was performed using dexamethasone 24 h before measurement of free-calcium concentrations and trypsin secretion (**Figure 5.10**).

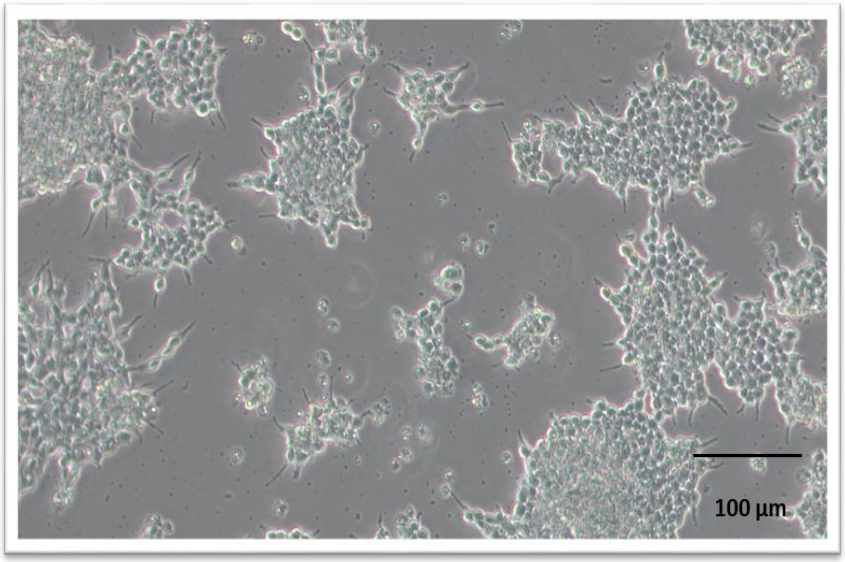

Figure 5.9 AR42J cells at desired confluence

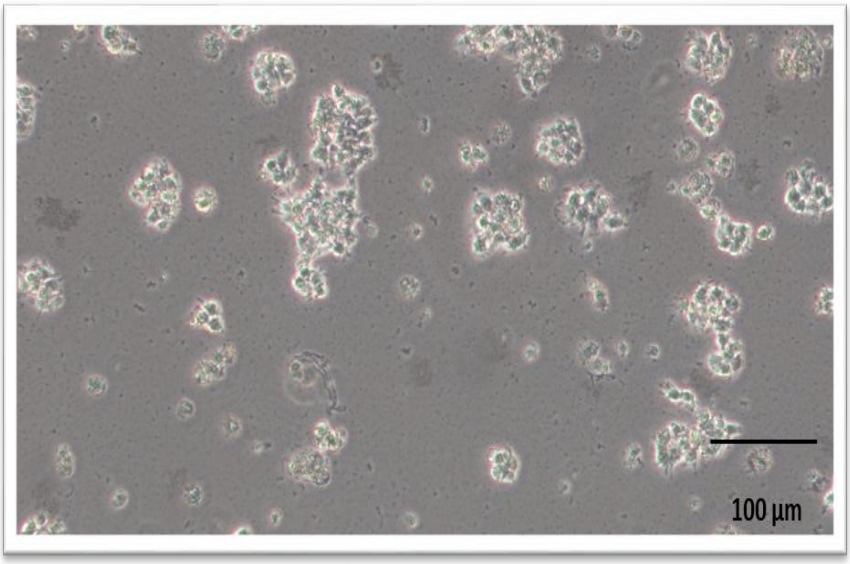

Figure 5.10 Exocrine phenotype of AR42J cells treated with dexamethasone

5.2.2 Cell viability

To investigate the effect of ACE and CARN on the viability of AR42J cells, a kinetic analysis was performed involving various concentrations. Staurosporine (stauro) at 2 µM served as a positive control to induce apoptosis in AR42J pancreatic cells.

ACE concentrations ranging from 0.1 to 100 µM did not significantly affect AR42J cell viability at 24-, 48-, and 72-hours post-treatment. Notably, only the positive control treatment demonstrated significant effects ($p < 0.05$) compared to the non-stimulated cells (n.s.), as illustrated in **Figure 5.11**.

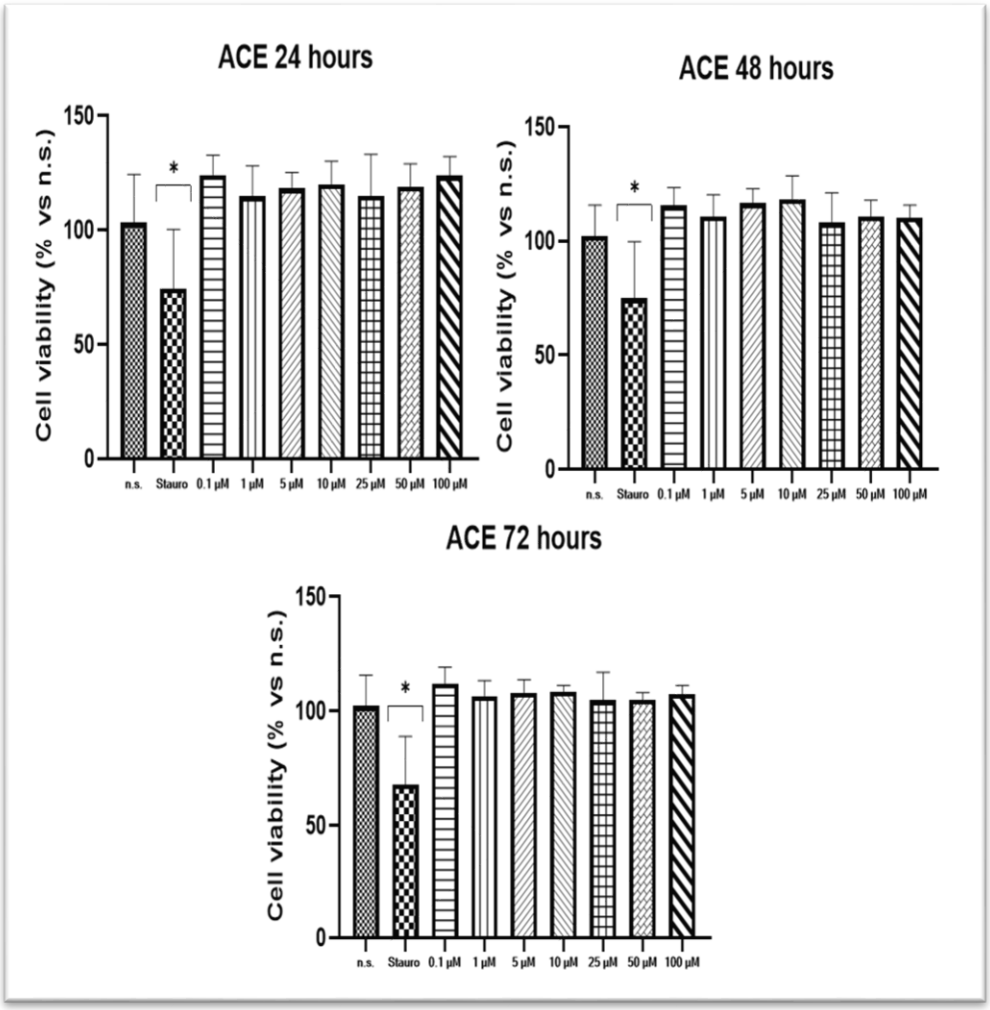

Figure 5.11 AR42J cell viability via treatment with different concentrations of ACE

*p < 0.05 as a significant difference in comparison to non-stimulated cells.

However, treatment with 50 mM of CARN induced cell death in AR42J cells after 24 hours, whereas 10 mM of CARN did not cause any notable changes in cell viability at the same time points (**Figure 5.12**).

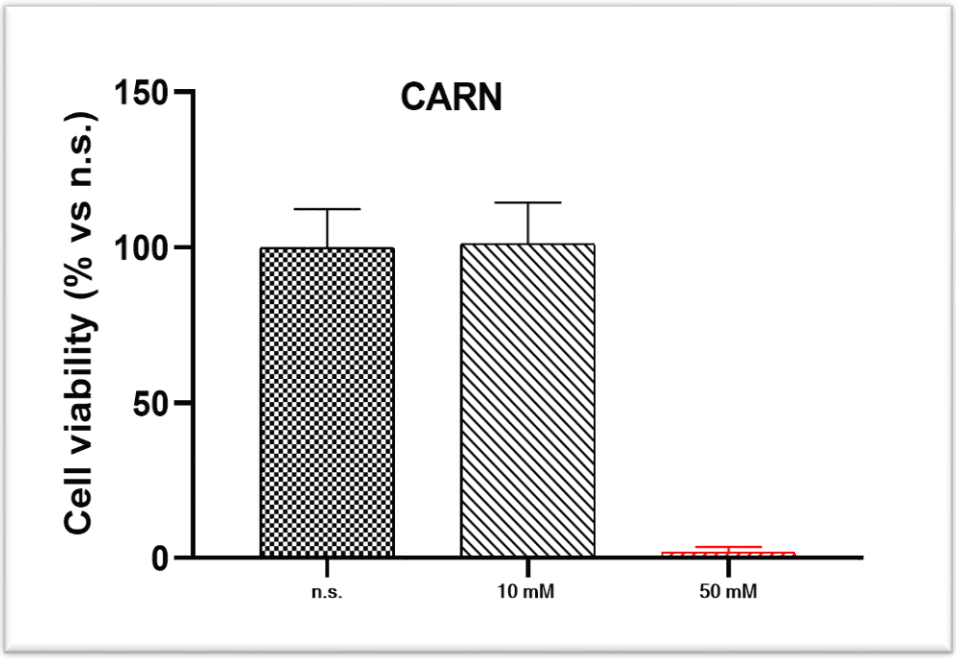

Figure 5.12 AR42J cell viability after treatment with CARN

Furthermore, ACE concentrations ranging from 0.5 to 2 mM exhibited an extremely significant increase in AR42J cell proliferation at 24-, 48-, and 72-hour post-treatments ($0.05 < p < 0.001$). Conversely, ACE at 4 -10 mM showed an extremely significant decrease in AR42J cell viability ($p \leq 0.001$). While treatment with Stauro was significant ($0.05 < p < 0.001$) compared to the non-stimulated cells (n.s.), as illustrated in (**Figure 5.13**).

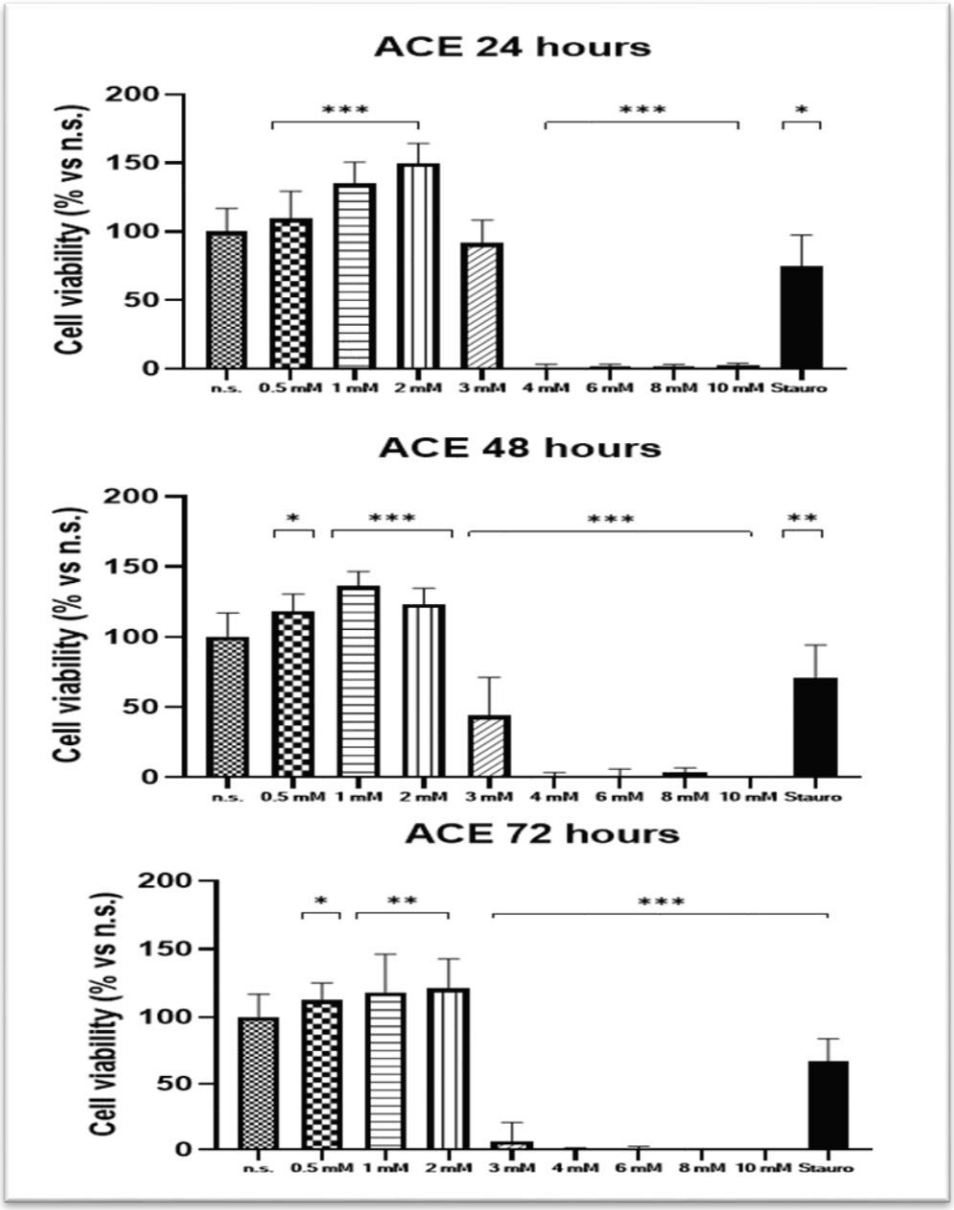

Figure 5.13 AR42J cell viability after ACE treatment with various concentrations

*p < 0.05, **p < 0.001, ***0.001 <p< 0.0001 as significant difference in comparison to non-stimulated cells.

Following these significant findings, further investigation was conducted into the cell viability of AR42J cells using a combination of ACE at 0.5-4 mM and 10 mM of

CARN treatment. The aim was to explore whether CARN could potentially mitigate the adverse effects of ACE.

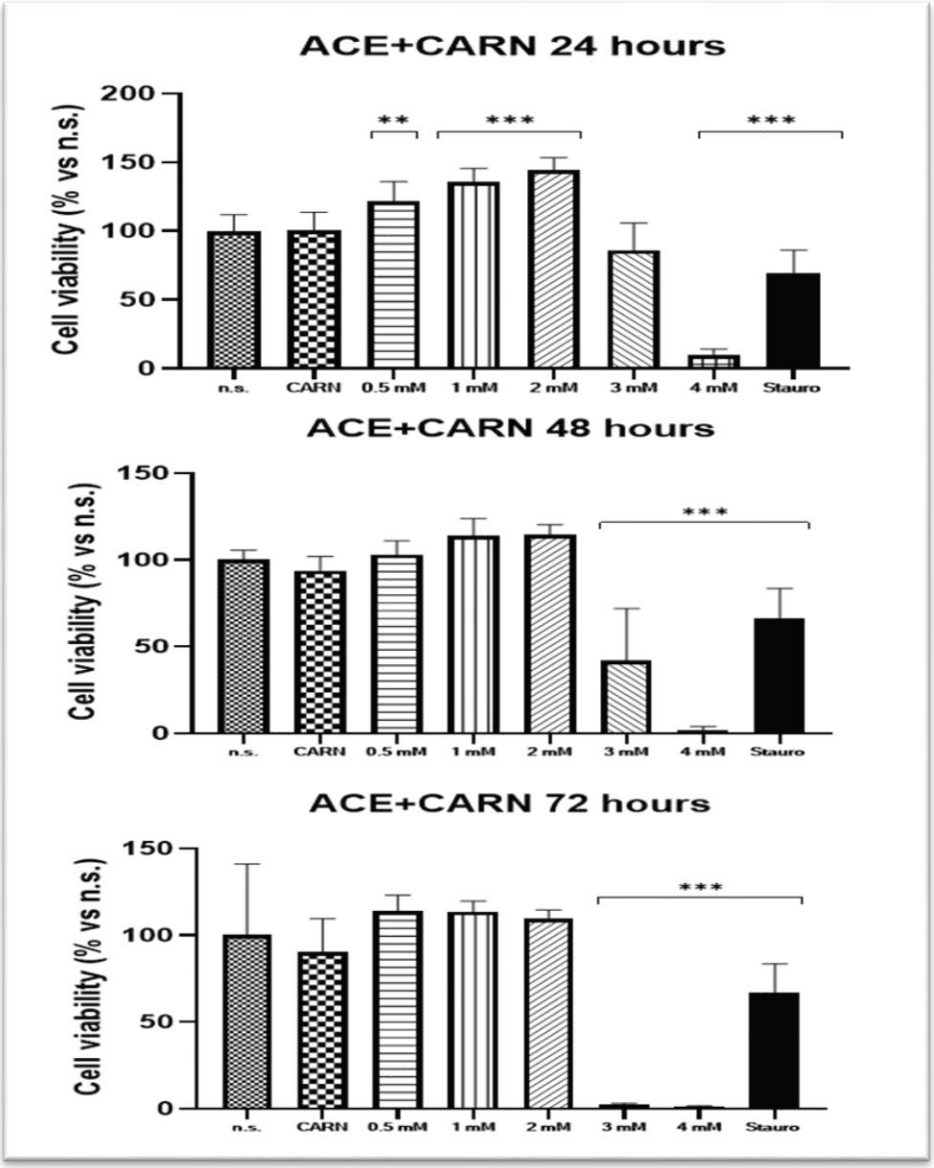

Figure 5.14 AR42J cell viability following combination treatment with ACE and CARN

**p < 0.001, ***0.001 < p < 0.0001 as significant differences in comparison to non-stimulated cells.

The co-treatment of AR42J cells with ACE and CARN showed a comparable effect to ACE treatment alone after 24 hours. However, beyond the initial 24-hour period, CARN

reduced AR42J cell proliferation caused by ACE at concentrations ranging from 0.5 to 2 mM, suggesting a preventive effect of CARN administration. Conversely, CARN did not mitigate the decrease in cell viability observed at concentrations of 3 and 4 mM which were extremely significant compared to non-stimulated cells ($p < 0.001$) (**Figure 5.14**).

5.2.3 Quantification of proteins by Western blotting

To deeply understand the intracellular mechanisms involved in response to ACE and CARN administration in AR42J cells, we investigated the phosphorylated form of MAPKs pathways, namely p44/42, p38, and JNK. ß-actin was used as a loading control.

The phosphorylation of p44/42 was highly significant ($p < 0.01$) at 3 mM of ACE and in the presence of staurosporine. However, the combination of ACE with CARN across all tested concentrations (i.e., 0.5-3 mM) significantly showed a high decrease in p44/42 phosphorylation in pncreatic AR42J cells compared to the non-stimulated cells ($0.05<p < 0.01$), as shown in **Figure 5.15**.

Yet, ACE treatment at 2 and 3 mM significantly increased the phosphorylation form of p38, similar to staurosporine ($0.05<p < 0.001$), compared to the non-stimulated cells. In contrast, the combined treatment with ACE and CARN at 1-3 mM led to a highly significant decrease in the phosphorylated form of p38 ($0.001<p < 0.0001$), as depicted in **Figure 5.16**.

On the other hand, the phosphorylated form of JNK was significantly increased in response to ACE treatment at 3 mM and staurosporine ($p < 0.05$), when compared to non-stimulated AR42J cells. The combination of ACE and CARN did not affect significant changes at all tested concentrations (**Figure 5.17**).

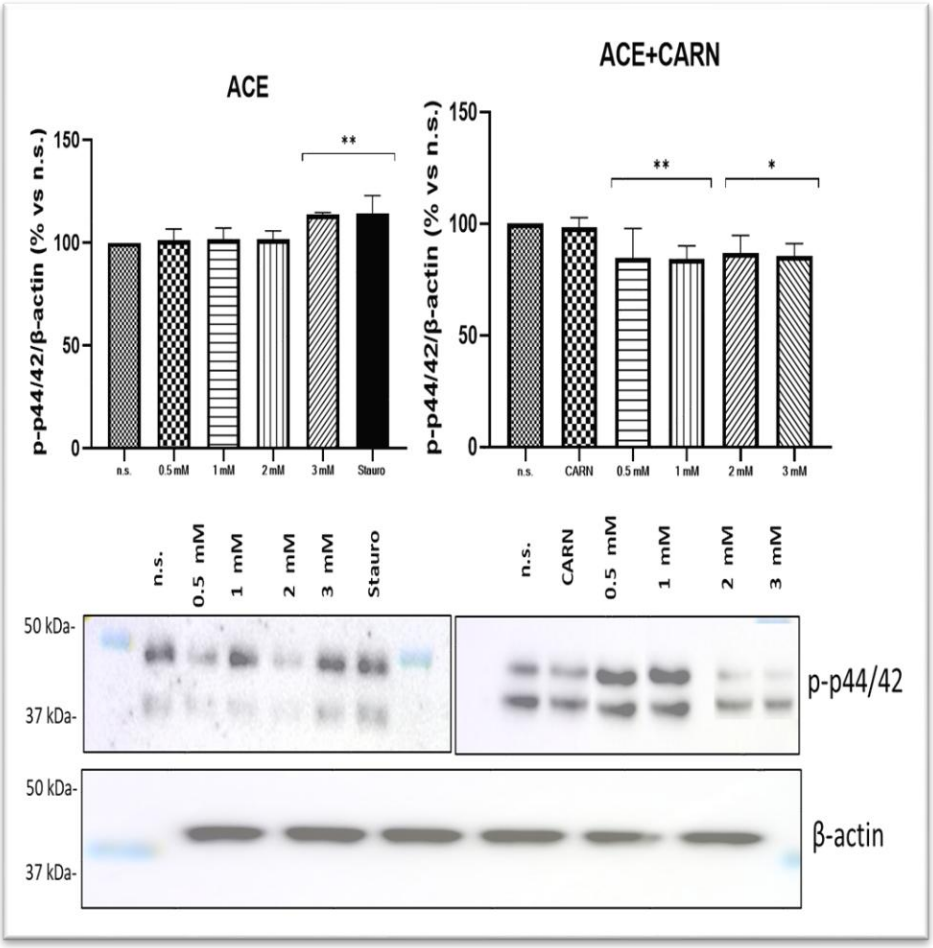

Figure 5.15 Effect of ACE and/or CARN administration on the expression of the phosphorylated form of p44/42

*p < 0.05, **p < 0.01, as significant difference in comparison to non-stimulated cells.

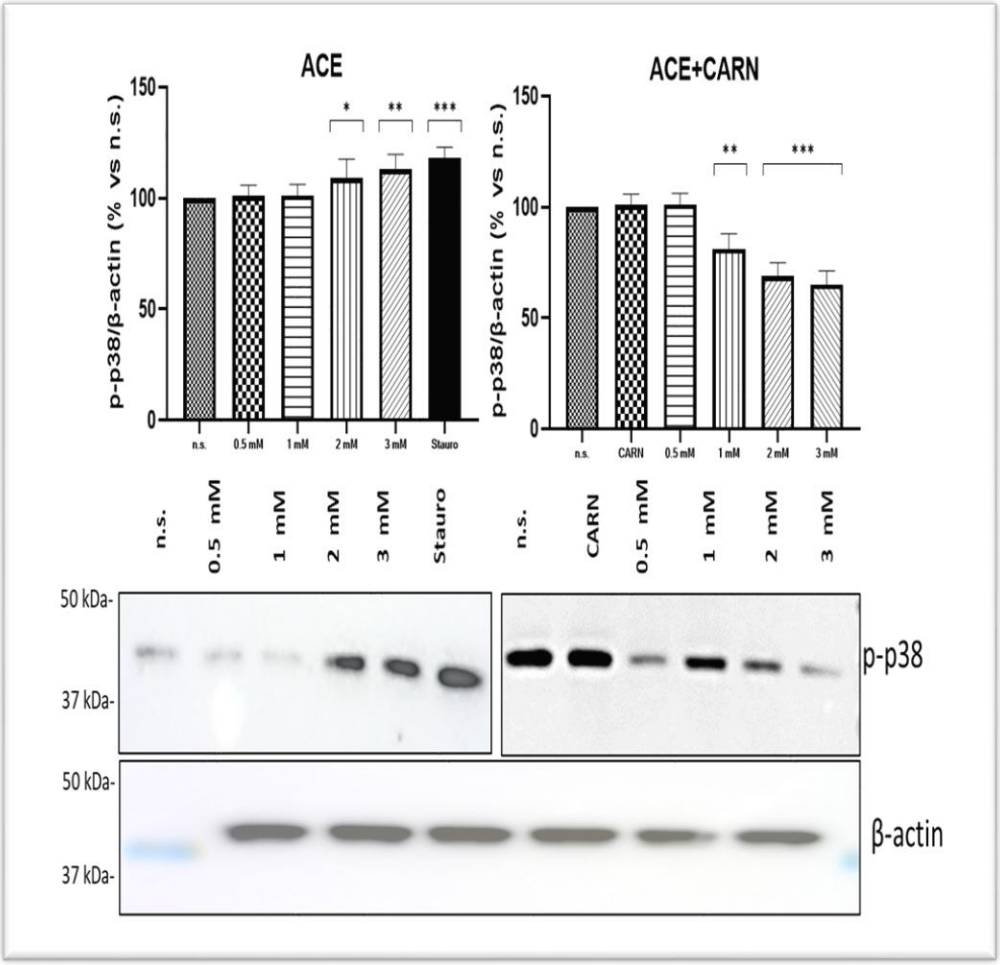

Figure 5.16 Effect of ACE and/or CARN administration on the expression of the phosphorylated form of p38

*p < 0.05, **p < 0.01, ***p < 0.0001 as significant difference in comparison to non-stimulated cells.

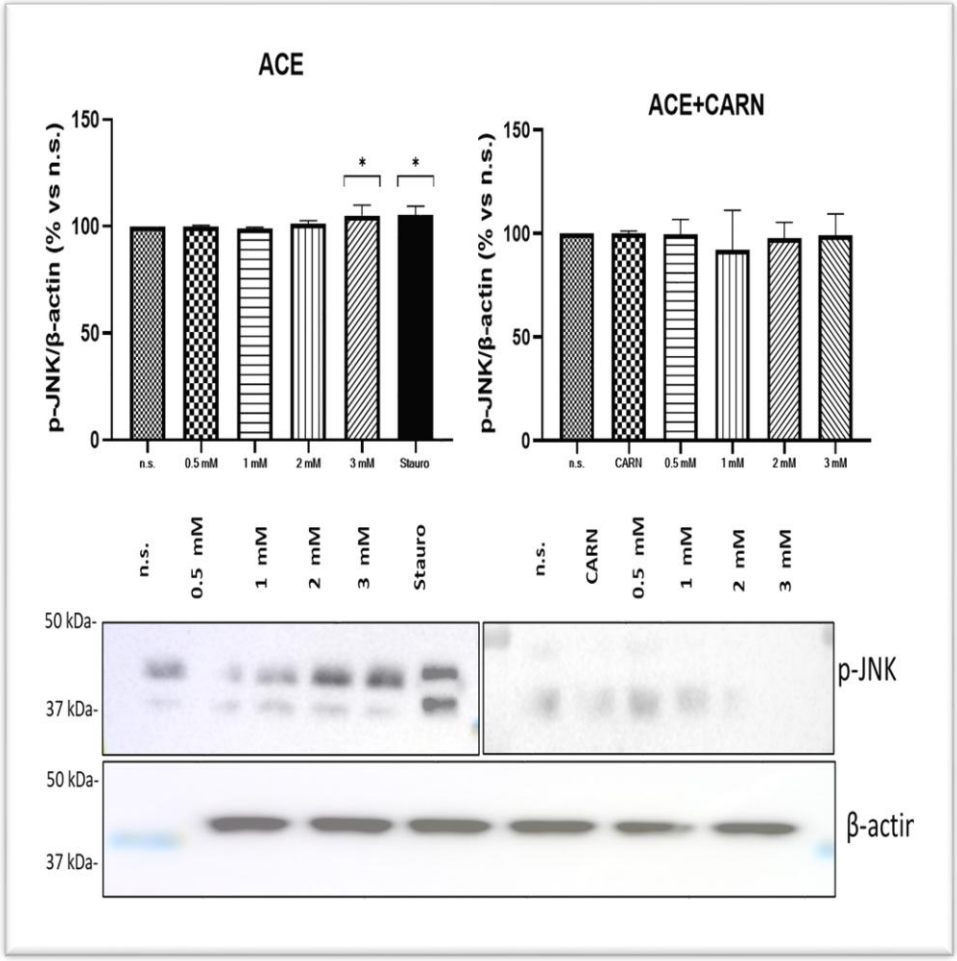

Figure 5.17 Effect of ACE and/or CARN administration on the expression of the phosphorylated form of JNK

*$p < 0.05$ as a significant difference in comparison to non-stimulated cells.

5.2.4 Calcium mobilization

Since Ca^{2+} mobilization plays a crucial role in regulating the physiology of pancreatic cells, we aimed to investigate whether ACE influences $[Ca^{2+}]_i$ in AR42J cells using Fura-2/AM (**Figure 5.18**).

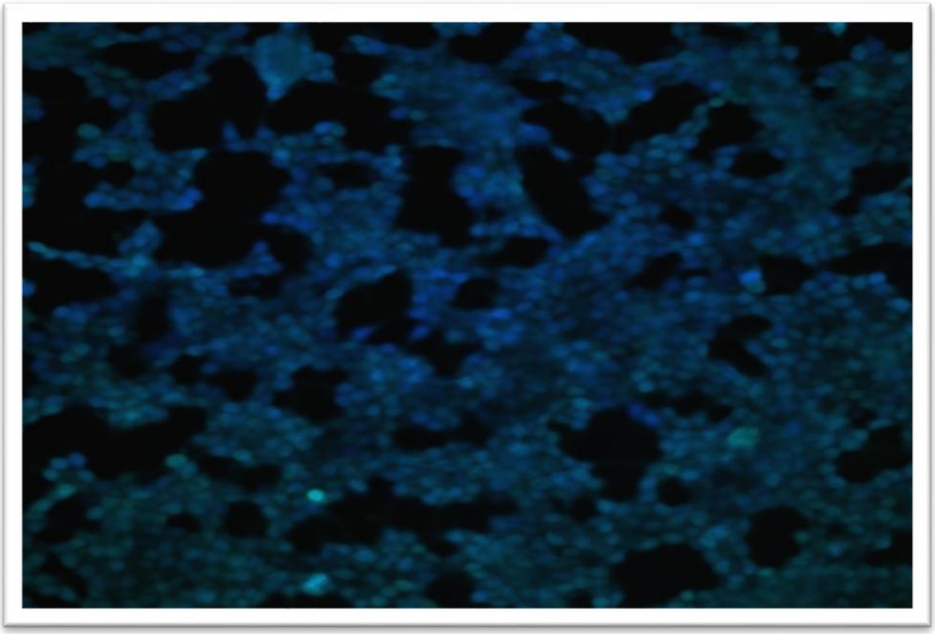

Figure 5.18 Fura-2/AM Fluorescence in AR42J Cells (20X)

The initial assessment of calcium mobilization was conducted using two concentrations of ACE (1 mM and 4 mM). The stimulation with 1 mM ACE resulted in a transient increase in intracellular Ca^{2+} levels ($[Ca^{2+}]_i$, followed by stabilization at a level that was slightly elevated compared to the baseline (pre-stimulation), as demonstrated in (**Figure 5.19A**). However, the stimulation of the cells with 4 mM ACE provoked a significant release in $[Ca2+]_i$ (**Figure 5.19.B**), indicating that this concentration induced direct cell death.

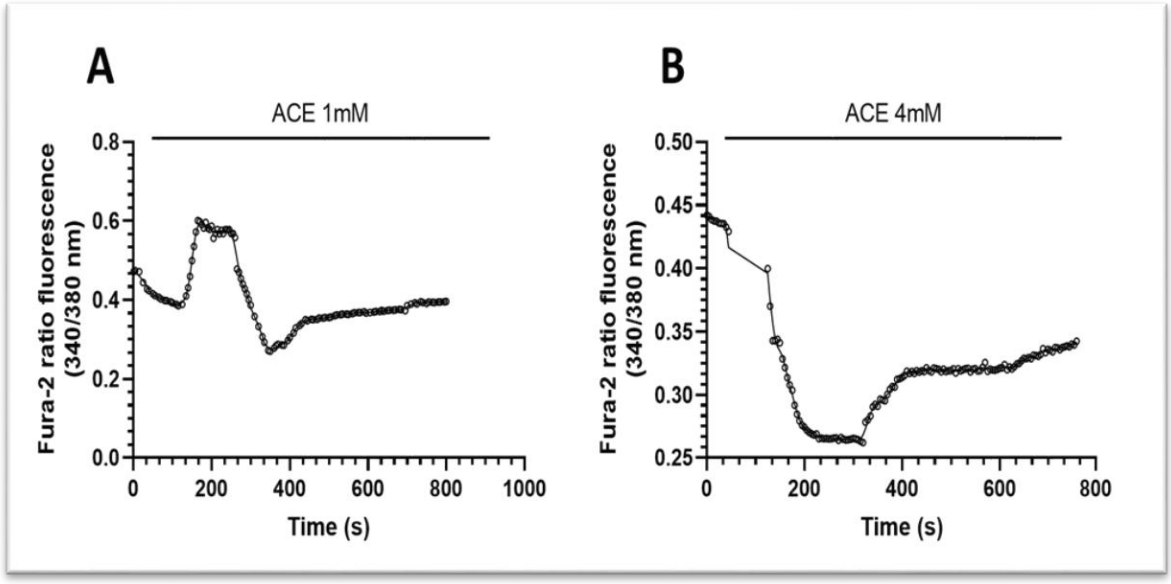

Figure 5.19 Variations in [Ca2+]i levels in AR42J cells following exposure to ACE. A) changes in fura-2 ratio fluorescence in AR42J cells treated with 1 mM of ACE. B) changes in fura-2 ratio fluorescence in AR42J cells treated with 4 mM of ACE.

Afterward, we examined the source of Ca^{2+} mobilization influenced by 1 mM of ACE. For this purpose, the cells were treated with ACE and Thapsigargin (Tps), a sarcoendoplasmic reticulum Ca^{2+} ATPase (SERCA) inhibitor, in a Ca^{2+} free medium. Similar to the earlier experiment, 1 mM of ACE induced an elevation in $[Ca^{2+}]_i$, which subsequently reverted to a consistent value above the initial (pre-stimulation) level (**Figure 5.20.A**). Stimulation with 1 µM of Tps alone, resulted in a marked elevation in $[Ca^{2+}]_i$ by depleting functional Ca^{2+} stores (**Figure 5.20.B**). Following the addition of 1 µM Tps after stimulation with 1 mM ACE, a transient and modest increase in intracellular Ca2+ levels ($[Ca^{2+}]_i$) was observed, which subsequently declined to a steady level above the baseline (**Figure 5.20.C**). When cells were further treated with 1 Mm ACE after the SERCA inhibitor, there was no additional Ca2+ mobilization (**Figure 5.20.D**).

Furthermore, cumulative Ca^{2+} mobilization in response to ACE was significantly reduced in the absence of extracellular Ca^{2+} compared to its presence ($P < 0.05$), as shown in (**Figure 5.21.A)**. Moreover, the cumulative Ca^{2+} mobilization in response to Tps alone or following ACE treatment indicated a significant difference, with greater

mobilization observed in response to Tps alone ($P < 0.001$) (**Figure 5.21.B**). These findings indicate that ACE-induced Ca^{2+} mobilization originates from intracellular sources, and that ACE facilitates Ca^{2+}release from Tps-sensitive stores.

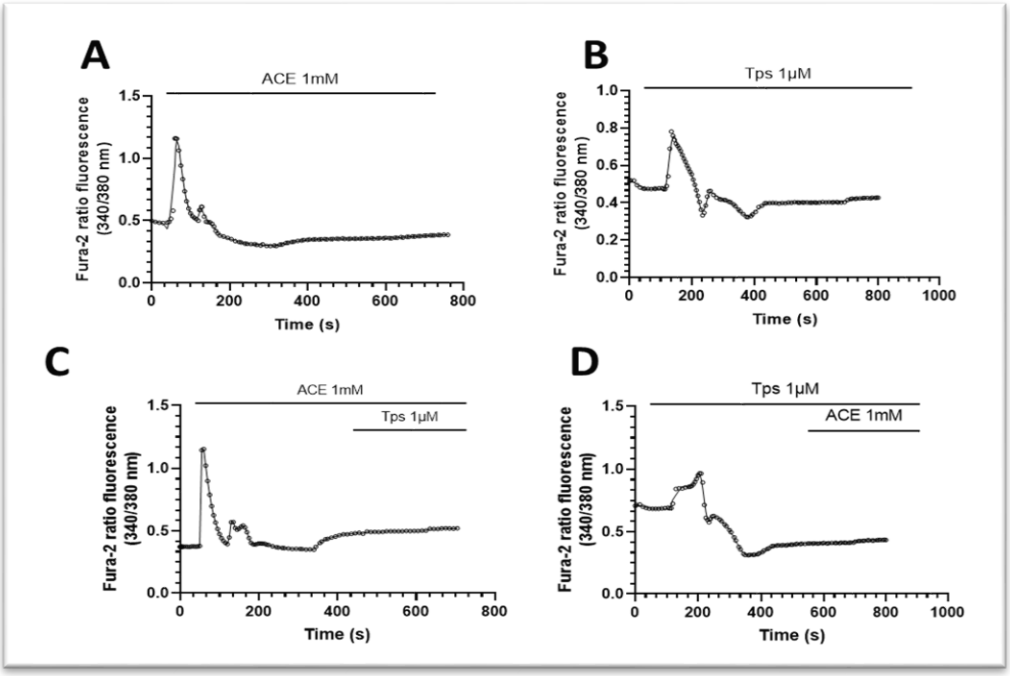

Figure 5.20 Variations in [Ca2+]i levels in AR42J cells following exposure to ACE and Tps. A) changes in fura-2 ratio fluorescence after treatment with ACE. B) changes in fura-2 ratio fluorescence after treatment with Tps. C) changes in fura-2 ratio fluorescence after treatment with Tps following ACE. D) changes in fura-2 ratio fluorescence after treatment with ACE following Tps.

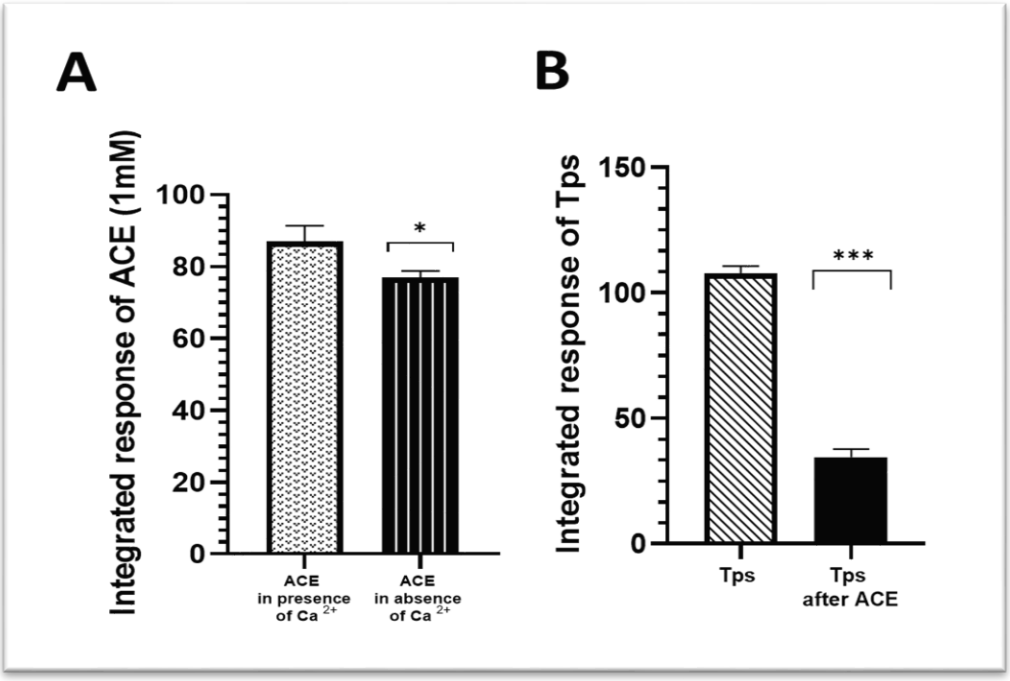

Figure 5.21 Total calcium mobilization in AR42J cells after exposure to ACE and Tps. A) The integrated response of the increase in [Ca2+]i following the addition of ACE in the presence and absence of Ca 2+in the media. B) the integrated response of the increase in [Ca2+]i following the addition of Tps after ACE stimulation. *p < 0.05, ***p < 0.0001 as a significant difference in comparison to the other group.

5.2.5 Trypsin secretion

To investigate the probable effect of ACE and/or CARN on digestive enzyme release, we examined the trypsin secretion in response to stimulation with CCK and combination with ACE, CARN, and CCK in the exocrine phenotype of AR42J cells. The results demonstrated that stimulation with CCK alone induced trypsin release in a concentration-dependent manner, reaching a peak at 10^{-10} M. However, co-incubation with ACE and CCK or the combination of ACE, CARN, and CCK, did not induce any significant changes in trypsin secretion compared to CCK stimulation alone, as observed in **Figure 5.22**.

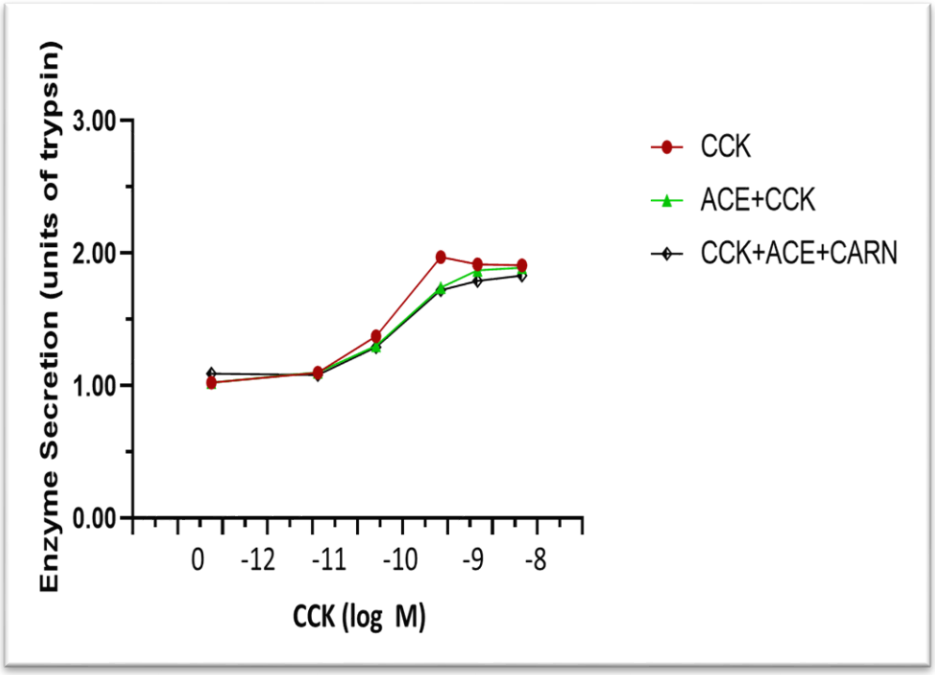

Figure 5.22 Trypsin secretion in AR42J cells after stimulation with CCK, ACE, and CARN

CHAPTER 6

DISCUSSION

CHAPTER 6

DISCUSSION

Neonicotinoid insecticides, a novel category of organochlorine pesticides structurally similar to nicotine, were developed as safer alternatives to carbamate and organophosphate compounds **(Gomez et al., 2020)**. Among these, ACE is characterized by its low environmental persistence and relatively low toxicity to mammals. Nevertheless, the widespread use of ACE has raised concerns, prompting research into its potential toxicity and adverse health impacts on mammals, including humans **(Erdemli et al., 2020)**.

CARN represents a naturally occurring dipeptide that is found in skeletal muscle. It acts as a preventive measure against several physiological functions by acting as a copper chelator, quencher of reactive oxygen and carbonyl species, and eliminator of aberrant proteins **(Aloisi et al., 2013; Barca et al., 2018; Kohen et al., 1988)**. Up to date, numerous studies have investigated its impact in various health conditions such as enhancing neural function in patients with Alzheimer's and Parkinson's diseases **(Gasmi et al., 2024; Kulikova et al., 2024; Shen et al., 2024)**, exerting an antitumor effect against colorectal and prostate cells **(Habra et al., 2024; Hsieh et al., 2024)**, and maintaining glycemic control in both *in-vivo* and *in-vitro* models **(Matthews et al., 2024)**.

However, the toxicity of the exocrine pancreas remains poorly investigated, as it is infrequently considered a target organ for chemicals **(Martínez-Morcillo et al., 2019)**. However, the disruption of exocrine secretion by xenobiotics, such as neonicotinoid insecticides, has been demonstrated to occur through the damage of the acinus and islets of Langerhans, which are responsible for endocrine secretion **(Rünzi et al., 1992; Sheets et al., 2016)**. In light of this evidence, the present study was initiated with the objective of investigating the effect of ACE on exocrine pancreatic tissue, employing both *in vivo* and *in vitro* approaches. Additionally, the potential preventive effect of CARN on exocrine pancreatic tissue was explored.

Our *in-vivo* findings reflected the toxic effect of ACE on the exocrine pancreas of male Wistar rats. This toxicity was evident through clinical toxicological signs, in

biochemical alterations, and several histopathological changes, all observed in a correlational manner. Whereas CARN exhibited a preventive role, mitigating these adverse effects. Besides, our *in-vitro* results revealed ACE-induced toxicity, while CARN countered these effects by preserving cell viability, regulating MAPK signaling pathways, and preventing excessive intracellular calcium mobilization in AR42J cells.

6.1 Effect of ACE on clinical signs, body weight, and PSI

A deep comprehension and application of clinical toxicity signs across various animal models and research domains are essential for furnishing crucial insights into the potential side effects and hazard risks linked to the tested substance **(Silva et al., 2021)**. In the groups treated with ACE (III and IV), clinical toxicity signs observed, such as piloerection, plowing, and increased salivation, likely indicate early symptoms of toxicity and the stressful effects of this insecticide. Furthermore, these symptoms are consistent with the activation of the autonomic nervous system, influenced by ACE's binding to nAChRs.

In mice, ACE has also been reported to cause other clinical symptoms such as respiratory depression, corner-sitting behavior, and signs of depression and lethargy **(Singh et al., 2012)**. These observed behaviors further underscore ACE's potential to disrupt normal neurological function and compromise overall neurological health.

The rats treated with CARN (groups II, V, and VI) did not exhibit any signs of toxicity. This observation may be attributed to the preventive effect of CARN on the neurological system, as multiple studies have demonstrated this specific effect through complex mechanisms **(Distefano et al., 2022; Kubota et al., 2020; Shen et al., 2024; Solana-Manrique et al., 2022)**.

Furthermore, the observed decrease in body weight and PSI in ACE-treated groups could be attributed to the compound's toxicity, anorectic properties, and its stressogenic effects on the animals' growth rates. Both low (21,7 mg/kg) and high (43,4 mg/kg) doses of ACE resulted in a significant decrease in body weight and PSI, suggesting a dose-dependent effect. These findings aligns with previous studies, such as Mondal et al. **(2015)**, who reported a significant reduction in body weight in Sprague Dawley rats after 13 weeks of chronic exposure to ACE at low and high doses (5, 20, and 40 mg/kg). Similarly, sub-acute toxicity of ACE at high doses (100, and 200 mg/kg)

led to reduced body weight of Wistar rats **(Mondal et al., 2009)**. Singh et al. **(2012)** also documented A comparable effect in mice administered a high dose of ACE (40 mg/kg) for 28 consecutive days.

The reduction in relative organ weight has been previously investigated. In a similar vein, Marzouki et al. **(2017)**, reported that administration of ACE at a low dose of ACE (5 mg/kg) provoked a decrease in relative spleen weight of male Swiss albino mice after 60-days of treatment. Hence, a reduction in relative brain weight was observed following 90 days of ACE administration at a very low dose of 3.14 mg/kg **(G. Gasmi et al., 2016)**. Additionally, the relative weight of the ovaries was reduced after 90 days administering imidacloprid at low dose (20 mg/kg) in female rats **(Kapoor et al., 2011)**.

While Lonare et al. **(2016)** noted a loss in epididymal weight in Wistar rats following high doses (45 and 90 mg/kg) of ACE administration for 28 consecutive days. In contrast to these results, Chakroun et al. **(2016)** observed an increase in relative liver weight in male Wistar rats treated with both low (21.7 mg/kg) and high (43.4 mg/kg) doses of ACE, indicating that the effects of ACE may be tissue-specific.

On the other hand, 200 mg/kg of CARN provided a slight preventive effect against weight loss in the body and the pancreas. Similar results were observed in the study of Kamel et al. **(2020)**, where CARN (at 250 mg/kg) protected body weight and relative testicular weight of male rats against a protein-deficient diet. Interestingly, Albrecht et al. **(2017)** reported a decrease in kidney weight ratio after 28 days of CARN treatment at 4 mM in mice with type 2 diabetes mellitus. In addition, doses of 25 and 30 mg/kg of CARN have been shown to reduce relative lung weight in male albino rats following sepsis.

Although scarce data is available on the direct impact of CARN and organ weight, its antioxidant and anti-inflammatory characteristics may indirectly aid in tissue repair and regeneration. This is consistent with findings by **Distefano et al. (2022)**, who demonstrated that CARN enhanced neuronal cell viability by counteracting the toxicity of Aß1–42 oligomers through the inhibition of insulin-degrading enzyme activity.

Moreover, CARN demonstrated anti-inflammatory effects on microglial cells by mitigating oxidative stress. This was achieved through reductions in intracellular nitric

oxide (NO) and superoxide anion (O2−•) levels, as well as the downregulation of inducible nitric oxide synthase (iNOS) and NADPH oxidase enzymes. Similarly, CARN lowered the production of pro-inflammatory cytokines such as interleukin-1ß (IL-1ß), while concurrently elevating the levels of interleukin-10 and transforming growth factor-beta 1 (TGF-ß1) **(Caruso et al., 2019)**.

6.2 Effect of ACE on enzyme pancreatic secretion

The examination of exocrine pancreatic toxicity is closely linked to the evaluation of amylase and lipase secretion, both of which are facilitated by the exocrine function of acinar cells **(Röder et al., 2016)**. These enzymes serve as crucial biomarkers for numerous pancreatic diseases (i.e., exocrine pancreatic injury and acute/chronic pancreatitis)**(Usborne et al., 2014)**. Also, glucose levels serve as a direct indicator of insulin and glucagon secretion. In the present study, a significant increase in serum lipase and glucose levels, accompanied by a decrease in amylase levels, was observed in all treated groups (III, IV, V, and VI) compared to the control group.

Several studies have aligned with these results. For instance, Khayal & Ahmed **(2019)** demonstrated that chlorpyriphos administration significantly altered pancreatic secretion leading to an elevation of lipase and glucose levels alongside a reduction in amylase levels following daily oral dosing at low dose of 6.75 mg/kg for eight weeks. In the same manner, oral gavage administration of diazinon at a high dosage of 335 mg/kg in Wistar rats resulted in decreased amylase levels and increased lipase levels **(Gokalp et al., 2005)**.

Furthermore, Mesallam et al. **(2018)** stated similar results in male albino rats after dimethoate insecticide at low dose of 20 mg/kg. Indeed, the level of serum amylase level was reduced in albino male rats following parastar administration at low dose of 6.23 mg/kg for 64 days as highlighted by Akono et al. **(2019)**. While Imizamox has been shown to raise serum glucose levels in male Sprague-Dawley rats following intraperitoneal injections at both doses of 24 and 36 mg/kg over 72 hours **(Sevim et al., 2019)**.

In this context, ACE might affect pancreatic enzyme secretions through both direct and indirect pathways, akin to other insecticides. The direct effects of ACE could involve disruptions in insulin secretion and glucose homeostasis, potentially due to

impaired ß-cell function. This is supported by the present study's findings of a reduced number of islets of Langerhans, which may contribute to hyperglycemia and insulin resistance. For instance, imidacloprid has been shown to impact insulin signaling by reducing the phosphorylated form of protein kinase B (AKT) and ribosomal S6 kinase, a downstream mediator of the AKT pathway that regulate insulin signaling—in hepatocytes, myotubes, and adipocytes **(Kim et al., 2013)**.

Indirectly, ACE could disrupt glucose homeostasis by affecting glucagon secretion. Malathion exposure has been associated with elevated voltage-gated K+ channels in both beta and alpha cells, which can disrupt the release of both glucagon and insulin **(Martins et al., 2023)**. Additionally, ACE might induce inflammation and oxidative stress in endocrine pancreatic cells, further impacting glucose homeostasis. Chronic exposure of beta cells to persistent organic pollutants can dysregulate key antioxidant enzymes, including catalase, peroxiredoxins, glutathione peroxidase, and thioredoxins. This dysregulation leads to increased ROS production, which impairs insulin secretion and exacerbates metabolic dysfunction **(Bresson & Ruzzin, 2024)**.

An interesting hypothesis suggests that ACE mimics the metabolic effects of nicotine in promoting hyperglycemia. Short-term nicotine administration to insulin-sensitive C57BL/J6 mice has been found to increase blood glucose levels and decrease insulin sensitivity, mainly due to nAChR activation and the stimulation of glycogenolysis in hepatocytes. However, chronic nicotine exposure appears to elicit contrasting effects by activating phosphatidylinositol 3-kinase signaling. This activation enhances Akt and glycogen synthase kinase (GSK-3ß) phosphorylation while decreasing cAMP response element-binding protein (CREB) phosphorylation. These molecular changes suppress the expression of critical gluconeogenic genes, such as phosphoenolpyruvate carboxykinase (PEPCK) and glucose-6-phosphatase (G6Pase), thereby mitigating hyperglycemia during prolonged exposure **(Vu et al., 2014)**.

Regarding exocrine pancreatic secretion, ACE can disrupt the secretion process. The high levels of lipase secretion might be influenced by complex neurohormonal mechanisms, including the involvement of cholecystokinin, secretin, and the cholinergic pathway **(Borovicka et al., 1997)**. Each of these molecules facilitates enzymatic secretion by binding to its cognate receptors. For instance, when CCK binds to its CCK1 receptor, it activates intracellular signaling pathways that trigger exocytosis, the

process by which enzymes are released from zymogen granules at the apical surface of acinar cells. The same is true for CCK and acetylcholine (ACh) when they interact with their respective receptors. In contrast, secretin increases the levels of intracellular cyclic AMP (cAMP) levels, which then drives the exocytosis response **(Mössner, 2010)**. On the other hand, the decreased amylase secretion could be due to enzyme retention within acinar cells or moving from the apical to the basolateral domains **(Gaisano & Gorelick, 2009)**.

To sum up, ACE such as other insecticides could alter the enzyme pancreatic secretion. However, there is limited research on the effects of ACE and other insecticides on these specific mechanisms.

Our research has demonstrated the effectiveness of 200 mg/kg of CARN in inhibiting lipase increase, enhancing amylase reduction, and having a minor effect on glycemia increase. In fact, few studies have examined these effects in adult diabetic rats, which serve as a relevant model for investigating the impact of metabolic disorders associated with diabetes, as they exhibit altered enzyme activity and glucose metabolism. In a study by Vahdatpour et al. **(2019)** and Albrecht et al. **(2017)**, CARN administration at doses of 100 and 200 mg/kg was shown to prevent elevated blood glucose, enhancing ß-cell function, and lowering hemoglobin A1C. At the cellular level, CARN was found to lower the levels of Insulin-like Growth Factor Binding Protein 1 (IGFBP1), a key regulator of glucose homeostasis. This reduction occurred through a complex mechanism that included both direct and indirect actions. Directly, CARN suppressed the induction of IGFBP1 by hypoxia-inducible factor-1 alpha (HIF-1α). Indirectly, CARN increased circulating insulin levels. These combined effects resulted in decreased blood glucose levels and elevated plasma Insulin-like Growth Factor 1 (IGF-1) levels in HepG2 cells **(Forsberg et al., 2015)**.

Nevertheless, lipase and amylase secretion related to CARN treatment had not been earlier evaluated, making the current study one of the few to investigate the synergistic effects of CARN and ACE on the rat exocrine pancreas.

6.3 Effect of ACE on MDA level in pancreatic tissue homogenate

The measurement of MDA levels directly indicates lipid peroxidation, thereby reflecting disturbances in oxidative balance. The present study showed a significant

increase in MDA levels in the pancreatic tissue homogenate of III, IV, and V groups. This finding suggests that ACE insecticide causes pancreatic oxidative stress in a dose-dependent manner.

These results align with the findings of the study by Chakroun et al. **(2016)**, which reported increased MDA levels in the liver following administration of both the high and the low doses of ACE (21.7 and 43.4 mg/kg). While Hassanen et al. **(2022)**, reported that imidacloprid and hexaflumuron insecticides (at 1/10 of LD_{50}) significantly elevated MDA level in liver and kidney tissue homogenates following sub-acute toxicity in male Wistar rats. Equally, at low doses, imidacloprid (9 mg/kg), chlorpyrifos (1.9 mg/kg), and cypermethrin (5 mg/kg) raised MDA levels in kidney tissue homogenate of male Wistar rats following a 28 days treatment period **(Taha et al., 2022)**.

Indeed, Gasmi et al. **(2017)** stated the increase of MDA levels in the brain tissue of male Wistar rats as a direct effect of ACE toxicity at low dose (3.14 mg/kg) for over 90 days. Similar to this study, Karaca et al. **(2019)** investigated the increase of plasma MDA levels in male Sprague-Dawley rats following exposure to the same dose and duration. Furthermore, Afolabi et al. **(2019)** highlighted the same effect in brain tissue homogenate of male rats after 25 mg/kg of cypermethrin administration for 14 days.

Whereas Arıcan et al. **(2020)** and Issam et al. **(2009)** investigated the MDA levels increase in testes of male rats following administration of ACE at 35 mg/kg and deltamethrin at 200 ppm for 60 days, respectively. All these findings demonstrate that ACE, as other insecticides, induced MDA level increase across various tissues and animal models, which indicates oxidative stress.

This oxidative stress likely arises from disruption in cellular redox balance. For instance, **Wang et al., (2022)** demonstrated that ACE disrupts the glutathione metabolism pathway in neuro-2a cells. This disruption involves affections in glutathione peroxidase, oxidized glutathione, and reduced glutathione levels, while also leading to increased ROS generation, reducing intracellular lipid hydroperoxides, elevated caspase 7 levels, and lactate dehydrogenase levels.

Similarly, in SH-SY5Y cells, ACE caused an increase in ROS production and endoplasmic reticulum stress, mediated through interactions with binding immunoglobulin protein 90 and inositol-requiring enzyme 1-alpha, along with an

upregulation of mitogen-activated protein kinase-8 protein levels. These mechanisms collectively led to apoptosis, indicating that cell death was initiated by internally generated signals, consistent with previous research **(Öztaş et al., 2021)**. This oxidative stress highlights the detrimental impact of insecticide exposure, particularly ACE, on cellular health and underscores the association between insecticide exposure and oxidative stress across diverse tissues and models.

Regarding the effect of CARN, our results observed an insignificant preventive effect of 200 mg/kg CARN against the ACE-induced increase in MDA levels in pancreatic tissue homogenates. However, previous studies suggest a potential for MDA level decrease in other experimental settings. Lee et al. **(2005)** observed a decrease in MDA levels in diabetic mice following CARN administration at 0.5, 1 g/l for 4 weeks. Relatively, S. Aydın et al. **(2010)** and Aydın et al. **(2016)** reported a similar effect of CARN on serum MDA level after 250 mg/kg treatment for 1 and 2 months, respectively. A. Aydın et al. **(2010)** also demonstrated the same effect of CARN (i.e., 250 mg/kg) on MDA level of the liver, brain, and the heart tissues of aged rats. Additionally, Ziling **(2007)** demonstrated a similar effect of CARN on serum MDA levels in a model of reoxygenation injury in male Wistar rats. In light of these findings, the antioxidant properties of CARN may be influenced by dose-dependence or may exhibit tissue specificity.

6.4 ACE-induced histopathologic changes in the pancreas

The histological examination of the pancreatic tissue showed various pathological alterations, particularly in Group III (high dose of ACE). These results were in line with our biochemical results. Several findings assessed identical lesions. In a 2017 study, Khalil et al. investigated the effects of imidacloprid, administered at low doses of 0.5 and 1.0 mg/kg on the pancreas of male rats over 60 days. The authors revealed significant pathological changes, including islet infiltration, congestion, hemorrhage, and duct hyperplasia. Furthermore, lambda-cyhalothrin insecticide at both low and high doses (5 and 50 mg/kg/day) led to acinar architecture disruption, hemorrhage, acinar shrinkage, and cytoplasmic vacuolation in albino rats **(Elhalwagy et al., 2015)**. Hence, administration of dimethoate insecticide at a low dose of 20 mg/kg resulted from similar lesions in the same animal model **(Mesallam et al., 2018)**.

Indeed, these observed lesions were also detected in the pancreatic tissue of animal models after induction of acute pancreatitis. After hydrogen peroxide injection in Wistar rats, severe edema and hemorrhage were detected serving as important signs of acute pancreatitis **(Tamura et al., 1992)**.

Thus, in fatty acid ethyl ester-induced pancreatitis, acinar vacuolization, severe edema, and trypsinogen activation were the major alterations observed in rats **(Werner et al., 2002)**. In another study conducted by Novaes et al. **(2002)**, injection with venom-induced acute/chronic pancreatitis, lymphocytic infiltration, vacuolization of acinar cells, and degranulation were detected 10 min afterward the treatment.

Mumcu et al. **(2005)** conducted a similar investigation, which revealed a notable presence of edema and infiltration in the rat pancreas following the induction of acute pancreatitis by glycodeoxycholic acid. Likewise, Usborne et al. **(2014)** illustrated a significant incidence of interstitial edema, exocrine gland inflammation, atrophy, and cellular vacuolization in the rat pancreas after the administration of 50 and 150mg/kg cyanohydroxybutene.

Certainly, our observations of acinar changes suggest that ACE can induce pancreatic toxicity and dysfunction by impacting acinar cell degeneration. This multifaceted process involves several factors and mechanisms, as supported by previous research. One potential explanation is the endoplasmic reticulum (ER) stress hypothesis. ER stress can occur when there is an increased demand for protein synthesis, such as trypsinogen, chymotrypsinogen, lipase, and lysosomal enzyme cathepsin B, coupled with a reduced capacity of the cell to process and recycle misfolded proteins. This can activate a cellular stress response known as the unfolded protein response (UPR) in response to pancreatic toxins. If the UPR cannot resolve the stress, it can lead to apoptosis **(Lee & Papachristou, 2019)**.

Additionally, ductal hypertension could play a role by activating the transcription factor 3 pathway and the signal transducer, leading to clinical manifestations such as interlobular and intralobular edema **(Bhanot & Möller, 2009)**. These mechanisms collectively contribute to the pancreatic toxicity and dysfunction observed with ACE exposure, highlighting the complex interplay of factors involved in this process and suggesting that all these pathological alterations could potentially compromise both the

exocrine and endocrine functions of the pancreas, thereby raising the possibility that ACE could trigger acute pancreatitis or chronic pancreatic diseases.

Furthermore, CARN's capacity to impede ACE alteration was manifestly evident in the pancreatic tissue. Thus, it has been indicated that CARN protects pancreatic tissue against vacuolation in the cytoplasm of acini and infiltration of inflammatory cells induced by sodium fluoride at 10 mg/kg for 35 consecutive days in adult male Wistar rats **(Agha et al., 2012)**. Certainly, CARN emerges as a promising preventive agent for various diseases affecting both endocrine and exocrine pancreatic tissues, offering potential due to its multifaceted protective mechanisms mainly through scavenging ROS, reactive nitrogen species, and foiling the formation of nitrotyrosine and 4-hydroxynonenal species **(Cripps et al., 2017; Miceli et al., 2018)**.

6.5 Effect of ACE and CARN on cell viability

The effect of (ACE) on the viability of AR42J cells exhibited a biphasic pattern that was concentration dependent. At lower concentrations (0.5 to 2 mM), ACE induced a mitogenic response, promoting cell proliferation. However, at higher concentrations (4 to 10 mM), ACE exerted a cytotoxic effect, leading to cell death. Of particular interest is that the effects observed with lower ACE concentrations were analogous to nicotine's impact on the same cell line. At 100 µM of nicotine, Bose et al. **(2005)**. These findings suggest a potential shared mechanism between ACE and nicotine in modulating cholinergic signaling pathways, which may involve receptor-mediated signaling cascades or downstream cellular events. Further investigations stated that the increase in cell viability was 25.6% compared to control cells.

Indeed, Walker et al. **(2008)** demonstrated that nicotine significantly increased AR42J cell proliferation, surpassing the effects induced by 20 µM of H_2O_2. They conclude that nicotine provoked a mitogenic that was analogous to that of growth factors. Hence, ACE at 50 µM enhanced the proliferation of 4T1-Luc breast cancer cells **(Li et al., 2022)**. Furthermore, chlorfluazuron, an insecticide, caused an accelerated the proliferation of Hek293 and HepG2 human cells, beyond their control level at 4.96 µM **(Huang et al., 2015)**. In contrast to our results, KARA et al. **(2020)** reported the occurrence of cytotoxic and genotoxic effects of ACE on AR42J cells at concentrations ranging from 1 to 6 mM, as measured via the MMT assay. Several factors may account

for these inconsistencies, including differences in the purity of the ACE compounds utilized in each study, variations in measurement sensitivity the distinct assay kits utilized in each investigation.

At higher concentrations exceeding 3 mM, the presence of ACE induced cytotoxic effects, resulting in AR42J cell death. This result was in line with assorted studies. Permethrin exerted an identical effect on human endothelial cells at different concentrations beyond 24h of treatment, without affecting apoptosis or necrosis processes **(H.S. Lee et al., 2022)**. Hence, Abdel-Halim & Osman **(2020)** investigated the cytotoxic effects of imidacloprid and glyphosate on the cell viability of the WPM-Y1 cell line, which is derived from human prostate epithelial cells. While Lamberti et al. **(2014)** stated the same effect of pyriproxyfen at 10-500 ppm on HepG2 cell viability. The cell viability of PC12 cells, a rat-derived adrenal pheochromocytoma cell line, was also decreased following exposure to the bipyridilium herbicide at a concentration of 1.4 $\times 10^{-5}$ mol/L **(Zhang et al., 2012)**.

The Proliferation of human lymphocytes was also altered by the insecticide bioallethrin at 200 μM, in the study of **Arif et al. (2021)**. Moreover, bifenthrin has been shown to reduce the viability of HCT-116 cells, a human colorectal cell line, via disrupting the oxidative balance **(Bouaziz et al., 2020)**. Conclusively, these findings strongly support the ability of ACE, and other chemicals, to alter cell viability in a dose-dependent manner.

On the other hand, the co-treatment with CARN mitigated the accelerated increase in cell viability induced by ACE beyond 48h of treatment. This cytoprotective effect of CARN (at 10 mM) was also observed in endocrine pancreatic cells, where this dipeptide protected beta cells from the accelerated growth induced by H_2O_2, inhibited caspase-3 activation and promoted insulin secretion **(Miceli et al., 2018)**. Additionally, CARN (1 g/L) enhanced glucose levels and the expression of insulin genes in induced diabetes in mice **(Barca et al., 2018)**.

In another cell line, CARN at 1, 5, and 10mM exhibited a protective effect on PC12 cells against the cytotoxic effect of morphine **(Sharifi, 2014)**. In hepatocytes of rat, CARN exerted a cytoprotective effect at concentrations of 50 and 100 μM by reducing oxidative stress and cytotoxicity induced by isoniazid **(Eftekhari et al., 2018)**. However, the effect of CARN on exocrine pancreatic cells has not been previously

investigated. Nonetheless, our findings following the literature suggest that CARN may be a potent agent in preventing various toxic effects exerted by several chemicals.

6.6 Effect of ACE and CARN on MAPKs pathway

MAPK signaling pathways are responsible for translating external signals into various cellular responses. Resulting in gene expression, proliferation, metabolism, stress response, apoptosis, viability, and cellular differentiation **(Cargnello & Roux, 2011)**. Our results showed that ACE induced activation of p44/42 (at 3 mM), p38 (at 2 and 3 mM), and JNK (at 3 mM) through their phosphorylation which was in line with our cell viability results. It is noteworthy that these results closely align with those reported in previous studies.

A Similar effect was detected in AR42J cells treated with 100 µM of nicotine, where the phosphorylated form of p44/42 increased, reaching its peak effect 3 min after stimulation. However, the p38 and JNK pathways demonstrated no activation **(Bose et al., 2005)**.

In the study of Song et al. **(2012)**, the insecticide endosulfan provoked phosphorylation of JNK, p44/42, and p38 protein kinases at a concentration of 30 µM for 24h leading to macrophage activation. Additionally, the authors stated that the activation of these protein kinases involves c-Jun transcription, which leads to cell survival through ERK1/2 inflammation, and apoptosis via JNK and p38 activation.

Moreover, monocrotophos, an organophosphate pesticide, at 10^{-3} M induced significant phosphorylation of JNK in human cord blood stem cells, leading to mitochondrial apoptosis **(Kashyap et al., 2013)**. Besides, Ki et al. **(2012)** demonstrated that the insecticide fipronil induced cell death in SH-SY5Y cells through the activation of p38, JNK, and p44/42 proteins, with peak phosphorylation observed 2h after stimulation. Furthermore, cypermethrin was shown to activate JNK and p44/42 the RAW 264.7 cell line, while also causing DNA damage, oxidative stress, and apoptosis **(Huang et al., 2016)**.

An interesting study conducted by Zhu et al. **(2021)** demonstrated that Avermectin affected neurotoxicity by promoting cell death in SH-SY5Y, PC-12, and SK-N-SH cells, primarily through the downregulation of ERK pathway. This phenomenon

was accompanied by a decrease in the phosphorylation levels of MSK1, p90Rsk, and Elk1/2 proteins, which are crucial for gene expression, cell growth, and differentiation. Interestingly, the p38 and JNK pathways were unaffected following the insecticide treatment.

Lower concentrations of ACE (0.5-2mM) did not affect the MAPKs pathway, potentially due to the involvement of an alternative signaling pathway. In the study of Wang et al. **(2023)**, ivermectin induced a decrease in p-mTOR levels and an increase in p-AMPK levels in RAW264.7 cells. Furthermore, it was shown that vinclozolin (at 100 nM and 1 μM) led to an elevation in p-mTOR and p-Akt levels, resulting in the upregulation of ADAM12 in SH-SY5Y cells. ADAM12, a protein that mediates cell growth and potentially contributes to oncogenesis, was found to be associated with these effects **(Graziosi et al., 2022)**.

CARN demonstrated a significant suppression of the ACE-induced increase in the phosphorylation levels of p-p44/42, p-p38, and p-JNK. This dipeptide has previously been shown to inhibit MAPKs pathway activation under various conditions. In the finding of Guo et al. **(2019)**, CARN prevented the increase in MAPKs signaling pathway in retinal vascular endothelial cells of diabetic rats. Moreover, accelerated cell proliferation of mesangial cells was reduced via inhibition of p44/42 and p38 phosphorylation after treatment with 20 mM of CARN **(Jia et al., 2009)**. In neuronal cells, treatment with 1 mM of CARN led to a reduction in JNK and ERK 1/2 activation, resulting in a decrease in free radical accumulation **(Kulebyakin et al., 2012)**.

Overall, the insecticide ACE could provoke its toxicity through altering cell signaling pathway, namely MAPKs. Additionally, CARN may prevent these adverse effects.

6.7 Effect of ACE on calcium mobilization

Calcium serves as a universal intracellular messenger in eukaryotic cells, governing diverse cellular processes such as cell growth, stress responses, apoptosis, and gene expression **(Rasaily et al., 2024)**. Studying calcium mobilization in the exocrine pancreas is crucial for understanding various physiological processes, including enzyme secretion, hormone-receptor interactions, cell membrane changes, zymogen granule architecture, pancreatic juice functionality, intracellular pH relationships, and acute pancreatitis mechanisms **(Williams & Yule, 2012)**. Our

findings indicated that ACE at 1 mM caused intracellular Ca^{2+} release in AR42J exocrine phenotype cells. ACE treatment after Tps did not elicit additional calcium release, this suggests that the endoplasmic reticulum serves as the primary source of Ca^{2+}.

This result aligns with previous studies involving different cell lines. In the study of Guzman-Vallejos et al. **(2024)**, ACE and imidacloprid at 500 µM provoked intracellular calcium mobilization in SH-SY5Y neurons. In addition, ACE at 50 µM affected free-calcium mobilization in 4T1-Luc cell line through G protein-coupled estrogen receptor **(Li et al., 2022)**. Furthermore, imidacloprid insecticide at 2.5 mM produced an analogous effect on neuroblastoma N1E-115 cells **(Tomizawa & Casida, 2002)**.

It should be noted that calcium mobilization in AR42J cells was previously investigated using various chemicals. Melatonin, CCK-8, and Tps have been observed to induce calcium release through the alteration of the endoplasmic reticulum **(del Castillo-Vaquero et al., 2010)**. Resveratrol, a natural phytoalexin, affected relative results along with a decrease in cell viability and JNK phosphorylation **(Garcia-Sanchez et al., 2012)**. Moreover, ebselen caused free-calcium mobilization with a concentration-dependent manner ranging from 1 to 40 µM **(Santofimia-Castaño et al., 2014)**. Besides, it was shown that gabapentin causes exocrine pancreatic cancer through intracellular Ca^{2+} mobilization in the AR42J cell model **(Dethloff et al., 2000)**.

This emphasizes that ACE, akin to other chemicals, could affect intracellular Ca^{2+} mobilization in the exocrine pancreas. This, in turn, can result in alterations to various physiological mechanisms, encompassing cell death/survival, stress and inflammation responses, and enzyme secretion.

6.8 Effect of ACE and CARN on trypsin secretion

Trypsinogen is released by the exocrine pancreas and is converted into trypsin by enterokinase in the duodenum. In the AR42J exocrine phenotype, trypsinogen occurs following CCK stimulation, and its disturbance serves as a significant biomarker for monitoring changes in the organ's physiological and pathophysiological conditions such as acute pancreatitis **(Vertiprakhov & Ovchinnikova, 2022)**.

Our findings indicated that neither ACE nor CARN elicited disruption in trypsin secretion after stimulation of AR42J exocrine cells with CCK. To the best of our knowledge, this study was the first to conduct such an effect. However, several studies have examined alterations in trypsin secretion under different conditions. Ameur et al. **(2018)** highlighted that sulfanilic acid at 100μM and 1 mM altered trypsin secretion, intracellular calcium concentrations, and oxidative balance in AR42J cells. Furthermore, lipopolysaccharide and cerulein induced comparable effects in the same cell line in a dose-dependent manner, ranging from 10 to 40 μM, and the protective effect of emodin against this observed effect **(Zhao et al., 2019)**.

A parallel investigation was undertaken by Qian et al. **(2021)**, in which taurolithocholic acid 3-sulfate disrupted trypsin and lipase secretion, with the preventive effect of salidroside noted.

In the current thesis, the toxic effects of ACE on the exocrine pancreas were assessed in both male Wistar rats and the AR42J cell line. The presented findings indicated significant impairment in pancreatic function following exposure to this insecticide, suggesting a potential health risk associated with these kinds of chemicals. Hence, the observed CARN effect indicates its potential as a preventive measure against insecticide-induced exocrine pancreatic damage. By unraveling the mechanisms underlying this toxicity, researchers will furnish valuable insights into pancreatic injury and identify potential preventive agents, such as CARN.

CONCLUSIONS

CONCLUSIONS

The present research thesis demonstrates that the exocrine pancreas may serve as a target organ for chemical toxins. Specifically, the neonicotinoid insecticide ACE has been shown to alter both the function and structure of exocrine pancreatic cells through various mechanisms, underscoring its potential role in the induction of pancreatic diseases. Additionally, this study provides new insights into the preventive role of CARN, as a natural dipeptide, in preventing and mitigating the adverse effects of ACE on the physiology of exocrine pancreatic cells.

In this work, we emphasized that ACE could alter the pancreatic somatic index and disrupt pancreatic secretion, primarily by decreasing amylase levels, increasing lipase levels, and raising blood glucose levels. These alterations reflect changes in insulin and glucagon secretion. Furthermore, ACE was found to increase MDA levels in tissue homogenates, serving as a direct marker of lipid peroxidation. Histological examination revealed several in the pancreatic tissue, including inflammatory infiltration, acinar cell vacuolization, atrophy, and hyperplasia. Meanwhile, CARN exhibited a potential preventive effect against these alterations in the exocrine pancreas.

At the molecular level, we observed that ACE induced a dose-dependent effect on AR42J cells viability, elevated the phosphorylated forms of p38, JNK, and p44/42 proteins, which are involved in various cellular processes. In contrast, CARN exhibited a potential preventive role by mitigating the damage induced by ACE in exocrine pancreatic cells. Finally, we found that ACE affected intracellular calcium release, presumably originating from the endoplasmic reticulum, which could disrupt various physiological mechanisms in AR42J cells.

While this study provides strong evidence, several avenues remain for future research. Building on the *in-vivo* findings, subsequent studies could investigate the long-term effects of ACE exposure beyond 30 days, assess varying dosages, and evaluate the efficacy of CARN in combination with other therapeutic agents. Furthermore, there is a need for more precise quantification of amylase and lipase secretion in tissue homogenate, as well as examining additional enzymes like trypsin and protease. Additionally, oxidative stress and lipid peroxidation in pancreatic tissue could be studied by analyzing additional

biomarkers such as ROS generation, superoxide dismutase, catalase, and reduced glutathione levels.

As well, immunohistochemistry studies have the potential to provide significant insights into the effects of ACE and/or CARN on various biomarkers within pancreatic tissue.

Although AR42J cells provided valuable insights into exocrine pancreatic physiology, they are tumor-derived rather than primary cells. Future studies should consider using primary acinar cells to gain a more accurate understanding of the mechanisms underlying ACE and CARN effects. Future research should also explore other signaling pathways involved in ACE-induced pancreatic damage, such as Akt, mTOR, and NF-κB pathways, which could yield a more comprehensive understanding of these toxic effects and help to elucidate the preventive role of CARN.

It is noteworthy that exocrine pancreatic cells within AR42J cells express nAChRs receptors, which are key targets of ACE, it would be of high interest to investigate whether this insecticide exerts similar effects as in neurons, including the involved. A complementary line of investigation would explore the synergistic effects of CARN in mitigating ACE-induced damage, with the potential to yield valuable insights. To further elucidate the effect of ACE on intracellular calcium mobilization in exocrine pancreatic cells, it is interesting to investigate its effect on calcium release from the mitochondrial matrix using Rhod-2 AM as well as its interaction with IP3 receptors using agonist substances.

To the best of our knowledge, ACE insecticide exposure can cause hazardous effects at various levels in non-target organisms, leading to serious changes in the exocrine pancreas. Therefore, its field application requires careful monitoring to minimize potential adverse effects on farm animals and occupationally exposed individuals. Given the limited data on exocrine pancreatic toxicity, further studies are mandatory to fully understand the mechanisms involved and explore the therapeutic potential of CARN and other agents in mitigating these effects.

Finally, future research should also investigate the clinical implications for human health, potentially through epidemiological studies examining the correlation between neonicotinoid exposure and pancreatic diseases. Exploring these areas could lead to the

development of innovative therapeutic strategies aimed at preventing or treating pancreatic diseases associated with environmental toxin exposure.

References

REFERENCES

Abd El-Kader, A. E.-K., Awadalla, E., Salah Eldin, A. E., Mohamed, Z., & Mohamed, O. (2022). Protective effect of curcumin against acetamiprid- induced neurotoxicity in male albino rats. *Aswan University Journal of Environmental Studies*, *3*(3), 303–312. https://doi.org/10.21608/aujes.2022.150987.1084

Abdallah, A. A., Marwa A. Ibrahim, Eman A. Ibrahim, Hossam El Din H. Abdelhafez, & Naglaa F. Mahmoud. (2021). Neuroprotective Effect of Moringa Oleifera Extract on Acetamiprid Induced Neurotoxicity and Apoptosis in Albino Rats. *Indian Journal of Forensic Medicine & Toxicology*, *15*(4), 711–719. https://doi.org/10.37506/ijfmt.v15i4.16790

Abdel-Halim, K. Y., & Osman, S. R. (2020). Cytotoxicity and Oxidative Stress Responses of Imidacloprid and Glyphosate in Human Prostate Epithelial WPM-Y.1 Cell Line. *Journal of Toxicology*, *2020*, e4364650. https://doi.org/10.1155/2020/4364650

Afolabi, O. K., Aderibigbe, F. A., Folarin, D. T., Arinola, A., & Wusu, A. D. (2019). Oxidative stress and inflammation following sub-lethal oral exposure of cypermethrin in rats: Mitigating potential of epicatechin. *Heliyon*, *5*(8), e02274. https://doi.org/10.1016/j.heliyon.2019.e02274

Agha, F. E., El-Badry, M., Hassan, D. A., & Elraouf, A. A. (2012). *Role of Vitamin E in Combination with Methionine and L- carnosine Against Sodium Fluoride-Induced Hematological, Biochemical, DNA Damage, Histological and Immunohistochemical Changes in Pancreas of Albino Rats.* https://www.semanticscholar.org/paper/Role-of-Vitamin-E-in-Combination-with-Methionine-L-Agha-El-Badry/0ed9031f83f9cf3600ae7da4f1de9887767655dd

Ahshin-Majd, S., Zamani, S., Kiamari, T., Kiasalari, Z., Baluchnejadmojarad, T., & Roghani, M. (2016). Carnosine ameliorates cognitive deficits in streptozotocin-induced diabetic rats: Possible involved mechanisms. *Peptides*, *86*, 102–111. https://doi.org/10.1016/j.peptides.2016.10.008

Akono, E. N., Sanda, A. K., Tsague, F. P. M., Tchewonpi, A. C., Kewir, T. S., Tashi, S., & Travert, C. (2019). Momordica Foetida (Cucurbitaceae) Extract Alleviates Parastar (Insecticide) -Induced Toxicity on Pancreatic and Duodenal α-amylase Activity in Male Rats. *Journal of Chemical Health Risks*, *9*(2), 97–105. https://doi.org/10.22034/jchr.2019.665820

Albrakati, A. (2024). The potential neuroprotective of luteolin against acetamiprid-induced neurotoxicity in the rat cerebral cortex. *Frontiers in Veterinary Science*, *11*, 1361792. https://doi.org/10.3389/fvets.2024.1361792

Albrecht, T., Schilperoort, M., Zhang, S., Braun, J. D., Qiu, J., Rodriguez, A., Pastene, D. O., Krämer, B. K., Köppel, H., Baelde, H., de Heer, E., Anna Altomare, A., Regazzoni, L., Denisi, A., Aldini, G., van den Born, J., Yard, B. A., & Hauske, S. J. (2017). Carnosine Attenuates the Development of both Type 2 Diabetes and Diabetic Nephropathy in BTBR ob/ob Mice. *Scientific Reports*, *7*(1), Article 1. https://doi.org/10.1038/srep44492

Aldini, G., de Courten, B., Regazzoni, L., Gilardoni, E., Ferrario, G., Baron, G., Altomare, A., D'Amato, A., Vistoli, G., & Carini, M. (2021). Understanding the antioxidant and carbonyl sequestering activity of carnosine: Direct and indirect

mechanisms. *Free Radical Research*, *55*(4), 321–330. https://doi.org/10.1080/10715762.2020.1856830

Aldini, G., Facino, R. M., Beretta, G., & Carini, M. (2005). Carnosine and related dipeptides as quenchers of reactive carbonyl species: From structural studies to therapeutic perspectives. *BioFactors (Oxford, England)*, *24*(1–4), 77–87. https://doi.org/10.1002/biof.5520240109

Aldini, G., Orioli, marica, & Carini, M. (2011). *Carnosine and related dipeptides as quenchers of reactive carbonyl species*. https://air.unimi.it/handle/2434/260907#

Ali, A. (2018). EFFECT OF ACETAMIPRID RESIDUES IN TOMATO FRUITS ON SOME BLOOD PROFILE PARAMETERS OF MALE MICE. *IRAQI JOURNAL OF AGRICULTURAL SCIENCES*, *49*(6). https://doi.org/10.36103/ijas.v49i6.149

Aloisi, A., Barca, A., Romano, A., Guerrieri, S., Storelli, C., Rinaldi, R., & Verri, T. (2013). Anti-Aggregating Effect of the Naturally Occurring Dipeptide Carnosine on Aß1-42 Fibril Formation. *PLOS ONE*, *8*(7), e68159. https://doi.org/10.1371/journal.pone.0068159

Aloisi, A., Barca, A., Romano, A., Guerrieri, S., Storelli, C., Rinaldi, R., & Verri, T. (2013). Anti-Aggregating Effect of the Naturally Occurring Dipeptide Carnosine on Aß1-42 Fibril Formation. *PLOS ONE*, *8*(7), e68159. https://doi.org/10.1371/journal.pone.0068159

Ameur, F. Z., Mehedi, N., Kheroua, O., Saïdi, D., Salido, G. M., & Gonzalez, A. (2018). Sulfanilic acid increases intracellular free-calcium concentration, induces reactive oxygen species production and impairs trypsin secretion in pancreatic AR42J cells. *Food and Chemical Toxicology: An International Journal Published for the British Industrial Biological Research Association*, *120*, 71–80. https://doi.org/10.1016/j.fct.2018.07.001

Andou, A., Hisamatsu, T., Okamoto, S., Chinen, H., Kamada, N., Kobayashi, T., Hashimoto, M., Okutsu, T., Shimbo, K., Takeda, T., Matsumoto, H., Sato, A., Ohtsu, H., Suzuki, M., & Hibi, T. (2009). Dietary Histidine Ameliorates Murine Colitis by Inhibition of Proinflammatory Cytokine Production From Macrophages. *Gastroenterology*, *136*(2), 564-574.e2. https://doi.org/10.1053/j.gastro.2008.09.062

Ansari, D., Tingstedt, B., Andersson, B., Holmquist, F., Sturesson, C., Williamsson, C., Sasor, A., Borg, D., Bauden, M., & Andersson, R. (2016). Pancreatic cancer: Yesterday, today and tomorrow. *Future Oncology (London, England)*, *12*(16), 1929–1946. https://doi.org/10.2217/fon-2016-0010

Arakawa, T., Satoh, H., Nakamura, A., Nebiki, H., Fukuda, T., Sakuma, H., Nakamura, H., Ishikawa, M., Seiki, M., & Kobayashi, K. (1990). Effects of zinc L-carnosine on gastric mucosal and cell damage caused by ethanol in rats. Correlation with endogenous prostaglandin E2. *Digestive Diseases and Sciences*, *35*(5), 559–566. https://doi.org/10.1007/BF01540402

Arıcan, E. Y., Gökçeoğlu Kayalı, D., Ulus Karaca, B., Boran, T., Öztürk, N., Okyar, A., Ercan, F., & Özhan, G. (2020). Reproductive effects of subchronic exposure to acetamiprid in male rats. *Scientific Reports*, *10*(1), 8985. https://doi.org/10.1038/s41598-020-65887-0

Arıcan, E. Y., Gökçeoğlu Kayalı, D., Ulus Karaca, B., Boran, T., Öztürk, N., Okyar, A., Ercan, F., & Özhan, G. (2020). Reproductive effects of subchronic exposure to acetamiprid in male rats. *Scientific Reports*, *10*, 8985. https://doi.org/10.1038/s41598-020-65887-0

Arif, A., Quds, R., & Mahmood, R. (2021). Bioallethrin enhances generation of ROS, damages DNA, impairs the redox system and causes mitochondrial dysfunction

in human lymphocytes. *Scientific Reports*, *11*(1), 8300. https://doi.org/10.1038/s41598-021-87799-3

Artioli, G. G., Sale, C., & Jones, R. L. (2019). Carnosine in health and disease. *European Journal of Sport Science*, *19*(1), 30–39. https://doi.org/10.1080/17461391.2018.1444096

Artioli, G. G., Sale, C., & Jones, R. L. (2019). Carnosine in health and disease. *European Journal of Sport Science*, *19*(1), 30–39. https://doi.org/10.1080/17461391.2018.1444096

Aryal, A., Harmon, A. C., & Dugas, T. R. (2021). Particulate matter air pollutants and cardiovascular disease: Strategies for intervention. *Pharmacology & Therapeutics*, *223*, 107890. https://doi.org/10.1016/j.pharmthera.2021.107890

Asatoor, A. M., Bandoh, J. K., Lant, A. F., Milne, M. D., & Navab, F. (1970). Intestinal absorption of carnosine and its constituent amino acids in man. *Gut*, *11*(3), 250–254. https://doi.org/10.1136/gut.11.3.250

Aydın, A. F., Çoban, J., Doğan-Ekici, I., Betül-Kalaz, E., Doğru-Abbasoğlu, S., & Uysal, M. (2016). Carnosine and taurine treatments diminished brain oxidative stress and apoptosis in D-galactose aging model. *Metabolic Brain Disease*, *31*(2), 337–345. https://doi.org/10.1007/s11011-015-9755-0

Aydın, A. F., Çoban, J., Doğan-Ekici, I., Betül-Kalaz, E., Doğru-Abbasoğlu, S., & Uysal, M. (2016). Carnosine and taurine treatments diminished brain oxidative stress and apoptosis in D-galactose aging model. *Metabolic Brain Disease*, *31*(2), 337–345. https://doi.org/10.1007/s11011-015-9755-0

Aydın, A., Küskü-Kiraz, Z., Doğru-Abbasoğlu, S., & Uysal, M. (2010). Effect of carnosine treatment on oxidative stress in serum, apoB-containing lipoproteins fraction and erythrocytes of aged rats. *Pharmacological Reports : PR*, *62 4*, 733–739. https://doi.org/10.1016/S1734-1140(10)70331-5

Babizhayev, M. A. (2009). Potentiation of intraocular absorption and drug metabolism of N-acetylcarnosine lubricant eye drops: Drug interaction with sight threatening lipid peroxides in the treatment for age-related eye diseases. *Drug Metabolism and Drug Interactions*, *24*(2–4), 275–323. https://doi.org/10.1515/dmdi.2009.24.2-4.275

Bachem, M. G., Schneider, E., Groß, H., Weidenbach, H., Schmid, R. M., Menke, A., Siech, M., Beger, H., Grünert, A., & Adler, G. (1998). Identification, culture, and characterization of pancreatic stellate cells in rats and humans. *Gastroenterology*, *115*(2), 421–432. https://doi.org/10.1016/S0016-5085(98)70209-4

Bando, K., Ichihara, K., Shimotsuji, T., Toyoshima, H., Koda, K., Hayashi, C., & Miyai, K. (1986). Reduced serum carnosinase activity in hypothyroidism. *Annals of Clinical Biochemistry*, *23 (Pt 2)*, 190–194. https://doi.org/10.1177/000456328602300208

Baran, E. J. (2000). Metal complexes of carnosine. *Biochemistry. Biokhimiia*, *65*(7), 789–797.

Barca, A., Gatti, F., Spagnolo, D., Ippati, S., Vetrugno, C., & Verri, T. (2018). Responsiveness of Carnosine Homeostasis Genes in the Pancreas and Brain of Streptozotocin-Treated Mice Exposed to Dietary Carnosine. *International Journal of Molecular Sciences*, *19*(6), 1713. https://doi.org/10.3390/ijms19061713

Barreto-Chang, O. L., & Dolmetsch, R. E. (2009). Calcium Imaging of Cortical Neurons using Fura-2 AM. *Journal of Visualized Experiments : JoVE*, *23*, 1067. https://doi.org/10.3791/1067

Barski, O. A., Xie, Z., Baba, S. P., Sithu, S. D., Agarwal, A., Cai, J., Bhatnagar, A., & Srivastava, S. (2013). Dietary Carnosine Prevents Early Atherosclerotic Lesion Formation in Apolipoprotein E–Null Mice. *Arteriosclerosis, Thrombosis, and Vascular Biology*, *33*(6), 1162–1170. https://doi.org/10.1161/ATVBAHA.112.300572

Bass, C., Denholm, I., Williamson, M. S., & Nauen, R. (2015). The global status of insect resistance to neonicotinoid insecticides. *Pesticide Biochemistry and Physiology*, *121*, 78–87. https://doi.org/10.1016/j.pestbp.2015.04.004

Bellia, F., Vecchio, G., & Rizzarelli, E. (2014). Carnosinases, Their Substrates and Diseases. *Molecules*, *19*(2), 2299–2329. https://doi.org/10.3390/molecules19022299

Beyer, G., Habtezion, A., Werner, J., Lerch, M. M., & Mayerle, J. (2020). Chronic pancreatitis. *Lancet (London, England)*, *396*(10249), 499–512. https://doi.org/10.1016/S0140-6736(20)31318-0

Bhanot, U. K., & Möller, P. (2009). Mechanisms of parenchymal injury and signaling pathways in ectatic ducts of chronic pancreatitis: Implications for pancreatic carcinogenesis. *Laboratory Investigation*, *89*(5), 489–497. https://doi.org/10.1038/labinvest.2009.19

Bharadwaj, L. A., Davies, G. F., Xavier, I. J., & Ovsenek, N. (2002). L-carnosine and verapamil inhibit hypoxia-induced expression of hypoxia inducible factor (HIF-1 alpha) in H9c2 cardiomyoblasts. *Pharmacological Research*, *45*(3), 175–181. https://doi.org/10.1006/phrs.2001.0911

Bhatia, M., Wong, F. L., Cao, Y., Lau, H. Y., Huang, J., Puneet, P., & Chevali, L. (2005). Pathophysiology of acute pancreatitis. *Pancreatology*, *5*(2), 132–144. https://doi.org/10.1159/000085265

Biswas, Md. S., & Mano, J. (2021). Lipid Peroxide-Derived Reactive Carbonyl Species as Mediators of Oxidative Stress and Signaling. *Frontiers in Plant Science*, *12*. https://www.frontiersin.org/articles/10.3389/fpls.2021.720867

Boldyrev, A. A., & Severin, S. E. (1990). The histidine-containing dipeptides, carnosine and anserine: Distribution, properties and biological significance. *Advances in Enzyme Regulation*, *30*, 175–194. https://doi.org/10.1016/0065-2571(90)90017-V

Boldyrev, A. A., Aldini, G., & Derave, W. (2013). Physiology and Pathophysiology of Carnosine. *Physiological Reviews*, *93*(4), 1803–1845. https://doi.org/10.1152/physrev.00039.2012

Boldyrev, A. A., Gallant, S. C., & Sukhich, G. T. (1999). Carnosine, the protective, anti-aging peptide. *Bioscience Reports*, *19*(6), 581–587. https://doi.org/10.1023/a:1020271013277

Bondareva, L., & Fedorova, N. (2021). Pesticides: Behavior in Agricultural Soil and Plants. *Molecules (Basel, Switzerland)*, *26*(17), 5370. https://doi.org/10.3390/molecules26175370

Bonner, A. B., Swann, M. E., Marway, J. S., Heap, L. C., & Preedy, V. R. (1995). Lysosomal and nonlysosomal protease activities of the brain in response to ethanol feeding. *Alcohol (Fayetteville, N.Y.)*, *12*(6), 505–509. https://doi.org/10.1016/0741-8329(95)00035-6

Borovicka, J., Schwizer, W., Mettraux, C., Kreiss, C., Remy, B., Asal, K., Jansen, J. B., Douchet, I., Verger, R., & Fried, M. (1997). Regulation of gastric and pancreatic lipase secretion by CCK and cholinergic mechanisms in humans. *The American Journal of Physiology*, *273*(2 Pt 1), G374-380. https://doi.org/10.1152/ajpgi.1997.273.2.G374

Bose, C., Zhang, H., Udupa, K. B., & Chowdhury, P. (2005). Activation of p-ERK1/2 by nicotine in pancreatic tumor cell line AR42J: Effects on proliferation and secretion. *American Journal of Physiology-Gastrointestinal and Liver Physiology*, *289*(5), G926–G934. https://doi.org/10.1152/ajpgi.00138.2005

Bouaziz, C., Graiet, I., Salah, A., Ben Salem, I., & Abid, S. (2020). Influence of bifentrin, a pyrethriod pesticide, on human colorectal HCT-116 cells attributed to alterations in oxidative stress involving mitochondrial apoptotic processes. *Journal of Toxicology and Environmental Health, Part A*, *83*(9), 331–340. https://doi.org/10.1080/15287394.2020.1755756

Bresson, S. E., & Ruzzin, J. (2024). Persistent organic pollutants disrupt the oxidant/antioxidant balance of INS-1E pancreatic ß-cells causing their physiological dysfunctions. *Environment International*, *190*, 108821. https://doi.org/10.1016/j.envint.2024.108821

Brunet, J.-L., Maresca, M., Fantini, J., & Belzunces, L. P. (2008). Intestinal absorption of the acetamiprid neonicotinoid by Caco-2 cells: Transepithelial transport, cellular uptake and efflux. *Journal of Environmental Science and Health, Part B*, *43*(3), 261–270. https://doi.org/10.1080/03601230701771446

Burger, G., & Diehl, S. (2013). *Widefield Calcium Imaging with Calcium Indicator Fura2*. https://www.leica-microsystems.com/science-lab/life-science/widefield-calcium-imaging-with-calcium-indicator-fura2/

Calza, P., Guarino, B., Dal Bello, F., Dioni, A., Bergero, M., & Medana, C. (2022). Integrated approach for the analysis of neonicotinoids in fruits and food matrices. *Food Chemistry*, *372*, 131153. https://doi.org/10.1016/j.foodchem.2021.131153

Carbo, L., Martins, E. L., Dores, E. F. G. C., Spadotto, C. A., Weber, O. L. S., & De-Lamonica-Freire, E. M. (2007). Acetamiprid, carbendazim, diuron and thiamethoxam sorption in two Brazilian tropical soils. *Journal of Environmental Science and Health, Part B*, *42*(5), 499–507. https://doi.org/10.1080/03601230701389439

Cargnello, M., & Roux, P. P. (2011). Activation and Function of the MAPKs and Their Substrates, the MAPK-Activated Protein Kinases. *Microbiology and Molecular Biology Reviews : MMBR*, *75*(1), 50. https://doi.org/10.1128/MMBR.00031-10

Caruso, G., Caraci, F., & Jolivet, R. B. (2019). Pivotal role of carnosine in the modulation of brain cells activity: Multimodal mechanism of action and therapeutic potential in neurodegenerative disorders. *Progress in Neurobiology*, *175*, 35–53. https://doi.org/10.1016/j.pneurobio.2018.12.004

Caruso, G., Caraci, F., & Jolivet, R. B. (2019). Pivotal role of carnosine in the modulation of brain cells activity: Multimodal mechanism of action and therapeutic potential in neurodegenerative disorders. *Progress in Neurobiology*, *175*, 35–53. https://doi.org/10.1016/j.pneurobio.2018.12.004

Casida, J. E. (2018). Neonicotinoids and Other Insect Nicotinic Receptor Competitive Modulators: Progress and Prospects. *Annual Review of Entomology*, *63*, 125–144. https://doi.org/10.1146/annurev-ento-020117-043042

Cesak, O., Vostalova, J., Vidlar, A., Bastlova, P., & Student, V. (2023). Carnosine and Beta-Alanine Supplementation in Human Medicine: Narrative Review and Critical Assessment. *Nutrients*, *15*(7), 1770. https://doi.org/10.3390/nu15071770

Chakroun, S., Ezzi, L., Grissa, I., Kerkeni, E., Neffati, F., Bhouri, R., Sallem, A., Najjar, M. F., Hassine, M., Mehdi, M., Haouas, Z., & Ben Cheikh, H. (2016). Hematological, biochemical, and toxicopathic effects of subchronic acetamiprid

toxicity in Wistar rats. *Environmental Science and Pollution Research International*, *23*(24), 25191–25199. https://doi.org/10.1007/s11356-016-7650-9

Chakroun, S., Ezzi, L., Grissa, I., Kerkeni, E., Neffati, F., Bhouri, R., Sallem, A., Najjar, M. F., Hassine, M., Mehdi, M., Haouas, Z., & Ben Cheikh, H. (2016). Hematological, biochemical, and toxicopathic effects of subchronic acetamiprid toxicity in Wistar rats. *Environmental Science and Pollution Research International*, *23*(24), 25191–25199. https://doi.org/10.1007/s11356-016-7650-9

Chakroun, S., Ezzi, L., Grissa, I., Kerkeni, E., Neffati, F., Bhouri, R., Sallem, A., Najjar, M. F., Hassine, M., Mehdi, M., Haouas, Z., & Ben Cheikh, H. (2016). Hematological, biochemical, and toxicopathic effects of subchronic acetamiprid toxicity in Wistar rats. *Environmental Science and Pollution Research International*, *23*(24), 25191–25199. https://doi.org/10.1007/s11356-016-7650-9

Choi, H. S., Lim, J.-Y., Chun, H. J., Lee, M., Kim, E. S., Keum, B., Seo, Y. S., Jeen, Y.-T., Um, S. H., Lee, H. S., Kim, C. D., Ryu, H. S., & Sul, D. (2013). The effect of polaprezinc on gastric mucosal protection in rats with ethanol-induced gastric mucosal damage: Comparison study with rebamipide. *Life Sciences*, *93*(2–3), 69–77. https://doi.org/10.1016/j.lfs.2013.05.019

Ciaffaglione, V., & Rizzarelli, E. (2023). Carnosine, Zinc and Copper: A Menage a Trois in Bone and Cartilage Protection. *International Journal of Molecular Sciences*, *24*(22), 16209. https://doi.org/10.3390/ijms242216209

Colín-Barenque, L., Bizarro-Nevares, P., González Villalva, A., Pedraza-Chaverri, J., Medina-Campos, O. N., Jimenez-Martínez, R., Rodríguez-Rangel, D. S., Reséndiz, S., & Fortoul, T. I. (2018). Neuroprotective effect of carnosine in the olfactory bulb after vanadium inhalation in a mouse model. *International Journal of Experimental Pathology*, *99*(4), 180–188. https://doi.org/10.1111/iep.12285

Cossi, P. F., Herbert, L. T., Yusseppone, M. S., Pérez, A. F., & Kristoff, G. (2020). Toxicity evaluation of the active ingredient acetamiprid and a commercial formulation (Assail® 70) on the non-target gastropod Biomphalaria straminea (Mollusca: Planorbidae). *Ecotoxicology and Environmental Safety*, *192*, 110248. https://doi.org/10.1016/j.ecoenv.2020.110248

Cripps, M. J., Hanna, K., Lavilla, C., Sayers, S. R., Caton, P. W., Sims, C., De Girolamo, L., Sale, C., & Turner, M. D. (2017). Carnosine scavenging of glucolipotoxic free radicals enhances insulin secretion and glucose uptake. *Scientific Reports*, *7*(1), 13313. https://doi.org/10.1038/s41598-017-13649-w

de Courten, B., Jakubova, M., de Courten, M. P., Kukurova, I. J., Vallova, S., Krumpolec, P., Valkovic, L., Kurdiova, T., Garzon, D., Barbaresi, S., Teede, H. J., Derave, W., Krssak, M., Aldini, G., Ukropec, J., & Ukropcova, B. (2016). Effects of carnosine supplementation on glucose metabolism: Pilot clinical trial. *Obesity (Silver Spring, Md.)*, *24*(5), 1027–1034. https://doi.org/10.1002/oby.21434

de Melo Reis, R. A., Freitas, H. R., & de Mello, F. G. (2020). Cell Calcium Imaging as a Reliable Method to Study Neuron–Glial Circuits. *Frontiers in Neuroscience*, *14*. https://www.frontiersin.org/journals/neuroscience/articles/10.3389/fnins.2020.569361

del Castillo-Vaquero, A., Salido, G. M., & Gonzalez, A. (2010). Garcia-. *Journal of Pineal Research*, *49*(3), 256–263. https://doi.org/10.1111/j.1600-079X.2010.00790.x

Dembiński, A., Warzecha, Z., Ceranowicz, P., Dembiński, M., Cieszkowski, J., Pawlik, W. W., Tomaszewska, R., Konturek, S. J., & Konturek, P. C. (2006). Effect of ischemic preconditioning on pancreatic regeneration and pancreatic expression

of vascular endothelial growth factor and platelet-derived growth factor-A in ischemia/reperfusion-induced pancreatitis. *Journal of Physiology and Pharmacology: An Official Journal of the Polish Physiological Society*, *57*(1), 39–58.

Derave, W., Everaert, I., Beeckman, S., & Baguet, A. (2010). Muscle carnosine metabolism and beta-alanine supplementation in relation to exercise and training. *Sports Medicine (Auckland, N.Z.)*, *40*(3), 247–263. https://doi.org/10.2165/11530310-000000000-00000

Dethloff, L., Barr, B., Bestervelt, L., Bulera, S., Sigler, R., LaGattuta, M., & de La Iglesia, F. (2000). Gabapentin-induced mitogenic activity in rat pancreatic acinar cells. *Toxicological Sciences: An Official Journal of the Society of Toxicology*, *55*(1), 52–59. https://doi.org/10.1093/toxsci/55.1.52

Devan, R. K. S., Mishra, A., Prabu, P. C., Mandal, T. K., & Panchapakesan, S. (2015). Sub-chronic oral toxicity of acetamiprid in Wistar rats. *Toxicological & Environmental Chemistry*, *97*(9), 1236–1252. https://doi.org/10.1080/02772248.2015.1092542

Dhouib, I. B., Annabi, A., Doghri, R., Rejeb, I., Dallagi, Y., Bdiri, Y., Lasram, M. M., Elgaaied, A., Marrakchi, R., Fazaa, S., & Gati, A. (2017). Neuroprotective effects of curcumin against acetamiprid-induced neurotoxicity and oxidative stress in the developing male rat cerebellum: Biochemical, histological, and behavioral changes. *Environmental Science and Pollution Research International*, *24*(35), 27515–27524. https://doi.org/10.1007/s11356-017-0331-5

Didenko, M. M., Yastrub, T. O., Hrygorieva, K. V., & Dontsova, D. O. (2022). DOSE DEPENDENCE OF SUBCHRONIC INFLUENCING OF ACETAMIPRID ON THE ORGANISM OF RATS FROM DATA OF MORPHOLOGICAL RESEARCHES. *Wiadomości Lekarskie*, *75*(12), 2987–2993. https://doi.org/10.36740/WLek202212116

Diniz, F. C., Hipkiss, A. R., & Ferreira, G. C. (2022). The Potential Use of Carnosine in Diabetes and Other Afflictions Reported in Long COVID Patients. *Frontiers in Neuroscience*, *16*. https://www.frontiersin.org/articles/10.3389/fnins.2022.898735

Distefano, A., Caruso, G., Oliveri, V., Bellia, F., Sbardella, D., Zingale, G. A., Caraci, F., & Grasso, G. (2022). Neuroprotective Effect of Carnosine Is Mediated by Insulin-Degrading Enzyme. *ACS Chemical Neuroscience*, *13*(10), 1588–1593. https://doi.org/10.1021/acschemneuro.2c00201

Drozak, J., Piecuch, M., Poleszak, O., Kozlowski, P., Chrobok, L., Baelde, H. J., & de Heer, E. (2015). UPF0586 Protein C9orf41 Homolog Is Anserine-producing Methyltransferase. *The Journal of Biological Chemistry*, *290*(28), 17190–17205. https://doi.org/10.1074/jbc.M115.640037

Drozak, J., Veiga-da-Cunha, M., Vertommen, D., Stroobant, V., & Van Schaftingen, E. (2010). Molecular Identification of Carnosine Synthase as ATP-grasp Domain-containing Protein 1 (ATPGD1)*. *Journal of Biological Chemistry*, *285*(13), 9346–9356. https://doi.org/10.1074/jbc.M109.095505

EFSA Panel on Plant Protection Products and their Residues (PPR), Hernandez Jerez, A., Adriaanse, P., Berny, P., Coja, T., Duquesne, S., Focks, A., Marinovich, M., Millet, M., Pelkonen, O., Pieper, S., Tiktak, A., Topping, C., Widenfalk, A., Wilks, M., Wolterink, G., Rundlöf, M., Ippolito, A., Linguadoca, A., … Aldrich, A. (2022). Statement on the active substance acetamiprid. *EFSA Journal*, *20*(1), e07031. https://doi.org/10.2903/j.efsa.2022.7031

Eftekhari, A., Heidari, R., Ahmadian, E., & Eghbal, M. A. (2018). Cytoprotective Properties of Carnosine against Isoniazid-Induced Toxicity in Primary Cultured Rat Hepatocytes. *Pharmaceutical Sciences*, *24*(4), Article 4. https://doi.org/10.15171/PS.2018.38

Efthymakis, K., & Neri, M. (2022). The role of Zinc L-Carnosine in the prevention and treatment of gastrointestinal mucosal disease in humans: A review. *Clinics and Research in Hepatology and Gastroenterology*, *46*(7), 101954. https://doi.org/10.1016/j.clinre.2022.101954

El Sayed, S. A., & Mukherjee, S. (2024). Physiology, Pancreas. In *StatPearls*. StatPearls Publishing. http://www.ncbi.nlm.nih.gov/books/NBK459261/

Elbarbary, N. S., Ismail, E. A. R., El-Naggar, A. R., Hamouda, M. H., & El-Hamamsy, M. (2018). The effect of 12 weeks carnosine supplementation on renal functional integrity and oxidative stress in pediatric patients with diabetic nephropathy: A randomized placebo-controlled trial. *Pediatric Diabetes*, *19*(3), 470–477. https://doi.org/10.1111/pedi.12564

El-Gendy, K. S., Aly, N. M., Mahmoud, F. H., & Allah, D. A. (2022). Toxicological assessment of sublethal dose of acetamiprid in male mice and the efficacy of quercetin. *Pesticide Biochemistry and Physiology*, *184*, 105078. https://doi.org/10.1016/j.pestbp.2022.105078

Elhalwagy, M. E., Abd-Alrahman, S. H., Nahas, A., Ziada, R. M., & Mohamady, A. H. (2015). Hepatopancreatic intoxication of lambda cyhalothrin insecticide on albino rats. *International Journal of Clinical and Experimental Medicine*, *8*(5), 7297–7305.

El-Nagdy, S. A., Elfakharany, Y. M., Morsy, M. M., Ahmad, M. M., Abd El-Fatah, S. S., & Khayal, E. E.-S. (2024). The role of fenugreek seed extract in alleviating pancreatic toxic effects and altering glucose homeostasis induced by acetamiprid via modulation of oxidative stress, apoptosis, and autophagy. *Tissue & Cell*, *86*, 102265. https://doi.org/10.1016/j.tice.2023.102265

Erdemli, M. E., Zayman, E., Erdemli, Z., Gul, M., Gul, S., & Gozukara Bag, H. (2020). Protective effects of melatonin and vitamin E in acetamiprid-induced nephrotoxicity. *Environmental Science and Pollution Research International*, *27*(9), 9202–9213. https://doi.org/10.1007/s11356-019-06754-y

Fadda, L. M., Ali, H. M., Mohamed, A. M., & Hagar, H. (2020). Prophylactic administration of carnosine and melatonin abates the incidence of apoptosis, inflammation, and DNA damage induced by titanium dioxide nanoparticles in rat livers. *Environmental Science and Pollution Research International*, *27*(16), 19142–19150. https://doi.org/10.1007/s11356-019-05059-4

Fasnabi, P. A., Remya, C., & Madhu, G. (2012). *Degradation of Acetamiprid in Wastewater by Ozonation*. https://www.semanticscholar.org/paper/Degradation-of-Acetamiprid-in-Wastewater-by-Fasnabi-Remya/c42d5cc717eb72a66162f35d765bece9490b558b

Fatih Aydın, A., Küçükgergin, C., Bingül, İ., Doğan-Ekici, I., Doğru-Abbasoğlu, S., & Uysal, M. (2017). Effect of Carnosine on Renal Function, Oxidation and Glycation Products in the Kidneys of High-Fat Diet/Streptozotocin-Induced Diabetic Rats. *Experimental and Clinical Endocrinology & Diabetes: Official Journal, German Society of Endocrinology [and] German Diabetes Association*, *125*(5), 282–289. https://doi.org/10.1055/s-0043-100117

Feehan, J., Hariharan, R., Buckenham, T., Handley, C., Bhatnagar, A., Baba, S. P., & Courten, B. de. (2022). Carnosine as a potential therapeutic for the management

of peripheral vascular disease. *Nutrition, Metabolism and Cardiovascular Diseases*, *32*(10), 2289–2296. https://doi.org/10.1016/j.numecd.2022.07.006

Fogel, M. N., Schneider, M. I., Desneux, N., González, B., & Ronco, A. E. (2013). Impact of the neonicotinoid acetamiprid on immature stages of the predator Eriopis connexa (Coleoptera: Coccinellidae). *Ecotoxicology (London, England)*, *22*(6), 1063–1071. https://doi.org/10.1007/s10646-013-1094-5

Fontana, M., Pinnen, F., Lucente, G., & Pecci, L. (2002). Prevention of peroxynitrite-dependent damage by carnosine and related sulphonamido pseudodipeptides. *Cellular and Molecular Life Sciences: CMLS*, *59*(3), 546–551. https://doi.org/10.1007/s00018-002-8446-2

Fonteh, A. N., Harrington, R. J., Tsai, A., Liao, P., & Harrington, M. G. (2007). Free amino acid and dipeptide changes in the body fluids from Alzheimer's disease subjects. *Amino Acids*, *32*(2), 213–224. https://doi.org/10.1007/s00726-006-0409-8

Formaziuk, V. E., Gorshkova, T. I., Boldyrev, A. A., & Sergienko, V. I. (1992). [Characteristics of chloramine complexes of carnosine with hypochlorite anion]. *Biokhimiia (Moscow, Russia)*, *57*(9), 1324–1329.

Forsberg, E. A., Botusan, I. R., Wang, J., Peters, V., Ansurudeen, I., Brismar, K., & Catrina, S. B. (2015). Carnosine decreases IGFBP1 production in db/db mice through suppression of HIF-1. *The Journal of Endocrinology*, *225*(3), 159–167. https://doi.org/10.1530/JOE-14-0571

Foster, J. R. (2014). A review of animal models of nonneoplastic pancreatic diseases. *Toxicologic Pathology*, *42*(1), 243–259. https://doi.org/10.1177/0192623313508479

Fresta, C. G., Fidilio, A., Lazzarino, G., Musso, N., Grasso, M., Merlo, S., Amorini, A. M., Bucolo, C., Tavazzi, B., Lazzarino, G., Lunte, S. M., Caraci, F., & Caruso, G. (2020). Modulation of Pro-Oxidant and Pro-Inflammatory Activities of M1 Macrophages by the Natural Dipeptide Carnosine. *International Journal of Molecular Sciences*, *21*(3), 776. https://doi.org/10.3390/ijms21030776

Fry, J. (1985). Gastro-Intestinal Diseases—The Clinical Spectrum. In J. Fry (Ed.), *Common Diseases: Their Nature Incidence and Care* (pp. 195–198). Springer Netherlands. https://doi.org/10.1007/978-94-009-4924-9_22

Gacem, H., Bendali-Saoudi, F., Serradj, N., Houmani, M., & Soltani, N. (2023). RISK ASSESSMENT OF THE NEONICOTINOID INSECTICIDE ACETAMIPRID ON TWO NON-TARGET SPECIES, DAPHNIA MAGNA STRAUS, 1820 (CRUSTACEA, CLADOCERA) AND PLEA MINUTISSIMA LEACH, 1817 (INSECTA, HETEROPTERA). *Applied Ecology and Environmental Research*, *21*(2), 1143–1155. https://doi.org/10.15666/aeer/2102_11431155

Gaisano, H. Y., & Gorelick, F. S. (2009). New insights into the mechanisms of pancreatitis. *Gastroenterology*, *136*(7), 2040–2044. https://doi.org/10.1053/j.gastro.2009.04.023

Gapp, J., Tariq, A., & Chandra, S. (2024). Acute Pancreatitis. In *StatPearls*. StatPearls Publishing. http://www.ncbi.nlm.nih.gov/books/NBK482468/

Garcia-Sanchez, L., Santofimia-Castaño, P., Miro-Moran, A., Tapia, J. A., Salido, G. M., & Gonzalez, A. (2012). *Molecular and Cellular Biochemistry*, *362*(1–2), 15–23. https://doi.org/10.1007/s11010-011-1123-8

Gardner, M. L., Illingworth, K. M., Kelleher, J., & Wood, D. (1991). Intestinal absorption of the intact peptide carnosine in man, and comparison with intestinal permeability to lactulose. *The Journal of Physiology*, *439*, 411–422.

Gasmi, G., R, R., M, K., A, S., S, B., N, T., C, T., S, H., Z, B., & B, D. (2016). Neurotoxicity of Acetamiprid in Male Albino Rats and the Opposite Effect of Quercetin. *BioTechnology: An Indian Journal*, *12*(12). https://www.tsijournals.com/abstract/neurotoxicity-of-acetamiprid-in-male-albino-rats-and-the-opposite-effect-of-quercetin-10123.html

Gasmi, G., R, R., M, K., A, S., S, B., N, T., C, T., S, H., Z, B., & B, D. (2016). Neurotoxicity of Acetamiprid in Male Albino Rats and the Opposite Effect of Quercetin. *BioTechnology: An Indian Journal*, *12*(12). https://www.tsijournals.com/abstract/neurotoxicity-of-acetamiprid-in-male-albino-rats-and-the-opposite-effect-of-quercetin-10123.html

Gasmi, S., Chafaa, S., Lakroun, Z., Rouabhi, R., Touahria, C., Kebieche, M., & Soulimani, R. (2019). Neuronal Apoptosis and Imbalance of Neurotransmitters Induced by Acetamiprid in Rats. *Toxicology and Environmental Health Sciences*, *11*(4), 305–311. Scopus. https://doi.org/10.1007/s13530-019-0417-1

Gasmi, S., Kebieche, M., Rouabhi, R., Touahria, C., Lahouel, A., Lakroun, Z., Henine, S., & Soulimani, R. (2017). Alteration of membrane integrity and respiratory function of brain mitochondria in the rats chronically exposed to a low dose of acetamiprid. *Environmental Science and Pollution Research International*, *24*(28), 22258–22264. https://doi.org/10.1007/s11356-017-9901-9

Gasmi, S., Kebieche, M., Rouabhi, R., Touahria, C., Lahouel, A., Lakroun, Z., Henine, S., & Soulimani, R. (2017). Alteration of membrane integrity and respiratory function of brain mitochondria in the rats chronically exposed to a low dose of acetamiprid. *Environmental Science and Pollution Research International*, *24*(28), 22258–22264. https://doi.org/10.1007/s11356-017-9901-9

Gokalp, O., Buyukvanlı, B., Cicek, E., Ozer, M. K., Koyu, A., Altuntas, I., & Koylu, H. (2005). The effects of diazinon on pancreatic damage and ameliorating role of vitamin E and vitamin C. *Pesticide Biochemistry and Physiology*, *81*(2), 123–128. https://doi.org/10.1016/j.pestbp.2004.11.001

Golson, M. L., & Kaestner, K. H. (2017). Epigenetics in formation, function, and failure of the endocrine pancreas. *Molecular Metabolism*, *6*(9), 1066–1076. https://doi.org/10.1016/j.molmet.2017.05.015

Gomez, S. D., Bustos, P. S., Sánchez, V. G., Ortega, M. G., & Guiñazú, N. (2020). Trophoblast toxicity of the neonicotinoid insecticide acetamiprid and an acetamiprid-based formulation. *Toxicology*, *431*, 152363. https://doi.org/10.1016/j.tox.2020.152363

Gopko, A. V., Kulibin, A. Y., Semenova, M. L., & Zakhidov, S. T. (2005). Carnosine-induced changes in the development of spermatogenic epithelial cells in senescence accelerated SAM mice. *Bulletin of Experimental Biology and Medicine*, *140*(2), 235–237. https://doi.org/10.1007/s10517-005-0454-4

Graziosi, A., Sita, G., Corrieri, C., Angelini, S., d'Emmanuele di Villa Bianca, R., Mitidieri, E., Sorrentino, R., Hrelia, P., & Morroni, F. (2022). Effects of Subtoxic Concentrations of Atrazine, Cypermethrin, and Vinclozolin on microRNA-Mediated PI3K/Akt/mTOR Signaling in SH-SY5Y Cells. *International Journal of Molecular Sciences*, *23*(23), 14538. https://doi.org/10.3390/ijms232314538

Greco, V., Naletova, I., Ahmed, I. M. M., Vaccaro, S., Messina, L., La Mendola, D., Bellia, F., Sciuto, S., Satriano, C., & Rizzarelli, E. (2020). Hyaluronan-carnosine conjugates inhibit Aß aggregation and toxicity. *Scientific Reports*, *10*(1), Article 1. https://doi.org/10.1038/s41598-020-72989-2

Grynkiewicz, G., Poenie, M., & Tsien, R. Y. (1985). A new generation of Ca2+ indicators with greatly improved fluorescence properties. *Journal of Biological Chemistry*, *260*(6), 3440–3450. https://doi.org/10.1016/S0021-9258(19)83641-4

Guiotto, A., Ruzza, P., Babizhayev, M. A., & Calderan, A. (2007). Malondialdehyde scavenging and aldose-derived Schiff bases' transglycation properties of synthetic histidyl-hydrazide carnosine analogs. *Bioorganic & Medicinal Chemistry*, *15*(18), 6158–6163. https://doi.org/10.1016/j.bmc.2007.06.029

Gulewitsch, Wl., & Amiradžibi, S. (1900). Ueber das Carnosin, eine neue organische Base des Fleischextractes. *Berichte Der Deutschen Chemischen Gesellschaft*, *33*(2), 1902–1903. https://doi.org/10.1002/cber.19000330275

Guo, Y., Guo, C., Ha, W., & Ding, Z. (2019). Carnosine improves diabetic retinopathy via the MAPK/ERK pathway. *Experimental and Therapeutic Medicine*. https://doi.org/10.3892/etm.2019.7223

Gusev, E., Sarapultsev, A., Solomatina, L., & Chereshnev, V. (2022). SARS-CoV-2-Specific Immune Response and the Pathogenesis of COVID-19. *International Journal of Molecular Sciences*, *23*(3), 1716. https://doi.org/10.3390/ijms23031716

Guzman-Vallejos, M. S., Ramirez-Cando, L. J., Aguayo, L., & Ballaz, S. J. (2024). Molecular Docking Analysis at the Human α7-nAChR and Proliferative and Evoked-Calcium Changes in SH-SY5Y Cells by Imidacloprid and Acetamiprid Insecticides. *Neurotoxicity Research*, *42*(2), 16. https://doi.org/10.1007/s12640-024-00697-0

Hall, C. (2001). *Sources of natural antioxidants: Oilseeds, nuts, cereals, legumes, animal products and microbial sources*. 159–209.

Hampton, R. F., Jimenez-Gonzalez, M., & Stanley, S. A. (2022). Unravelling innervation of pancreatic islets. *Diabetologia*, *65*(7), 1069–1084. https://doi.org/10.1007/s00125-022-05691-9

Harada, K. H., Tanaka, K., Sakamoto, H., Imanaka, M., Niisoe, T., Hitomi, T., Kobayashi, H., Okuda, H., Inoue, S., Kusakawa, K., Oshima, M., Watanabe, K., Yasojima, M., Takasuga, T., & Koizumi, A. (2016). Biological Monitoring of Human Exposure to Neonicotinoids Using Urine Samples, and Neonicotinoid Excretion Kinetics. *PLOS ONE*, *11*(1), e0146335. https://doi.org/10.1371/journal.pone.0146335

Hassanen, E. I., Hussien, A. M., Mehanna, S., Ibrahim, M. A., & Hassan, N. H. (2022). Comparative assessment on the probable mechanisms underlying the hepatorenal toxicity of commercial imidacloprid and hexaflumuron formulations in rats. *Environmental Science and Pollution Research*, *29*(19), 29091–29104. https://doi.org/10.1007/s11356-021-18486-z

Hataba, A. A., Keshta, A. T., Mead, HalaM. I., & El-Shafey, NouranM. (2014). Hematological, Biochemical and Histological alterations induced by oral administration of Thiamethoxam and Acetamiprid in male rats. *Biochemistry Letters*, *9*(1), 113–125. https://doi.org/10.21608/blj.2014.63858

Henry, B. M., Skinningsrud, B., Saganiak, K., Pękala, P. A., Walocha, J. A., & Tomaszewski, K. A. (2019). Development of the human pancreas and its vasculature—An integrated review covering anatomical, embryological, histological, and molecular aspects. *Annals of Anatomy - Anatomischer Anzeiger*, *221*, 115–124. https://doi.org/10.1016/j.aanat.2018.09.008

Hipkiss, A. R., & Gaunitz, F. (2014). Inhibition of tumour cell growth by carnosine: Some possible mechanisms. *Amino Acids*, *46*(2), 327–337. https://doi.org/10.1007/s00726-013-1627-5

Hipkiss, A. R., Preston, J. E., Himswoth, D. T., Worthington, V. C., & Abbot, N. J. (1997). Protective effects of carnosine against malondialdehyde-induced toxicity towards cultured rat brain endothelial cells. *Neuroscience Letters*, *238*(3), 135–138. https://doi.org/10.1016/s0304-3940(97)00873-2

Hipkiss, A. R., Worthington, V. C., Himsworth, D. T., & Herwig, W. (1998). Protective effects of carnosine against protein modification mediated by malondialdehyde and hypochlorite. *Biochimica Et Biophysica Acta*, *1380*(1), 46–54. https://doi.org/10.1016/s0304-4165(97)00123-2

Hisamatsu, T., Ono, N., Imaizumi, A., Mori, M., Suzuki, H., Uo, M., Hashimoto, M., Naganuma, M., Matsuoka, K., Mizuno, S., Kitazume, M. T., Yajima, T., Ogata, H., Iwao, Y., Hibi, T., & Kanai, T. (2015). Decreased Plasma Histidine Level Predicts Risk of Relapse in Patients with Ulcerative Colitis in Remission. *PLoS ONE*, *10*(10), e0140716. https://doi.org/10.1371/journal.pone.0140716

Hobart, L. J., Seibel, I., Yeargans, G. S., & Seidler, N. W. (2004). Anti-crosslinking properties of carnosine: Significance of histidine. *Life Sciences*, *75*(11), 1379–1389. https://doi.org/10.1016/j.lfs.2004.05.002

Hoffman, J. R., Varanoske, A., & Stout, J. R. (2018). Effects of ß-Alanine Supplementation on Carnosine Elevation and Physiological Performance. *Advances in Food and Nutrition Research*, *84*, 183–206. https://doi.org/10.1016/bs.afnr.2017.12.003

Holdaj, M., Gorzka, D., & Soika, G. (2020). Effectiveness of acetamiprid in reducing rosy apple aphid population (Dysaphis plantaginea, Passerini) analysed in selected apple orchards. *Progress in Plant Protection*, *60*(4). https://doi.org/10.14199/ppp-2020-035

Holeček, M. (2020). Histidine in Health and Disease: Metabolism, Physiological Importance, and Use as a Supplement. *Nutrients*, *12*(3), 848. https://doi.org/10.3390/nu12030848

HOLEČEK, M. (2022). Side Effects of Amino Acid Supplements. *Physiological Research*, *71*(1), 29–45. https://doi.org/10.33549/physiolres.934790

Holliday, R., & McFarland, G. A. (1996). Inhibition of the growth of transformed and neoplastic cells by the dipeptide carnosine. *British Journal of Cancer*, *73*(8), 966–971. https://doi.org/10.1038/bjc.1996.189

Huang, F., Liu, Q., Xie, S., Xu, J., Huang, B., Wu, Y., & Xia, D. (2016). Cypermethrin Induces Macrophages Death through Cell Cycle Arrest and Oxidative Stress-Mediated JNK/ERK Signaling Regulated Apoptosis. *International Journal of Molecular Sciences*, *17*(6), Article 6. https://doi.org/10.3390/ijms17060885

Huang, Q., Wu, X., Yu, X., Zhang, L., Lu, M., & Tao, L. (2015). Comparison of the cytotoxic impact of chlorfluazuron on selected insect and human cell lines. *Environmental Toxicology and Chemistry*, *34*(7), 1675–1682. https://doi.org/10.1002/etc.2969

Igarashi, A., & Yamaguchi, M. (2003). Great increase in bone 66 kDa protein and osteocalcin at later stages with healing rat fractures: Effect of zinc treatment. *International Journal of Molecular Medicine*, *11*(2), 223–228.

Ihara, H., Kakihana, Y., Yamakage, A., Kai, K., Shibata, T., Nishida, M., Yamada, K.-I., & Uchida, K. (2019). 2-Oxo-histidine-containing dipeptides are functional oxidation products. *The Journal of Biological Chemistry*, *294*(4), 1279–1289. https://doi.org/10.1074/jbc.RA118.006111

Issam, C., Samir, H., Zohra, H., Monia, Z., & Hassen, B. C. (2009). Toxic responses to deltamethrin (DM) low doses on gonads, sex hormones and lipoperoxidation in

male rats following subcutaneous treatments. *The Journal of Toxicological Sciences*, *34*(6), 663–670. https://doi.org/10.2131/jts.34.663

Jablan, J. (2016). Spectrophotometric Determination of Malondialdehyde in Urine Suitable for Epidemiological Studies. *Croatica Chemica Acta*. https://www.academia.edu/56452687/

Jia, H., Qi, X., Fang, S., Jin, Y., Han, X., Wang, Y., Wang, A., & Zhou, H. (2009). Carnosine inhibits high glucose-induced mesangial cell proliferation through mediating cell cycle progression. *Regulatory Peptides*, *154*(1–3), 69–76. https://doi.org/10.1016/j.regpep.2008.12.004

Jukić, I., Kolobarić, N., Stupin, A., Matić, A., Kozina, N., Mihaljević, Z., Mihalj, M., Šušnjara, P., Stupin, M., Ćurić, Ž. B., Selthofer-Relatić, K., Kibel, A., Lukinac, A., Kolar, L., Kralik, G., Kralik, Z., Széchenyi, A., Jozanović, M., Galović, O., … Drenjančević, I. (2021). Carnosine, Small but Mighty—Prospect of Use as Functional Ingredient for Functional Food Formulation. *Antioxidants*, *10*(7), 1037. https://doi.org/10.3390/antiox10071037

Jun(1), I., Lee(1), M. G., & Muallem(2), S. (2017). Molecular Mechanisms of Pancreatic Bicarbonate Secretion. *Pancreapedia: The Exocrine Pancreas Knowledge Base*. https://doi.org/10.3998/panc.2017.01

Kagawa, N., & Nagao, T. (2018). Neurodevelopmental toxicity in the mouse neocortex following prenatal exposure to acetamiprid. *Journal of Applied Toxicology: JAT*, *38*(12), 1521–1528. https://doi.org/10.1002/jat.3692

Kamei, J., Ohsawa, M., Miyata, S., & Tanaka, S. (2008). Preventive effect of L-carnosine on changes in the thermal nociceptive threshold in streptozotocin-induced diabetic mice. *European Journal of Pharmacology*, *600*(1–3), 83–86. https://doi.org/10.1016/j.ejphar.2008.10.002

Kamel, O., Ramadan, B., Abd Elwahab, A., Mohamed, S., & Ali, H. (2020). The possible ameliorative effect of carnosine in protein deficient diet induced testicular damage. *Journal of Recent Advances in Medicine*, *1*(2), 96–103. https://doi.org/10.21608/jram.2020.22346.1033

Kanna, S., Karuppuchamy, P., Kuttalam, S., & Sivasamy, N. (2007). Bio-efficacy of acetamiprid 20 sp against Aphis gossypii and Amrasca biguttula biguttula in cotton. *Annals of Plant Protection Sciences*. https://www.semanticscholar.org/paper/Bio-efficacy-of-acetamiprid-20-sp-against-Aphis-and-Kanna-Karuppuchamy/9ebf3ba066c205f1e416890e4fcc72972e066fc2

Kapoor, U., Srivastava, M. K., & Srivastava, L. P. (2011). Toxicological impact of technical imidacloprid on ovarian morphology, hormones and antioxidant enzymes in female rats. *Food and Chemical Toxicology: An International Journal Published for the British Industrial Biological Research Association*, *49*(12), 3086–3089. https://doi.org/10.1016/j.fct.2011.09.009

KARA, M., ÖZTAŞ, E., & ÖZHAN, G. (2020). Acetamiprid-induced Cyto- and Genotoxicity in the AR42J Pancreatic Cell Line. *Turkish Journal of Pharmaceutical Sciences*, *17*(5), 474–479. https://doi.org/10.4274/tjps.galenos.2019.89719

Kara, M., Yumrutas, O., Demir, C. F., Ozdemir, H. H., Bozgeyik, I., Coskun, S., Eraslan, E., & Bal, R. (2015). Insecticide imidacloprid influences cognitive functions and alters learning performance and related gene expression in a rat model. *International Journal of Experimental Pathology*, *96*(5), 332–337. https://doi.org/10.1111/iep.12139

Karaca, B. U., Arican, Y. E., Boran, T., Binay, S., Okyar, A., Kaptan, E., & Özhan, G. (2019a). Effects of subchronic oral acetamiprid exposure in ratsToxic. *Toxicology and Industrial Health*, *35*(11–12), 679–687. https://doi.org/10.1177/0748233719893203

Karaca, B. U., Arican, Y. E., Boran, T., Binay, S., Okyar, A., Kaptan, E., & Özhan, G. (2019b). Toxic effects of subchronic oral acetamiprid exposure in rats. *Toxicology and Industrial Health*, *35*(11–12), 679–687. https://doi.org/10.1177/0748233719893203

Karaca, B. U., Arican, Y. E., Boran, T., Binay, S., Okyar, A., Kaptan, E., & Özhan, G. (2019). Effects of subchronic oral acetamiprid exposure in ratsToxic. *Toxicology and Industrial Health*, *35*(11–12), 679–687. https://doi.org/10.1177/0748233719893203

Karpińska, M., & Czauderna, M. (2022). Pancreas—Its Functions, Disorders, and Physiological Impact on the Mammals' Organism. *Frontiers in Physiology*, *13*. https://doi.org/10.3389/fphys.2022.807632

Kashyap, M. P., Singh, A. K., Kumar, V., Yadav, D. K., Khan, F., Jahan, S., Khanna, V. K., Yadav, S., & Pant, A. B. (2013). Pkb/Akt1 Mediates Wnt/GSK3ß/ß-Catenin Signaling-Induced Apoptosis in Human Cord Blood Stem Cells Exposed to Organophosphate Pesticide Monocrotophos. *Stem Cells and Development*, *22*(2), 224–238. https://doi.org/10.1089/scd.2012.0220

Kebièche, M., Lakroun, Z., Mraïhi, Z., & Soulimani, R. (2011). Effet antidiabétogène et cytoprotecteur de l'extrait butanolique de Ranunculus repens L. et de la quercétine sur un modèle expérimental de diabète alloxanique. *Phytothérapie*, *9*(5), 274–282. https://doi.org/10.1007/s10298-011-0651-4

Khalil, S. R., Awad, A., Mohammed, H. H., & Nassan, M. A. (2017). Imidacloprid insecticide exposure induces stress and disrupts glucose homeostasis in male rats. *Environmental Toxicology and Pharmacology*, *55*, 165–174. Scopus. https://doi.org/10.1016/j.etap.2017.08.017

Khayal, E., & Ahmed, M. (2019). Evaluating Chloropyrifos Induced Diabtes Mellitus, Pancreatic Toxic Effects in Adult Albino Rats and Whether This Insult Is Permanent or Temporary. *Ain Shams Journal of Forensic Medicine and Clinical Toxicology*, *33*(2), 92–103. https://doi.org/10.21608/ajfm.2019.41229

Ki, Y.-W., Lee, J. E., Park, J. H., Shin, I. C., & Koh, H. C. (2012). Reactive oxygen species and mitogen-activated protein kinase induce apoptotic death of SH-SY5Y cells in response to fipronil. *Toxicology Letters*, *211*(1), 18–28. https://doi.org/10.1016/j.toxlet.2012.02.022

Kilis-Pstrusinska, K. (2020). Carnosine and Kidney Diseases: What We Currently Know? *Current Medicinal Chemistry*, *27*(11), 1764–1781. https://doi.org/10.2174/0929867326666190730130024

Kim, J., Park, Y., Yoon, K. S., Clark, J. M., & Park, Y. (2013). Imidacloprid, a neonicotinoid insecticide, induces insulin resistance. *The Journal of Toxicological Sciences*, *38*(5), 655–660. https://doi.org/10.2131/jts.38.655

Kim, Y., & Kim, Y. (2020). L-histidine and L-carnosine exert anti-brain aging effects in D-galactose-induced aged neuronal cells. *Nutrition Research and Practice*, *14*(3), 188–202. https://doi.org/10.4162/nrp.2020.14.3.188

Kitazawa, M., Medeiros, R., & LaFerla, F. M. (2012). Transgenic Mouse Models of Alzheimer Disease: Developing a Better Model as a Tool for Therapeutic Interventions. *Current Pharmaceutical Design*, *18*(8), 1131–1147.

Klebanov, G. I., Teselkin YuO, null, Babenkova, I. V., Popov, I. N., Levin, G., Tyulina, O. V., Boldyrev, A. A., & Vladimirov YuA, null. (1997). Evidence for a direct

interaction of superoxide anion radical with carnosine. *Biochemistry and Molecular Biology International*, *43*(1), 99–106. https://doi.org/10.1080/15216549700203861

Kleeff, J., Whitcomb, D. C., Shimosegawa, T., Esposito, I., Lerch, M. M., Gress, T., Mayerle, J., Drewes, A. M., Rebours, V., Akisik, F., Muñoz, J. E. D., & Neoptolemos, J. P. (2017). Chronic pancreatitis. *Nature Reviews. Disease Primers*, *3*, 17060. https://doi.org/10.1038/nrdp.2017.60

Ko, E. A., Park, Y. J., Yoon, D. S., Lee, K.-M., Kim, J., Jung, S., Lee, J. W., & Park, K. H. (2022). Drug repositioning of polaprezinc for bone fracture healing. *Communications Biology*, *5*(1), 462. https://doi.org/10.1038/s42003-022-03424-7

Kohen, R., Yamamoto, Y., Cundy, K. C., & Ames, B. N. (1988). Antioxidant activity of carnosine, homocarnosine, and anserine present in muscle and brain. *Proceedings of the National Academy of Sciences*, *85*(9), 3175–3179. https://doi.org/10.1073/pnas.85.9.3175

Kolanczyk, R. C., Tapper, M. A., Sheedy, B. R., & Serrano, J. A. (2020). *In vitro* metabolism of imidacloprid and acetamiprid in rainbow trout and rat. *Xenobiotica*, *50*(7), 805–814. https://doi.org/10.1080/00498254.2019.1694197

Kulebyakin, K., Karpova, L., Lakonsteva, E., Krasavin, M., & Boldyrev, A. (2012). Carnosine protects neurons against oxidative stress and modulates the time profile of MAPK cascade signaling. *Amino Acids*, *43*(1), 91–96. https://doi.org/10.1007/s00726-011-1135-4

Kulikova, O. I., Berezhnoy, D. S., Stvolinsky, S. L., Lopachev, A. V., Orlova, V. S., & Fedorova, T. N. (2018). Neuroprotective effect of the carnosine—α-lipoic acid nanomicellar complex in a model of early-stage Parkinson's disease. *Regulatory Toxicology and Pharmacology: RTP*, *95*, 254–259. https://doi.org/10.1016/j.yrtph.2018.03.025

Kulikova, O. I., Stvolinsky, S. L., Migulin, V. A., Andreeva, L. A., Nagaev, I. Y., Lopacheva, O. M., Kulichenkova, K. N., Lopachev, A. V., Trubitsina, I. E., & Fedorova, T. N. (2020). A new derivative of acetylsalicylic acid and carnosine: Synthesis, physical and chemical properties, biological activity. *Daru: Journal of Faculty of Pharmacy, Tehran University of Medical Sciences*, *28*(1), 119–130. https://doi.org/10.1007/s40199-019-00323-x

Kundoo, A., Dar, S., Mushtaq, M., Bashir, Z., Dar, M. S., Gul, S., Ali, M. T., & Gulzar, S. (2018). Role of neonicotinoids in insect pest management: A review. *Journal of Entomology and Zoology Studies*. https://www.semanticscholar.org/paper/Role-of-neonicotinoids-in-insect-pest-management%3A-A-Kundoo-Dar/9c87b45f41a9a9631f08a6470a6f538bbba345d7

Kurata, H., Fujii, T., Tsutsui, H., Katayama, T., Ohkita, M., Takaoka, M., Tsuruoka, N., Kiso, Y., Ohno, Y., Fujisawa, Y., Shokoji, T., Nishiyama, A., Abe, Y., & Matsumura, Y. (2006). Renoprotective effects of l-carnosine on ischemia/reperfusion-induced renal injury in rats. *The Journal of Pharmacology and Experimental Therapeutics*, *319*(2), 640–647. https://doi.org/10.1124/jpet.106.110122

Lamberti, M., Stellavato, A., Pirozzi, A., & D'Agostino, A. (2014). Effects of Pyriproxyfen on Viability and Increase of Intracellular Lipids in HepG2 Cell Line. *Occupational Medicine & Health Affairs*, *02*(05). https://doi.org/10.4172/2329-6879.1000189

Lee, H.-S., Song, H.-J., Park, Y., Smolensky, D., & Lee, S.-H. (2022). Permethrin inhibits tube formation and viability of endothelial cells. *Journal of the Science of Food and Agriculture*, *102*(10), 4079–4085. https://doi.org/10.1002/jsfa.11757

Lee, P. J., & Papachristou, G. I. (2019). New insights into acute pancreatitis. *Nature Reviews. Gastroenterology & Hepatology*, *16*(8), 479–496. https://doi.org/10.1038/s41575-019-0158-2

Lee, Y.-T., Hsu, C., Lin, M., Liu, K., & Yin, M. (2005). Histidine and carnosine delay diabetic deterioration in mice and protect human low density lipoprotein against oxidation and glycation. *European Journal of Pharmacology*, *513 1-2*, 145–150. https://doi.org/10.1016/J.EJPHAR.2005.02.010

Lee, Y.-T., Hsu, C., Lin, M., Liu, K., & Yin, M. (2005). Histidine and carnosine delay diabetic deterioration in mice and protect human low density lipoprotein against oxidation and glycation. *European Journal of Pharmacology*, *513 1-2*, 145–150. https://doi.org/10.1016/J.EJPHAR.2005.02.010

Li, B., Xia, X., Wang, J., Zhu, L., Wang, J., & Wang, G. (2018). Evaluation of acetamiprid-induced genotoxic and oxidative responses in Eisenia fetida. *Ecotoxicology and Environmental Safety*, *161*, 610–615. https://doi.org/10.1016/j.ecoenv.2018.06.022

Li, X., He, S., Xiao, H., He, T.-T., Zhang, J.-D., Luo, Z.-R., Ma, J.-Z., Yin, Y.-L., Luo, L., & Cao, L.-Y. (2022). Neonicotinoid insecticides promote breast cancer progression via G protein-coupled estrogen receptor: In vivo, in vitro and in silico studies. *Environment International*, *170*, 107568. https://doi.org/10.1016/j.envint.2022.107568

Lonare, M., Kumar, M., Raut, S., More, A., Doltade, S., Badgujar, P., & Telang, A. (2016). Evaluation of ameliorative effect of curcumin on imidacloprid-induced male reproductive toxicity in wistar rats. *Environmental Toxicology*, *31*(10), 1250–1263. https://doi.org/10.1002/tox.22132

Longnecker, D. S. (2014). Anatomy and Histology of the Pancreas. *Pancreapedia: The Exocrine Pancreas Knowledge Base*. https://doi.org/10.3998/panc.2014.3

Lopachev, A. V., Kazanskaya, R. B., Khutorova, A. V., & Fedorova, T. N. (2020). An overview of the pathogenic mechanisms involved in severe cases of COVID-19 infection, and the proposal of salicyl-carnosine as a potential drug for its treatment. *European Journal of Pharmacology*, *886*, 173457. https://doi.org/10.1016/j.ejphar.2020.173457

Love, J. A., Yi, E., & Smith, T. G. (2007). Autonomic pathways regulating pancreatic exocrine secretion. *Autonomic Neuroscience*, *133*(1), 19–34. https://doi.org/10.1016/j.autneu.2006.10.001

Lu, Z., Ye, W., Feng, P., Dai, M., Bian, D., Ren, Y., Zhu, Q., Mao, T., Su, W., Li, F., Sun, H., Wei, J., & Li, B. (2021). Low concentration acetamiprid-induced oxidative stress hinders the growth and development of silkworm posterior silk glands. *Pesticide Biochemistry and Physiology*, *174*, 104824. https://doi.org/10.1016/j.pestbp.2021.104824

Mahai, G., Wan, Y., Xia, W., Wang, A., Qian, X., Li, Y., He, Z., Li, Y., & Xu, S. (2022). Exposure assessment of neonicotinoid insecticides and their metabolites in Chinese women during pregnancy: A longitudinal study. *The Science of the Total Environment*, *818*, 151806. https://doi.org/10.1016/j.scitotenv.2021.151806

Mahmood, A., FitzGerald, A. J., Marchbank, T., Ntatsaki, E., Murray, D., Ghosh, S., & Playford, R. J. (2007). Zinc carnosine, a health food supplement that stabilises small bowel integrity and stimulates gut repair processes. *Gut*, *56*(2), 168–175. https://doi.org/10.1136/gut.2006.099929

Martínez-Morcillo, S., Pérez-López, M., Soler-Rodríguez, F., & González, A. (2019). The organophosphorus pesticide dimethoate decreases cell viability and induces changes in different biochemical parameters of rat pancreatic stellate cells. *Toxicology in Vitro*, *54*, 89–97. https://doi.org/10.1016/j.tiv.2018.09.011

Martins, J. R. N., Lopes, S., Hurtado, H. N., da Silva, F. N., Villard, D. R., Taboga, S. R., Souza, K. L. A., Quesada, I., Soriano, S., & Rafacho, A. (2023). Acute and chronic effects of the organophosphate malathion on the pancreatic α and ß cell viability, cell structure, and voltage-gated K+ currents. *Environmental Toxicology and Pharmacology*, *98*, 104046. https://doi.org/10.1016/j.etap.2022.104046

Marzouki, S., Bini Dhouib, I., Benabdessalem, C., Rekik, R., Doghri, R., Maroueni, A., Bellasfar, Z., Fazaa, S., Bettaieb, J., Barbouche, M. R., & Ben Ahmed, M. (2017). Specific immune responses in mice following subchronic exposure to acetamiprid. *Life Sciences*, *188*, 10–16. https://doi.org/10.1016/j.lfs.2017.08.022

Matsumaru, D., & Motohashi, H. (2021). The KEAP1-NRF2 System in Healthy Aging and Longevity. *Antioxidants*, *10*(12), 1929. https://doi.org/10.3390/antiox10121929

Matsuo, H., Tomizawa, M., & Yamamoto, I. (1998). Structure-activity relationships of acyclic nicotinoids and neonicotinoids for insect nicotinic acetylcholine receptor/ion channel complex. *Archives of Insect Biochemistry and Physiology*, *37*(1), 17–23. https://doi.org/10.1002/(SICI)1520-6327(1998)37:1<17::AID-ARCH3>3.0.CO;2-S

Matthews, J. J., Artioli, G. G., Turner, M. D., & Sale, C. (2019). The Physiological Roles of Carnosine and ß-Alanine in Exercising Human Skeletal Muscle. *Medicine and Science in Sports and Exercise*, *51*(10), 2098–2108. https://doi.org/10.1249/MSS.0000000000002033

Maurin, M., & Garnuszek, P. (2010). Radiochemical synthesis and preliminary in vivo evaluation of new radioactive platinum complexes with carnosine. *Applied Radiation and Isotopes: Including Data, Instrumentation and Methods for Use in Agriculture, Industry and Medicine*, *68*(2), 317–324. https://doi.org/10.1016/j.apradiso.2009.10.053

Mayerle, J., Sendler, M., Hegyi, E., Beyer, G., Lerch, M. M., & Sahin-Tóth, M. (2019). Genetics, Cell Biology, and Pathophysiology of Pancreatitis. *Gastroenterology*, *156*(7), 1951-1968.e1. https://doi.org/10.1053/j.gastro.2018.11.081

McFarland, G. A., & Holliday, R. (1994). Retardation of the senescence of cultured human diploid fibroblasts by carnosine. *Experimental Cell Research*, *212*(2), 167–175. https://doi.org/10.1006/excr.1994.1132

Menini, S., Iacobini, C., Ricci, C., Scipioni, A., Fantauzzi, C. B., Giaccari, A., Salomone, E., Canevotti, R., Lapolla, A., Orioli, M., Aldini, G., & Pugliese, G. (2012). D-carnosine octylester attenuates atherosclerosis and renal disease in ApoE null mice fed a Western diet through reduction of carbonyl stress and inflammation. *British Journal of Pharmacology*, *166*(4), 1344–1356. https://doi.org/10.1111/j.1476-5381.2012.01834.x

Menon, K., Marquina, C., Hoj, P., Liew, D., Mousa, A., & de Courten, B. (2020). Carnosine and histidine-containing dipeptides improve dyslipidemia: A systematic review and meta-analysis of randomized controlled trials. *Nutrition Reviews*, *78*(11), 939–951. https://doi.org/10.1093/nutrit/nuaa022

Mesallam, D. I. A., Abdel Hamid, O. I., & Ibrahem, N. E. (2018). Ethanolic extract of fenugreek seeds moderates dimethoate-induced pancreatic damage in male rats.

Environmental Science and Pollution Research International, *25*(4), 3894–3904. https://doi.org/10.1007/s11356-017-0749-9

Miceli, V., Pampalone, M., Frazziano, G., Grasso, G., Rizzarelli, E., Ricordi, C., Casu, A., Iannolo, G., & Conaldi, P. G. (2018). Carnosine protects pancreatic beta cells and islets against oxidative stress damage. *Molecular and Cellular Endocrinology*, *474*, 105–118. https://doi.org/10.1016/j.mce.2018.02.016

Mitsika, E. E., Christophoridis, C., & Fytianos, K. (2013). Fenton and Fenton-like oxidation of pesticide acetamiprid in water samples: Kinetic study of the degradation and optimization using response surface methodology. *Chemosphere*, *93*(9), 1818–1825. https://doi.org/10.1016/j.chemosphere.2013.06.033

Mondal, S. (2015). Haematobiochemical Profile in Chronic Acetamiprid Exposure in Sprague Dawley Rats. *Advances in Animal and Veterinary Sciences*, *3*(7), 384–394. https://doi.org/10.14737/journal.aavs/2015/3.7.384.394

Mondal, S., Ghosh, R. C., Mate, M. S., & Karmakar, D. B. (2009). Effect of subacute exposure of acetamiprid on organ toxicity and growth of wistar rat. *Indian J. Anim. Health*, *48*, 67–72.

Mössner, J. (2010). New advances in cell physiology and pathophysiology of the exocrine pancreas. *Digestive Diseases (Basel, Switzerland)*, *28*(6), 722–728. https://doi.org/10.1159/000324279

Mou, Y., Wen, S., Li, Y.-X., Gao, X.-X., Zhang, X., & Jiang, Z.-Y. (2020). Recent progress in Keap1-Nrf2 protein-protein interaction inhibitors. *European Journal of Medicinal Chemistry*, *202*, 112532. https://doi.org/10.1016/j.ejmech.2020.112532

Mumcu, S., Alhan, E., Türkyilmaz, S., Kural, B. V., Erçin, C., & Kalyoncu, N. I. (2005). Effects of N-acetylcysteine on acute necrotizing pancreatitis in rats. *European Surgical Research. Europaische Chirurgische Forschung. Recherches Chirurgicales Europeennes*, *37*(3), 173–178. https://doi.org/10.1159/000085965

Mustafa, I. M., Hapipah, M. A., Abdulla, M. A., & Ward, T. R. (2009). Synthesis, structural characterization, and anti-ulcerogenic activity of schiff base ligands derived from tryptamine and 5-chloro, 5-nitro, 3,5-ditertiarybutyl salicylaldehyde and their nickel(II), copper(II), and zinc(II) complexes. *Polyhedron*, *28*(18), 3993–3998. https://doi.org/10.1016/j.poly.2009.10.004

Nagai, K., & Suda, T. (1986). [Antineoplastic effects of carnosine and beta-alanine—Physiological considerations of its antineoplastic effects]. *Nihon Seirigaku Zasshi. Journal of the Physiological Society of Japan*, *48*(11), 741–747.

Nagai, K., Suda, T., Kawasaki, K., & Yamaguchi, Y. (1990). [Acceleration of metabolism of stress-related substances by L-carnosine]. *Nihon Seirigaku Zasshi. Journal of the Physiological Society of Japan*, *52*(7), 221–228.

Nagasawa, T., Yonekura, T., Nishizawa, N., & Kitts, D. D. (2001). In vitro and in vivo inhibition of muscle lipid and protein oxidation by carnosine. *Molecular and Cellular Biochemistry*, *225*(1-), 29–34. https://doi.org/10.1023/a:1012256521840

Naranjo, S., & Akey, D. (2004, May 1). *Comparative Efficacy and Selectivity of Acetamiprid for the Management of Bemisia tabaci*. https://www.semanticscholar.org/paper/Comparative-Efficacy-and-Selectivity-of-Acetamiprid-Naranjo-Akey/67cddb96330b11a21dc9fe0cc38dacb3b68d6575

Nawaz, A., Niaz, A., Ilyas, M., Shah, S. S. H., Asi, M. R., & Ahmad, Z. A. (2015). Determination and Extraction of Acetamiprid Residues in Fruits and Vegetables. *International Journal of Food and Allied Sciences*, *1*(2), 63. https://doi.org/10.21620/ijfaas.2015263-66

Nicoll, R. A., Alger, B. E., Jahr, C. E., & Morley, J. S. (1980). Peptides as Putative Excitatory Neurotransmitters: Carnosine, Enkephalin, Substance P and TRH [and Discussion]. *Proceedings of the Royal Society of London. Series B, Biological Sciences*, *210*(1178), 133–149.

Nimako, C., Ikenaka, Y., Akoto, O., Fujioka, K., Taira, K., Arizono, K., Kato, K., Takahashi, K., Nakayama, S. M. M., Ichise, T., & Ishizuka, M. (2021). Simultaneous quantification of imidacloprid and its metabolites in tissues of mice upon chronic low-dose administration of imidacloprid. *Journal of Chromatography. A*, *1652*, 462350. https://doi.org/10.1016/j.chroma.2021.462350

Ning, H., Marshall, F. D., Henn, F. A., & Sellström, A. (1977). Metabolism of carnosine and homocarnosine in subcellular fractions and neuronal and glial cell-enriched fractions of rabbit brain. *Journal of Neurochemistry*, *28*(2), 449–452. https://doi.org/10.1111/j.1471-4159.1977.tb07770.x

Niu, H., Álvarez-Álvarez, I., Guillén-Grima, F., & Aguinaga-Ontoso, I. (2017). Prevalence and incidence of Alzheimer's disease in Europe: A meta-analysis. *Neurologia (Barcelona, Spain)*, *32*(8), 523–532. https://doi.org/10.1016/j.nrl.2016.02.016

Novaes, G., Queiroz, A. C., Queiroz, A. P., Santos, R. R., Flores, D. G., Henkes, G., & Fernandes, B. J. D. (2002). Estudo histopatológico do pâncreas de ratos intoxicados pelo veneno bruto do escorpião Tityus serrulatus. *Revista de Ciências Médicas e Biológicas*, *1*(1), Article 1. https://doi.org/10.9771/cmbio.v1i1.4041

Omary, M. B., Lugea, A., Lowe, A. W., & Pandol, S. J. (2007). The pancreatic stellate cell: A star on the rise in pancreatic diseases. *The Journal of Clinical Investigation*, *117*(1), 50–59. https://doi.org/10.1172/JCI30082

Orioli, M., Aldini, G., Benfatto, M. C., Maffei Facino, R., & Carini, M. (2007). HNE Michael Adducts to Histidine and Histidine-Containing Peptides as Biomarkers of Lipid-Derived Carbonyl Stress in Urines: LC−MS/MS Profiling in Zucker Obese Rats. *Analytical Chemistry*, *79*(23), 9174–9184. https://doi.org/10.1021/ac7016184

Öztaş, E., Kara, M., Boran, T., Bişirir, E., Karaman, E. F., Kaptan, E., & Özhan, G. (2021). Cellular Stress Pathways Are Linked to Acetamiprid-Induced Apoptosis in SH-SY5Y Neural Cells. *Biology*, *10*(9), 820. https://doi.org/10.3390/biology10090820

Pan, C., Yu, J., Yao, Q., Lin, N., Lu, Z., Zhang, Y., Zhao, S., Wang, Z., Lei, X., Tian, Y., & Gao, Y. (2022). Prenatal neonicotinoid insecticides Exposure, oxidative Stress, and birth outcomes. *Environment International*, *163*, 107180. https://doi.org/10.1016/j.envint.2022.107180

Panteghini, M., Bonora, R., & Pagani, F. (2001). Measurement of pancreatic lipase activity in serum by a kinetic colorimetric assay using a new chromogenic substrate. *Annals of Clinical Biochemistry*, *38*(4), 365–370. https://doi.org/10.1258/0004563011900876

Pepper, E. D., Farrell, M. J., Nord, G., & Finkel, S. E. (2010). Antiglycation effects of carnosine and other compounds on the long-term survival of Escherichia coli. *Applied and Environmental Microbiology*, *76*(24), 7925–7930. https://doi.org/10.1128/AEM.01369-10

Peters, V., Jansen, E. E. W., Jakobs, C., Riedl, E., Janssen, B., Yard, B. A., Wedel, J., Hoffmann, G. F., Zschocke, J., Gotthardt, D., Fischer, C., & Köppel, H. (2011). Anserine inhibits carnosine degradation but in human serum carnosinase (CN1)

is not correlated with histidine dipeptide concentration. *Clinica Chimica Acta; International Journal of Clinical Chemistry*, *412*(3–4), 263–267. https://doi.org/10.1016/j.cca.2010.10.016

Peters, V., Klessens, C. Q. F., Baelde, H. J., Singler, B., Veraar, K. A. M., Zutinic, A., Drozak, J., Zschocke, J., Schmitt, C. P., & de Heer, E. (2015). Intrinsic carnosine metabolism in the human kidney. *Amino Acids*, *47*(12), 2541–2550. https://doi.org/10.1007/s00726-015-2045-7

Phogat, A., Singh, J., Sheoran, R., Hasanpuri, A., Singh, V., Kumar, V., Prakash, C., & Malik, V. (2023). *Acetamiprid Exposure-Induces Molecular and Structural Changes in Liver and Kidney Tissues of Rats* (2023122173). Preprints. https://doi.org/10.20944/preprints202312.2173.v1

Potts, J., Jones, D. L., Macdonald, A., Ma, Q., & Cross, P. (2022). Acetamiprid fate in a sandy loam with contrasting soil organic matter contents: A comparison of the degradation, sorption and leaching of commercial neonicotinoid formulations. *Science of The Total Environment*, *842*, 156711. https://doi.org/10.1016/j.scitotenv.2022.156711

Price, D. L., Rhett, P. M., Thorpe, S. R., & Baynes, J. W. (2001). Chelating Activity of Advanced Glycation End-product Inhibitors*. *Journal of Biological Chemistry*, *276*(52), 48967–48972. https://doi.org/10.1074/jbc.M108196200

Pua, L. J. W., Mai, C.-W., Chung, F. F.-L., Khoo, A. S.-B., Leong, C.-O., Lim, W.-M., & Hii, L.-W. (2022). Functional Roles of JNK and p38 MAPK Signaling in Nasopharyngeal Carcinoma. *International Journal of Molecular Sciences*, *23*(3), 1108. https://doi.org/10.3390/ijms23031108

Qamruzzaman, Q., & Nasar, A. (2014). Treatment of acetamiprid insecticide from artificially contaminated water by colloidal manganese dioxide in the absence and presence of surfactants. *RSC Adv.*, 10.1039.C4RA09685A. https://doi.org/10.1039/C4RA09685A

Qian, J., Wang, X., Weng, W., Zhou, G., Zhu, S., & Liu, C. (2021). Salidroside alleviates taurolithocholic acid 3-sulfate-induced AR42J cell injury. *Biomedicine & Pharmacotherapy = Biomedecine & Pharmacotherapie*, *142*, 112062. https://doi.org/10.1016/j.biopha.2021.112062

Quintana, M. M., Rivero Osimani, V., Magnarelli, G., Rovedatti, M. G., & Guiñazú, N. (2018). The insecticides chlorpyrifos and acetamiprid induce redox imbalance in umbilical cord blood erythrocytes in vitro. *Pesticide Biochemistry and Physiology*, *148*, 87–92. Scopus. https://doi.org/10.1016/j.pestbp.2018.04.001

Raghuraman, M., Birah, A., & Gupta, G. (2008). Bioefficacy of acetamiprid on sucking pests in cotton. *Indian Journal of Entomology*. https://www.semanticscholar.org/paper/Bioefficacy-of-acetamiprid-on-sucking-pests-in-Raghuraman-Birah/1484806428615127a124b627dd381c7c2dd80b9a

Rasaily, M., Ngiimei D, S., Thaosen, R. K., Gupta, S., Deka, S., & Tamuli, R. (2024). Methods for the detection of intracellular calcium in filamentous fungi. *MethodsX*, *12*, 102570. https://doi.org/10.1016/j.mex.2024.102570

Reddy, V. P., Garrett, M. R., Perry, G., & Smith, M. A. (2005). Carnosine: A Versatile Antioxidant and Antiglycating Agent. *Science of Aging Knowledge Environment*, *2005*(18), pe12–pe12. https://doi.org/10.1126/sageke.2005.18.pe12

Renaud, M., Akeju, T., Natal-da-Luz, T., Leston, S., Rosa, J., Ramos, F., Sousa, J. P., & Azevedo-Pereira, H. M. V. S. (2018). Effects of the neonicotinoids acetamiprid and thiacloprid in their commercial formulations on soil fauna. *Chemosphere*, *194*, 85–93. https://doi.org/10.1016/j.chemosphere.2017.11.102

Riedl, E., Pfister, F., Braunagel, M., Brinkkötter, P., Sternik, P., Deinzer, M., Bakker, S. J. L., Henning, R. H., van den Born, J., Krämer, B. K., Navis, G., Hammes, H.-P., Yard, B., & Koeppel, H. (2011). Carnosine prevents apoptosis of glomerular cells and podocyte loss in STZ diabetic rats. *Cellular Physiology and Biochemistry: International Journal of Experimental Cellular Physiology, Biochemistry, and Pharmacology*, *28*(2), 279–288. https://doi.org/10.1159/000331740

Rocha, C. C., Kawai, G. K. V., de Agostini Losano, J. D., Angrimani, D. de S. R., Rui, B. R., de Cássia Bicudo, L., da Silva, B. do C. S., Alonso, M. A., Mendes, C. M., Ortiz D'Avila Assumpção, M. E., Pereira, R. J. G., Barnabe, V. H., & Nichi, M. (2018). Carnosine as malondialdehyde scavenger in stallion seminal plasma and its role in sperm function and oxidative status. *Theriogenology*, *119*, 10–17. https://doi.org/10.1016/j.theriogenology.2018.06.016

Rocha, S., Rufino, A. T., Freitas, M., Silva, A. M. S., Carvalho, F., & Fernandes, E. (2023). Methodologies for Assessing Pancreatic Lipase Catalytic Activity: A Review. *Critical Reviews in Analytical Chemistry*, *0*(0), 1–28. https://doi.org/10.1080/10408347.2023.2221731

Röder, P. V., Wu, B., Liu, Y., & Han, W. (2016). Pancreatic regulation of glucose homeostasis. *Experimental &Amp; Molecular Medicine*, *48*, e219.

Röder, P. V., Wu, B., Liu, Y., & Han, W. (2016). Pancreatic regulation of glucose homeostasis. *Experimental &Amp; Molecular Medicine*, *48*, e219.

Rünzi, M., Müller, M. K., Schmid, P., von Schönfeld, J., & Goebell, H. (1992). Stimulatory and inhibitory effects of galanin on exocrine and endocrine rat pancreas. *Pancreas*, *7*(6), 619–623. https://doi.org/10.1097/00006676-199211000-00001

Saadah, L. M., Deiab, G. I. A., Al-Balas, Q., & Basheti, I. A. (2020). Carnosine to Combat Novel Coronavirus (nCoV): Molecular Docking and Modeling to Cocrystallized Host Angiotensin-Converting Enzyme 2 (ACE2) and Viral Spike Protein. *Molecules (Basel, Switzerland)*, *25*(23), 5605. https://doi.org/10.3390/molecules25235605

Sakai, M., Kani, K., Karasawa, N., Yoshida, M., & Nagatsu, I. (1988). Carnosine-like immunoreactivity in the olfactory bulb of the rat: An electron microscopic study. *Brain Research*, *438*(1), 335–338. https://doi.org/10.1016/0006-8993(88)91359-5

Santofimia-Castaño, P., Garcia-Sanchez, L., Ruy, D. C., Fernandez-Bermejo, M., Salido, G. M., & Gonzalez, A. (2014). The seleno-organic compound ebselen impairs mitochondrial physiology and induces cell death in AR42J cells. *Toxicology Letters*, *229*(3), 465–473. https://doi.org/10.1016/j.toxlet.2014.07.025

Sasawatari, S., Okamura, T., Kasumi, E., Tanaka-Furuyama, K., Yanobu-Takanashi, R., Shirasawa, S., Kato, N., & Toyama-Sorimachi, N. (2011). The solute carrier family 15A4 regulates TLR9 and NOD1 functions in the innate immune system and promotes colitis in mice. *Gastroenterology*, *140*(5), 1513–1525. https://doi.org/10.1053/j.gastro.2011.01.041

Sastre, J., Sabater, L., & Aparisi, L. (2005). Fisiología de la secreción pancreática. *Gastroenterología y Hepatología*, *28*, 3–9. https://doi.org/10.1157/13071380

Schön, M., Mousa, A., Berk, M., Chia, W. L., Ukropec, J., Majid, A., Ukropcová, B., & de Courten, B. (2019). The Potential of Carnosine in Brain-Related Disorders: A Comprehensive Review of Current Evidence. *Nutrients*, *11*(6), 1196. https://doi.org/10.3390/nu11061196

Sedlmeier, J. E., Grass, I., Bendalam, P., Höglinger, B., Walker, F., Gerhard, D., Piepho, H.-P., Brühl, C. A., & Petschenka, G. (2024). *The neonicotinoid acetamiprid is highly toxic to wild non-target insects*. https://doi.org/10.1101/2024.04.11.589033

Segawa, Y., Tsuzuike, N., Itokazu, Y., Tagashira, E., & Yamaguchi, M. (1992). Beta-Alanyl-L-histidinato zinc prevents hydrocortisone-induced disorder of bone metabolism in rats. *Research in Experimental Medicine. Zeitschrift Fur Die Gesamte Experimentelle Medizin Einschliesslich Experimenteller Chirurgie*, *192*(5), 317–322. https://doi.org/10.1007/BF02576288

Sevim, Ç., Çomaklı, S., Taghizadehghalehjoughi, A., Özkaraca, M., Mesnage, R., Kovatsi, L., Burykina, T. I., Kalogeraki, A., Antoniou, M. N., & Tsatsakis, A. (2019). An imazamox-based herbicide causes apoptotic changes in rat liver and pancreas. *Toxicology Reports*, *6*, 42–50. https://doi.org/10.1016/j.toxrep.2018.11.008

Shahid, Z., & Singh, G. (2024). Physiology, Islets of Langerhans. In *StatPearls*. StatPearls Publishing. http://www.ncbi.nlm.nih.gov/books/NBK542302/

Shakthi Devan, R. K., Prabu, P. C., & Panchapakesan, S. (2015). Immunotoxicity assessment of sub-chronic oral administration of acetamiprid in Wistar rats. *Drug and Chemical Toxicology*, *38*(3), 328–336. https://doi.org/10.3109/01480545.2014.966382

Shamsi, M., Soodi, M., Shahbazi, S., & Omidi, A. (2021). Effect of Acetamiprid on spatial memory and hippocampal glutamatergic system. *Environmental Science and Pollution Research International*, *28*(22), 27933–27941. https://doi.org/10.1007/s11356-020-12314-6

Sharifi, A. M. (2014). Effect of Carnosine on the Prevention of High-Dose Morphine-Induced Apoptosis of PC12 Cells. *Journal of Medical and Bioengineering*. https://www.academia.edu/86060805/Effect_of_Carnosine_on_the_Prevention_of_High_Dose_Morphine_Induced_Apoptosis_of_PC12_Cells

She, J., Fu, L., Zheng, X., Li, J., Wang, L., Yu, B., & Ju, J. (2022). Characterization of a new L-carnosine synthase mined from deep-sea sediment metagenome. *Microbial Cell Factories*, *21*(1), 129. https://doi.org/10.1186/s12934-022-01854-w

Sheets, L. P., Li, A. A., Minnema, D. J., Collier, R. H., Creek, M. R., & Peffer, R. C. (2016). A critical review of neonicotinoid insecticides for developmental neurotoxicity. *Critical Reviews in Toxicology*, *46*(2), 153–190. https://doi.org/10.3109/10408444.2015.1090948

Sheets, L. P., Li, A. A., Minnema, D. J., Collier, R. H., Creek, M. R., & Peffer, R. C. (2016). A critical review of neonicotinoid insecticides for developmental neurotoxicity. *Critical Reviews in Toxicology*, *46*(2), 153–190. https://doi.org/10.3109/10408444.2015.1090948

Shen, F., Regmi, D., Islam, M., Raja Somu, D., Merk, V., & Du, D. (2022). Effects of zinc and carnosine on aggregation kinetics of Amyloid-ß40 peptide. *Biochemistry and Biophysics Reports*, *32*, 101333. https://doi.org/10.1016/j.bbrep.2022.101333

Silva, A. V., Norinder, U., Liiv, E., Platzack, B., Öberg, M., & Törnqvist, E. (2021). Associations between clinical signs and pathological findings in toxicity testing. *ALTEX*, *38*(2), 198–214. https://doi.org/10.14573/altex.2003311

Singh, T. B. (2012). Acetamiprid Induces Toxicity in Mice under Experimental Conditions with Prominent Effect on the Hematobiochemical Parameters. *Journal of Drug Metabolism and Toxicology*, *3*(6), 1–5. https://doi.org/10.4172/2157-7609.1000134

Singh, T. B., Mukhopadhayay, S. K., Sar, T. K., & Ganguly, S. (2012). Induced Acetamiprid Toxicity in Mice: A Review. *Journal of Drug Metabolism & Toxicology*, *0*(0), 1–2.

Solana-Manrique, C., Sanz, F. J., Martínez-Carrión, G., & Paricio, N. (2022). Antioxidant and Neuroprotective Effects of Carnosine: Therapeutic Implications in Neurodegenerative Diseases. *Antioxidants*, *11*(5), 848. https://doi.org/10.3390/antiox11050848

Song, M. O., Lee, C.-H., Yang, H. O., & Freedman, J. H. (2012). Endosulfan upregulates AP-1 binding and ARE-mediated transcription via ERK1/2 and p38 activation in HepG2 cells. *Toxicology*, *292*(1), 23–32. https://doi.org/10.1016/j.tox.2011.11.013

Song, Y. R., Kim, J.-K., Lee, H.-S., Kim, S. G., & Choi, E.-K. (2020). Serum levels of protein carbonyl, a marker of oxidative stress, are associated with overhydration, sarcopenia and mortality in hemodialysis patients. *BMC Nephrology*, *21*(1), 281. https://doi.org/10.1186/s12882-020-01937-z

Spaas, J., Franssen, W. M. A., Keytsman, C., Blancquaert, L., Vanmierlo, T., Bogie, J., Broux, B., Hellings, N., van Horssen, J., Posa, D. K., Hoetker, D., Baba, S. P., Derave, W., & Eijnde, B. O. (2021). Carnosine quenches the reactive carbonyl acrolein in the central nervous system and attenuates autoimmune neuroinflammation. *Journal of Neuroinflammation*, *18*(1), 255. https://doi.org/10.1186/s12974-021-02306-9

Stuerenburg, H. J. (2000). The roles of carnosine in aging of skeletal muscle and in neuromuscular diseases. *Biochemistry. Biokhimiia*, *65*(7), 862–865.

Suwannarin, N., Prapamontol, T., Isobe, T., Nishihama, Y., Hashimoto, Y., Mangklabruks, A., Pantasri, T., Chantara, S., Naksen, W., & Nakayama, S. F. (2021). Exposure to Organophosphate and Neonicotinoid Insecticides and Its Association with Steroid Hormones among Male Reproductive-Age Farmworkers in Northern Thailand. *International Journal of Environmental Research and Public Health*, *18*(11), 5599. https://doi.org/10.3390/ijerph18115599

Swenson, T. L., & Casida, J. E. (2013). Aldehyde oxidase importance in vivo in xenobiotic metabolism: Imidacloprid nitroreduction in mice. *Toxicological Sciences: An Official Journal of the Society of Toxicology*, *133*(1), 22–28. https://doi.org/10.1093/toxsci/kft066

Taha, M., Badawy, M., Abdel-razik, R., Younis, H., & Abo-el-saad, M. (2022). Effects of sub-chronic exposure of male albino rats to some insecticides on mitochondrial dysfunction and oxidative stress in the kidney with molecular docking. *Journal of Cellular Neuroscience and Oxidative Stress*, *13*(3), Article 3. https://doi.org/10.37212/jcnos.1080039

Taira, K., Fujioka, K., & Aoyama, Y. (2013). Qualitative Profiling and Quantification of Neonicotinoid Metabolites in Human Urine by Liquid Chromatography Coupled with Mass Spectrometry. *PLoS ONE*, *8*(11), e80332. https://doi.org/10.1371/journal.pone.0080332

Tallon, M. J., Harris, R. C., Maffulli, N., & Tarnopolsky, M. A. (2007). Carnosine, taurine and enzyme activities of human skeletal muscle fibres from elderly subjects with osteoarthritis and young moderately active subjects. *Biogerontology*, *8*(2), 129–137. https://doi.org/10.1007/s10522-006-9038-6

Tamang, S. (2024, April 7). *Pancreatic Cells: Types, Structure, Functions, Diseases*. https://microbenotes.com/pancreatic-cells/

Tamura, K., Manabe, T., Andoh, K., Kyogoku, T., Oshio, G., & Tobe, T. (1992). Effect of intraarterial active oxygen species on the rat pancreas. *Hepato-Gastroenterology*, *39*(2), 152–157.

Tang, X., Li, X., Ma, D.-L., Lu, L., & Qu, B. (2018). A label-free triplex-to-G-qadruplex molecular switch for sensitive fluorescent detection of acetamiprid. *Talanta*, *189*, 599–605. https://doi.org/10.1016/j.talanta.2018.07.025

Tapia, J. A., González, A., Salido, G., & Lj, G. (1997). Trypsinogen secretion from the isolated guinea-pig pancreas in response to secretagogues. *Biogenic Amines*. https://www.semanticscholar.org/paper/Trypsinogen-secretion-from-the-isolated-guinea-pig-Tapia-Gonz%C3%A1lez/971fd7deaa6c03569a1f5549092bd4291b28ef79

Terayama, H., Qu, N., Endo, H., Ito, M., Tsukamoto, H., Umemoto, K., Kawakami, S., Fujino, Y., Tatemichi, M., & Sakabe, K. (2018). Effect of acetamiprid on the immature murine testes. *International Journal of Environmental Health Research*, *28*(6), 683–696. https://doi.org/10.1080/09603123.2018.1504897

Thomas, H., Nisbet, T. R., & Willoughby, I. H. (2023). Acetamiprid used to prevent *Hylobius abietis* damaging young trees poses a very low risk of causing water contamination provided good forestry practices are followed. *Forestry: An International Journal of Forest Research*, *96*(2), 207–216. https://doi.org/10.1093/forestry/cpac041

Toghan, R., Amin, Y. A., Ali, R. A., Fouad, S. S., Ahmed, M. A.-E. B., & Saleh, S. M. M. (2022). Protective effects of Folic acid against reproductive, hematological, hepatic, and renal toxicity induced by Acetamiprid in male Albino rats. *Toxicology*, *469*, 153115. https://doi.org/10.1016/j.tox.2022.153115

Tomizawa, M., & Casida, J. E. (2002). Desnitro-imidacloprid Activates the Extracellular Signal-Regulated Kinase Cascade via the Nicotinic Receptor and Intracellular Calcium Mobilization in N1E-115 Cells. *Toxicology and Applied Pharmacology*, *184*(3), 180–186. https://doi.org/10.1006/taap.2002.9503

Torreggiani, A., Tamba, M., & Fini, G. (2000). Binding of copper(II) to carnosine: Raman and IR spectroscopic study. *Biopolymers*, *57*(3), 149–159. https://doi.org/10.1002/(SICI)1097-0282(2000)57:3<149::AID-BIP3>3.0.CO;2-G

Toviwek, B., Suwanasopee, T., Koonawootrittriron, S., Jattawa, D., & Pongprayoon, P. (2023). Binding Modes of Carnostatine, Homocarnosine, and Ophidine to Human Carnosinase 1. *ACS Omega*, *8*(45), 42966–42975. https://doi.org/10.1021/acsomega.3c06139

Travagli, T. B. and R. A. (2016). Neural Control of the Pancreas. *Pancreapedia: The Exocrine Pancreas Knowledge Base*. https://doi.org/10.3998/panc.2016.27

Turner, M. D., Sale, C., Garner, A. C., & Hipkiss, A. R. (2021). Anti-cancer actions of carnosine and the restoration of normal cellular homeostasis. *Biochimica et Biophysica Acta (BBA) - Molecular Cell Research*, *1868*(11), 119117. https://doi.org/10.1016/j.bbamcr.2021.119117

Usborne, A., Smith, A. T., Engle, S., Watson, D., Sullivan, J., & Walgren, J. L. (2014). Biomarkers of Exocrine Pancreatic Injury in 2 Rat Acute Pancreatitis Models. *Toxicologic Pathology*, *42*, 195–203. https://doi.org/10.1177/0192623313512030

Vertiprakhov, V. G., & Ovchinnikova, N. V. (2022). The activity of trypsin in the pancreatic juice and blood of poultry increases simultaneously in the postprandial period. *Frontiers in Physiology*, *13*, 874664. https://doi.org/10.3389/fphys.2022.874664

Vincent, A., Herman, J., Schulick, R., Hruban, R. H., & Goggins, M. (2011). Pancreatic cancer. *Lancet (London, England)*, *378*(9791), 607–620. https://doi.org/10.1016/S0140-6736(10)62307-0

Vu, C. U., Siddiqui, J. A., Wadensweiler, P., Gayen, J. R., Avolio, E., Bandyopadhyay, G. K., Biswas, N., Chi, N.-W., O'Connor, D. T., & Mahata, S. K. (2014). Nicotinic acetylcholine receptors in glucose homeostasis: The acute hyperglycemic and chronic insulin-sensitive effects of nicotine suggest dual opposing roles of the receptors in male mice. *Endocrinology*, *155*(10), 3793–3805. https://doi.org/10.1210/en.2014-1320

Walker, A., Udupa, K. B., & Chowdhury, P. (2008). Mitogenic and functional responses by nicotine and hydrogen peroxide in AR42J cells: A comparative study. *Tobacco Induced Diseases*, *4*(July). https://doi.org/10.1186/1617-9625-4-5

Wallace, D. R. (2024). Acetamiprid. In P. Wexler (Ed.), *Encyclopedia of Toxicology (Fourth Edition)* (pp. 53–59). Academic Press. https://doi.org/10.1016/B978-0-12-824315-2.00267-0

Wang, G., Yue, W., Liu, Y., Li, F., Xiong, M., & Zhang, H. (2013). Biodegradation of the neonicotinoid insecticide Acetamiprid by bacterium Pigmentiphaga sp. Strain AAP-1 isolated from soil. *Bioresource Technology*, *138*, 359–368. https://doi.org/10.1016/j.biortech.2013.03.193

Wang, X., Qiu, J., Xu, Y., Pan, Y., Chen, H., Jia, Q., & Qian, Y. (2022). Different cellular mechanism of imidacloprid and acetamiprid by a combined targeted lipidomics and metabolomics approach in Neuro-2a cells. *Toxicology in Vitro: An International Journal Published in Association with BIBRA*, *83*, 105426. https://doi.org/10.1016/j.tiv.2022.105426

Wang, X., Wang, J., Zhang, P., Zhang, C., Wang, W., Wu, M., Xu, W., Tao, L., Li, Z., & Zhang, Y. (2023). Cytotoxicity and Autophagy Induced by Ivermectin via AMPK/mTOR Signaling Pathway in RAW264.7 Cells. *Molecules (Basel, Switzerland)*, *28*(5), 2201. https://doi.org/10.3390/molecules28052201

Wang-Eckhardt, L., Bastian, A., Bruegmann, T., Sasse, P., & Eckhardt, M. (2020). Carnosine synthase deficiency is compatible with normal skeletal muscle and olfactory function but causes reduced olfactory sensitivity in aging mice. *The Journal of Biological Chemistry*, *295*(50), 17100–17113. https://doi.org/10.1074/jbc.RA120.014188

Waqas, M. S., Qian, L., Shoaib, A. A. Z., Cheng, X., Zhang, Q., Elabasy, A. S. S., & Shi, Z. (2019). Lethal and Sublethal Effects of Neonicotinoid Insecticides on the Adults of Phenacoccus solenopsis (Hemiptera: Pseudococcidae) on Tomato Plants. *Journal of Economic Entomology*, *112*(3), 1314–1321. https://doi.org/10.1093/jee/toy427

Wassif, W. S., Sherwood, R. A., Amir, A., Idowu, B., Summers, B., Leigh, N., & Peters, T. J. (1994). Serum carnosinase activities in central nervous system disorders. *Clinica Chimica Acta; International Journal of Clinical Chemistry*, *225*(1), 57–64. https://doi.org/10.1016/0009-8981(94)90027-2

Wassif, W. S., Sherwood, R. A., Amir, A., Idowu, B., Summers, B., Leigh, N., & Peters, T. J. (1994). Serum carnosinase activities in central nervous system disorders. *Clinica Chimica Acta; International Journal of Clinical Chemistry*, *225*(1), 57–64. https://doi.org/10.1016/0009-8981(94)90027-2

Werner, J., Saghir, M., Warshaw, A. L., Lewandrowski, K. B., Laposata, M., Iozzo, R. V., Carter, E. A., Schatz, R. J., & Fernández-Del Castillo, C. (2002). Alcoholic pancreatitis in rats: Injury from nonoxidative metabolites of ethanol. *American*

Journal of Physiology. Gastrointestinal and Liver Physiology, *283*(1), G65-73. https://doi.org/10.1152/ajpgi.00419.2001

Wijaya, W., Pang, S., Labuza, T. P., & He, L. (2014). Rapid Detection of Acetamiprid in Foods using Surface-Enhanced Raman Spectroscopy (SERS). *Journal of Food Science*, *79*(4). https://doi.org/10.1111/1750-3841.12391

Williams, J. A. (2010). Regulation of Acinar Cell Function in The Pancreas. *Current Opinion in Gastroenterology*, *26*(5), 478–483. https://doi.org/10.1097/MOG.0b013e32833d11c6

Williams, J. A., & Yule, D. I. (2012). Chapter 50—Stimulus-secretion Coupling in Pancreatic Acinar Cells. In L. R. Johnson, F. K. Ghishan, J. D. Kaunitz, J. L. Merchant, H. M. Said, & J. D. Wood (Eds.), *Physiology of the Gastrointestinal Tract (Fifth Edition)* (pp. 1361–1398). Academic Press. https://doi.org/10.1016/B978-0-12-382026-6.00050-6

Wu, G. (2020). Important roles of dietary taurine, creatine, carnosine, anserine and 4-hydroxyproline in human nutrition and health. *Amino Acids*, *52*(3), 329–360. https://doi.org/10.1007/s00726-020-02823-6

Wu, J. W., Liu, K.-N., How, S.-C., Chen, W.-A., Lai, C.-M., Liu, H.-S., Hu, C.-J., & Wang, S. S.-S. (2013). Carnosine's Effect on Amyloid Fibril Formation and Induced Cytotoxicity of Lysozyme. *PLoS ONE*, *8*(12), e81982. https://doi.org/10.1371/journal.pone.0081982

Yang, H., Hou, X., Xing, L., & Tian, F. (2022). Carnosine and bone (Review). *Molecular Medicine Reports*, *27*(1), 12. https://doi.org/10.3892/mmr.2022.12899

Yeargans, G. S., & Seidler, N. W. (2003). Carnosine promotes the heat denaturation of glycated protein. *Biochemical and Biophysical Research Communications*, *300*(1), 75–80. https://doi.org/10.1016/s0006-291x(02)02796-1

Yeter, O., & Aydın, A. (2014). Determination of Acetamiprid and IM-1-2 in PostMortem Human Blood, Liver, Stomach Contents by HPLC-DAD. *Journal of Forensic Sciences*, *59*(1), 287–292. https://doi.org/10.1111/1556-4029.12368

You, Z., & Jiao, Q. (2006). Synthesis, Crystal Structures and Antibacterial Activities of Two Schiff Base Zinc(II) Complexes. *Synthesis and Reactivity in Inorganic, Metal-Organic, and Nano-Metal Chemistry*, *36*(10), 713–717. https://doi.org/10.1080/15533170601028165

Yu, X.-Y., Mu, C.-L., Gu, C., Liu, C., & Liu, X.-J. (2011). Impact of woodchip biochar amendment on the sorption and dissipation of pesticide acetamiprid in agricultural soils. *Chemosphere*, *85*(8), 1284–1289. https://doi.org/10.1016/j.chemosphere.2011.07.031

Zafer, J. B., Dede, S., & Karakuş, E. (2021). α-Amylase assay with starch–iodine–sodium fluorescein-based fluorometric method in human serum samples. *Preparative Biochemistry & Biotechnology*, *51*(6), 599–606. https://doi.org/10.1080/10826068.2020.1843177

Zhang, H., Bai, X., Zhang, T., Song, S., Zhu, H., Lu, S., Kannan, K., & Sun, H. (2022). Neonicotinoid Insecticides and Their Metabolites Can Pass through the Human Placenta Unimpeded. *Environmental Science & Technology*, *56*(23), 17143–17152. https://doi.org/10.1021/acs.est.2c06091

Zhang, J.-J., Wang, Y., Xiang, H.-Y., Li, M.-X., Li, W.-H., Ma, K.-G., Wang, X.-Z., & Zhang, J.-H. (2011). Oxidative Stress: Role in Acetamiprid-Induced Impairment of the Male Mice Reproductive System. *Agricultural Sciences in China*, *10*(5), 786–796. Scopus. https://doi.org/10.1016/S1671-2927(11)60063-1

Zhang, Q., Wang, C., Liu, W., Zhang, X., & Zhuang, S. (2012). Evidence for DNA-diquat interaction and cytotoxicity in in vitro rat cells. *Environmental Chemistry Letters*, *10*(1), 35–39. https://doi.org/10.1007/s10311-011-0325-3

Zhang, X., Huang, Y., Chen, W.-J., Wu, S., Lei, Q., Zhou, Z., Zhang, W., Mishra, S., Bhatt, P., & Chen, S. (2023). Environmental occurrence, toxicity concerns, and biodegradation of neonicotinoid insecticides. *Environmental Research*, *218*, 114953. https://doi.org/10.1016/j.envres.2022.114953

Zhang, Z., Miao, L., Wu, X., Liu, G., Peng, Y., Xin, X., Jiao, B., & Kong, X. (2014). Carnosine Inhibits the Proliferation of Human Gastric Carcinoma Cells by Retarding Akt/mTOR/p70S6K Signaling. *Journal of Cancer*, *5*(5), 382–389. https://doi.org/10.7150/jca.8024

Zhao, J., Posa, D. K., Kumar, V., Hoetker, D., Kumar, A., Ganesan, S., Riggs, D. W., Bhatnagar, A., Wempe, M. F., & Baba, S. P. (2019). Carnosine protects cardiac myocytes against lipid peroxidation products. *Amino Acids*, *51*(1), 123–138. https://doi.org/10.1007/s00726-018-2676-6

Zhao, J.-Y., Wang, J.-Q., Wu, L., Zhang, F., Chen, Z.-P., Li, W.-D., Cai, H., & Liu, X. (2019). Emodin attenuates cell injury and inflammation in pancreatic acinar AR42J cells. *Journal of Asian Natural Products Research*, *21*(2), 186–195. https://doi.org/10.1080/10286020.2017.1408594

Zhao, Z., & Liu, W. (2020). Pancreatic Cancer: A Review of Risk Factors, Diagnosis, and Treatment. *Technology in Cancer Research & Treatment*, *19*, 1533033820962117. https://doi.org/10.1177/1533033820962117

Zharikov, A. Y., Kalnitsky, A. S., Mazko, O. N., Makarova, O. G., & Bobrov, I. P. (2023). Effect of Carnosine on the Activity of Matrix Metalloproteinase-2 and Oxidative Stress in the Kidneys in Experimental Urate Nephrolithiasis. *Bulletin of Experimental Biology and Medicine*, *174*(3), 326–329. https://doi.org/10.1007/s10517-023-05701-9

Zhu, T., Liu, X., Song, J., Li, D., Pang, X.-J., Wang, S.-H., Li, Q.-R., Fu, D.-J., Zhang, S.-Y., & Xie, H.-Z. (2021). Ras/Raf/MEK/ERK pathway axis mediated neurotoxicity induced by high-risk pesticide residue-Avermectin. *Environmental Toxicology*, *36*(5), 984–993. https://doi.org/10.1002/tox.23086

Ziling, W. (2007). Effect of Carnosine on the Expression of HSP70 and Inflammatory Factors in a Rat Ischemia-Reperfusion Injury Model. *Journal of Medical Molecular Biology*. https://consensus.app/papers/carnosine-expression-hsp70-inflammatory-factors-ziling/63d3213b4a305adc903b244faa8a1283/

Zuščíková, L., Bažány, D., Greifová, H., Knížatová, N., Kováčik, A., Lukáč, N., & Jambor, T. (2023). Screening of Toxic Effects of Neonicotinoid Insecticides with a Focus on Acetamiprid: A Review. *Toxics*, *11*(7), Article 7. https://doi.org/10.3390/toxics11070598

APPENDIX

1. Composition of physiological Na-HEPES solution

Composition	Molecular weight	Concentration (g/l)
NaCL	58.44	8.1816
KCL	74.56	0.350432
CaCL2	147.02	0.191126
MgCL2*6H2O	203.3	0.2033
Hepes	238.3	2.383
Glucose	180.16	1.8016

2. Composition of supplemented RPMI medium

RPMI -1640 Medium	FBS 10%	Horse serum 4%	Streptomycin	Penicillin
500 ml	58.1 ml	23.3 ml	0.1 mg/ml	100 IU

3. Composition of blocking solution

Composition	Molarity	Quantity
Tris	50 mM	6.05 g
NaCL	150 mM	8.76 g
H_2O	-	1000 g
Nonfat dried milk	-	50 g

4. Composition of lysis buffer

Composition	Volume
Lysis solution	700 µL
Protease inhibitor	7 µL
Orthophosphate	1.4 µL

5. Composition of running buffer

Composition	Molarity	Quantity
Tris base	25 mM	100 mL
Glycine	192 mM	14.4 g
SDS	0.1% (w/v)	1 g
H_2O	-	900 mL

6. Composition of transfer buffer

Composition	Volume
Transfer buffer 10X	100 mL
Methanol	200 mL
H_2O	700 mL